Caracterización microclimática mediante sensores de humedad y temperatura de obras de arte con fines de conservación preventiva

Programa de Doctorado en Estadística y Optimización

Valencia, Octubre 2015

Autor: **Paloma Merello Giménez**

Directores: **Dr. Fernando Juan García Diego**
Dr. Manuel Zarzo Castelló
Dra. Carmen Pérez García

Universitat Politècnica de València

Departamento de Estadística e Investigación Operativa Aplicadas y Calidad

Agradecimientos

Quiero agradecer a mis directores toda la ayuda prestada. A Fernando, por guiarme a lo largo del camino y trabajar día a día conmigo. A Manolo, por compartir conmigo sus conocimientos y su buen saber hacer. A Carmen, porque es un lujo escuchar sus indicaciones fruto de una carrera tan consolidada.

A mi padre, por sembrar en mí el amor por la Ciencia y el Arte. A mi madre, mi padre y mi hermano, por compartir conmigo tantos momentos divertidos.

Por último, agradecer también a Ángel Fernández-Navajas, Jorge Curiel, y el resto de coautores, su colaboración.

A mis prícipes, mi marido y mi hijo.

Resumen

Esta tesis doctoral trata sobre el análisis estadístico multivariante de datos microclimáticos para la conservación preventiva en patrimonio cultural: la casa de Ariadna (Pompeya, Italia), el Museo arqueológico de l'Almoina (Valencia, España) y la iglesia mudéjar de Santa María en Ateca (Ateca, España) . El objetivo principal de esta tesis es proponer una metodología de análisis estadístico de datos microclimáticos extensible a conservadores y restauradores. Se demuestra la utilidad de la metodología propuesta, ya que ha sido posible caracterizar los sitios del patrimonio cultural estudiados. Además, se han propuesto y adoptado acciones correctivas de acuerdo con los resultados obtenidos del análisis de los datos registrados en la casa de Ariadna y el Museo arqueológico de l'Almoina. La efectividad de dichas medidas correctoras ha sido evaluada a través de una segunda campaña de monitorización.

En el caso de la casa de Ariadna, dos campañas de monitorización se llevaron a cabo. Durante la primera, en 2008, el análisis de los datos recogidos demostró que los tejados de policarbonato transparente instalados en los años 70 estaban provocando un efecto invernadero muy perjudicial para la conservación de los frescos. Los sensores permitieron además identificar diferencias entre orientaciones y alturas. Bajo las recomendaciones realizadas, en 2010 los tejados fueron cambiados por unos opacos de fibrocemento, y los datos termo-higrométricos recogidos en una segunda campaña de monitorización permitieron evaluar la adecuación de la medida correctiva en la configuración de un microclima más estable.

El Museo arqueológico de l'Almoina se encuentra expuesto a los viandantes a través de una claraboya que cubre parte de las ruinas. Una primera campaña de monitorización en 2010 permitió caracterizar termo-higrométricamente el museo e identificar la influencia significativa de la claraboya sobre la temperatura y la humedad relativa, causando fuertes aumentos y caídas durante las horas de luz del día, así como un aporte de humedad de una acequia colindante. En 2013 se llevaron a cabo dos

medidas correctivas que fueron evaluadas a través de una segunda monitorización microclimática.

La iglesia mudéjar de Santa María está situada en Ateca, una población de la provincia de Zaragoza caracterizada por fríos inviernos y cálidos veranos. Esta fría climatología invernal condiciona la iglesia al uso de un sistema de climatización. El resultado de nuestros análisis ha puesto de manifiesto que el sistema de climatización solo se enciende para la celebración de misas o festividades religiosas, media hora antes de que entre el público en la iglesia, provocando extremos ciclos de temperatura y humedad relativa, más notables en las partes altas del retablo por el ascenso del aire caliente (incremento horario de 7 °C en la temperatura y un descenso del 11 % de la humedad relativa) que resultan perjudiciales para la conservación de éste.

Resum

Aquesta Tesi doctoral tracta sobre l'anàlisi estadístic multivariant de dades microclimàtics per a la conservació preventiva en patrimoni cultural: la casa d'Ariadna (Pompeia, Itàlia), el Museu arqueològic de l'Almoina (València, Espanya) i l'església mudèjar de Santa María en Ateca (Saragossa, Espanya).

L'objectiu principal d'aquesta tesi és proposar una metodologia d'anàlisi estadístic de dades microclimàtics extensible a conservadors i restauradors. Es demostra la utilitat de la metodologia proposada, ja que ha sigut possible caracteritzar els llocs del patrimoni cultural estudiats.

A més, s'han proposat i adoptat accions correctives d'acord amb els resultats obtinguts de l'anàlisi de les dades registrades en la casa d'Ariadna i el Museu arqueològic de l'Almoina. L'efectivitat d'aquestes mesures correctores ha sigut avaluada a través d'una segona campanya de monitoratge.

En el cas de la casa d'Ariadna, dues campanyes de monitoratge es van dur a terme. Durant la primera, en 2008, l'anàlisi de les dades enregistrades va demostrar que les teulades de policarbonat transparent instal·lades en els anys 70 estaven provocant un efecte hivernacle molt perjudicial per a la conservació dels frescs. Els sensors van permetre a més identificar diferències entre orientacions i altures. Sota les recomanacions realitzades, en 2010 les teulades van ser canviades per unes opaques de fibrociment, i les dades termo-higromètriques arreplegades en una segona campanya de monitoratge van permetre avaluar l'adequació de la mesura correctiva en la configuració d'un microclima més estable.

El Museu arqueològic de l'Almoina es troba exposat als vianants a través d'una claraboia que cobreix part de les ruïnes. Una primera campanya de monitoratge en 2010 va permetre caracteritzar termo-higromètricament el museu i identificar la

influència significativa de la claraboia sobre la temperatura i la humitat relativa, causant forts augments i caigudes durant les hores di*ü*rnes, així com una aportació d'humitat d'una sèquia confrontant. En 2013 es van dur a terme dues mesures correctives que van ser avaluades a través d'un segon monitoratge microclimàtic.

L'església mudèjar de Santa María està situada en Ateca, una població de la província de Saragossa caracteritzada per freds hiverns i càlids estius. Aquesta freda climatologia hivernal condiciona l'església a l'ús d'un sistema de climatització. El resultat de les nostres anàlisis ha posat de manifest que el sistema de climatització solament s'encén per a la celebració de misses o festivitats religioses, mitja hora abans que entre el públic en l'església, provocant extrems cicles de temperatura i humitat relativa, més notables en les parts altes del retaule per l'ascens de l'aire calent (increment horari de 7 °C en la temperatura i un descens del 11 % de la humitat relativa) que resulten perjudicials per a la conservació d'aquest.

Abstract

This PhD dissertation deals with the multivariate statistical analysis of microclimatic data for preventive conservation of cultural heritage in several locations: Ariadne's house (Pompeii, Italy), l'Almoina Archaeological Museum (Valencia, Spain) and mudejar church of Santa Maria in Ateca (Zaragoza, Spain).

The main objective of this thesis is to propose a methodology for statistical analysis of microclimatic data which can be extended to curators and restorers. The usefulness of the proposed methodology is shown, as it has been successfully applied to the studied cultural heritage sites.

Furthermore, corrective actions have been proposed and taken in accordance with the results obtained from the analysis of data recorded at Ariadne's house and the Archaeological Museum of l'Almoina. The effectiveness of such corrective measures has been evaluated through a second monitoring campaign.

In the case of Ariadne's house, two monitoring campaigns were conducted. During the first, in 2008, the analysis of the recorded data showed that the transparent polycarbonate roof installed in the 1970s was causing a greenhouse effect harmful to the conservation of the frescoes. The sensors also helped identifying differences between orientations and heights. Following our recommendations, in 2010 the roofs were changed by some opaque fibrocement and thermo-hygrometric data recorded in a second monitoring campaign allowed us evaluating the adequacy of the corrective actions in configuring a more stable microclimate.

The Archaeological Museum of l'Almoina is exposed to passers-by through a skylight that covers part of the ruins. A first monitoring campaign in 2010 allowed the thermo-hygrometric characterization of the inner microclimate and the identification of the significant influence of the skylight on the temperature and relative

humidity values, causing sharp rises and falls during the daylight hours. In 2013 two corrective measures were implemented and evaluated subsequently through a second microclimatic monitoring campaign conducted at the museum.

The mudejar church of Santa Maria is located in Ateca, a town in the province of Zaragoza characterised by cold winters and warm summers. Given the low temperatures in winter, a heating system is used. The results of our analysis have shown that the heating system is turned on only for the celebration of Mass or religious festivities (half hour before the entrance of public at the church), causing extreme cycles of temperature and humidity, especially at the upper parts of the altarpiece due to the rising of hot air (hourly increase of 7 °C in temperature and a decrease of 11 % relative humidity) that are detrimental for the conservation of this artwork.

Index

Chapter 1

Introduction

Preventive conservation of archaeological sites is understood as the whole control process of the deterioration factors in order to prevent damage to the cultural heritage before it occurs and minimise future interventions [1].

Currently, preventive conservation measures are acknowledged as important for safeguarding cultural heritage (CH, from here on), both in terms of preserving CH and also reducing the cost of future conservation measures [2].

The practical application of a preventive conservation plan involves the study and control of the risks of deterioration. The objects are influenced by their environment, in terms of stress caused by physical agents such as temperature, humidity, radiation, and chemical agents (e.g., CO_2, SO_2, O_3, mineral salts, etc.), and creating sometimes harmful conditions for preservation [3] - [6]. Specifically, both abrupt changes and values of temperature and relative humidity (RH) outside the recommended ranges [7], can cause serious damage to the structure of objects, such as non-isotropic material deformation or detachment in materials of several layers. In hygroscopic materials, such as wood panels, which are the mainstay of many artworks, mechanical changes and deformations can occur [8]. In the case of frescoes, moisture and soluble salts are the very common causes of degradation; therefore an early detection of inadequate values of these physical parameters is essential to avoid this kind of damage [9]. In the case of closed or buried archaeological sites (hypogeum) under climate control systems, it is very important to control the operation of the latter, as well as to prevent harmful combinations of temperature and

relative humidity that may lead to the appearance of fungi (high temperature and humidity) or drying of the substrate.

It is important to characterise a cultural heritage site with a view to carrying out comparative studies in the future for its preventive conservation, either regularly, in order to verify whether the conditions are constant, or occasionally, when the boundary conditions are altered. It is also important after any change in the environment to first ascertain if the resulting microclimate is suitable according to the experience of other researchers and standards, and, secondly, if deterioration in the site occurs, to know the microclimate that has led to this phenomenon.

Currently, there is growing interest in monitoring the climatic parameters in cultural heritage [10] - [21].

The measurement of thermo-hygrometric parameters such as temperature and relative humidity (RH) is a priority [7]. Microclimatic conditions are routinely controlled in museums [22] - [27] given the importance of maintaining RH and temperatures within the recommended optimum intervals [7], which is easily achieved in most cases given the current technology of air conditioning systems.

Several works have also studied the indoor environment in churches [28], [29], [16], [18], which often contain valuable artworks. The control of microclimatic conditions inside these buildings is rarely a technical challenge, and undoubtedly the most complex problem consists of achieving an optimum conservation environment in open-air sites. In such cases, it is of interest to evaluate the effect of climatic parameters on the conservation of artworks in order to propose corrective actions.

Few works have studied microclimatic conditions in semi-confined [21],[17],[30] or open-air archaeological sites aimed at preventive conservation [12],[31].

The environmental monitoring is performed by a regular data collection, whose frequencies are typically between one datum every hour (1 datum/hour) or every day (1 datum/day) [22], [12].

Furthermore, regarding the characterisation of cultural heritage sites, it is necessary to install a microclimatic monitoring system comprised by several sensors in different locations at the place of interest. The registered data will provide information on different ambient conditions among these locations. The statistical analysis can be conducted by means of descriptive methods using summary statistics (e.g. average, median and variance). These methods are often applied in this context [12],[31],[32] as they are of simple application for curators and restorers. However, multivariate statistical tools like principal components analysis (PCA) or Cluster analysis are more powerful, but their application is not yet widely used in cultural

heritage. Notice that few studies have been published using PCA in microclimatic monitoring of cultural heritage [16],[18],[33].

This PhD dissertation deals with the data analyses of microclimatic monitoring data for characterising the microclimate and quantitatively assessing the effect of corrective measures implemented in three cultural heritage sites: Ariadne's house (Pompeii, Italy), l'Almoina archaeological site (Valencia, Spain) and the mudejar church of Santa Maria in Ateca (Zaragoza, Spain). The recorded thermo-hygrometric data is discussed through exploratory and multivariate techniques. Also, an efficient methodology of data analysis to obtain relevant results as simple as possible to be applied by curators and restorers is proposed. Furthermore, a proper experimental design is important, however it is not always possible to take into account the deficiencies of the design and employ techniques to overcome them taking advantage of our frequency of data recording, which is also of great interest.

The results of our studies have led to eight scientific publications in international journals indexed in the Journal Citations Report(JCR ®), all of which are inserted in the present document. The author of this PhD dissertation appears as first author of four of these publications, as second author of two articles, and as third or fourth author of two publications. The reason is that these works have been performed by a multidisciplinary research team, and in most cases all coauthors have contributed equally to the work. Actually, this remark ("all authors contributed equally to this work") has been indicated in the papers.

Since this PhD dissertation is composed by articles, we have tried to be as faithful as possible to the original structure and appearance of these. The reader is able to find some differences between the chapters of results due to the different format of the journals where the articles were published.

This PhD dissertation is structured as follows. The objectives of this work are explained in chapter 2. Following, the different papers (published in JCR indexed journals) are presented in separated chapters. Thus, chapters 3 - 6 deal with the detailed study of Ariadne's House in Pompeii, from the preliminary studies of microclimate and materials (Chapter 3), through the data analyses by descriptive techniques of the first (chapter 4) and second (chapter 5) monitoring campaign, and ending with a PCA analysis of the 2008 data (chapter 6). Chapters 7 and 8 deal, respectively, with the microclimatic characterisation of l'Almoina Archaeological Museum in Valencia and the subsequent evaluation of the corrective actions carried out. Chapter 9 shows the analyses of data recorded at the Mudéjar church of Santa Maria in Ateca and the effect of its heating system. On the other hand, improvements made in software Burrito implementing the methodology developed in this PhD dissertation are shown in chapter 10. Finally, chapters 11 and 12 deal

with the discussion of results and the conclusions respectively.

1.1. Ariadne's House in Pompeii (Italy)

Pompeii was a village of ancient Rome located about 26 km southeast of the modern city of Naples (Italy).

Around the year 62 AD, an earthquake severely damaged Pompeii and other nearby locations. Since then, the city was rebuilt until the eruption of Mount Vesuvius in 79 AD. Pompeii at that time had a population of about 15,000 inhabitants. The violent eruption of this volcano buried the city and preserved the ruins for centuries.

Thick layers of ash covered Pompeii and Herculaneum, both towns placed at the base of Mount Vesuvius. Their names and locations were forgotten until the 18th century when a new interest for antiquity led to excavations [34]. Herculaneum was rediscovered in 1738 and Pompeii in 1748. Since then, a campaign was launched to unearth both cities, revealing many intact buildings and valuable wall paintings. Pompeii offers a picture of Roman life in the first century. The forum, baths, many houses, and some villas remained in a surprisingly good state of conservation.

The site was declared World Heritage by UNESCO in 1997 and has become a popular tourist destination, with 2.5 million visitors in 2007. Pompeii is an open-air museum of 1,500 buildings comprising around 20,000 m^2 of mural fresco paintings [35]. Pompeian interior frescoes have become a main source of knowledge about Roman painting up to 79 AD, not because the city was so important at that time but because its tragic end has preserved in good conditions all its wall frescoes for posterity to study [36].

An imposed moratorium stopped excavations in the site to focus the efforts in maintaining the unburied ruins and leaving the remaining excavations for future generations. At present, the access to the ruins is more restricted for tourists, and less than one third of the houses open in the 1960s are currently available for public visits. This is due to the endless maintenance works to prevent the deterioration of buildings already unearthed [37]. Apart from ruin fallings, at least 150 m2 of fresco paintings and plaster works are lost every year due to lack of maintenance.

Ariadne's house is a Pompeian domus (i.e., a singlefamily house owned by the upper classes) situated in aprivileged location at the city center (Regio VII, insula 4). It is a domus of Hellenistic inspiration with an extension of 1,700 m^2. The house was

built at the end of the second century BC and was heavily damaged during the earthquake of 62 AD, not having been finished its reconstruction on the fateful date of Mount Vesuvius eruption [34]. Most inner walls of the house were originally decorated with frescoes.

Ariadne's House was excavated between 1832 and 1835 and during the 19th century it was one of the most famous and visited Pompeian houses, later to sink into oblivion afterwards [38]. A 3-D view of the place obtained from a photogrametric scan of the whole ruins [39] shows the remarkable quality of some wall paintings. Detailed pictures of all lodgings in Ariadne's house are available [40]. The complete pictorial collection of Ariadne's house has a remarkable quality and was probably created by the same artists' team. Although most interior walls were originally ornamented with frescoes, the paintings have suffered severe damages since the excavation of Ariadne's house in 1832-1835.

Pompeii has been preserved in an enviable conservation state under the layers of ash, but most buildings suffered serious damages during the volcanic eruption and the majority of roofs came down. An aerial view (http://maps.google.es) of Ariadne's house (40° 44' 57.77" N, 14° 29' 14.37" E) and nearby buildings reveals that they are well preserved but the roof is lacking in most of them.

This is the case of Ariadne's house, with only one room (marked as 4 in Figure 4.1) partly covered with a roof of ceramic tiles (14 m^2) that was settled in the 1950's. After a preventive actuation in the 1970s, roofs made of transparent polycarbonate sheets supported by metallic structures were established in three rooms of the house (1, 2 and 3 in Figure 4.1) in order to protect the frescoes inside from rainwater. During the following decades, mural frescoes in all rooms that had been left uncovered were seriously damaged due to direct contact with rainwater and the unfavorable thermohygrometric conditions mainly during the summer [34]. Room 2 is comprised by four walls, the northwest one with a large window and a doorway in the SW wall. As a result, the indoor microclimate is more isolated from the outside environment compared with the other rooms under study that are delimited by three walls. Rooms 1 and 3 are open to the courtyard by their NE side. Room 4 is open to the atrium by its west side. It is the largest one and has only one wall decorated with frescoes that presents a semicircular shape (Figure 4.1).

Room 3 (exedra, coded as lodging 18 in [40]) displays a mosaic of Hellenistic inspiration on the floor (84 × 77 cm) protected with a glass box. The mosaic is probably from the second century BC, and the rest of the floor is paved with tiles of a different style (first century AD). The mosaic is covered with a box composed by five glass sheets of three millimeter.

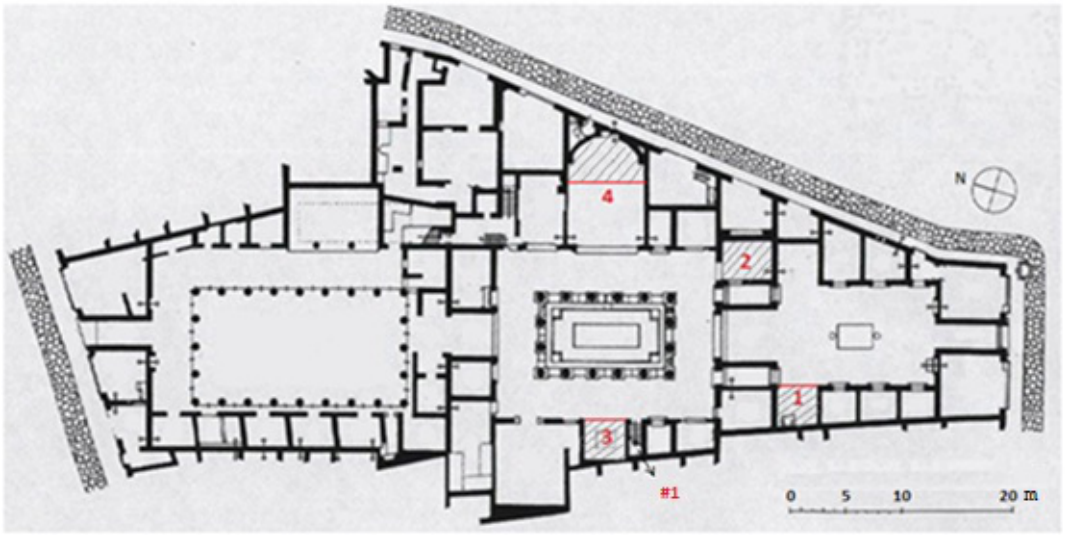

Figure 1.1: Plan of Ariadne's house. Lodgings marked as 1 to 4 are the only roofed ones (parallel tilted lines delimit the covered area). Data-logger ♯1 was located on the top of an outside wall next to room 3 at 3 m from the ground level and it was covered with a ceramic tile.

Between 2004 and 2008, a multidisciplinary team led by the Archaeological Research Section of the City of Valencia, in collaboration with a number of researchers linked to different scientific institutions, carried out 18 surveys from one extreme to another of Ariadne's House finding archeological remains from all of the periods of the house [41].

The main problems affecting Ariadne's house are biological colonization (superior plants and animals) and water problems caused by rains due to the long absence of a roof. In 2010 the transparent polycarbonate sheets were changed for an isolated non transparent roof as consequence of the results described in this PhD dissertation.

1.2. L'Almoina Archaeological Museum (Valencia, Spain)

The city of Valentia (Valencia, Spain) was founded by the Romans in 138 BC, and the exact founding point where the city started is located in Plaza de l'Almoina. Evidence of Roman settlement can still be seen in the excavated remains of the Romanforum and baths [42].

Figure 1.2: Archaeological remains of l'Almoina Archaeological Museum (Valencia, Spain).

The l'Almoina Archaeological Centre (Valencia, Spain) comprises an area of about $2,500\ m^2$. It houses the archaeological excavations performed between 1985 and 2005 in the city of Valencia [43]. This work has led to the discovery of several monumental buildings, inscriptions, loose architectural elements, more than $1,000$ coins and 500 exhibition quality ceramic pieces [44], and has also given rise to a vast body of technical documentation.

The most interesting facet of this site is the buildings, a continuous overlapping of constructs, forming a complete and well-preserved compendium of history and urban development of the city of Valencia from its founding to the present. Among them, we find the Islamic Alcazar [45], the first city (the Republican) represented by the thermals [46], the remains of the Roman Empire (the forum and the Curia) [47], [48], and martyrdom and Episcopal area from the Vizigothic stage [48], [49].

An intervention was conducted in the years 2005-2007 for the development and construction of the Archaeological Centre. To protect the ruins, a concrete structure adapted to the unique archaeological site was built. In addition, a glass cover (25

Figure 1.3: Plan of the archaeological remains in the Museum of l'Almoina.

× 25 m) was installed, which allowed passers-by a glimpse of the archaeological remains.

L'Almoina is an archaeological museum located in a building about 3 m below the current city sidewalk level. The archaeological remains are covered by a concrete structure, which forms an elevated plaza above the sidewalk. This cover connects with sidewalks through steps with different heights along its perimeter due to the slope of the sidewalk. There is no vertical retaining wall inside the museum to isolate the remains from water diffusion through capillarity from the surrounding areas.Preventive conservation of the archaeological site at Plaza de l'Almoina includes maintaining stable and adequate temperature and relative humidity levels and managing light exposure, among others.

In early summer 2013, water leaks from the skylight occurred, dripping onto the archaeological site. As an initial solution, Valencia City Council, which manages the archaeological site, eliminated the water from the skylight to prevent further leaks.

Later, in August, the City Council placed a waterproof canvas over the skylight, preventing rainfall leakage and the direct impact of sunlight.

Moreover, in the year 2011 a water ditch built with porous bricks passing near the archaeological site [50] was substituted by a 110 mm PVC pipe.

1.3. Mudéjar church of Santa Maria in Ateca (Ateca, Spain)

Ateca is a village in the province of Zaragoza in the Autonomous Community of Aragon (Spain). Located at the southwest of the province, at the confluence of the rivers Jalón and Manubles, Ateca is at 606 m above sea level (Latitude: 41Â°19'51" N, Longitude: 1Â°47'36" O) [51].

In the village centre there stands the mudejar parish church of Santa María. Mudejar is a style of Iberian architecture and decoration, particularly in Aragon and Castile, dating to the 12th to 16th centuries and strongly influenced by Moorish taste. In contrast to other churches of the same period, mudejar churches are mainly made of brick and plaster, instead of ashlar stone [52]. Santa María of Ateca is a temple of a single nave, a seven-sided polygonal apse and chapels between the buttresses. It has a square tower and two sections, minaret structure with stairs covered by barrel vaults and simple ribbing. The tower was built during the second half of the thirteenth century while the mudejar church was constructed in the fourteenth century.

The altarpiece (Figure 9.1.b) develops the most important events in the life of the Virgin Mary, and was made between 1650 and 1657. The author of the relief was Martin of Almunia, from Ateca. Bernardo Ibañes was the author of the sculptures, and they were polychromed by Juan Lobera and his sons Jusepe and Francisco Lobera [53].

Ateca features an extreme climate, with a mean daily RH between 91.97 % and 11.94 % and a mean daily temperature between 38.48 Â°C and -5.59 Â°C. Therefore, a single heating strategy is adopted. The church is heated rapidly, shortly before and during services, to a more comfortable temperature [54], [55] with a hot air heating system through the floor of the church.

The vault had repainting and detachment problems. Thus, in 2011, a restoration work performed by the company Albarium S.L. began. It was decided to implement

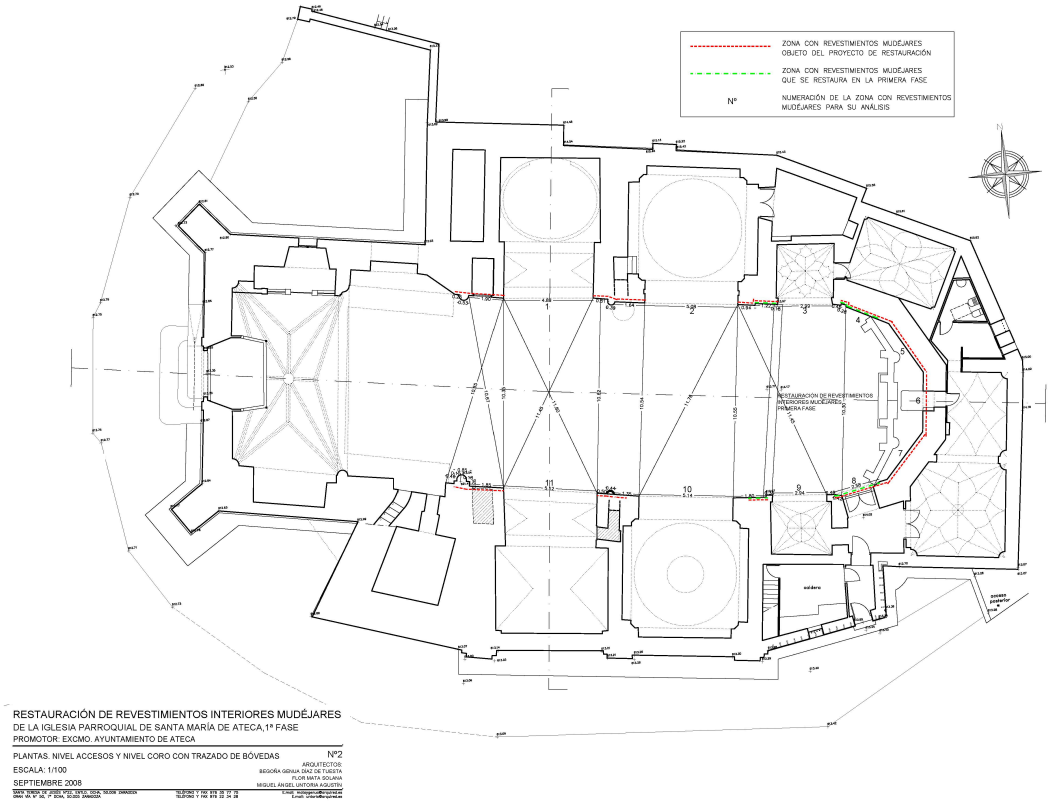

Figure 1.4: Plan of mudejar parish church of Santa María, Ateca. Choir level with plotting of vaults.

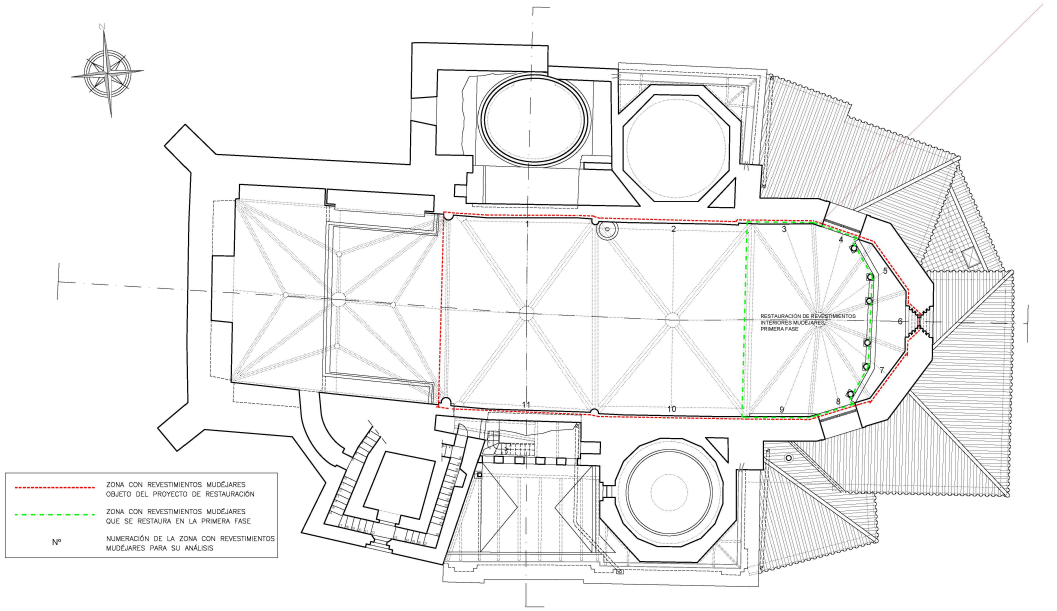

Figure 1.5: Plan of mudejar parish church of Santa María, Ateca. Entrances level.

a monitoring system for recording a full year of data of the physical parameters involved in conservation.

Chapter 2

Objectives

The lack of previous studies about microclimatic monitoring with high frequency data collection and a detailed analysis methodology hinders a proper and quantitative assessment of thermo-hygrometric conservation conditions of cultural heritage. Therefore, this PhD dissertation aims to characterize the microclimate and quantitatively evaluate the effect of corrective measures implemented in archaeological and cultural heritage sites of significant interest from a multivariate approach, using the most appropriate statistical analyses applied to thermo-hygrometric data collected with greater frequency than 1 data/hour through a system specifically designed for this purpose.

The following general and specific objectives arise:

- **O1**[1]: Study the background of monitoring thermo-hygrometric parameters applied to preventive conservation of cultural heritage.
  - **O1.1**: In semi-confined archaeological sites.
  - **O1.2**: In underground archaeological remains.
  - **O1.3**: In churches.

[1] Although this is not a typical objective, as implicitly any scientific study requires a preliminary study of the literature, being an article thesis we have tried to specify that the background has been divided into the various works that compose the dissertation as is justified in chapter 11.

- **O2**: Characterize the microclimate conditions at Ariadne's House (Pompeii, Italy) using multivariate statistical techniques such as principal component analysis (PCA).
  - **O2.1**: Discuss the most suitable data pre-treatment for the detection of anomalous trajectories.
  - **O2.2**: Perform a division of the monitored period using CUSUM charts.
  - **O2.3**: Characterise the different rooms using PCA, identifying differences between heights, orientations and type of roof.
  - **O2.4**: Provide a physical interpretation to the PCA components.

- **O3**: Characterise and analyse the effects of the heating system in the mudejar Church of Santa María (Ateca).
  - **O3.1**: Characterise the microclimate inside the church and around the Altarpiece.
  - **O3.2**: Quantify the effects of the heating system on temperature and RH.
  - **O3.3**: Determine when the heating effects are more pronounced and their hourly evolution.

- **O4**: Propose a methodology for data analysis that can be applied by curators and non-experts in statistics for the characterization of cultural heritage sites.
  - **O4.1**: Combine descriptive techniques like mean trajectories or bivariate plots.
  - **O4.2**: Compare the obtained results with those obtained by simpler techniques.
  - **O4.3**: Compare the results with those obtained by more complex techniques.

- **O5**: Implement the developed methodology in software capable of managing microclimatic monitoring data.

- **O6**: Propose corrective measures from the results of the data analysis methodology proposed, serving as an example for other cultural heritage sites in the future.
  - **O6.1**: Ariadne's house (Pompeii, Italy)

  - **O6.1.1**: Characterize the monitored rooms and quantify differences between orientations, heights and roof type using the proposed methodology.
  - **O6.1.2**: Propose the most suitable corrective actions.

- **O6.2**: Archaeological Museum l'Almoina
  - **O6.2.1**: Characterize the different areas of the museum and quantify differences between heights, type of cover and proximity to groundwater using the proposed methodology.
  - **O6.2.2**: Propose appropriate solutions.

- **O7**: Analyse the corrective actions taken in Ariadne's House (Pompeii) and the archaeological Museum of l'Almoina, using the proposed methodology.
  - **O7.1**: Ariadne's house (Pompeii, Italy)
    - **O7.1.1**: Characterise the monitored rooms after the corrective action, using the proposed methodology.
    - **O7.1.2**: Determine whether the new microclimate suits the recommendations of the international standards.
  - **O7.2**: Archaeological Museum l'Almoina
    - **O7.2.1**: Characterise the different areas of the museum and quantify the variation after the corrective action, using the proposed methodology.
    - **O7.2.2**: Determine whether the new microclimate suits the recommendations of the international standards.

Chapter 3

Ariadne's house (Pompeii, Italy) wall paintings: A multidisciplinary study of its present state focused on a future restoration and preventive conservation

Ariadne's house (Pompeii, Italy) wall paintings: A multidisciplinary study of its present state focused on a future restoration and preventive conservation. Pérez, M.C.; García-Diego, F. J.; Merello, P.; D'Antoni, P.; Fernández Navajas, A.; Ribera i Lacomba, A.; Ferrazza, L.; Pérez Miralles, J.; Baró, J.L.; Merce, P.; D'Antoni, H., Curiel Esparza, J. *Materiales De Construcción* 2013, Vol. 63 (311), 449-467

ABSTRACT: This paper deals with the development of a multidisciplinary study on the current state of conservation of Ariadne's house (Pompeii, Italy), a domus of great archaeological value. The aim of this study is to undertake the preventive conservation actions required and increase the knowledge about its conservation and to generate discussions and points of view for a future restoration. Environmental studies, electromagnetic radiation measurements, study of materials and a photographical study were carried out. Those studies revealed that the rooftops covering the analyzed rooms resulting in adverse weather conditions causing grave damage to the conservation of the wall paintings.

Thus, between 2009-2010 the rooftops were changed and new environmental studies were conducted. Studies of materials showed that the paintings match in execution and composition with those reported by other authors.

The salts from modern mortars from previous restorations were affecting frescoes, also it is described a thin grayish surface layer from environmental contaminants.

Keywords: Pompeii; preventive conservation; materials; environmental monitoring; photography.

3.1. Introduction

Ariadne's House or "dei Capitelli Colorati" is located in the "Regio" VII, insula 4 (Pompeii, Italy), in a privileged location at the center of the city, less than 100 meters from the forum. With 1700 m^2 it is one of the biggest stately domus of the private Pompeian architecture [41].

Ariadne's House was excavated between 1832 and 1835 and during the 19th century it was one of the most famous and visited Pompeian houses, later to sink into oblivion afterwards [38].

The rooms considered in this work are: numbers 1, 2, 3 and 4 (Fig. 3.1). These four rooms are decorated with mural paintings from the first to the fourth Pompeian style [41].

During the 1970´s a rooftop consisting of a metallic structure holding transparent polycarbonate sheets was installed on three rooms of the house (coded as rooms 1, 2 and 3 in Fig. 3.1).

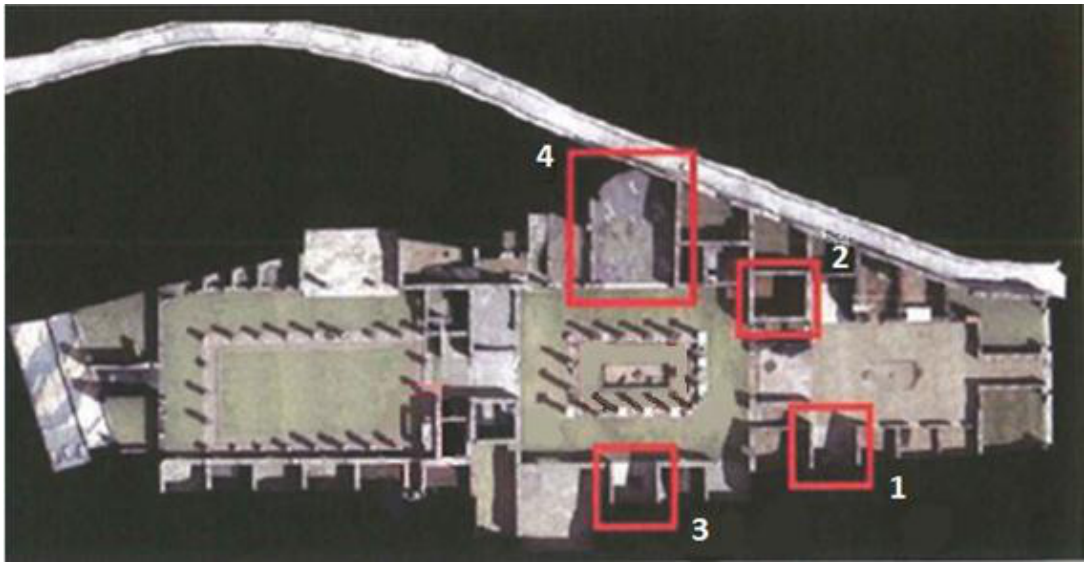

Figure 3.1: Plan of Ariadne's house. This map was made by the City Council of Valencia.

In 2010 the transparent polycarbonate sheets were changed by an isolated non transparent roof. Room 4 (Fig. 3.1) is partially covered with a tile rooftop.

In room 3, there is a mosaic as a central emblem of the plan of the room. The Hellenistic tradition mosaic measures 84×77 cm^2. It is thought to have been made within the late 2^{nd} century BC or at the beginning of 1^{st} BC. The floor of the rest of the room is formed by a different, more modern, paving from the 1st century AD. The mosaic is covered with a box composed by five glass sheets of three millimeter.

Between 2004 and 2008, a multidisciplinary team led by the Archaeological Research Section of the City of Valencia, in collaboration with a number of researchers linked to different scientific institutions, carried out 18 surveys from one extreme to another of Ariadne's House finding archeological remains from all of the periods of the house [41].

The main problems affecting Ariadne's house are biological colonization (superior plants and animals) and water problems caused by rains due to the long absence of a roof.

During the last decades, an increasing interest in all areas of conservation with an multidisciplinary approach has been developed. Preventive conservation, as a method of work, aims to control the state of conservation of the artwork before the

deterioration occurs. Currently, preventive conservation measures are acknowledged as important for safeguarding cultural heritage (CH, from here on), both in terms of preserving CH and also reducing the cost of future conservation measures [2].

In the case of wall paintings, the deterioration process is determined by factors such as petrographical and chemical characteristics of the materials, presence of mineral salts and organic substances on the surfaces, air pollution, sunlight, temperature, water content of the surface, etc. [56]. Hence, preventive conservation requires knowledge of a set of parameters connected to a specific CH site, including microclimatic conditions [57], mineralogical, textural, petrophysical, and durability characterization studies of mortars. In our case, as documented in the literature on outdoor stone because it is difficult to find frescoes in these conditions [58], other biological factors such as cyanobacteria, lichen, etc., are negligible in front of the above mentioned factors.

The study of the techniques originally used is essential for conservation and restoration, is required in order to understand the original and added materials present both on the surface and within the painting's stratigraphy [59]-[62].

In addition, analytical results can improve a conservator's overall awareness of deterioration processes and mechanisms that influence the condition of wall paintings in general [63], [64] providing necessary data for a future restoration [65], [66]. It is known that external wall paintings are especially affected by changes in temperature and humidity, deteriorating phenomena associated with soluble salts, microbiological activity, or damage due to vandalism, iconoclasm and tourism [64]. In many cases new mortars, whether due to their soluble salt content, their greater mechanical resistance or their different physical properties, had a negative effect on the conservation of CH [67].Therefore, different studies are needed before a restoration begins in order to know which kinds of phenomena are affecting the artwork.

The objective of this paper is to document the conservation conditions and the causes of deterioration of the wall paintings of Ariadne's house to develop a future restoration trying to prolong its conservation as much as possible.

Multidisciplinary studies were developed prior to intervention, including environmental studies, measurements of electromagnetic radiation, study of materials used in the execution of the paintings and in recent restorations that could generate the appearance of salts, as well as a photographic study.

Specifically, the goal of materials analysis techniques will be twofold, on one hand the characterization of the wall paintings in order to proceed to the comparison with the extensive existing literature on the subject [59], [68], [69], on the other

hand the differentiation between the original materials of the work and added ones in successive conservation interventions, studying the phenomena of degradation of the original materials of the wall paintings, and interactions with the new ones, as in the case of the problems caused by the crystallization of salts [70], [56].

3.2. Materials and methods

3.2.1. Environmental study

The application of temperature and RH sensors permits for a full, accurate and secure monitoring of the environmental conditions and allows for the prediction of physicalchemical mechanisms of degradation, as well as of the most suitable procedures for controlling them [71].

In order to perform an environmental study, 26 probes were placed, each one containing a temperature and a relative humidity (RH) sensor. One of these probes was placed outside of the house serving as a control.

Each sensor was developed by Maxim Integrated Products, Inc. (Sunnyvale, CA, USA). RH was recorded by a DS1923 with an accuracy of ± 5 %RH, and temperature by a DS1922L with an accuracy of ± 0.5 °C. RH sensors were calibrated prior to their installation as described in [18].

Two environmental studies were performed. The first one was performed between 2008 and 2009 (from 7/23/2008 to 7/30/2009) and since the most conflicting data appeared in summer, the second study was conducted within the summer of 2010 (from 7/15/2010 to 10/16/2010), to evaluate the consequences of the rooftop change performed. The data are taken every half an hour.

On the other hand, microclimatic studies have been combined with infrared thermography in order to complete the results obtained. Infrared thermography is a technique that allows us, at certain distance and without direct contact, to measure and display with an infrared sensor the infrared radiation emitted by an object [72]. The camera used is a NEC Corporation (Tokyo, Japan) TH9260 with an infrared matrix of 640x480 pixels, a resolution of 0.06 °C and a spectral range from 8 to 14 μm.

3.2.2. Electromagnetic radiation measurements

Electromagnetic radiation measurements are particularly useful for the control of archeological monuments [73].

CCD spectrometers allow in situ investigation on artworks and the measurement of harmful agents related to electromagnetic radiation wavelengths [73], [74].

In this work, the measurements were carried out by a portable spectrophotometer. Relative reflectivity calibrated to Munsell's White 9. A computerized xenon light source that emits in the 200 to 1100 nm range (traceable to the U.S. National Institute of Standards and Technology, NIST) was used to illuminate the target points. An advanced CCD grating spectrometer consisting of a SONY ILX511 detector with 2048 pixels was used to measure normal (90°) reflectivity in the 220 to 850 nm range. The signals were collected by 1860 pixels of the 2040 linear array, with 0.37 nm mean resolution and stray light correction.

All the components of the equipment worked according to specifications when tested in the Plant Science Laboratory of NASA Ames Research Center in California, using a calibrating light source "seasoned" at the NIST. Throughout the investigation a portable calibrating device was used to verify the wavelength calibration. No new adjustments were needed.

3.2.3. Study of materials

The observations and stratigraphic analysis of samples of wall paintings from Pompeii have been performed with optical microscopy and scanning electron microscopy. The optical microscope is from NIKON Corporation (Tokyo, Japan) ECLIPSE 80i with a DS-Fi1 camera. Samples have been observed in reflected light at magnifications ranging from 5x to 50x. The scanning electron microscopy with microanalysis (SEM-EDX) was performed with a scanning electron microscope of variable pressure from Hitachi LTD (VP-SEM) S-3400N, equipped with energy dispersive X-ray spectrometer (EDX) by Bruker Corporation XFlash ® with Silicon Drift Droplet detector (SD3), supra light element window/8 μm Dura-Beryllium window, and an energetic resolution of 125 eV. With working conditions: accelerating voltage 20 kV, measuring time between 30 and 100 s, working distance 10 mm. This research has been performed taking small samples of different materials from the mortars and pictorial layers of frescoes, which have been included in a bi-component polyester resin of self-curing (Presi, MECAPREX SS) and prepared in cross section. This preparation allows for observations and elemental chemical analysis of the strati-

graphic sequence of each sample and the observations of appearance, texture, grain size, thickness and color observations of each layer [75], [76].

The identification of different crystalline phases has been performed by X-ray diffraction (XRD) by the method of crystalline powder method. XRD data were obtained with a Bruker Corporation (MA, USA) D4 Endeavor AXS diffractometer, with Cu Ka_1 radiation. The measures were taken with 40 kV and 20 mA, in a range of 15-70th (2θ), a step of 0.05^{o} and a collection time of 1.5 s.

For the analytical of mortars a Fourier transform infrared spectrometer (FTIR) from Bruker Corporation Vertex 70, in the range 4000-400 cm-1 with a resolution of 4 cm-1 was used. Sample tablets were prepared (diameter 13 mm), pressed by dry potassium bromide (1 mg/100 mg KBr) at a pressure of 10 tons for 4 minutes in vacuum.

3.2.4. Photography

The digital treatment of images has been widely used in many different fields, as for instance, astrophysical, medical, geographical and military research. In the last years, digital elaboration of the images has also been used in the field of CH conservation [77]. In fact, professional photography specialized in art and restoration, gives a new vision for scientific photographical documentation [78].

A digital camera Hasselblad USA Inc. (WA, USA) with a 55 x 41 cm CCD of 6496 x 4872 pixels was used. The shots were taken with a shutter speed of 1/125 and f16 or f11 aperture. The number of taken images taken exceeds 700.

As the solar light falling on the paintings is inadequate and provides very low quality results, in this study we used a Bron Elektronik AG (Allschwil, Switzerland) Broncolor Verso A4 with a diffusing screen and fully protected from UV radiation.

The flashes were placed approximately two meters away from the object at an incident angle of 45 degrees.

False-color infrared (IR) photographs were taken by a SONY Corporation (Tokyo, Japan) camera, model DSC-F828 equipped with a Super HAD CCD. This camera is capable of removing the visible filter (IR-cut filter).

To obtain a false-color infrared photograph a modified [79] technique has been used. The blue channel was substituted by a new channel from IR photography. This technique is widely used [80].

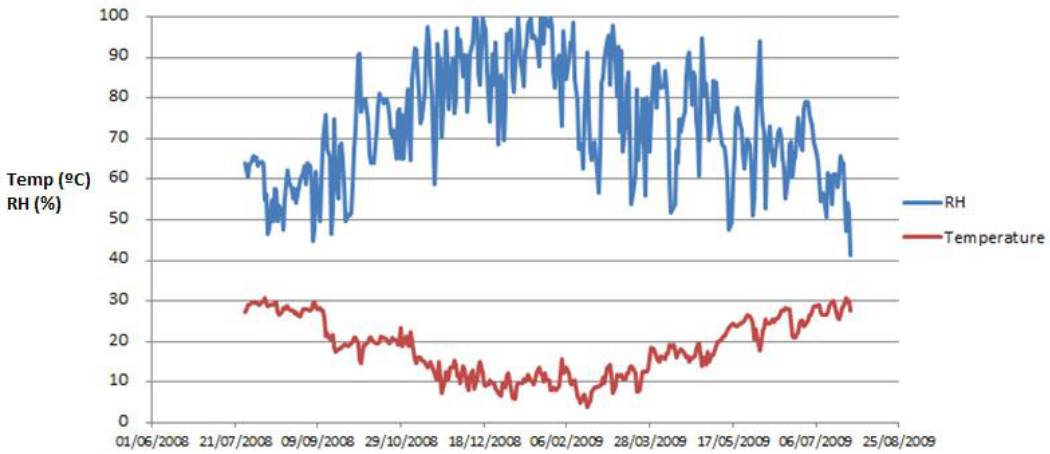

Figure 3.2: Ariadne's house daily values of outdoor temperature and RH from 07/23/2008 to 07/30/2009.

3.3. Results and discussion

By combining different methodological approaches (studies of environmental conditions, study of materials, photography, etc.) it was possible to determine the main problems affecting Ariadne's house for preventive conservation and for a future decision of the most convenient techniques of restoration to be used [81].

3.3.1. Environmental study

The roman city of Pompeii presents an extreme weather (Fig. 3.2), with big fluctuations between night and day, in summer 2008 an average of 15 % for RH and 6.5 °C for temperature.

Abrupt weather fluctuations are detrimental to conservation since extreme changes produce deterioration [82].

As an open-air archaeological site, the outdoor climate determines the climate of the rooms, thus, the technical actions should aim to cushion these jumps, smoothing the maximums and minimums for a uniform environment whenever possible.

Exploratory analysis performed in 2008-2009 showed that different microclimates occurred in the rooms depending on the covers and roofs used. A microclimate for

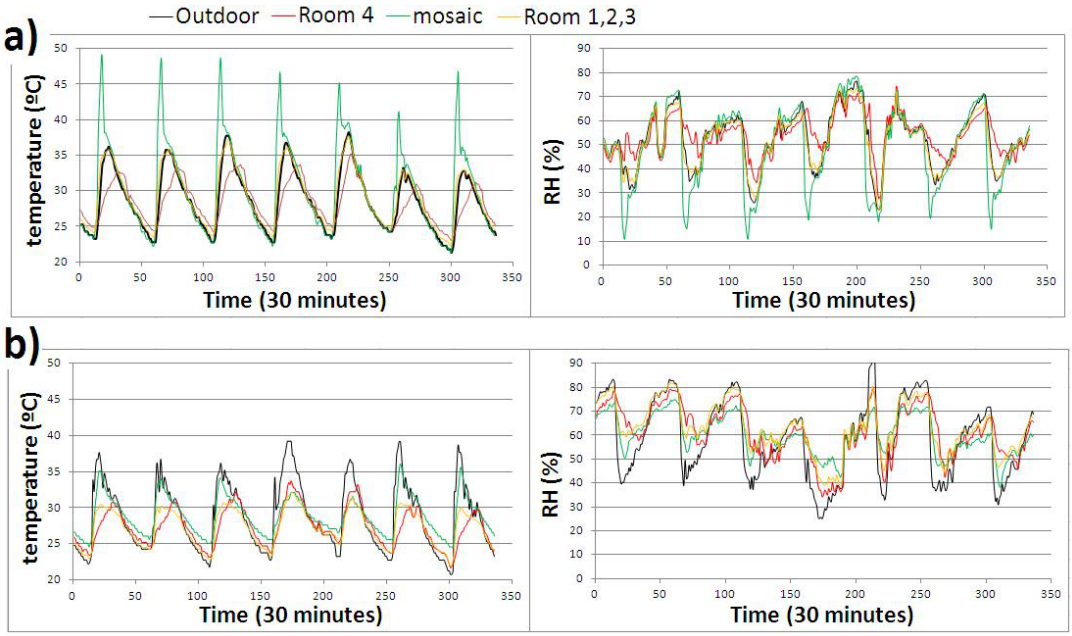

Figure 3.3: Comparison of values of temperature (ºC) and RH (%) of a summer week in a) 2008 and b) 2010, for the different microclimates of Ariadne's house. Time 0 corresponds to August 11th 2008, 00:00 hours. Data every half hour.

the tile roof (room 4, Fig. 3.1), another for the polycarbonate covers (rooms 1, 2 and 3, Fig. 3.1) and yet another for the glass cover (mosaic) were detected (Fig. 3.3.a). The opaque cover (room 4) configured a suitable microclimate in summer, dimming the exterior climate changes, both in temperature as in RH. During winter it had a similar effect, but of less intensity.

However, the transparent polycarbonate cover (rooms 1, 2 and 3, Fig. 3.1) produced a greenhouse effect, with similar weather parameter values to the outdoor microclimate (Fig. 3.3.a).

Finally, the glass coverage of the fish mosaic provides the most damaging conditions of all micro-climates due to large variations in temperature and RH (Fig. 3.3). It is advised not to put this covering on the mosaic since it is protected from rain by the roof of the room.

After having these results, decisions for solutions were taken in order to palliate the effects of this kind of covers.

Thus, a rooftop change was performed in rooms 1, 2 and 3 where opaque covers

were installed. Environmental conditions further away from those recommended in the standard UNI 10829 [83] for the conservation of frescoes appeared in summer, when abrupt day/night temperature shifts as well as in RH appeared.

Thus, in order to evaluate the effects of the roof change, a second microclimate study was performed only for the summer months in 2010. The obtained results from exploratory analysis show how temperatures and RH have suffered a positive variation from summer 2008 to summer 2010 as a consequence of the rooftop change performed.

In 2010 the average temperature in the room decreased with respect to the outside, due to the decrease of the maximum temperature (Fig. 3.3.a). Also in 2010, the RH increased on average with respect to the exterior, due to the increase of the minimum. Temperature and RH have stabilized, reducing its variability and smoothing those extreme daily changes. On the other hand, in 2010 the main differences between microclimates obtained in 2008 for RH and temperature have disappeared (Fig. 3.3).

On the other hand, the use of a complementary technique, thermography, allowed us to assess the changes obtained with the new roofs. The results have shown that changing the rooftops has generated a substantial modification in the temperature gradient and values of the rooms (Fig. 3.4), as well as the microclimatic study showed.

Thermography has an advantage over the data-loggers since it allowed evaluating areas with lower temperature due to evaporation of water or problems such as cavities or uprisings.

Summarizing, the environmental study has allowed us to acknowledge the detrimental microclimatic conditions in Ariadne's house rooms, providing an adequate solution (change of roofs). Also it has been possible to evaluate the positive consequences of changing the rooftops (Fig. 3.4). We can see that the difference in temperature gradient in summer 2008 is 22 ^{o}C, while in 2010 this gradient is reduced to about only 7 ^{o}C.

Note that if a roof change had not been performed a future restoration would have been useless.

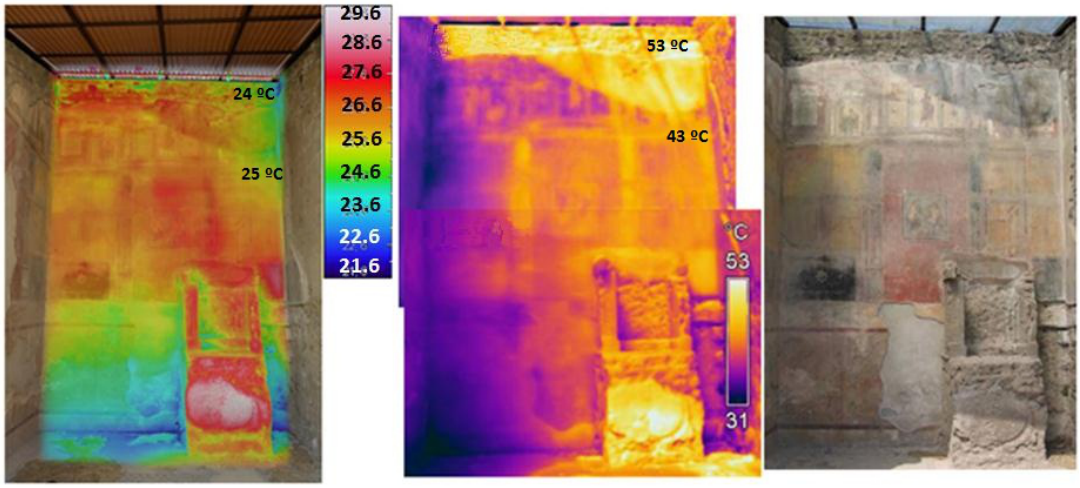

Figure 3.4: Room 1, from left to right: 2010 thermography, 2008 thermography, 2008 real image (room 1). These figures show the roof change performed and its subsequent benefits on temperature.

3.3.2. Electromagnetic radiation measurements

The murals in Ariadne's house in Pompeii are exposed daily to the sunlight. Considering the possible damages of this electromagnetic radiation to the paintings, particularly ultraviolet, measurements of solar radiation and of filters have been taken in the different rooms of the house.

As mentioned, polycarbonate rooftops were installed on rooms 1-3 (Fig. 3.1) of the house where frescoes cover the walls from top to bottom. Some areas of the frescoes are exposed to direct sunlight, because the rooftops not cover completely the artworks. Furthermore, the filtering properties of the polycarbonate change over the years losing the capacity to absorb some of the harmful radiation and transparency to the visible light [84].

The effectiveness of the installed filters was measured and they were compared with others that were considered as possible options to protect the paintings, such as different types of acrylic filters.

We considered filters such as Reflectiv (Bonneuil sur Marne, France) SOL 259 interior, which is a 36 microns polyester film that has smoke color. It blocks 95 % of the Ultraviolet radiation without canceling the visible light with an 11 % transmission, which allows for daylight viewing with a reduction of the greenhouse effect and a blockage of the UV radiation. Another filter considered was the UVA 109 filter that

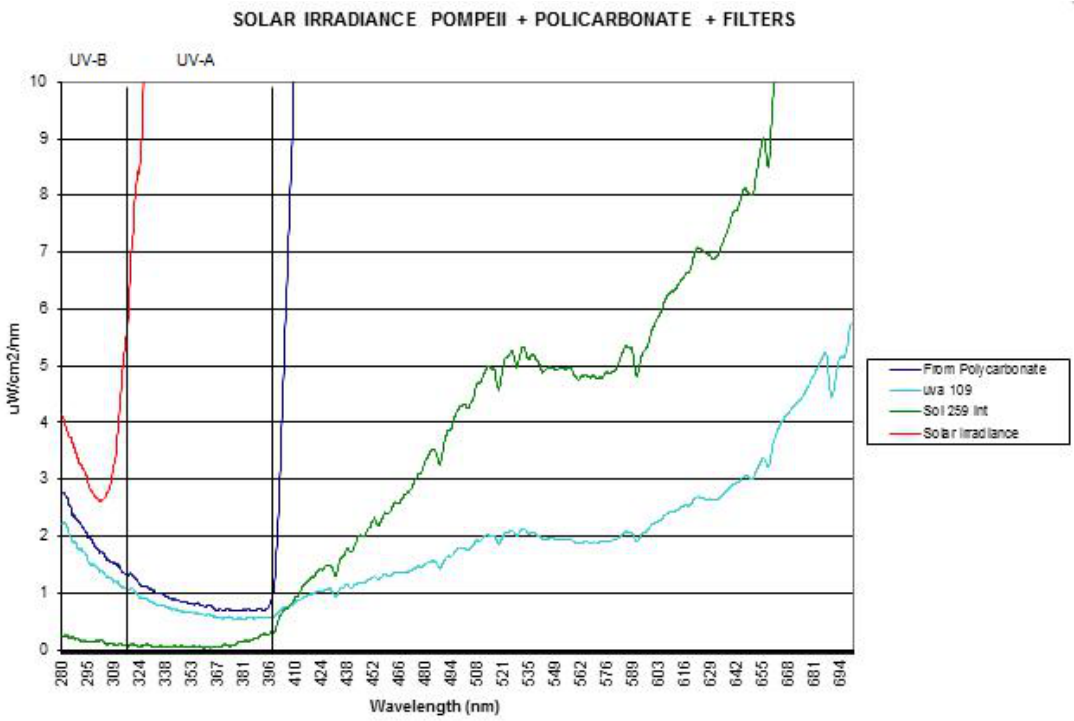

Figure 3.5: Comparison of the effectiveness of polycarbonate and polyester filters (Sol 259, UVA 109) under the influence of solar radiation. All these filters are efficient, but Sol 259 has the best filtering properties in the Ultraviolet band (280-400 nm) while it is the most transparent to the visible light.

has similar characteristics and is also a 36 micron polyester film, but it has the advantage that it blocks UV radiation up to 99 % and is also more transparent to visible light, allowing 73 % transmission.

The analysis (Fig. 3.5) shows that the polycarbonate absorbs/reflects a great portion of Ultraviolet, but this is further enhanced when another filter is added. Polyester filters do not block enough the harmful solar ultraviolet radiation.

If these filters were replaced by a non-transparent roof, such as wood or tiles, the harmful radiation reaching the paintings from the roof would be close to zero.

In turn, some areas of the frescoes are exposed to direct sunlight, because the rooms have large outdoor vertical openings. Results without filters at 12:30 PM in summer were: 6 $\mu W/cm^2/nm$ of Ultraviolet B at 280 nm and 9 $\mu W/cm^2/nm$ at 319 nm. In the UV-A band 10 $\mu W/cm^2/nm$ at 322 nm and 48 $\mu W/cm^2/nm$ at 390 nm.

Considering that the UV must be as close to cero as possible, these data showed the necessity of using a solar filter to preserve the paintings.

The data obtained in this work shows a considerable amount of solar radiation that bathes the frescoes in Ariadne's house. Therefore, as a conclusion of this electromagnetic radiation study in coincidence with other techniques applied in the present work, the polycarbonate roofs are affecting the wall paintings preservation.

3.3.3. Study of materials

Below the results from the stratigraphic layer outermost to the innermost are showed.

First, note that the polychrome surface is affected by the presence of a thin layer of diffuse grayish hue. The SEM-EDX analysis has identified compounds based on calcium sulfate and silicon compounds, aluminum and potassium, elements usually present in the volcanic soil of sedimentation and pollutants from the environment of the archaeological site of Pompeii [85].

Secondly, by optic microscopy, a study of the layers of paint was performed. It was determined that the thickness of the paint layers is not regular; it varies from a minimum of 10-20 microns to a maximum of approximately 110 microns. In the SEM-EDX study of the paint layers (Fig. 3.6) was also detected the presence of calcium. Elements attributed to the use of lime (carbonation of fresh mortar or mixture of water lime with pigments) that appeared constantly in the samples.

The studies described above have identified the various layers of preparation, allowing to demonstrate that some paintings were executed with the painting technique "al fresco" and others with the technique "al secco" [86]. The identified pigments are shown in Table 3.1.

Third, the results of stratigraphic and mortars studies using instrumental techniques such as optical microscopy, scanning electron microscopy analysis with microanalysis (SEM-EDX) and X-ray diffraction (XRD) show that the wall paintings have a stratigraphy composed of at least 3 layers of mortars of different thicknesses (Fig. 3.7), on which lie the layers of polychromy.

The lower layer of gray mortar (*arriccio*) identified, is made with a white binder of calcium carbonate, and silicate-based aggregate of hydrates of aluminum, silica, iron oxide, potassium, sodium and magnesium (*pozzolana*).

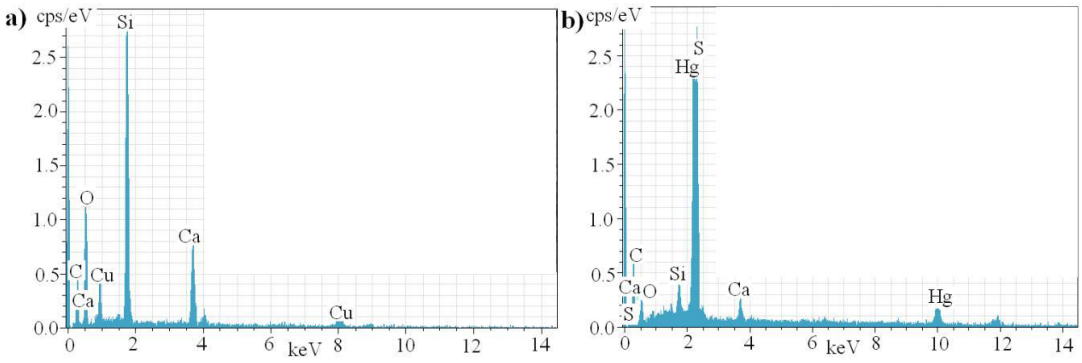

Figure 3.6: SEM-EDX study of the paint layers: a) Microanalysis detecting the presence of calcium, copper and silicon, that suggest the presence of copper silicate (Blue Pompeii or Cearuleum). b) Microanalysis detecting the presence of mercury and sulfur that suggest the presence of cinnabar (Red Pompeii or minium).

Color	Old name	Composition
White	*Creta calcarea*	Calcium carbonate
Yellow	*Ochra*	Yellow ochre iron hydroxide base
Red	*Rubricae*	Red Ochre based on iron oxides with Si, Al, Ca and Mg
	Minium	Cinnabar
Green	*Creta viridis*	Green earth from clay colored by iron silicates
Blue	*Caeruleum*	Egyptian blue based on copper and calcium silicate

Table 3.1: Pigments identified in the wall paintings of Ariadne's House in Pompeii.

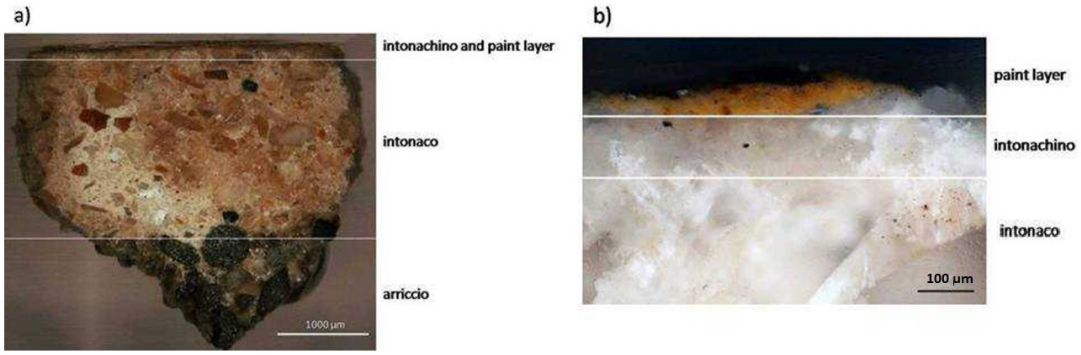

Figure 3.7: a) Cross-section obtained with optical microscopy (2x). b) Cross-section obtained with optical microscopy (50x). The different layers of mortar and the yellow paint layers are observed. From top to bottom, paint layer, *intonachino*, *intonaco* and *arriccio*.

Successive layers of mortar are presented in white color (*intonaco* and *intonachino*), prepared with a calcium carbonate binder and arid formed by calcite, with minor amounts of quartz, ferrocalcite, dolomite calcite and clay compounds. *Intonachino* is thinner and has lower arids aggregated than *intonaco*.

On the other hand, X-ray diffraction (XRD) and Fourier transform infrared spectroscopy (FTIR) was used to analyze samples of original mortars and those of mortars that have been added in previous building interventions [87].

The results of these studies generally show the presence of coated based mortar of lime, hydraulic lime or cement mortar. Also show the use of materials of the archeological site (lava material, pumice, refractory material, etc.), creating coated or filled materials of cement nature with the presence of aggregates and other components of different composition.

Finally, the more worrying phenomenon for the future conservation of wall paintings was detected, that is the crystallization of soluble salts below the layer of polychrome.

This phenomenon affects all paint layers and their visible effects are the appearance of large areas of polychrome with a dusty appearance (Fig. 3.8.a) and detachment of the outermost layers of paint. By optic microscopy (Fig. 3.8.b), it was observed that the crystallization was developed inside the supporting structure, causing the detachment of the more superficial layers (sub-efflorescence phenomenon). Note that after highlighting the existence of salts at the time of a future restoration will be required a comprehensive mapping of the area to determine specific affected

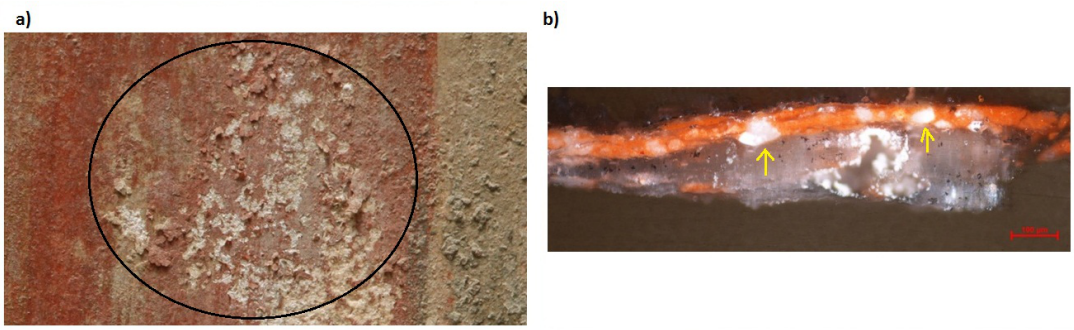

Figure 3.8: a) Detail of Ariadne's house mural painting in Pompeii. The alteration of the polychrome layer by crystallization of salts is observed (circle). b) Section of a sample of red polychromy by light microscope (10x). Crystallization of sulfates is observed below the stratum polychrome (arrows).

areas.

The salts, which have been characterized by XRD analysis are mainly determined by the presence of calcium sulfate (gypsum), sodium sulfate and potassium sulfate, products that can be generated by the presence of alkaline salts (Na_2O and K_2O) in the building materials used in recent times [88] (gypsum, ettringite and thaumasite, which originate through the reaction of Portland cement with sulfur compounds).

The deterioration affecting Ariadne's house wall paintings, produced by salt crystallization, requires the elimination or reduction of the contributions of salt solutions, i.e. the mechanical removal of the mortars used in the past century for the structural consolidation of the paintings.

However, since these wall paintings are placed at their original context, in an outdoor archaeological site, the measure to eliminate or reduce pollutant concentrations is not easy to apply as these can come from the adjacent houses or the floor. Among the solutions that can slow the deterioration process we may highlight a control of the evaporation-crystallization cycles through monitoring the environmental parameters and creating barriers to moisture in the walls of the house to prevent moisture by capillary.

Furthermore it is necessary a direct conservative intervention on frescoes, to prevent detachment of paint layers by applying specific restoration methodologies, such as pre-consolidation, salt elimination treatments and consolidation of the layers of color to its support and further protection.

Summarizing, it is important to emphasize the need for regular monitoring of in-

terventions, through a control of the frescoes state of conservation [89], [90], the study of their support [91] and the compatibility of restoration materials with the work and environmental contaminants.

3.3.4. Photography

The results obtained with high resolution digital photography, IR photography and infrared false-color photography can be very useful in restoration. With them we get information that often eludes our vision especially if complemented or joined with other techniques like in this work, such as infrared reflectography, multispectral, thermography, etc.

Infrared false-color photography is a useful supplementary technique for the examination and characterization of objects, especially pigment identification [79].

Fig. 3.9 is useful for a more thorough explanation of this technique, where we can see more details and a greater definition of the lines and contours that would be essential in a future restoration.

3.4. Conclusions

The studies developed in this work (environmental study, electromagnetic radiation measurement, the study of materials and photography) allowed documenting the state of conservation of Ariadne's house and evaluating the most convenient procedures for a preventive conservation as well as increasing the knowledge about the materials used in its construction, its pictorial procedure and what has been the process of deterioration for the discussion of a future restoration.

The studies suggest that the deterioration process has been accelerated due to the transparent rooftop used.

Then, it was determined that the optimal cover should be opaque and as isolated as possible and, if feasible, covering the walls and the doors to prevent the entry of rain water and sunlight and raising the deck a little to achieve the ventilation of the room.

Therefore the decision on changing the rooftops was taken and within 2009-2010 they were replaced. As consequence, the variability of the environmental conditions

Figure 3.9: Infrared reflectography comparison. This Fig. allows us to appreciate subtleties (e.g. the black square) needed in order to make accurate judgments about archeological objects. From left to right: digital RGB photography, infrared photography (IR) and false-color IR photography (IR-RG).

has been considerably reduced and the values have approximated to the optimal ones.

The multidisciplinary approach has been fundamental to achieve the goal of this work. The study of materials and the photographic study have also shown the relevance of monitoring the environmental conditions in order to stop the deterioration caused by salts crystallization, together with the application of specific techniques for fixing the polychrome, providing valuable knowledge for a possible restoration in the future. In addition, these studies reveal the current state of conservation of the frescoes that will get worse over the years.

Chapter 4

Microclimate monitoring of Ariadne's house (Pompeii, Italy) for preventive conservation of fresco paintings

Microclimate monitoring of Ariadne's house (Pompeii, Italy) for preventive conservation of fresco paintings. Merello, P., García-Diego, F.-J., Zarzo, M. *Chemistry Central Journal* 2012, 6 (1), art. no. 145.

This chapter basically corresponds to the publication mentioned above, after correcting a few mistakes and adding some sentences for clarification.

Abstract: Background: Ariadne's house, located at the city center of ancient Pompeii, is of great archaeological value due to the fresco paintings decorating several rooms. In order to assess the risks for long-term conservation affecting the valuable mural paintings, 26 temperature data-loggers and 26 relative humidity data-loggers were located in four rooms of the house for the monitoring of ambient conditions.

Results: Data recorded during 372 days were analyzed by means of graphical descriptive methods and analysis of variance (ANOVA). Results revealed an effect of the roof type and number of walls of the room. Excessive temperatures were observed during the summer in rooms covered with transparent roofs, and corrective actions were taken. Moreover, higher humidity values were recorded by sensors on the floor level.

Conclusions: The present work provides guidelines about the type, number, calibration and position of thermohygrometric sensors recommended for the microclimate monitoring of mural paintings in outdoor or semi-confined environments.

Keywords: Multivariate monitoring, temperature and relative humidity sensors, cultural heritage, preservation of open-air frescoes.

4.1. Background

Pompeii was a village of ancient Rome located about 26 km southeast of the modern city of Naples (Italy). Around the year 62 AD, an earthquake severely damaged Pompeii and other nearby locations. Since then, the city was rebuilt until the eruption of Mount Vesuvius in 79 AD. Pompeii at that time had a population of about 15,000 inhabitants. The violent eruption of this volcano buried the city and preserved the ruins for centuries.

Thick layers of ash covered Pompeii and Herculaneum, both towns placed at the base of Mount Vesuvius. Their names and locations were forgotten until the 18th century when a new interest for antiquity led to excavations [34]. Herculaneum was rediscovered in 1738 and Pompeii in 1748. Since then, a campaign was launched to unearth both cities, revealing many intact buildings and valuable wall paintings. Pompeii offers a picture of Roman life in the first century.

The forum, baths, many houses, and some villas remained in a surprisingly good state of conservation.

The site was declared World Heritage by UNESCO in 1997 and has become a popular tourist destination, with 2.5 million visitors in 2007. Pompeii is an open-air museum of 1,500 buildings comprising around 20,000 m^2 of mural fresco paintings [35]. Pompeian interior frescoes have become a main source of knowledge about Roman painting up to 79 AD, not because the city was so important at that time but because its tragic end has preserved in good conditions all its wall frescoes for posterity to study [36].

An imposed moratorium stopped excavations in the site to focus the efforts in maintaining the unburied ruins and leaving the remaining excavations for future generations. At present, the access to the ruins is more restricted for tourists, and less than one third of the houses open in the 1960s are currently available for public visits. This is due to the endless maintenance works to prevent the deterioration of buildings already unearthed [37]. Apart from ruin fallings, at least 150 m^2 of fresco paintings and plaster works are lost every year due to lack of maintenance.

4.1.1. Description of Ariadne's house

Ariadne's house is a Pompeian domus (i.e., a single-family house owned by the upper classes) situated in a privileged location at the city center (Regio VII, insula 4). It is a domus of Hellenistic inspiration with an extension of 1,700 m^2. The elevation above sea level of Pompeii is about 14 m. The prevailing wind directions are northeast (October to February) and south (March to September), with an average wind speed of approximately 2.57 m/s (http://es.windfinder.com). The house was built at the end of the second century BC and was heavily damaged during the earthquake of 62 AD, not having been finished its reconstruction on the fateful date of Mount Vesuvius eruption [34]. Most inner walls of the house were originally decorated with frescoes.

The complete pictorial collection of Ariadne's house has a remarkable quality and was probably created by the same artists' team.

Pompeii has been preserved in an enviable conservation state under the layers of ash, but most buildings suffered serious damages during the volcanic eruption and the majority of roofs came down. An aerial view (http://maps.google.es) of Ariadne's house (40° 44' 57.77" N, 14° 29' 14.37" E) and nearby buildings reveals that they are well preserved but the roof is lacking in most of them.

This is the case of Ariadne's house, with only one room (marked as 4 in Fig. 4.1) partly covered with a roof of ceramic tiles (14 m^2) that was settled in the 1950's. After a preventive actuation in the 1970s, roofs made of transparent polycarbonate

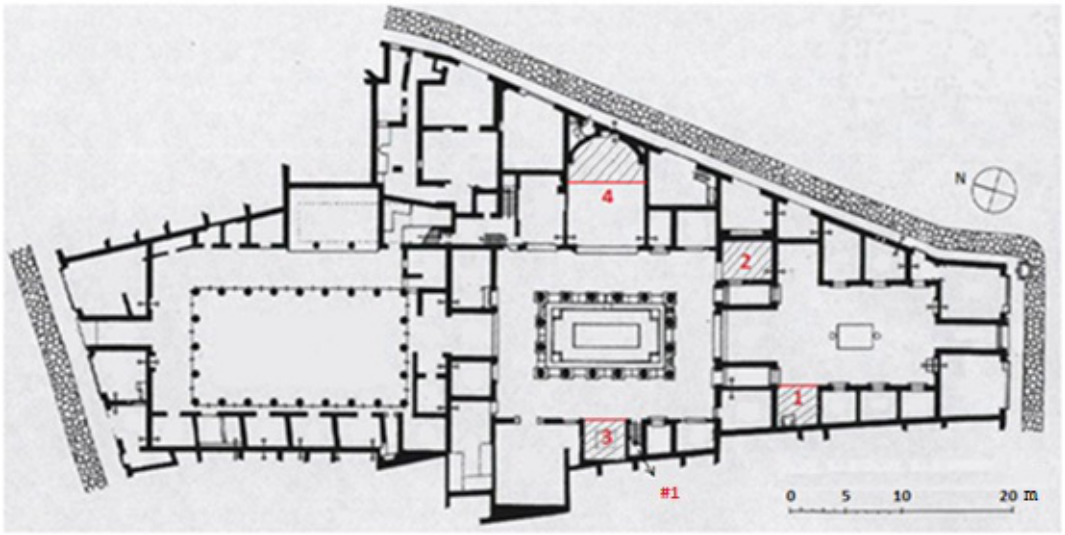

Figure 4.1: Plan of Ariadne's house. Lodgings marked as 1 to 4 are the only roofed ones (parallel tilted lines delimit the covered area). Data-logger ♯1 was located on the top of an outside wall next to room 3 at 3 m from the ground level and it was covered with a ceramic tile.

sheets supported by metallic structures were established in three rooms of the house (1, 2 and 3 in Fig. 4.1) in order to protect the frescoes inside from rainwater. During the following decades, mural frescoes in all rooms that had been left uncovered were seriously damaged due to direct contact with rainwater and the unfavorable thermohygrometric conditions mainly during the summer [34].

Room 2 is comprised by four walls, the northwest one with a large window and a doorway in the SW wall. As a result, the indoor microclimate is more isolated from the outside environment compared with the other rooms under study that are delimited by three walls. Rooms 1 and 3 are open to the courtyard by their NE side. Room 4 is open to the atrium by its west side. It is the largest one and has only one wall decorated with frescoes that presents a semicircular shape (Fig. 4.1).

An extensive scientific literature is available about the analysis of materials and characterization of mural paintings in Pompeii [59], [68], [92], [93] and other Roman cities [69], [94]. In the benchmark of a conservation project started in 2008, a series of works were carried out in Ariadne's house: microclimate monitoring, electromagnetic radiation measurements, study of materials, and photographic report. The purpose was to assess the conservation state of frescoes and the most convenient future restoration works of Ariadne's lodgings still containing mural paintings. These were all covered rooms (1 to 4 in Fig. 4.1), whose roofs have preserved wall

frescoes during the last decades.

The multidisciplinary team has studied the problems of salt efflorescence, atmospheric pollution and other pathologies associated with the materials in order to determine the causes of fresco degradation and propose conservation actions [21]. It was found that all pigments are from inorganic origin. The deterioration of frescoes due to inappropriate temperatures in the rooms assessed by thermography was also discussed. The multidisciplinary approach has been fundamental to provide the basic guidelines for future in-depth restoration works.

Regarding the microclimate study, a set of 26 thermohygrometric probes comprised by temperature and relative humidity (RH) data-loggers were installed for monitoring ambient conditions inside the roofed rooms. The statistical analysis of data recorded by these sensors will be the subject of the present research.

Different reported studies have measured air temperature, RH and other parameters inside museums for the preventive conservation of their collections [22], [57], [95], [96].

Similar works have monitored the indoor environment in churches, as they contain valuable artifacts [16], [18], [28], [29], [97], [98].

However, very few studies have characterized ambient conditions of outdoor archaeological sites [12], [31], [99] or semi-confined environments [17]. The present work reports for the first time a microclimate research conducted in the ruins of Pompeii, which is of relevant interest because inappropriate conditions of temperature and RH are causing severe damages on the valuable fresco paintings. Moreover, results reported here will provide guidelines to establish thermohygrometric monitoring systems in similar open-air archaeological sites for preventive conservation.

4.2. Experimental

4.2.1. Description of data-loggers

The use of autonomous devices was the best option in this case due to the lack of electric supply in Ariadne's house. Each RH data-logger (Datalog Hygrochron DS1923) contains a humidity sensor with an accuracy of $\pm 5\,\%$ [100].

Although this model can also record temperatures, it was decided to use inde-

pendent devices (Datalog Thermochron DS1922L) for the temperature monitoring [101], which has the same accuracy (±0.5°C) as DS1923. The reason was to expand the data storage capacity of the monitoring system.

A set of 52 data-loggers, 26 of each model, were purchased directly from the manufacturer (Maxim Integrated Products, Inc., Sunnyvale, CA) and they were calibrated prior to their installation as described ahead. These devices resemble button-like batteries, with 17.4 mm of diameter and 5.9 mm of height. Given their small size, each pair of DS1923 and DS1922L data-loggers were assembled together by means of a metallic structure and will be referred to hereafter as thermohygrometric probe. This probe is isolated by an external PVC structure of dark-gray color, which allows a convenient fixing to the wall, and has a cylindrical shape with a diameter of 6 cm. It is filled with polyurethane foam to isolate the data-loggers from the PVC structure. The assembly allows both data-loggers to be directly in contact with the ambient air, and therefore it was assumed that the supporting structure had a negligible effect on the recorded data.

4.3. Results and discussion

4.3.1. Calibration of sensors

The time series of temperature or RH recorded by one data-logger reflects the parameter evolution along the time, and it is often so-called as trajectory. Fig. 4.2 shows that the differences among average time series were slight in the calibration experiment. As all trajectories are quite parallel, the average registered during the calibration period by each data-logger is a representative value. If average temperatures obtained in the first period are compared with those from the second calibration stage, it turns out that the correlation is statistically significant (r =0.934, p <0.0001). This result implies certain bias that should be corrected. For the first period, the bias was calculated as the mean temperature recorded by each data-logger minus the average from all of them, which was regarded as the exact value. The same procedure was applied for the second period.

Next, the mean of both bias estimations was calculated (shown in Table 4.1) resulting a range from −0.44 °C (♯18) to +0.53 °C (♯13), which is consistent with the measurement error of ±0.5 °C indicated by the manufacturer [101]. Probe ♯2 was the one with highest RH values recorded in the second period (Fig. 4.2.c, bias =1.9 %), but it was the third one with lowest RH in the first stage (Fig. 4.2.a, bias

$= -1.1\,\%$). Thus, from the first to the second period, the shift is $1.1 + 1.9 = 3\,\%$. This error seems too high as the purpose of the present study is to discuss the slight differences recorded among sensors, and no bias correction was applied to ♯2. This abnormal performance was caused by an accidental water drop over this data-logger during its uninstallation. If RH data from ♯2 are disregarded for the calibration study, it turns out that the correlation between the average RH recorded by each data-logger in the first vs. the second calibration period is statistically significant ($r = 0.701$, $p = 0.0001$). Again, this result reveals certain bias, and the same procedure described for temperature was applied to estimate the errors.

The resulting bias estimations range from $-1.5\,\%$ (♯19) to $+0.8\,\%$ (♯5). This range is much lower than the measurement error of $\pm 5\,\%$ indicated in the manufacturer's data sheet [100]. It was decided to correct all temperature and RH values collected in Ariadne's house according to the estimated biases (Table 4.1) in order to improve the reproducibility of the monitoring system.

In order to determine more accurately the real bias, a further experiment was conducted with aqueous solutions of two salts. Results confirmed that the bias was small and irrelevant for the purpose of the present study.

4.3.2. Descriptive data analysis of mean trajectories

Knowledge about ideal or limit values of microclimate parameters for conservation of cultural heritage is still poor [32]. The Italian UNI 10829 [83] and DM 10/2001 [7] are currently the approved standards on this issue. They do not provide guidelines for the conservation of outdoor paintings, but nevertheless the admissible values of RH and temperature indicated by both standards can be taken as a reference for the conservation of Pompeian frescoes. According to [83], the recommended range of RH and temperature for mural paintings is $55-65\,\%$ and $10-24$°C, respectively. These ranges are narrower than the ones suggested by [7]: $45-60\,\%$ and $6-25$°C.

Taking into account that both standards were developed for indoor conditions, we decided to consider here the intervals given by [7], which are wider and could be better extrapolated for outdoor conditions.

Fig. 4.3 shows the evolution of RH and temperature recorded by all probes in a period of one year. It turns out that the mean RH was out of the range recommended by the standard in 272 days during one year, while the mean temperature was higher than 25°C in 116 days. Thus, ambient conditions are too humid in winter and too hot in summer for the preservation of fresco paintings. The conservation risk is even more serious taking into account the marked daily variations of temperature and

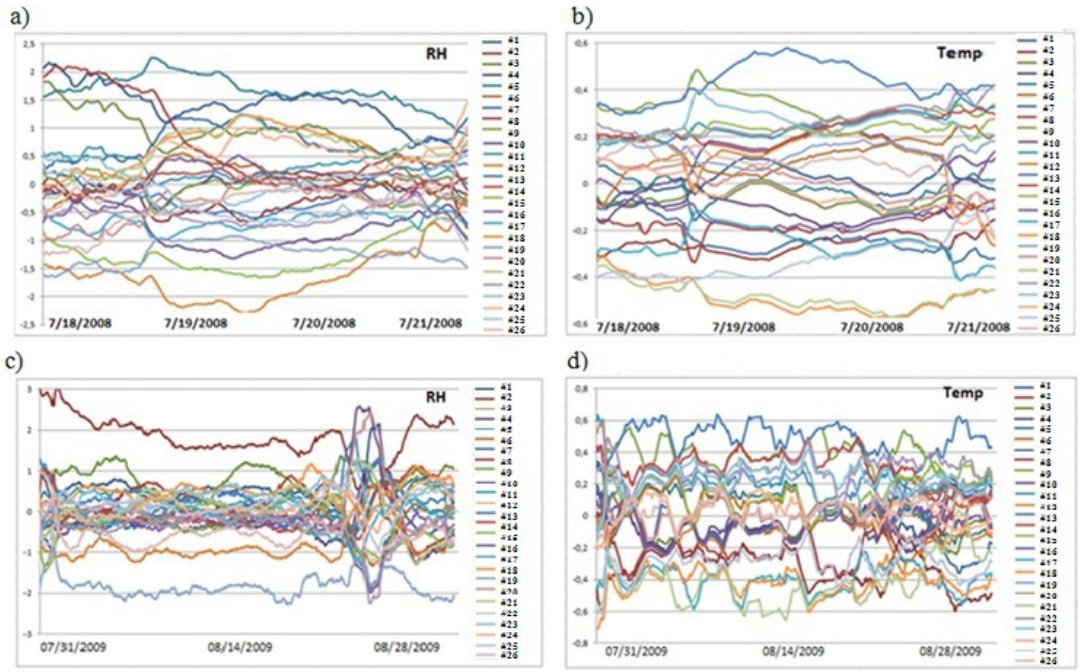

Figure 4.2: Calibration of RH and temperature sensors. Difference between RH and temperature recorded by each probe with respect to the average from all probes in two different calibration periods: first, from 18^{th} to 21^{st} July 2008 (a: RH; b: temperature) or second, from July 31^{st} to August 28^{th} 2009 (c: RH, d: temperature). Trajectories were smoothed using a moving average with a window size of one day.

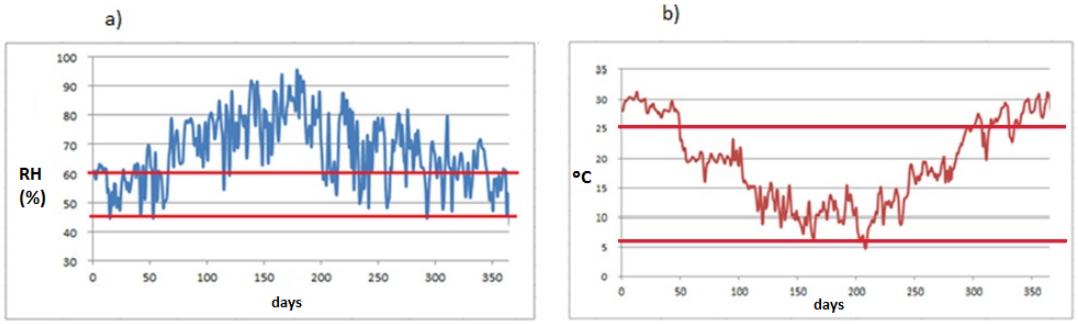

Figure 4.3: Smoothed time series of RH and temperature. Average RH (a) and temperature (b) recorded by all probes (except ♯1) during one year (day 0 corresponds to July 23^{rd} 2008). The time series was smoothed using a moving average with a window size of one day. Horizontal lines in red correspond to the ranges recommended by the standard DM 10/2001 for the conservation of mural paintings.

Code	Height[b]	T_{bias}	RH_{bias}	Code	Height[b]	T_{bias}	RH_{bias}
#1		−0.015	0.647	#14	0	0.405	−0.096
#2	185	−0.321	0.425	#15	30	0.175	−0.351
#3	290	−0.088	0.714	#16	0	0.027	−0.532
#4	153	−0.119	−0.365	#17	338	−0.298	−0.084
#5	0	0.018	0.760	#18	300	−0.438	0.495
#6	0	0.064	−0.208	#19	310	0.206	−1.506
#7	163	−0.168	0.372	#20	290	0.035	−0.198
#8	0	−0.204	0.342	#21	175	−0.424	0.464
#9	189	0.305	0.059	#22	240	0.291	−0.555
#10	240	−0.029	−0.550	#23	330	0.224	0.613
#11	0	0.199	0.204	#24	117	0.010	0.308
#12	210	−0.115	−1.112	#25	54	−0.304	0.233
#13	0	0.529	0.435	#26	15	0.036	−0.512

Table 4.1: Height and bias of temperature and RH data-loggers. [a]Temperature bias (T_{bias} in °C) and relative humidity bias (RH_{bias} in %), averaged for both calibration periods (codes as in Fig. 17). [b]Distance to the floor level (cm).

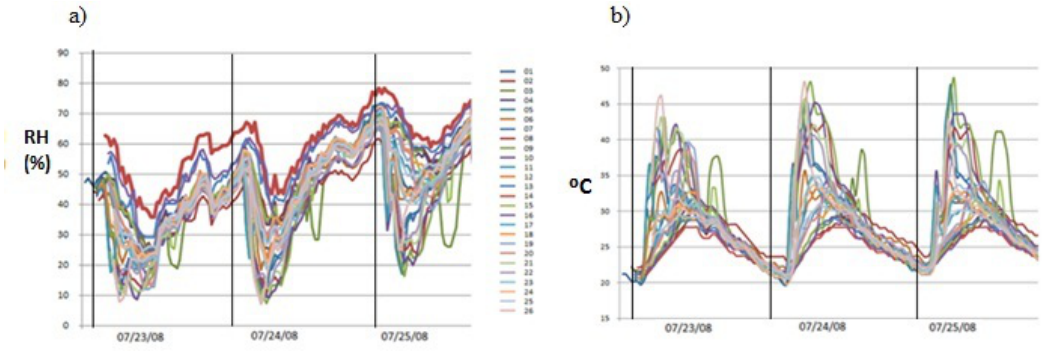

Figure 4.4: Trajectories of RH (a) and temperature (b) recorded by all probes during three summer days (23^{rd} to 25^{th} July 2008). Vertical lines correspond to midnight (0:00 hr).

RH (Fig. 4.4) and given that high peaks of temperature can be reached in summer. Actually, 31.2 % of all recorded temperatures were above 25°C, and 73.1 % of RH data were above 60 %.

Daily oscillations of temperature and RH in summer can be up to 25°C and 40 %, respectively (Fig. 4.4). High variability is inappropriate for the conservation of fresco paintings, which encourages some kind of corrective action to reduce the temperature at least in summer [7].

A monitoring system will be necessary to study the effectiveness of any action of this kind, and to assess the risks for the long-term conservation of frescoes.

Fig. 4.4.a shows that all RH trajectories are quite parallel. Thus, the average RH of all values recorded by each sensor during the monitoring study characterizes the basic dissimilarities among RH time series.

In the case of temperature, not all trajectories follow the same pattern. Consequently, the average value is not enough to describe conveniently the differences among temperature trajectories, and additional parameters were studied using bivariate plots and analysis of variance as described below.

4.3.3. Detection of outliers

Certain atypical shapes are observed in Fig. 4.4.b. Thus, prior to comparing average values, it is convenient to discuss those trajectories with abnormal deviations from the average temperature recorded by data-loggers in the same room. For this

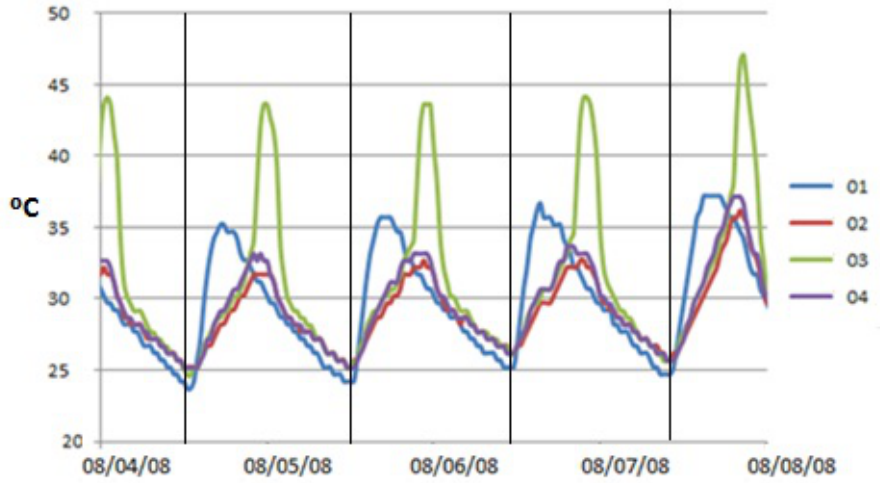

Figure 4.5: Temperatures in room 4. Temperatures recorded by data-loggers in room 4 (♯2, ♯3 and ♯4) during four summer days (4^{th} to 8^{th} August 2008). Values of ♯1 are also shown for comparison.

purpose, all trajectories were carefully inspected.

Fig. 4.5 shows that probe ♯3 recorded an abnormal increase of temperature at about 2:00 PM, and recovered the common pattern at 8:00 PM approximately. By contrast, in the same time frame, its RH time series underwent a sudden decrease (Fig. 4.4.a). The reason seems to be an effect of direct sunshine radiation that heats the data-logger during this time period as reflected by Fig. 4.6.

In order to check if the atypical peaks of temperature recorded by ♯3 occurred all the year round, we calculated the differences between ♯3 and ♯4. The latter was taken as a reference data-logger in the same room with a normal performance. Next, the maximum value of this difference was calculated for the 48 time observations corresponding to each day: $MAX[(temp_{t_1}^{\sharp 3} - temp_{t_1}^{\sharp 4}) \cdots (temp_{t_{48}}^{\sharp 3} - temp_{t_{48}}^{\sharp 4})]$.

If this daily difference is plotted for the period under study (Fig. 4.7), it turns out that values are close to zero (i.e., both data-loggers presented very similar trajectories) from October 12^{th} 2008 to February 23^{rd} 2009.

Out of this period, however, the differences are remarkable. The reason seems to be that no direct sunlight reached data-logger ♯3 during this particular period. The abnormal temperature increase of ♯3 did not occur in a few days of spring and summer probably due to the presence of clouds or rainy conditions that reduced

Figure 4.6: Location of probes ♯2, ♯3 and ♯4 in room 4. The picture was taken at 1:05 PM. The brighter zone at the lower right corner corresponds to sunlight incident on the frescoes that affects ♯3 from 2:00 PM to 8:00 PM.

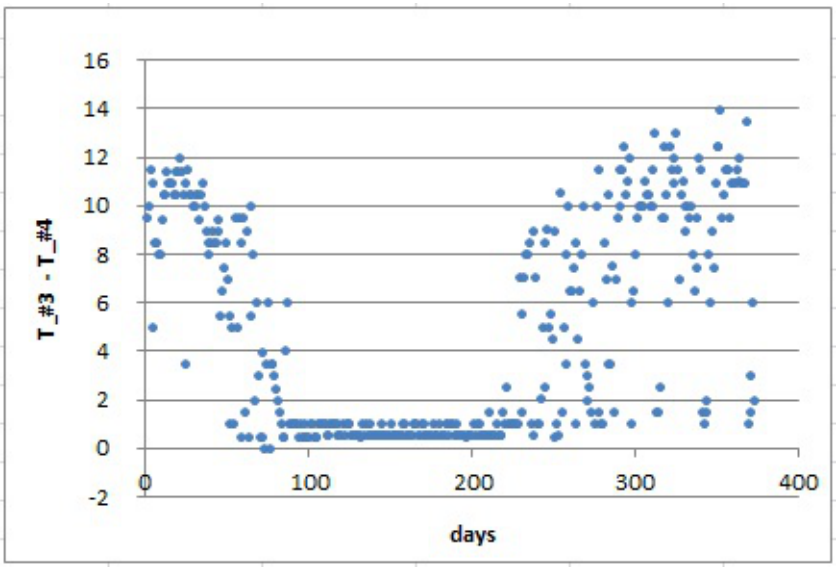

Figure 4.7: Maximum daily differences of temperature between data-loggers ♯3 and ♯4. Calculated for the 372 days of the period under study (day 0 corresponds to July 23^{rd} 2008).

sunshine.

Fig. 4.8 shows abnormal daily peaks of temperature recorded by ♯2 that occurred in winter from 2:30 PM to 6:30 PM approximately. Similarly, the temperature time series of ♯9 (room 3) also reflects sudden peaks (Fig. 4.8.b) in winter from about 8:30 AM to midday. In the same time frames, both data-loggers registered an atypical decrease of RH (Figs. not shown). Again, sunlight incident on these particular sensors seems to be the reason. The time series of ♯1 did not deviate from the common pattern in summer (Fig. 4.5) nor winter (Fig. 4.8.a) probably because this probe was covered with a tile and never received sunlight.

The sudden variations observed in certain trajectories at particular day frames can be seen as a mistake in the experimental setup. This is a problem for the statistical analysis, and the abnormal data of probes ♯2, ♯3 and ♯9 were discarded after carefully checking the values. Of course, direct sunshine on sensors produces abnormal temperature variations that should be avoided, but in long-term monitoring it is not evident how to determine the different trajectories of solar radiation incident on all walls during the year. This is an important recommendation for future studies of outdoor ambient monitoring.

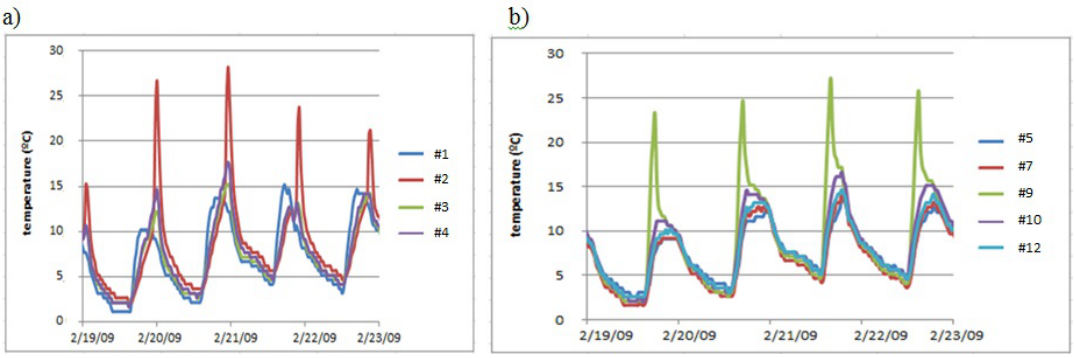

Figure 4.8: Abnormal peaks of temperature recorded in room 4 and 3. Temperatures recorded by probes in room 4 (a) and five probes in room 3 (b) during four winter days (19^{th} to 23^{rd} February 2009). Values from ♯1 are also included for comparison.

4.3.4. Daily mean trajectories

As the daily thermohygrometric variations are more prominent in summer, it was decided to check firstly the data recorded from July 23^{rd} until September 22^{nd} 2008 in order to better appreciate the differences among trajectories.

After discarding the abnormal values caused by incident sunlight, we calculated the average temperature recorded in summer by data-logger ♯1 at 0:00, 0:30, 1:00... and so on until 12:00 PM, resulting a daily mean time series. The same procedure was applied to all data-loggers. Daily trajectories of RH were also obtained (Fig. 4.9).

Daily variations of temperature are more pronounced in rooms 1 and 3 (Fig. 4.9.a). Ceramic tiles protecting room 4 reduce the amplitude of the daily cycles (Fig. 4.9.b), which clearly indicates that this type of roof seems more convenient for the conservation of frescoes than the transparent polycarbonate sheets covering the other rooms. Actually, marked oscillations of thermohygrometric parameters represent a serious risk for the long-term preservation of frescoes.

All temperature trajectories seem to converge at night to a common pattern, but their variability is much higher at midday, with a range of about 15°C comparing the values of ♯9 vs. ♯11. Moreover, the shape of these trajectories differs at midday as the maximum value is reached around 9:00 AM in some cases (e.g. ♯8, ♯9 or ♯21) while other probes registered the maximum temperature about 12:00 AM (e.g. ♯13, ♯14 or ♯20). In the case of RH, the highest variability is observed at about 10:00 AM. At this time, the range among daily RH trajectories is about 45 % (♯21 vs.

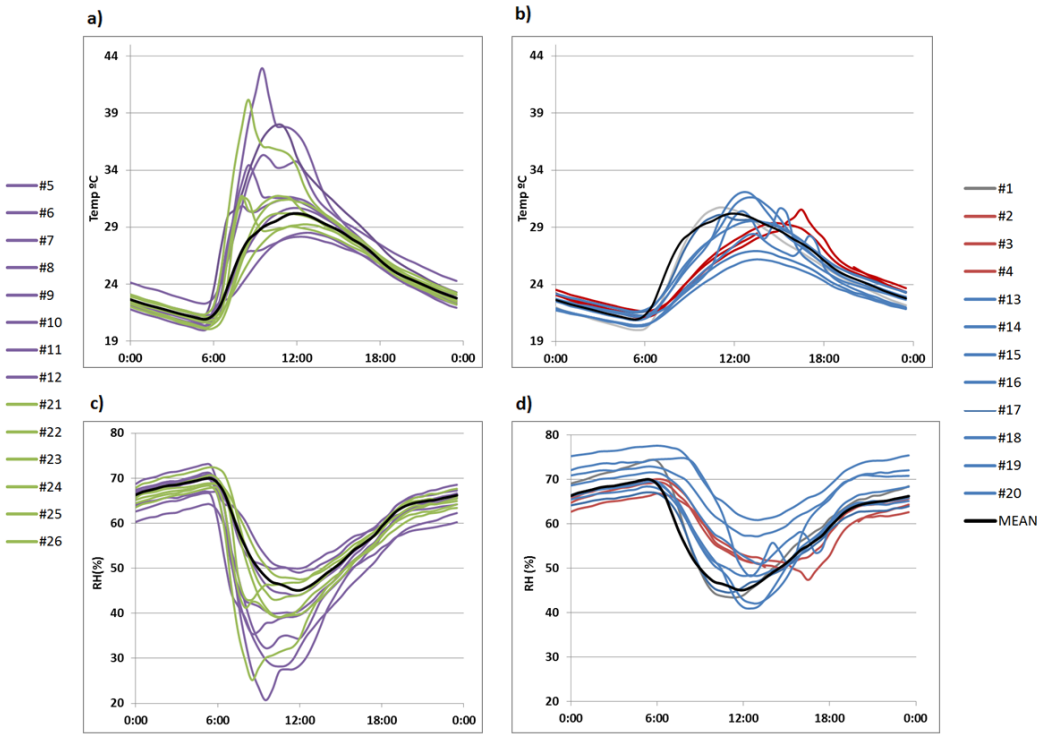

Figure 4.9: Mean daily trajectories of temperature and RH in summer. a) Temperature at rooms 1 and 3; b) temperature at rooms 2 and 4; c) RH at rooms 1 and 3; d) RH at rooms 2 and 4. Summer period: 7/23/2008 to 9/20/2008. Color codes indicate the location of probes: room 1 (green), room 2 (blue), room 3 (violet), room 4 (red). The thicker black line corresponds to the average time series of all probes.

♯25).

4.3.5. Analysis of variance (ANOVA)

Different statistical parameters were calculated for each day and each temperature data-logger: minimum ($Tmin$), maximum ($Tmax$) and average. Considering that monitoring frequencies normally used in cultural heritage are 1 datum/hour or 1 datum/day, a simulation has been performed to determine if the ANOVA results can be interesting in these data bases. For doing this, we have simulated a database with a recording frequency of 1 data per day. Daily data have been calculated as the daily average for each sensor.

Similarly, daily averages of RH, minimum ($RHmin$) and maximum ($RHmax$) values were also obtained. In order to study the effect of height and wall orientation where the probe was located, different ANOVA models were carried out with these parameters. In all cases, two factors were considered: day and data-logger.

The effect of day is not of interest here, and results will only be discussed according to the second factor. The best results were obtained with RH recorded in summer (from 7/24/2008 to 9/22/2008). Alternative ANOVAs using only winter data or both periods were also checked, but the interpretation was less clear.

Regarding room 2, the daily average RH in summer was higher in data-loggers on the floor than those hanging on the walls at about 3 m of height. LSD (Least Significant Difference) intervals of sensors on the ground (♯13, ♯14 and ♯16) do not overlap with LSD intervals of those at the upper position (♯17, ♯18, ♯19 and ♯20) (Fig. 4.10), which indicates that differences are statistically significant ($\alpha = 0.05$). Such significant differences of RH with respect to sensor height are not so apparent in the other lodgings. We hypothesize that the reason could be the different microclimate in room 2 given that it is the only one delimited by four walls, which probably provides more stable ambient conditions.

This result suggests that sensor height is more important than wall orientation for monitoring semi-confined environments with similar characteristics as room 2.

The mean RH of wall probes ♯18, ♯19 and ♯20 was nearly the same (Fig. 4.10). By contrast, the differences among floor sensors resulted statistically significant: mean RH recorded by the north-oriented probe (♯14) were higher than in the case of those oriented to the east (♯13) or south (♯16). Sensor ♯15 remains at 30 cm from the ground which is an intermediate position and, remarkably, the average RH recordings of this data-logger are also intermediate (Fig. 4.10).

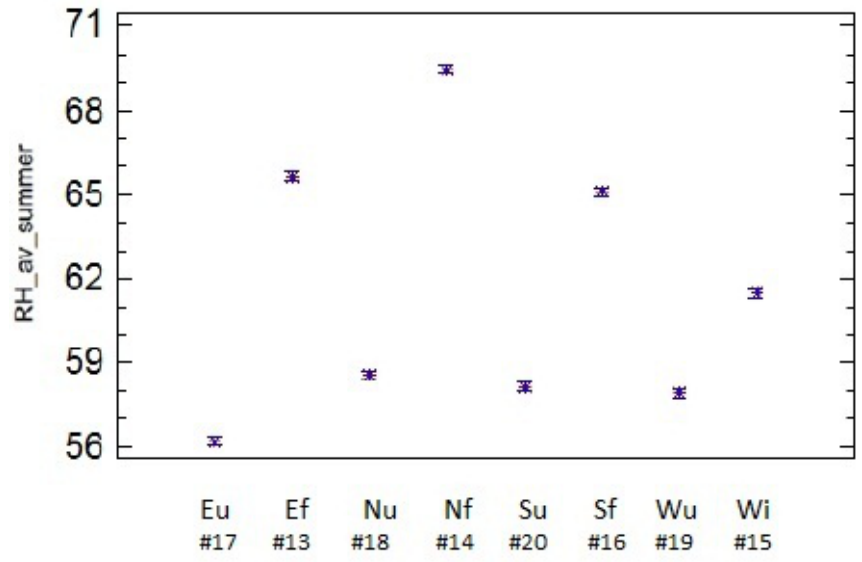

Figure 4.10: ANOVA results (room 2). ANOVA results showing the differences among probes in room 2 on the daily mean RH recorded in summer 2008. For each data-logger, the average and 95 % LSD interval is depicted. Codes indicate the wall orientation where each sensor is facing (N: north; S: south, E: east, W: west) and the height: f (floor level), u (upper) or i (intermediate).

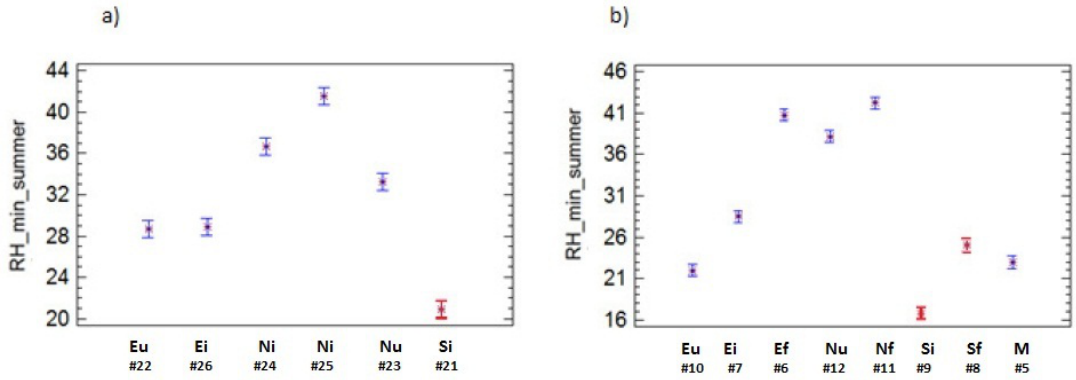

Figure 4.11: ANOVA results (rooms 1 and 3). ANOVA results (average and 95 % LSD intervals) showing the differences among probes in room 1 (a) and 3 (b) on the daily minimum RH recorded in summer 2008. The codes indicate the wall orientation (N: north; S: south, E: east, W: west) and the height: f (floor level), u (upper) or i (intermediate).

Figure 4.12: Mural frescoes in Ariadne's house (western wall of room 1). Three probes can be observed: ♯22, ♯25 and ♯26, which remain at 240, 54 and 15 cm from the floor, respectively.

Rooms 1 and 3 present a similar size and orientation (Fig. 4.1), both are comprised by three walls and are roofed with transparent polycarbonate sheets. Fig. 4.11 shows that probes facing to the south in both rooms (LSD intervals highlighted in red) tend to present lower $RHmin$ values than the rest. Conversely, north-oriented sensors in room 1 (♯23, ♯24 and ♯25) recorded significantly higher $RHmin$ values than east-oriented data-loggers (♯22 and ♯26). This outcome is intuitively appealing because the south orientation receives more sunlight along the day. The significant differences between probes ♯25 and ♯26 were somewhat unexpected because they are separated just 2 meters away (Fig. 4.12). The effect of orientation cannot be studied in room 4 because all sensors were basically located on the same semicircular wall.

An additional effect of sensor height is also apparent in room 3 (Fig. 4.11.b). Actually, comparing probes with the same orientation, those on the floor recorded significantly higher $RHmin$ values. Results reported here indicate that data-loggers located on the ground have a different pattern, and consequently all of them will be treated as an independent cluster in the bivariate plots presented in the next section. Different ANOVAs were also performed with daily average temperatures,

$Tmax$ and $Tmin$, but results did not provide a clear interpretation regarding the effect of height and wall orientation on these parameters. Further studies with multivariate statistical methods will be necessary for this purpose. The fact that RH provides more information than temperatures was also found in a recent study [18].

Summarizing, sensor height (floor vs. upper position) was the main cause of RH variability in the room with four walls. An additional effect of wall orientation on $RHmin$ was observed in rooms 1 and 3 that are quite similar. Consequently, it appears that the location of probes was appropriate, and similar criteria should be applied in further studies of outdoor monitoring. In closed rooms, it seems advisable to install sensors on the floor, and two different orientations might be enough for wall sensors.

By contrast, in outdoor sites or lodgings with a high rate of air exchange, special care should be taken in wall orientation. In all cases, direct sunlight on data-loggers should always be avoided to prevent abnormal measurements.

4.3.6. Bivariate plots

Fig. 4.13 shows that summer is characterized by more pronounced thermohygrometric differences between day and night. Moreover, mean temperatures are higher in summer while the opposite applies to RH. As a result, both parameters are negatively correlated. Marked cycles of RH which occur along the year are also reflected.

Winds like sirocco, tramontane and episodes of hot and persistent humid air are typically recorded in the Mediterranean basin. This work deals with a long-term monitoring (372 days), therefore the observed results are an average of the different wind effects along this period, avoiding their influence on the daily cycles and on the correlation between RH and temperature.

RH is defined as the partial pressure of water vapor in the air-water mixture divided by the saturated vapor pressure. At higher temperatures, the air can hold more water prior to reaching the saturation, which may partly explain the negative correlation between RH and temperature (r = -0.862) observed in Fig. 4.14.a.

Attempting to further describe the thermohygrometric variations along the year, mean values of absolute humidity (AH) are also depicted in Fig. 4.13. They were calculated using Equation 4.1 from [1] according to RH (%) and temperature (°C).

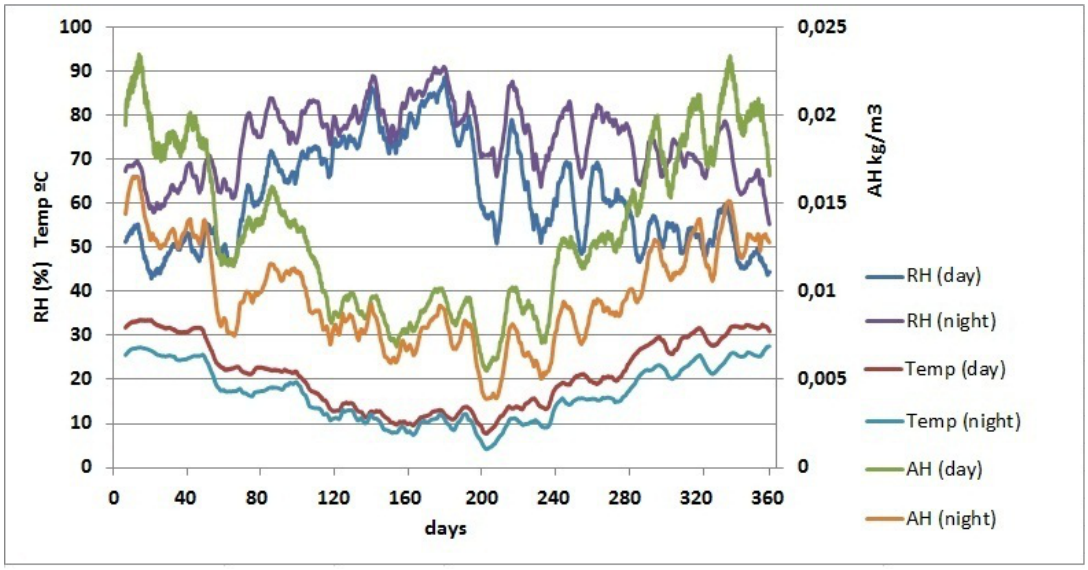

Figure 4.13: Evolution along the year of daily mean parameters: temperature, absolute humidity (AH) and RH. Data recorded by all probes during the daytime (8:00 AM to 8:00 PM) and night-time (8:00 PM to 8:00 AM). Day 0 corresponds to 24^{th} July 2008 (days< 60: summer; 60-151: autumn; 152-239: winter; 240-331: spring). Trajectories were smoothed using a moving average with a weekly window size.

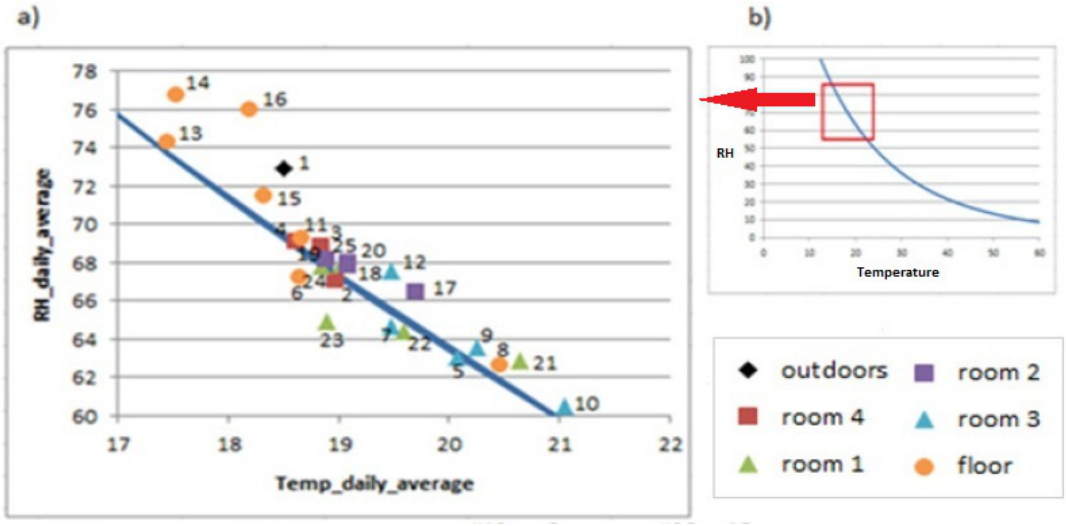

Figure 4.14: Bivariate plot of daily average RH vs. temperature. a) Bivariate plot of daily average RH from each probe with respect to daily average temperature, corresponding to the year 2008-2009 (372 days). b) Theoretical function relating RH and temperature (Equation 4.2), which is also depicted inside the bivariate plot.

$$AH = RH \frac{0.0132295}{273.16 + T} \times exp\left(\frac{17.2694 \times T}{283.3 + T}\right), \tag{4.1}$$

$$RH = 0.0109 \times \frac{273.16 + T}{0.0132295} \times exp\left(-\frac{17.2694 \times T}{283.3 + T}\right). \tag{4.2}$$

In order to characterize the dissimilarities among probes, different bivariate plots were obtained and visually inspected. Fig. 4.14.a displays average RH vs. average temperatures. Taking into account the relationship between RH and AH (Equation 4.1), RH was plotted as a function of temperature inside this figure by considering $AH = 0.0109\, kg/m^3$ (Equation 4.2). This value is the one that achieves the best goodness-of-fit in Fig. 4.14.a and it was estimated using non-linear regression after disregarding floor probes and ♯1.

Bivariate plots of $Tmax$, $Tmin$, $RHmax$ and $RHmin$ are also of interest to illustrate the differences among recorded trajectories. The comparison of $RHmin$ vs. $Tmin$ (Fig. 4.15) does not show any correlation, but the plot reveals three clusters of probes according to their location: (i) floor, (ii) rooms 1 and 3, and (iii) rooms 2 and 4.

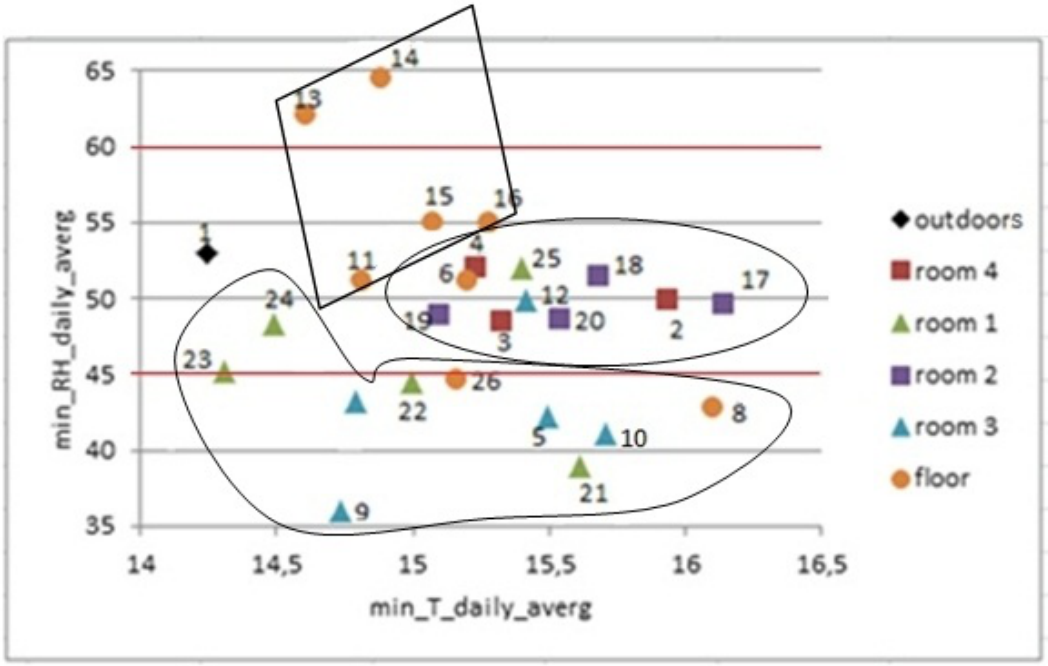

Figure 4.15: Bivariate plot of daily minimum RH from each probe vs. daily minimum temperature, averaged for all the 372 days. Horizontal lines in red (45-60 %) correspond to the range of RH recommended by the standard DM 10/2001 for the conservation of mural paintings.

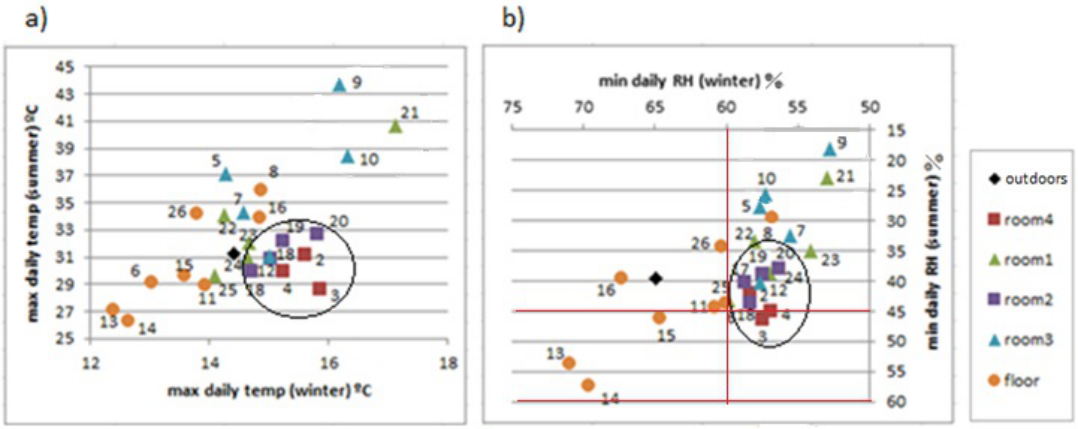

Figure 4.16: Bivariate plots (summer vs. winter). a) Bivariate plot of daily maximum temperature ($Tmax$) averaged for the summer period (7/24/ 2008 - 9/22/2008) vs. $Tmax$ averaged for the winter period (12/21/2008 - 3/31/2009). b) Bivariate plot of daily minimum RH ($RHmin$) in summer vs. $RHmin$ in winter. Axes were inverted in the right plot to ease the comparison. Lines in red (45-60 %) correspond to the range of RH recommended by the standard DM 10/2001.

Minimum temperatures tended to be cooler at the floor level. The bivariate plot of RHmax vs. Tmax (Fig. not shown) was also visually inspected, but clusters are better discriminated in Fig. 4.15.

Additional bivariate plots considering only the summer or winter periods were also inspected. The most interesting ones that reflect the different ambient conditions between the two seasons correspond to $Tmax$ (Fig. 4.16.a) and $RHmin$ (Fig. 4.16.b).

Sensors in rooms 2 and 4 are highlighted with an ellipse. The relative position of probes in both figures is very similar given the tight correlation between RH and temperature, which reveals certain redundant information. Based on this correlation, it is not justified to use the same number of data-loggers for recording both parameters in open-air archaeological sites.

According to Figs. 4.14, 4.15 and 4.16, probes on the floor recorded higher RH and lower temperatures. In particular, most of them yielded the highest mean RH along the year (Fig. 4.14.a), and the highest $RHmin$ values in winter (Fig. 4.16.b). Moreover, they yield the lowest mean temperatures along the year (Fig. 4.14.a) and the lowest $Tmax$ in winter (Fig. 4.16.a). As an exception, probe ♯8 registered much higher temperatures (Fig. 4.14.a). The reason is unclear, but taking into account

that ♯8 was oriented to the south, perhaps it received more diffuse solar radiation.

The same reason might explain why probes ♯9 and ♯21 recorded the highest $Tmax$ (Fig. 4.16.a) and the lowest $RHmin$ values (Figs. 4.11 and 4.16.b), given that they were also south-oriented. This hypothesis is mere speculation and further studies using more data-loggers will be necessary to investigate this issue.

Assuming that AH is constant inside all rooms, the curve depicted in Fig. 4.14.a highlights that floor probes ♯14 and ♯16 (room 2) deviate from the theoretical relationship between RH and temperature. The RH mean daily time series of both probes is also atypical (Fig. 4.9.d) as the daily decrease of RH registered at sunrise is delayed in about 30 min with respect to the other trajectories. This abnormal performance might be caused by diffusion of water vapor by capillarity through the ground to the boundary layer in contact with the data-logger. The fact that higher $RHmin$ values were recorded by floor sensors is also consistent with this hypothesis.

Room 2 is the only one comprised by four walls, but it is uncertain if this issue could also explain their atypical performance.

Probe ♯1 also appears as an outlier in Fig. 4.14, which suggests that AH outside Ariadne's house might be higher than indoors. Moreover, this probe recorded the lowest $Tmin$ (Fig. 4.15) and higher $RHmin$ values in winter with respect to wall sensors (Fig. 4.16.b). Results reveal that the microclimate reflected by ♯1 was slightly different, which suggests using one or more outside sensors in similar monitoring studies.

According to DM 10/2001 [7], the recommended interval of RH is 45-60 %. Regarding $RHmin$, only probes in room 4 satisfy this condition in summer and winter (Fig. 4.16.b). By contrast, $RHmin$ tends to be lower than 45 % in rooms 1 and 3 (Fig. 4.15), which indicates ambient conditions too dry for an appropriate conservation of frescoes particularly in summer.

Figs. 4.14, 4.15, 4.16 reveal that ambient conditions in rooms 2 and 4 were cooler in summer, more humid and more stable (i.e., with less variability among probes) than in rooms 1 and 3. In winter, temperatures in rooms 2 and 4 tended to be less cold (Fig. 4.16.a), which appears more appropriate for preserving the frescoes. The observed differences among lodgings can be explained by the roof type and number of walls of the room. Actually, room 2 is characterized by an environment more isolated from outdoor conditions and room 4 is partly covered with ceramic tiles that prevent incoming sunlight.

The others are roofed with transparent sheets that produce a greenhouse effect,

which tends to increase the temperature. Thus, opaque shelters seem more convenient.

Taking into account that probe ♯5 was located under a glass, the greenhouse effect could also explain the higher temperatures recorded by this data-logger with respect to the others on the floor of room 3 (Fig. 4.14.a).

Experts in restoration of frescoes are currently assessing the conservation state of paintings in Ariadne's house. Preliminary results suggest that frescoes in room 2 are better preserved that the rest, which is of interest because room 2 presents ambient conditions closer to the range recommended by DM 10/2001 [7]. This issue supports the use of this standard for discussing the statistical data analysis.

Given the unfavorable environment revealed in the present study, the transparent roof in rooms 1-3 was replaced in December 2009 by undulating roof sheets made of fiber cement with a thickness of about 5 mm.

The conclusion that transparent roofs are inappropriate for the conservation of outdoor wall paintings might seem obvious for experts in the field, but the competing authorities requested empirical evidence prior to approving the roof change. The effectiveness of this corrective measure will be assessed in a future study.

4.4. Conclusions

The statistical analysis of RH and temperatures recorded in Ariadne's house has revealed that autonomous data-loggers with a sampling rate of two readings per hour seem appropriate. Considering that few works have monitored microclimate environments of outdoor or semi-confined archaeological sites, results reported here are of interest for similar studies regarding the number, type and position of data-loggers, as well as for the subsequent statistical data analysis. The first step of the analysis should be the bias correction of all measurements based on the calibration experiment.

Descriptive tools have been effective for highlighting the dissimilarities among probes. The mean daily trajectories displayed in Fig. 4.9 provide useful information about the difference in average values and shapes among data-loggers. This type of plot is used in several fields of science to visualize and synthesize differences in recorded values, but it is rarely applied in microclimate monitoring where trajectories of a few days randomly chosen are usually presented.

By means of ANOVA and bivariate plots, it was found an effect of roof type, wall orientation and sensor height on microclimate conditions. Higher RH values were recorded by data-loggers on the floor, and the south orientation was characterized by lower RH values because it tended to receive more sunlight radiation.

The differences among probes suggest that at least four data-loggers per room would be required in similar studies to assess the effect of different factors and to detect abnormal trajectories. One or more control sensors are also recommended. Regarding the number of walls of the room, rooms with four walls will require less number of sensors at wall levels, where two different orientations might be enough. At floor level, north orientation and a complementary one (south or east) should also be monitored. If several lodgings present similar characteristics, orientation, size and number of walls, it seems sufficient to monitor just one of them.

A tight correlation was found between average RH and temperatures, which suggests that it is not necessary to use the same number of RH and temperature sensors in open-air archeological sites. Redundant information will also result if lodgings with very similar characteristic are monitored, which reveals the importance of choosing properly the right location for probes.

Results reveal that summer conditions in Pompeii are more unfavorable for the conservation of frescoes according to the standard DM 10/2001 because the microclimate was too dry and hot. Consequently, ambient conditions in similar studies should be basically monitored in summer. Transparent roofs produce a greenhouse effect that increases the temperature, which is undesirable. Based on the results, corrective measures were taken by replacing the type of roof. The effectiveness of such measures will be assessed in future studies.

4.5. Methods

4.5.1. Installation of data-loggers

The monitoring study started on July 23rd 2008 when 25 probes were installed in the four rooms under investigation (exact location shown in Fig. 4.17). One additional device (♯1 in Fig. 4.1) was placed oriented to the east on the top of an outside wall and it was covered with a ceramic tile to protect it against rainwater and sunlight.

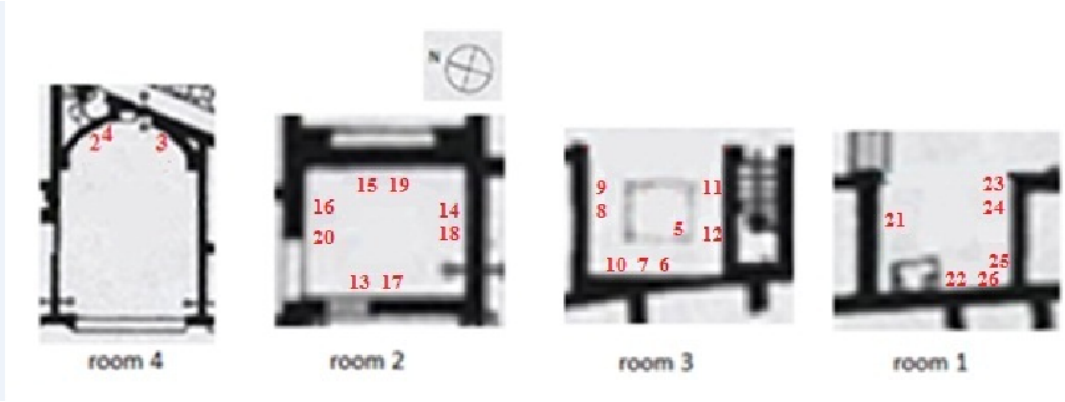

Figure 4.17: Position of thermohygrometric probes. Room code as in Fig. 4.1. Probe ♯5 was installed at the center of room 3 under a glass box on the ground protecting a mosaic. Probes ♯6, ♯8 and ♯11 were located on the floor level under a ceramic tile that was placed to protect them from accidental stepping.

Data recorded by ♯1 cannot be regarded as reference outdoor conditions like those of a meteorological station (due to the specific policy required for their installation). However, in this work ♯1 is used as a reference taking into account its limitations when analyzing the results.

Information about the position of probes (room and wall orientation) is indicated in Fig. 4.17. Table 4.1 shows the height with respect to floor level.

One target was to study the vertical gradient of RH and temperature. For this purpose, data-loggers were placed in the four rooms at three levels: floor, intermediate (15 - 200 cm) and upper position (200 - 338 cm). Thermographic studies carried out previously [21] were also taken into consideration to decide the best location of probes. The intermediate position was omitted in room 2 because it is more isolated from the outside environment and, hence, lower thermohygrometric gradients were expected. Data-loggers in room 4 were not located on the ground because the floor was full of rubble, which might result in microclimate conditions not directly comparable with respect to the floor of the other rooms.

Probe ♯5 was placed inside a glass box that protects a mosaic on the floor of room 3 in order to assess the microclimate inside this box. All probes on the ground except ♯5 were placed near the walls (Fig. 4.17), as otherwise they would hamper the free movement of visitors inside the room. The rest were installed hanging on walls except the reference probe ♯1.

All data-loggers were programmed to register two recordings per hour. Fig. 4.18

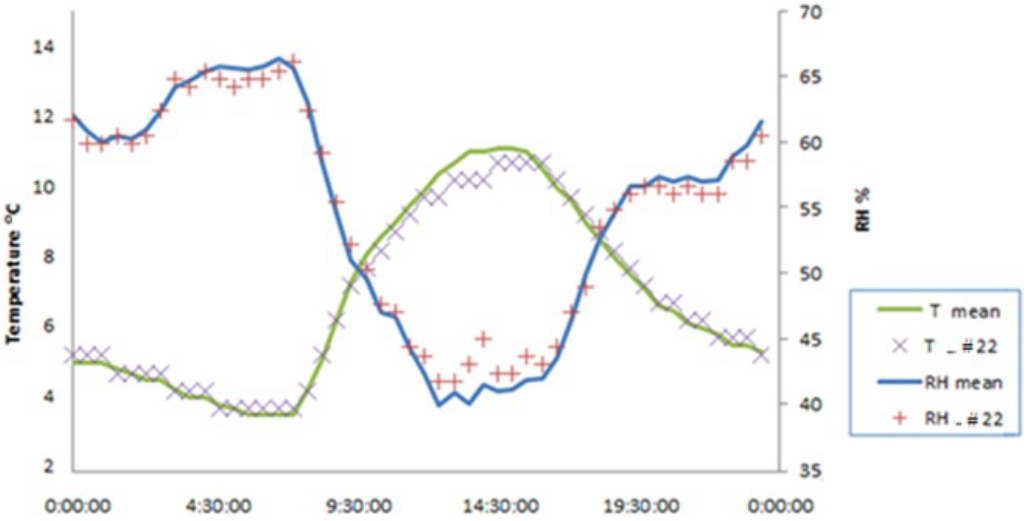

Figure 4.18: Daily time series of probe ♯22. Temperature and RH values registered by one specific probe (♯22) during a day randomly chosen (February 16th 2009) as well as average values collected by the 26 probes. One measurement was recorded every 30 min. According to the manufacturer, the accuracy is ±0.5°C and ±5 % for temperature and RH data-loggers, respectively.

shows that the daily cycles of temperature and RH are clearly reflected by the data of probe ♯22 chosen as example, which suggests that a sampling rate of one measurement every 30 minutes seems convenient.

4.5.2. Calibration of sensors

A calibration experiment is another compulsory step in a methodology of microclimate monitoring. Two different calibration experiments were conducted. The first was carried out in two periods (at the beginning and at the end of the experiment) in order to study if measurements from one or more sensors were biased with respect to the average recorded by all sensors. During both periods, all data-loggers were kept in a small compartment in contact with the indoor air of the laboratory whose conditions varied during the experiment.

For this calibration experiment, all data-loggers were confined inside an 8-liter compartment (20 × 10 × 40 cm) that was not sealed and allowed the inside air to reach an equilibrium of RH and temperature with respect to the outside. This experiment was carried out during a 3- day period (07/18/2008 to 07/21/2008)

prior to the installation of probes in Ariadne's house and during 28 days after the monitoring study (07/31/2009 to 08/28/2009), once all data-loggers were back in the laboratory.

In the first calibration period, temperature ranged from 27.5°C to 29.5°C and RH ranged from 49 % to 60 %. In the second period, the range of temperature was 21.5 - 26°C, and 58 - 82 % in the case of RH.

A further experiment was carried out with aqueous solutions of two salts (lithium chloride and sodium chloride) according to the standard ASTME 104-02 [102] in order to study the measurement errors of RH data-loggers.

4.5.3. Frequency of data recording

The monitoring study started on July 23rd 2008 and ended on July 30th 2009, resulting a period of 372 days.

All data-loggers were programmed to register one measurement every 30 minutes, which implies 1,440 recorded values per month (i.e., 30 days × 24 hours/day × 2 data/hour). Taking into account that these devices are able to store 8,192 registries, it turned out that they could operate for about 5.7 months, which allowed the scientific team to travel conveniently from Spain to Pompeii three times a year to collect the data.

4.5.4. Analysis of variance (ANOVA)

Taking into account that similarities and dissimilarities among trajectories might be different in summer versus winter, a summer period of 61 days was considered from 7/24/2008 to 9/22/2008 (i.e., from the first day of monitoring until the autumnal equinox). Similarly, a winter period of 90 days was considered from 12/21/2008 (winter solstice) to 31/3/2009. For each day and each data-logger, different statistical parameters of RH and temperature were calculated: daily averages, maximum and minimum values. These data were arranged in a matrix comprised by 3,926 rows (i.e., (61 + 90 days) × 26 data-logger). Four factors were considered and included in the matrix: day, season (summer or winter), data-logger code and room code. In order to study if the differences among probes in the same room were statistically significant, multifactor ANOVAs were carried out considering two factors (day and data-logger) and selecting data recorded in summer in one room.

Next, the analysis was repeated for each room and considering only the summer or

winter periods. All ANOVAs were performed using the software Statgraphics 5.1 [103].

Chapter 5

Evaluation of corrective measures implemented for the preventive conservation of fresco paintings in Ariadne's house (Pompeii, Italy)

Evaluation of corrective measures implemented for the preventive conservation of fresco paintings in Ariadne's house (Pompeii, Italy). P. Merello, F.-J. García-Diego, M. Zarzo. *Chemistry Central Journal* 2013, 7 (1), art. no. 87.

This chapter basically corresponds to the publication mentioned above, after correcting a few mistakes and adding some sentences for clarification.

Abstract:

Background: A microclimate monitoring study was conducted in 2008 aimed at assessing the conservation risks affecting the valuable wall paintings decorating Ariadne's House (Pompeii, Italy). It was found that thermohygrometric conditions were very unfavorable for the conservation of frescoes. As a result, it was decided to implement corrective measures, and the transparent polycarbonate sheets covering three rooms (one of them delimited by four walls and the others composed of three walls) were replaced by opaque roofs. In order to examine the effectiveness of this measure, the same monitoring system comprised by 26 thermohygrometric probes was installed again in summer 2010. Data recorded in 2008 and 2010 were compared.

Results: Microclimate conditions were also monitored in a control room with the same roof in both years. The average temperature in this room was lower in 2010, and it was decided to consider a time frame of 18 summer days with the same mean temperature in both years. In the rooms with three walls, the statistical analysis revealed that the diurnal maximum temperature decreased about 3.5°C due to the roof change, and the minimum temperature increased 0.5°C. As a result, the daily thermohygrometric variations resulted less pronounced in 2010, with a reduction of approximately 4°C, which is favorable for the preservation of mural paintings. In the room with four walls, the daily fluctuations also decreased about 4°C. Based on the results, other alternative actions are discussed aimed at improving the conservation conditions of wall paintings.

Conclusions: The roof change has reduced the most unfavorable thermohygrometric conditions affecting the mural paintings, but additional actions should be adopted for a long term preservation of Pompeian frescoes.

Keywords: Microclimate monitoring, Pompeii, archaeological preservation, temperature and relative humidity sensors.

5.1. Background

The long-term preservation of wall paintings in open-air sites or semi-confined environments is a challenge due to the difficulty in providing optimum ambient conditions. In such cases, the deterioration process of paintings is determined by many factors such as petrographical and chemical characteristics of the materials, presence of mineral salts and organic substances on the surfaces, air pollution, sunlight, heating, water content of the surface, etc. [104].

Weathering and disintegration of buildings, masonries and artifacts, as a result of salt efflorescence effects, have been widely studied. Rocks undergo deterioration processes due to temperature changes because most salts have high coefficients of volumetric expansion [105]. Moisture availability and insolation are also climatic variables affecting weathering [106]. Nonetheless, reported evidence indicates that the atmosphere has little corrosive effect on stone in the absence of water. Thus, it is important to monitor the presence of rainwater when assessing the damages caused by weathering in materials of different compositions [107]-[110]. Wide diurnal temperature fluctuations, sun intensity and sporadic heavy rain showers are the propelling factors for the chemical weathering [111].

Wall paintings are very sensitive to multiple factors such as (i) climatic conditions, especially temperature and humidity [12], [56], (ii) presence of soluble salts, (iii) microbiological activity, and (iv) external factors like vandalism or tourism [12]. Indoor environments are more appropriate for the conservation of wall paintings because rainwater is rarely a problem and climatic conditions can be controlled.

Many works have monitored thermohygrometric parameters inside museums for the preventive conservation of their collections [22], [95], [96] as well as in churches [16], [18], [28], [29] but few studies have characterized ambient conditions in semi-confined [17] or open-air archaeological sites [12], [31].

The house of Ariadne or dei *capitelli colorati* (of the colored capitals) is one of the most interesting places in ancient Pompeii (Italy). It is located at less than 100 m from the forum (Regio VII, insula 4) and presents a surface of 1,700 m^2 [41], being one of the largest domus of Pompeian architecture. A 3-D view of the place obtained from a photogrametric scan of the whole ruins [39] shows the remarkable quality of some wall paintings. Detailed pictures of all lodgings in Ariadne's house are available [40].

Although most interior walls were originally ornamented with frescoes, the paintings have suffered severe damages since the excavation of Ariadne's house in 1832-1835. At present, original frescoes are only conserved in three rooms that were sheltered with transparent polycarbonate sheets in the 1970s (coded as 1-3 in Fig. 5.1), and in one additional lodging (room 4, *apsidal exedra*) that was covered in the 1950s with a roof of ceramic tiles (see [40], web link to room number 29). Room 3 (exedra, coded as lodging 18 in [40]) displays a mosaic of Hellenistic inspiration on the floor (84 $\times$ 77 cm) protected with a glass box. The mosaic is probably from the second century BC, and the rest of the floor is paved with tiles of a different style (first century AD). Room 1 (west side of atrium, lodging 6 in [40]) is delimited by three walls, as well as rooms 1 and 4. By contrast, room 2 (oecus, coded as 12 in [40]) is composed of four walls.

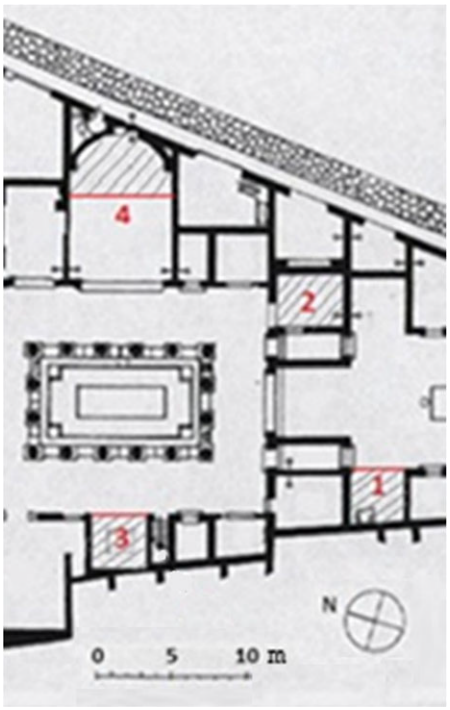

Figure 5.1: Plan of Ariadne's house displaying the four rooms under study. Parallel sloping lines define the roofed area. A more detailed plan of the whole house with pictures of each room is available in [40].

Code	Height[a]	Room	Pictures[b]	Code	Height[a]	Room	Pictures[b]
#3	153	4	3th, 4th at L29	#15	30	2	7th at L12
#4	290	4		#16	0	2	12th at L13
#5	0	3	1st at L18	#17	338	2	4th, 5th, 8th at L13
#6	0	3	1st at L18	#18	300	2	7th , 10th at L12
#7	163	3	1st , 6th at L18	#19	310	2	7th , 9th at L12
#8	0	3	1st, 2nd, 3rd at L18	#20	290	2	7th at L12
#9	189	3	1st, 3rd, 6th at L18	#21	175	1	2nd, 3rd, 17th at L6
#10	340	3	1st , 6th at L18	#22	240	1	3rd, 11th, 12th at L6
#11	0	3	1st , 8th at L18	#23	330	1	3rd, 15th at L6
#12	210	3	6th , 8th at L18	#24	117	1	2nd, 3rd, 15th at L6
#13	0	2	11h at L13	#25	54	1	3rd, 10th, 15th at L6
#14	0	2	2nd at L13	#26	15	1	10th, 11th, 13th at L6

Table 5.1: Position of thermohygrometric probes. [a]Distance to the ground level in cm. Probes ♯6, ♯8 and ♯11 were covered with a ceramic tile that can be seen in [40]. Probe ♯5 was located inside the glass box displayed in lodging 18 of [40]. [b]Pictures in [40] showing the exact position. For example, probe ♯7 appears in the 1^{st} and 6^{th} pictures displayed in [40] after following the link of lodging 18 (L18), which is coded as room 3 in Fig. 5.1. Lodgings (L) numbered as 6, 12 and 29 in the room plan of [40] (coded here as L6, L12 and L29) correspond to rooms 1, 2 and 4, respectively. The link to lodging 13 (L13) in [40] also shows pictures of room 2.

Mural paintings of Ariadne's house have undergone deterioration processes in the last decades, and a research project was launched in 2008 to assess their conservation state by means of microclimate monitoring, thermography, study of materials, solar radiation, characterization of salt efflorescence, etc. [21]. With respect to the microclimate monitoring, a set of 26 thermohygrometric probes were installed in July 2008 inside the covered rooms (Table 5.1).

Each probe was composed of one relative humidity (RH) data-logger and one temperature data-logger. It was found that the transparent roofs produced an unfavorable greenhouse effect causing excessive temperatures, particularly in summer [19]. As a result, the covering of rooms 1-3 was replaced in December 2009 by undulating opaque red roof sheets made of fiber cement with a thickness of about 6 mm, model ColorAGRI® rosso of Edilit SpA (Padova, Italy) [112].

Structural details about the initial roof in rooms 1 and 3 can be seen in [40], following the link to lodgings 6 (1^{st} and 3^{rd} pictures) and 18 (2^{nd} picture). The photographs were taken in March 2009 and show the roof slope as well as the metallic structure supporting the polycarbonate sheets. The water drainage gutter and downspout can also be observed. The uniform height of walls propitiated the roof installation directly fixed to the room upper perimeter (see pp. 97 of [113]),

leaving a negligible ventilation space through the roof borders (less than 5 cm between the shelter and wall top). Such reduced space is not a problem in this case because rooms 1 and 3 are composed of three walls, which allows appropriate ventilation. In room 2, the initial roof was also directly resting on the top of the four walls delimiting this lodging as shown in [40], following the link to lodgings 12 (12^{th} picture) and 13 (5^{th} picture).

The roof change of room 1 performed at the end of 2009 is clearly illustrated by comparing the 3^{rd} picture of lodging 6 [40] with a photograph of this room taken in 2010 [21]. The latter shows that three supporting metal square tubes were installed perpendicular to the existing ones to fix conveniently the fiber cement sheets.

It can also be noticed in this picture that the roof is not perfectly sealed to the wall borders, allowing certain ventilation. The distance between the wall top and the sheets is about 10 cm. Exhaustive details concerning the design of complex shelters mounted on open-air archaeological sites are described for the Villa Arianna at Castellammare di Stabia (see [113], pp. 307-312) and Punta d'Alaca in the Italian island of Vivara (see [113], pp. 319-323). A comprehensive description of the whole covering project is not addressed here because the shelters are relatively simple and the pictures in [40] provide clear information.

In order to assess the effectiveness of the roof change, the data-loggers used in the previous study [19] were installed in the same locations in summer 2010. The present work performs a comparative statistical analysis of data recorded in 2008 and 2010 (summer periods) aimed at evaluating the effect of roof change on the microclimate conditions surrounding the valuable fresco paintings. Results provide guidelines for additional corrective measures.

5.2. Results and discussion

5.2.1. Monitoring periods

As the summer season is the most hostile for the conservation of outdoor wall paintings given the high temperatures and daily variations, it was decided to conduct the study in this season. The monitoring period started on July 20^{th} 2010 and ended on September 15^{th} 2010, resulting a frame of 58 days.

Each temperature data-logger was paired with a RH data-logger by means of a

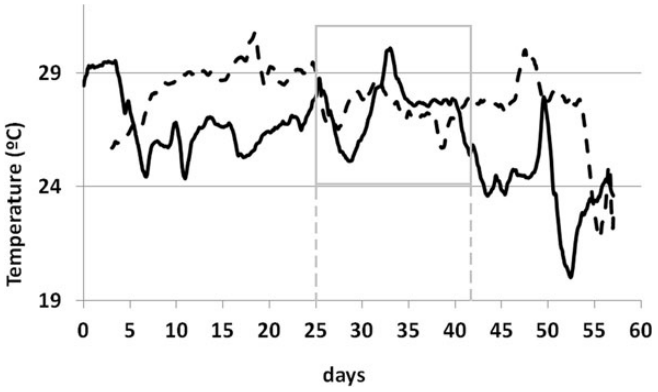

Figure 5.2: Average temperature in summer 2008 and 2010 recorded by data-loggers ♯3 and ♯4 (room 4). Day 0 corresponds to July 20th 2008 (dashed trajectory) and July 20th 2010 (continuous). A moving average with a window size of 48 data (i.e., one day) was applied to smooth both time series. The time frame from day 25 to 42 (highlighted in gray color) presents a similar average temperature in both years.

PVC structure. This assembly will be referred to hereafter as thermohygrometric probe (coded as ♯1 to ♯26 in Table 5.1). All probes were placed inside the 4 rooms under study except ♯1, which was located on the top of an outside wall to serve as a control. Unfortunately, data-loggers of probes ♯1 and ♯2 were wrongly programmed and they were disregarded.

Data recorded in 2008 and 2010 can only be directly compared in the case of similar thermohygrometric conditions outside the rooms. Meteorological data from a weather station in Pompeii would be necessary to check this issue. Unfortunately, the closest stations are located in Naples and Capri, too far away. Given that room 4 was the only one that maintained the same roof, probes located there (♯3 and ♯4) can be used as a reference to compare ambient conditions in both years. Fig. 5.2 shows the average trajectories of temperature in room 4 for the monitored period of 58 days. In this period, the mean temperature was 27.8°C in 2008 and 26.2°C in 2010. The fact that summer 2008 was hotter may lead to a misinterpretation of data from probes in rooms 1-3.

Thus, it is not possible to conclude if the observed differences of temperature in rooms 1-3 are caused by the roof change or are due to the different outside temperatures of each year, which implies that both effects are confounded.

Attempting to avoid this confusion of effects, it was decided to select a time frame of the monitoring period with a similar average temperature in both years inside

room 4. The interval chosen was August 14^{th} to 31^{st} (18 days), as indicated in Fig. 5.2. For probes in room 4, Fig. 5.3.a shows that the mean diurnal evolution of temperature in the 18-day period was nearly the same in 2008 and 2010. Moreover, the average RH was also similar in both years (Fig. 5.3.c). Thus, it was assumed that outside ambient conditions were similar in this time frame of both years. Data out of this interval were disregarded.

The time series recorded by each data-logger reflects the evolution of the measured parameter versus time, and it is commonly denoted as trajectory. By carefully inspecting all trajectories recorded in 2008, it was reported in the previous study [19] that certain probes underwent abnormal peaks of temperature at particular time frames, which was caused by solar radiation incident on the probes. Trajectories obtained in 2010 were also visually examined, and only probe ♯15 yielded atypical temperature peaks from about 5:00 PM to 8:00 PM caused by sunshine entering through the entryway of room 2. The abnormal data were removed.

5.2.2. Mean daily trajectories

The average daily trajectories recorded by data-loggers in the selected 18-day period are displayed in Fig. 5.3, which provides useful information to discuss the effect of roof change on thermohygrometric conditions. Minimum temperatures of each probe were similar in both years, but the maximum values in rooms 1-3 were obtained in 2008.

Similarly, trajectories of RH are also more pronounced in 2008. The microclimate was less hot and less dry after the roof change, which is more favorable from a preservation standpoint.

There is a lack of consensus about the ideal or limit values of thermohygrometric parameters for an optimum maintenance of frescoes. The Italian standard DM 10/2001 [7] indicates reference values for the conservation of cultural heritage. It does not provide guidelines for outdoor paintings, but nonetheless the admissible values suggested by this standard for indoor mural paintings (RH: 45 - 60 % and temperature: 6 - 25°C) can be taken as a reference for the present work.

Figs. 5.3.c and 5.3.d show that RH values below 45 % were recorded at midday in rooms 1-3 in 2008. By contrast, such dry conditions did not occur in 2010 except in room 3. Thus, the roof change has avoided the low RH registered in 2008 that could be regarded as harmful for the frescoes according to [7].

The daily variation of temperature (DVT) for a given day was computed as the

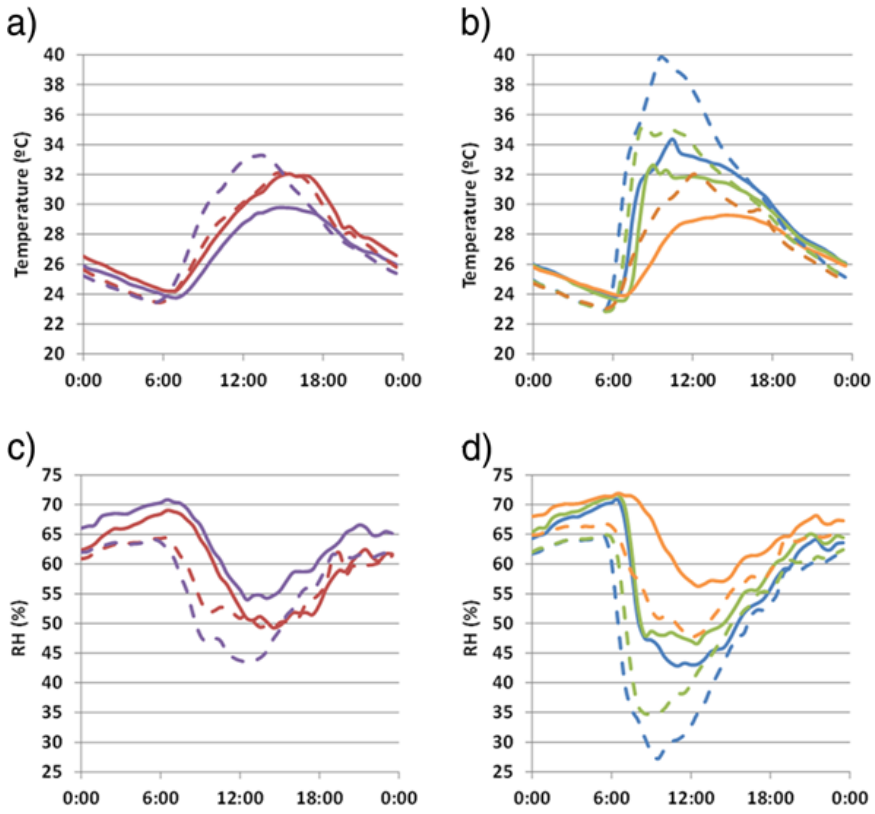

Figure 5.3: Mean daily trajectories of temperature and RH in summer. Figs. (a, b) depict temperature trajectories and (c, d) RH trajectories. Monitoring period: 14-31 August 2008 (dashed trajectories); 14-31 August 2010 (continuous). Trajectories were averaged for all data recorded in each room except by floor probes. Color codes: green (probes in room 1: ♯21 - ♯26); violet (room 2: ♯15, ♯17 - ♯20); blue (room 3: ♯7, ♯9, ♯10, ♯12); red (room 4: ♯3, ♯4); orange (floor probes: ♯6, ♯8, ♯11, ♯13, ♯14, ♯16). The probe inside the mosaic glass box (♯5) was not considered here.

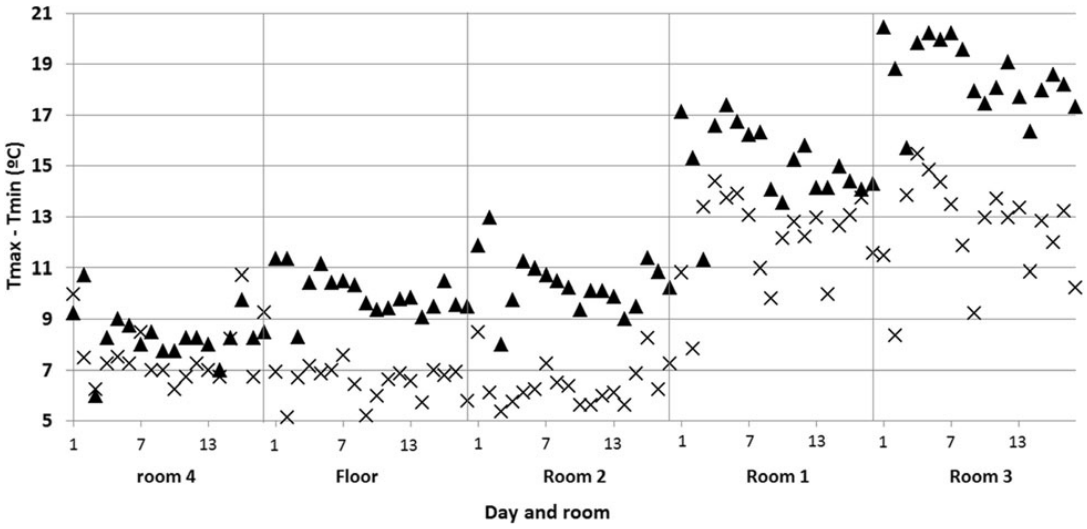

Figure 5.4: Daily variations of temperature for each room. Calculated as the difference between maximum and minimum temperatures recorded during the 18 days under study (filled triangles: 14-31 August 2008; crosses: 14-31 August 2010), averaged for probes in each room (except those in the floor).

difference of the maximum ($Tmax$) and minimum ($Tmin$) recorded values. It is well known that DVT should be kept as low as possible for an optimum conservation of wall paintings. DVT was calculated for the 18 days under study (Fig. 5.4). In 2010, the most stable conditions (i.e., lowest DVT) were found in rooms 2 and 4 as well as floor sensors ($DVT \approx 7$°C).

Room 4 also yielded a similar DVT in 2008 because the roof was maintained and the 18-day time frame was properly chosen to achieve an equal mean temperature in this room for both years.

In 2008, the lowest DVT was achieved in room 4, while data-loggers in room 2 and those on the floor yielded a DVT =10.2°C. Thus, DVT underwent a reduction of about 4°C in room 2 caused by the roof change, becoming the lodging with better conditions for the frescoes.

This room is delimited by four walls and presents a semi-confined environment more isolated from outside fluctuations, which would explain its low DVT in 2010.

DVT was 15.1°C (room 1) and 18.5°C (room 3) in 2008, but it decreased to 12.3°C in 2010. Although this reduction is favorable from a preservation viewpoint, there is still a need to achieve a further decrease of DVT, trying to reach the microcli-

mate of room 2. One option would be to insulate the roof with spray polyurethane foam. Another alternative, though more expensive, is to replace the undulating fiber cement sheets currently covering rooms 1-3 by foam-filled insulated roof sheets.

Although DVT is a good parameter to evaluate the effect of roof change, the opaque shelter has decreased the temperature in rooms 1 and 3 (Fig. 5.3.b) probably due to the different solar radiation incident on the walls through the roof. Preliminary measurements of direct light radiation were carried out in 2008 [21], and a detailed study about indirect light radiation in the rooms with the new coverage will be addressed as part of the on-going conservation project.

Results indicate that the roof change has improved the conditions for the preservation of wall paintings, but not enough. The goal would be to achieve a microclimate in rooms 1 and 3 similar to that in room 2. Thus, a general recommendation to reduce the deterioration of Pompeian frescoes in other houses would be to cover the lodgings with opaque roofs, preferentially containing thermal insulation. Another useful measure would be to avoid direct contact of sunshine radiation in summer by installing some kind of vertical curtains, shades or microperforated fabrics as a parapet hanging on the roof edge.

Probe ♯5 was installed inside the glass box protecting the mosaic in room 3. In 2008, the glass received direct sunshine through the transparent roof, causing a severe greenhouse effect with DVT up to 25°C (Fig. 5.5), which is extremely harmful. This effect was eliminated with the roof change, resulting a DVT of about 7°C, which is similar as in the case of floor probes (Fig. 5.4).

5.2.3. Analysis of variance (ANOVA)

Considering that monitoring frequencies normally used in cultural heritage are 1 datum/hour or 1 datum/day, a simulation has been performed to determine if the ANOVA results can be interesting in these data bases. For doing this, we have simulated a database with a recording frequency of 1 data per day. Daily data have been calculated as the daily average for each sensor.

Thus, in order to further study the effect of roof change, different parameters were calculated for each RH data-logger and each day in both periods under study (14-31 August): maximum ($RHmax$), minimum ($RHmin$) and average. Daily averages of temperature, $Tmax$ and $Tmin$ values were computed as well. Different ANOVAs were carried out considering two factors: data-logger and year.

An effect of sensor height in room 2 is reflected by Fig. 5.6.a. Floor probes recorded

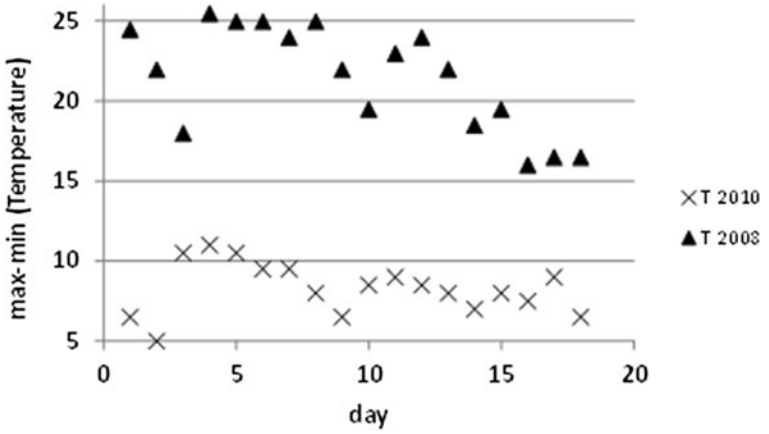

Figure 5.5: Daily variations of temperature for data-logger ♯5 (mosaic). Difference between maximum and minimum temperatures recorded during 18 days (filled triangles: 14-31 August 2008; crosses: 14-31 August 2010).

lower temperatures with a similar mean in both years. By contrast, probes at the upper position (♯17 - ♯20) registered higher values in 2008 due to the effect of solar radiation incident on the upper parts of walls before the roof change. The observed differences are statistically significant ($\alpha = 0.05$) because the LSD (Least Significant Difference) intervals do not overlap.

The pattern of temperature according to sensor height is inversely related to the pattern of RH (Fig. 5.6.b) because higher temperatures imply lower RH and vice-versa.

The observed differences of RH according to year are also statistically significant. Such clear effect of sensor height on thermohygrometric parameters is not so apparent in the other lodgings probably because room 2 is the only one delimited by four walls, which provides more stable conditions.

The $Tmax$ (averaged for the 18-day period) of probes in rooms 1 and 3 is shown in Figs. 5.7.a and 5.7.b, respectively. This parameter is remarkably different among probes in room 3, ranging from 31.5°C (♯11) to 49.1°C (♯9) in 2008 (Fig. 5.7.b). Such variability represents a serious risk for conservation purposes [7]. No significant differences between 2008 and 2010 are observed in probes that recorded the lowest $Tmax$ values (♯6, ♯11, ♯12, ♯24, and ♯25). All of these data-loggers (except ♯6) are located on walls facing to the north, which is the orientation receiving less solar radiation. By contrast, the highest $Tmax$ values, particularly in 2008, were basically recorded by sensors facing to the south (♯8, ♯9 and ♯21).

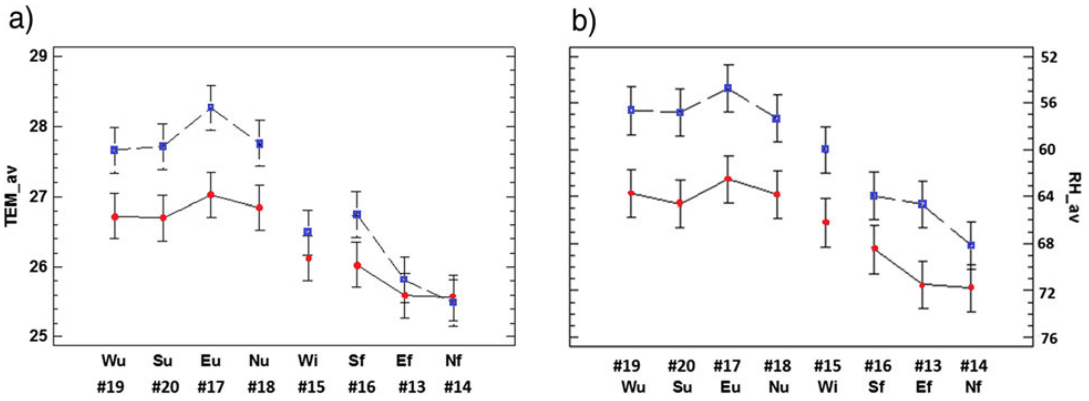

Figure 5.6: ANOVA results (room 2): interaction plot. Plot showing the effect of year (2008: blue squares; 2010: red circles) and data-logger on the daily mean temperatures (a) and RH (b) recorded in room 2 from 14^{th} to 31^{st} of August. Codes indicate the wall orientation (North, South, East or West) and the height (u: upper position; i: intermediate; f: floor level). For each data-logger, the average and 95 % LSD interval is illustrated.

The reduction of solar radiation incident on walls due to the opaque shelter has decreased $Tmax$ in rooms 1 and 3 (♯8, ♯9, ♯10, and ♯21), particularly in those positions that received more sunshine. The change of shelter has also produced a slight increase of $Tmin$ in about 0.6°C in rooms 1 and 3 (Fig. 5.8).

The differences are not statistically significant for all probes because some LSD intervals overlap, but the parallel trend is apparent in both rooms. The decrease of $Tmax$ caused by the roof change and the slight increase of $Tmin$ results in a lower DVT in 2010 (Fig. 5.4), which involves that the microclimate was more stable throughout the day and, hence, more appropriate for conservation purposes.

5.2.4. Bivariate plots

Fig. 5.9.a displays a scatterplot of $Tmax$ in 2010 vs. $Tmax$ in 2008. Probes ♯3 and ♯4 appear on the bisector line (i.e., equal mean values in both years), which indicates that the 18-day period was correctly selected. Some additional probes are also close to the bisector, but most of them yielded a lower $Tmax$ in 2010 as discussed above. The high $Tmax$ of ♯9, ♯10 or ♯21 is also reflected in Fig. 5.7, but Fig. 5.9.a provides complementary information because all probes are depicted. The bivariate plot of $Tmin$ in 2010 vs. $Tmin$ in 2008 (Fig. 5.9.b) is consistent with Fig. 5.8 and reveals that $Tmin$ was about 0.6°C higher in 2010 on average compared with 2008, except

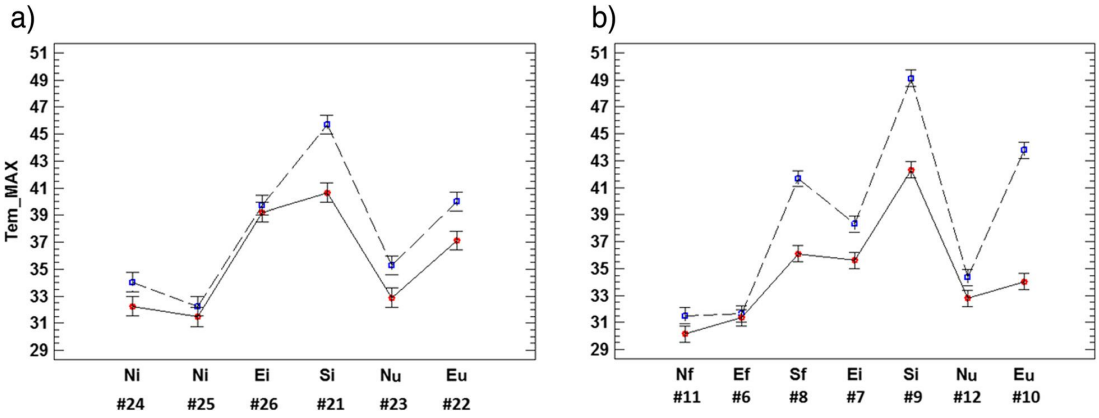

Figure 5.7: ANOVA results of $Tmax$ in rooms 1 and 3: interaction plot. Plot (average and 95 % LSD intervals) showing the effect of data-logger and year (2008: blue squares; 2010: red circles) on the daily maximum temperatures in room 1 (a) and room 3 (b) from August 14^{th} to 31^{st}. Codes as in Fig. 5.6.

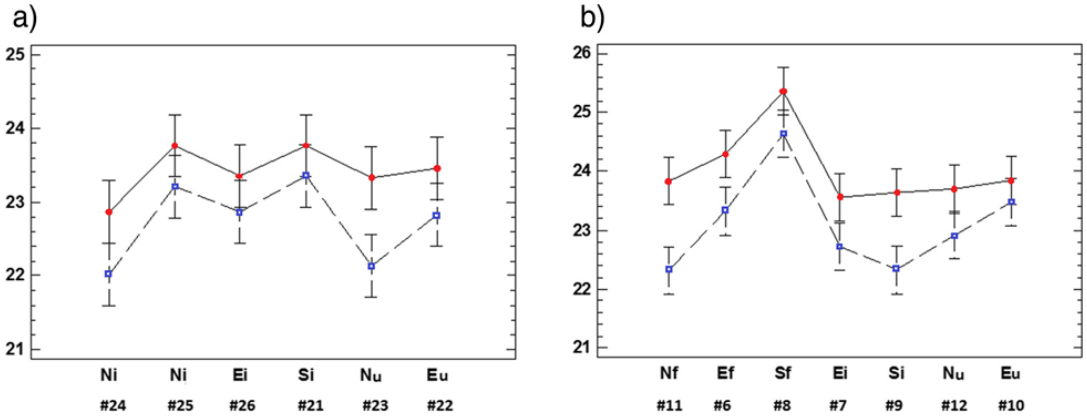

Figure 5.8: ANOVA results of $Tmin$ in rooms 1 and 3: interaction plot. Plot of factors data-logger and year (2008: blue squares; 2010: red circles) on the daily minimum temperatures in room 1 (a) and room 3 (b). Codes as in Fig. 5.6.

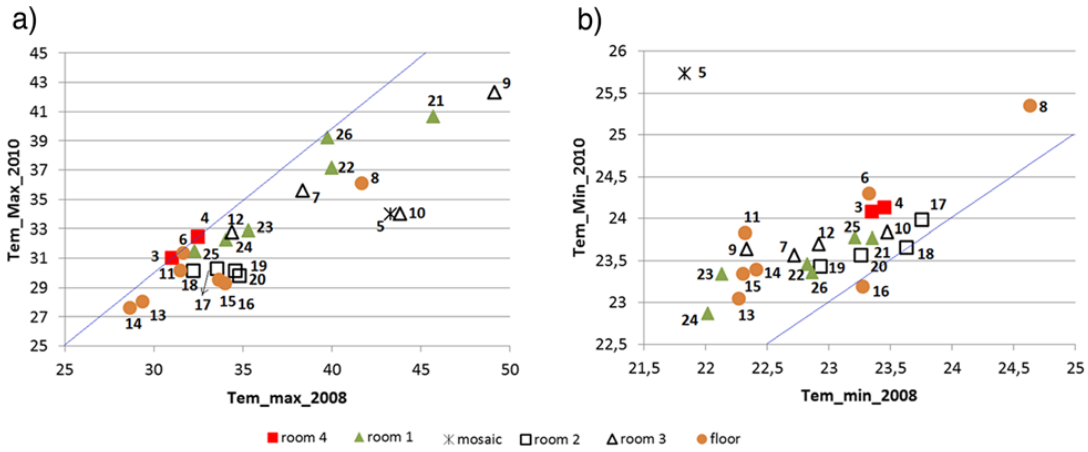

Figure 5.9: Bivariate plot of daily maximum ($Tmax$) and minimum ($Tmin$) temperatures in 2010 vs. 2008. Bivariate plot of $Tmax$ (a) and $Tmin$ (b) recorded from each probe in 2010 vs. 2008 (monitoring period: 14^{th} to 31^{st} of August). The tilted line is the bisector.

in the case of room 2 with 0.3°C of variation.

RH and temperatures measured during one day by a given probe were negatively correlated according to Fig. 5.3 because the maximum temperatures recorded at midday correspond to the minimum RH. Moreover, probes that yielded the highest temperatures ($Tmax$) also recorded the lowest RH ($RHmin$), which was also reported in the previous study [19]. This inverse relationship between $Tmax$ and $RHmin$ shows up by comparing Figs. 5.9.a and 5.10.a because the relative position of probes in both figures is basically the same. There is also certain similarity between $Tmin$ (Fig. 5.9.b) and $RHmax$ (Fig. 5.10.b).

In 2010, half of the probes registered $RHmin$ values above 45 %, but only two probes (♯13 and ♯14) satisfied this condition in 2008 (Fig. 5.10.a). Taking into account that 45-60 % is the recommended range of RH according to [7] for mural paintings, this result implies that the change of roof has improved the RH conditions from a conservation standpoint. In the case of $RHmax$ (Fig. 5.10.b), the points follow a linear trend, and it can be deduced that RH increased around 6 units in 2010 with respect to 2008.

Probe ♯5 was affected by a severe greenhouse effect in 2008 that is no longer present in 2010, but it behaves as an outlier in Figs. 5.9.b and 5.10.b, with an abnormal low $RHmax$ and a high $Tmin$. The interpretation is uncertain because ♯5 was the only probe inside the glass box protecting the mosaic. The microclimate inside this

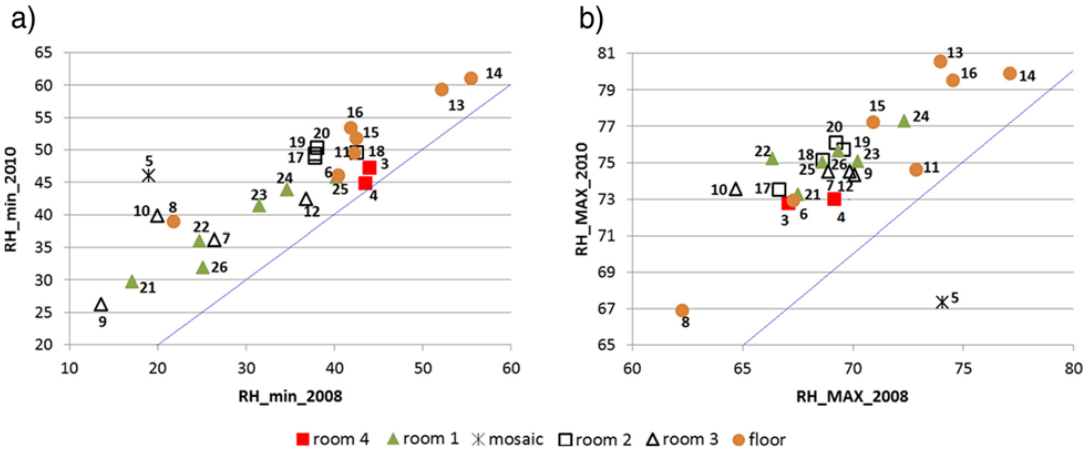

Figure 5.10: Bivariate plot of daily minimum ($RHmin$) and maximum ($Tmax$) relative humidities in 2010 vs. 2008. Bivariate plot of $RHmin$ (a) and $RHmax$ (b) recorded from each probe in 2010 vs. 2008 (14th to 31st of August). The tilted line is the bisector.

box is totally confined and cannot be directly compared with ambient conditions in the rooms.

5.2.5. Efficiency of transparent vs. opaque shelters

A list of 222 covered archaeological sites in Italy is available in the literature (see annex of [113]), 38.7 % of which are regarded as shelters with an intermediate efficiency and 59 % as highly efficient. The tile roof of room 4 appears in this list as highly efficient, with a score of 7.1 on a 0-10 scale, while transparent shelters covering the other rooms scored 5.5 (intermediate). However, these scores were calculated using qualitative criteria not based on microclimate studies. In our opinion, such efficiency index may provide a rough guidance for archaeological sites curators, but it could be improved by taking into consideration parameters derived from multivariate microclimate monitoring studies. The present work may provide guidelines for a methodology aimed at comparing the efficiency of shelters in different locations.

5.3. Experimental

5.3.1. Description and installation of data-loggers

The same set of RH and temperature data-loggers (models Hygrochron DS1923 [100] and Thermochron DS1922L [101], respectively) used in the previous study [19] was reinstalled in Ariadne's house in July 2010. According to the manufacturer (Maxim Integrated Products, Inc., Sunnyvale, CA), the accuracy is ±5 % RH [100]. All dataloggers were calibrated prior to their installation in 2008 as described in [19]. Based on the calibration experiment, it was obtained that the temperature biases ranged from −0.44°C to +0.53°C (see Table 1 of [19]), which is nearly coincident with the accuracy range (±0.5°C) indicated by the manufacturer [100]. These biases were corrected as described in [19] to improve the accuracy of temperature measurements. Another calibration experiment was carried out in 2010 with RH sensors by comparing their measurements with reference values of a standard procedure based on aqueous solutions of two salts (NaCl and LiCl) [102], resulting a bias below 1 % for all data-loggers. RH recordings were corrected taking into account the experimental biases to improve the accuracy.

Each probe was composed of one pair of DS1923 and DS1922L data-loggers assembled together by means of a PVC protective structure with a cylindrical shape (6 cm of diameter), which allows a convenient fixing to the wall. One measurement was recorded from each data-logger every 30 minutes, which involves 48 recordings per day. All probes were placed in the same positions as in the monitoring experiment of 2008 [19] in order to allow an appropriate data comparison of both years. The purpose was to locate data-loggers in the four rooms at three levels: floor (0 - 15 cm), intermediate (< 2 m) and upper position (> 2 m) (Table 5.1).

5.3.2. Statistical data analysis

Firstly, we computed the mean values recorded in 2010 by each data-logger at 0:00, 0:30, 1:00... and so on until 12:00 PM, resulting a daily mean trajectory. The calculation was performed with the set of 18 days under study (14-31 August), which were selected to achieve an equal mean temperature in room 4 in both years. All trajectories were visually inspected in order to detect abnormal peaks as those identified in the previous study [19].

Next, trajectories of probes in the same room were averaged, except those on the ground that were set aside (Fig. 5.3). This procedure was also applied to data

recorded in the same time frame of 2008, and the differences were discussed.

For each day and probe, the following parameters were computed: mean temperature, mean RH, $Tmax$, $Tmin$, $RHmax$, and $RHmin$. One important parameter frequently considered in the conservation of cultural heritage [7] is the daily variation of temperature (i.e., $Tmax$ - $Tmin$). This parameter was computed for the 18-day period of each year and it was averaged for probes in the same room, which provides useful information about the effect of roof change (Fig. 5.4). In order to study if the differences among probes in the same room were statistically significant, different multifactor ANOVAs were performed with the key thermohygrometric parameters considering two factors: year (2008 or 2010) and probes (Figs. 5.6, 5.7, 5.8). All ANOVA models were carried out with the software Statgraphics 5.1 [103].

Attempting to further characterize the differences among probes according to year, different bivariate plots (Figs. 5.9 and 5.10) were obtained with $Tmax$, $Tmin$, $RHmax$, and $RHmin$ (averaged for the 18 days). They provide further information about the relationship between RH and temperature. RH values were discussed according to the guidelines for indoor mural paintings indicated by the Italian standard DM 10/2001 [7].

5.4. Conclusions

The statistical analysis has revealed a considerable reduction of about 3.5°C in the maximum daily values reached in summer at rooms 1 and 3 caused by the roof change.

Results show that this corrective measure adopted in 2009 has lowered the maximum temperatures and has also increased the RH and minimum temperatures, which entails an attenuation of daily variations of thermohygrometric conditions. Thus, the roof change has created a microclimate more stable and less harmful for the conservation of frescoes.

The steadiest ambient conditions were found in room 2, which is intuitively appealing because this room is delimited by four walls and the microclimate inside is more isolated from outdoor fluctuations. The roof change has enhanced the conditions in rooms 1 and 3 from a preservation standpoint, but they can be further improved to resemble those in room 2. For this purpose, several additional corrective measures are proposed.

An effect of sensor height was detected in room 2. The higher temperatures recorded there at the upper positions were due to diffuse solar radiation incident on walls through the transparent roof in 2008. In rooms 1 and 3, it was also found that sensors facing to the south recorded higher temperatures particularly in 2008, probably because the south orientation received more solar radiation before the roof change.

The methodology of data analysis applied here is also of interest for similar studies aimed at comparing thermohygrometric data recorded in different periods, because it is necessary to avoid the confusion of effects that appears when the average conditions of the periods are different.

Chapter 6

Diagnosis of abnormal patterns in multivariate microclimate monitoring: a case study of an open-air archaeological site in Pompeii (Italy)

Diagnosis of abnormal patterns in multivariate microclimate monitoring: a case study of an open-air archaeological site in Pompeii (Italy). Merello, P., García-Diego, F.-J., Zarzo, M. *Science of the Total Environment* 2014, 488-489(1), 14-25. DOI: 10.1016/j.scitotenv.2014.04.068

This chapter basically corresponds to the publication mentioned above, after correcting a few mistakes and adding some sentences for clarification.

Abstract: Chemometrics has been applied successfully since the 1990s for the multivariate statistical control of industrial processes. A new area of interest for these tools is the microclimatic monitoring of cultural heritage. Sensors record climatic parameters over time and statistical data analysis is performed to obtain valuable information for preventive conservation. A case study of an open-air archaeological site is presented here. A set of 26 temperature and relative humidity data-loggers were installed in four rooms of Ariadne's house (Pompeii). If climatic values are recorded versus time at different positions, the resulting data structure is equivalent to records of physical parameters registered at several points of a continuous chemical process. However, there is an important difference in this case: continuous processes are controlled to reach a steady state, while open-air sites undergo tremendous fluctuations. Although data from continuous processes are usually column-centred prior to applying principal components analysis, it turned out that another pre-treatment (row-centred data) was more convenient for the interpretation of components and to identify abnormal patterns. The detection of atypical trajectories was more straightforward by dividing the whole monitored period into several sub-periods, because the marked climatic fluctuations throughout the year affect the correlation structures. The proposed statistical methodology is of interest for the microclimatic monitoring of cultural heritage, particularly in the case of open-air or semi-confined archaeological sites.

Keywords: multivariate monitoring, outlier detection, relative humidity sensors, temperature sensors, preventive conservation, cultural heritage.

6.1. Introduction

One of the requirements for the preventive conservation of cultural heritage is the monitoring of factors involved in deterioration processes of artworks [1]. The measurement of thermo-hygrometric parameters such as temperature and relative humidity (RH) is a priority [7]. Microclimatic conditions are routinely controlled in museums [22]-[27] given the importance of maintaining RH and temperatures within the recommended optimum intervals [7], which is easily achieved in most cases given the current technology of air conditioning systems. Several works have also studied the indoor environment in churches [16],[18],[28],[29] which often contain valuable artworks. The control of microclimatic conditions inside these buildings is rarely a technical challenge, and undoubtedly the most complex problem consists of achieving an optimum conservation environment in open-air sites. In such cases, it is of interest to evaluate the effect of climatic parameters on the conservation of

artworks in order to propose corrective actions.

Few works have studied microclimatic conditions in semi-confined [17],[21],[30] or open-air archaeological sites aimed at preventive conservation [12],[31]. Nava *et al.* [17] assessed air pollution threats to cultural heritage in a semi-confined environment by means of thermographic measurements on wall paintings, microclimatic analysis and gaseous pollutant monitoring. Another work has proposed a monitoring system for the biological control of historic timber structures aimed at preventing biodeterioration by fungi and insects [30]. Lillie *et al.* [12] performed a monthly monitoring of water levels, pH and redox potential in waterlogged crannogs of south-west Scotland. Maekawa *et al.* [31] gathered climatic data over two years to assess the effect of weather conditions on the conservation state of monuments in Tiwanaku (Bolivia).

Regarding the microclimate monitoring of open-air sites, it is necessary to install sensors in several locations at the place of interest. The registered data will provide information on different ambient conditions among these locations. The statistical analysis can be conducted by means of descriptive methods using summary statistics (e.g. average, median and variance) or bivariate plots, among other basic techniques. Despite their simplicity, these methods are often applied in this context [12],[19],[31] although multivariate statistical tools like principal components analysis (PCA) are more powerful. However, their application is not yet widely used in cultural heritage and few studies have been published [16],[18],[33]. The present work reports, probably for the first time, the advantages of PCA in the multivariate microclimate monitoring of an open-air archaeological site.

Microclimatic monitoring systems record several parameters at different positions. The resulting data structure is equivalent to measurements of variables like temperature or pressure registered vs. time at several points of a continuous chemical process. Thus, chemometric tools developed for the multivariate statistical control of industrial processes can also be applied for this case. In the field of process chemometrics, there is abundant literature available on multivariate methods for the monitoring, diagnosis and fault detection in continuous [114]-[117] and batch chemical processes [118]-[120].

As a case study, the present work applies PCA to identify abnormal patterns and to assess the differences among sensors installed in Ariadne's house (Pompeii). This *domus* (i.e., a single-family house owned by the upper classes) is situated in a privileged location at the city centre. It is a *domus* of Hellenistic inspiration composed of 31 rooms with an extension of 1,700 m^2. Ariadne's house is of great archaeological value because some walls still display fresco paintings of a remarkable quality, despite the destruction caused by the eruption of Mount Vesuvius in the

year 79 AD. The paintings exhibit an interesting decorative diversity and comprise different pictorial phases, from the first to the fourth Pompeian style [121].

To protect the frescoes from rainwater, in the 1970s three rooms of Ariadne's house were covered with polycarbonate sheets [21]. In the 1950s another room was partly sheltered with a roof of ceramic tiles. Fresco paintings in these covered lodgings have survived up to the present day, though in a delicate condition, but most frescoes in the other rooms have entirely disappeared due to the impact of rainwater and the unfavourable weather. Optimum conditions for the conservation of indoor paintings are indicated in the Italian standard UNI 10829 [83] and DM 10/2001 [7]. The latter recommends a range of 45 - 60 % for RH and 6 - 25°C for temperature, but no guidelines are provided for the preservation of outdoor frescoes.

Given the serious deterioration risks affecting the valuable paintings, a multidisciplinary conservation project was launched in 2008. The team studied the problems of atmospheric pollution, salt efflorescence and other pathologies associated with the materials in order to determine the causes of fresco degradation and propose conservation actions. It was found that the deterioration was mainly caused by inappropriate temperatures and RH inside the rooms [21]. Studying the different microclimatic conditions according to the room, sensor height and wall orientation is particularly important in summer due to the high temperatures, which represent a serious risk for the conservation of fresco paintings [19].

PCA is applied here to analyse temperature and RH values recorded in Ariadne's house during 372 days. Different objectives are proposed. First, it is of interest to identify abnormal trajectories that deviate from the common pattern of variability. Another target is to characterise the evolution of thermo-hygrometric parameters throughout the year.

6.2. Methodology

6.2.1. Monitoring system and sensor calibration

As part of the multidisciplinary conservation project, a microclimate monitoring system was set up to assess the environment surrounding fresco paintings in the four roofed rooms, coded as 1-4 in Fig.1 of [19]. Room 2 is delimited by four walls, but the north-east wall is missing in rooms 1 and 3. Room 4 is partly covered by an opaque roof that protects a semicircular wall oriented to the south-west. A detailed

plan of Ariadne's house (*Regio* VII, *insula* 4) with pictures of each room is available in [40].

One thermo-hygrometric probe (coded as ♯1) was placed on the top of an outside wall to monitor outdoor ambient conditions, and 25 probes of the same type were located inside the four covered rooms. Each probe consists of one temperature data-logger (model Thermochron DS1922L) and one RH data-logger (model Hygrochron DS1923) (see [19] for technical details). Some probes were placed on the floor (♯5, ♯6, ♯8, ♯11, ♯13, ♯14, and ♯16), others were installed on walls at more than 2 m from the ground level (♯4, ♯12, ♯17, ♯18, ♯19, ♯20, ♯22, and ♯23) and the rest at an intermediate position (see Table 1 of [19] for exact height). All data-loggers were calibrated in laboratory prior to their installation as described in [19].

Although the best monitoring system would be a centralized data acquisition system, in this particular case it could not be done this way because of the lack of power supply.

The monitoring experiment started on July 23^{rd} 2008 and ended on July 30^{th} 2009. During this period of 372 days, each data-logger recorded one measurement every 30 minutes.

6.2.2. Data structure and statistical analyses

The time series of a given parameter recorded by one sensor reflects the evolution vs. time of the measurements, and is often known as trajectory. In a previous analysis of the same dataset [19], part of the recordings from data-loggers ♯2, ♯3 and ♯9 were discarded because they were identified as abnormal by visually inspecting the trajectories. Nonetheless, all recorded data were considered here in order to discuss the most appropriate data pre-treatment and methodology for the detection of outliers. The initial data matrix of temperature consists of 17856 rows (i.e., time observations: 372 days $\times$ 48 data/day) by 26 variables in columns, one corresponding to each temperature data-logger. The dataset of RH presents the same structure, as there were also 26 RH data-loggers. Note that temperature and relative humidity data are analysed separately, as Ariadne's house is an open-air archaeological site, so temperature and relative humidity are not necessarily related, as there may be a contribution from outdoor humidity.

For the initial matrix of temperature, two types of data pre-treatment were applied. One option was to centre the columns by subtracting the mean (i.e., average value recorded by a given data-logger), so that the mean becomes null for all centred columns. This pre-treatment is frequently applied for the multivariate statistical

control of continuous chemical processes. An alternative method, which has been used in other reported studies [16],[18], was to centre the rows by subtracting the mean (i.e., average temperature recorded by all data-loggers in a certain instant of time). Next, PCA was carried out with each centred matrix in order to discuss the advantages and disadvantages of each type of data pre-treatment. All PCAs were performed using the software SIMCA-P (Umetrics, Umea, Sweden). Loading plots with different combinations of PCs were visually inspected to study which PCs were influenced by data-loggers with an abnormal performance. The distance to the PCA model was also used to identify outliers.

A common approach in multi-phase batch chemical processes is to fit a different statistical model for each stage [122]. In this case, it was decided to split the monitored period of 372 days into several sub-periods with similar climatic conditions, taking into account that relationships among data-loggers might be significantly altered from season to season. For this purpose, we used CUSUM charts (cumulative sums), which are widely applied in process control to detect shifts in a monitored variable. A reported work has employed these charts to detect shifts throughout the year in the performance of a batch chemical process [123]. CUSUM charts were obtained for the average daily temperature recorded all year round in Pompeii, as well as in two nearby weather stations (Capri and Naples). Based on the comparison of these charts, it was decided to split the temperature matrix into four sub-periods: warm, transition, cold and transition, with 6504, 2429, 6955 and 1968 time observations each, respectively. The RH matrix was divided into three sub-periods: dry, transition and humid, with 7152, 4272 and 6432 time observations, respectively. Next, PCA was applied to each sub-period except for the two transition stages of temperature. To further study the underlying latent structures responsible for the data variability, PCA models were repeated after discarding the atypical values recorded by some probes.

6.3. Results and Discussion

The results are presented in the following order. First (section 6.3.1), the data pre-treatment is discussed with the objective of identifying anomalous trajectories as well as possible. After identifying the most suitable pre-treatment (row-centred), a selection of periods is performed by determining trend changes in CUSUM charts of average daily data of the data-loggers and two nearby weather stations (section 6.3.2). According to these results, PCA of temperature and RH data are performed by periods (section 6.3.3), more rigorously identifying the anomalous trajectories

in this way. Finally, after excluding the outliers, PCA is performed by periods (section 6.3.4 and 6.3.5) with the interest of identifying the specific behaviour of sensors according to their position in Ariadne's house.

6.3.1. Discussion of data pre-treatment

Multivariate systems for the monitoring of microclimatic conditions are based on a set of sensors that register climatic values over time. The same data structure is obtained when temperatures or pressures are recorded in a continuous chemical process. Such processes are controlled to achieve the minimum deviations of variables from the optimum operative conditions once the process reaches the steady state [114],[116]. The data structure is a matrix of variables (in columns) recorded at multiple instants of time (observations) that is usually column-centred prior to the multivariate statistical analysis. The present case is an uncontrolled continuous process, given the tremendous fluctuations of thermo-hygrometric conditions registered throughout the year in open-air sites. Thus, it is relevant to discuss if the column-centre pre-treatment is the best option to study the relationships among data-loggers and to identify abnormal patterns. To this end, only the recordings of temperature were considered because they reflect atypical patterns in some data-loggers more clearly than in the case of RH (see Fig. 4 of [19]).

The initial temperature matrix was analysed with PCA after applying one of the pre-treatments. The percentage of explained variance for the 6 principal components is indicated in Table 1. The loading plot for the first and second principal components (PC1, PC2) according to the type of pre-treatment is shown in Fig. 6.1. If p[1] loadings of each pre-treatment are compared, it turns out that there is no correlation between them ($r = -0.311$, $p = 0.122$).

If temperatures are plotted vs. time for all data-loggers (see Fig. 4 of [19]), it can be observed that daily cycles are clearly marked, resulting in a common pattern of data variability. If all trajectories had been perfectly parallel, the mean temperature recorded by each data-logger would be the most representative value. This is not exactly the case here because some data-loggers undergo more pronounced daily fluctuations, but nonetheless their mean temperature is slightly correlated with p[1] loadings in the column-centred PCA ($r = -0.378$, $p = 0.047$) and strongly correlated in the row-centred PCA ($r = 0.919$, $p < 0.01$).

Thus, using the row-centre pre-treatment, PC1 provides a clearer physical interpretation and also PC2 provides information about the different shape of the trajectories, but the interpretation of PC2 is not so straightforward in the other pre-treatments.

	Column-centered data		Row-centered data		
PC	R^2	Q^2	R^2	Q^2	Q^2_{limit}
1	0.965	0,966	0.675	0.641	0.037
2	0.021	0,018	0.082	0.040	0.039
3	0.004	0,0021	0.066	0.050	0.040
4	0.002	-0,0012	0.031	0.005	0.042
5	0.001	0,0000	0.026	-0.001	0.044
6	0.001	-0,021	0.022	0.003	0.046

Table 6.1: Summary overview of the 6 principal components obtained from the initial matrix of temperature (monitoring period of 372 days) with two different types of data pretreatment: variance explained (R^2), cross-validated variance (Q^2) and threshold value (Q^2_{limit}).

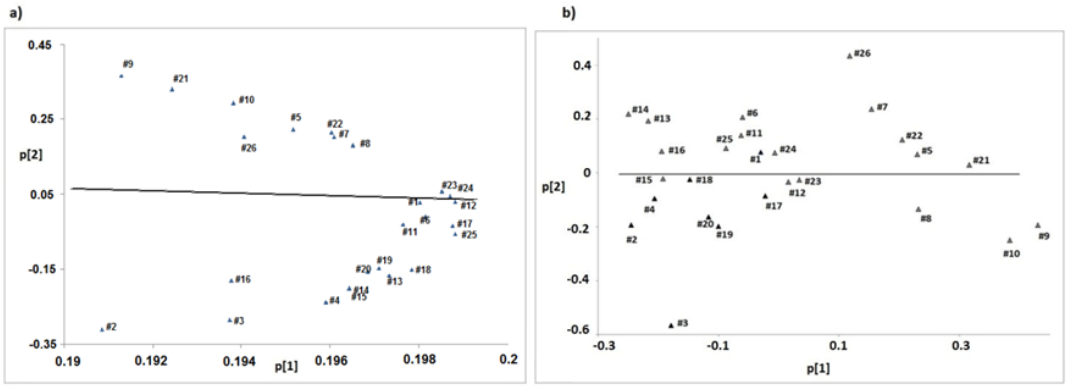

Figure 6.1: Loading plot (p[2] vs. p[1]) of the PCA applied to the initial matrix of temperature (monitoring period of 372 days). a) Column-centred data, b) row-centred data. The fitted regression line is also indicated ($R^2 = 0.036$ and $R^2 \approx 0$, respectively).

Regarding the number of PCs to be studied, it can be assumed that a given component provides relevant information if the cross-validated explained variance (Q^2) is higher than the threshold considered by the software (Q^2_{limit}). This criterion is not satisfied by PC2 in the case of column-centre pre-treatment (Table 6.1). In the case of row-centre pre-treatment, PC2 is significant and the results of some studies indicate that it provides relevant information (such as the detection of the anomalous trajectory of data-logger ♯3, figure 6.1.b). In the case of further components not satisfying the Q^2_{limit} criterion, some studies indicate that they provide relevant information regarding the detection of the anomalous trajectories (Figures 6.5-6.7).

This result is another indication that the row-pre-treatment seems more sensitive for the detection of relevant information.

PC3 satisfies the cross-validation criterion, but not PC5 or PC6 (Table 1). PC4 is very close to the threshold value, which requires further investigation. In order to check if PC4 accounts for systematic data variability, the loading plot for PC3 and PC4 was visually inspected (Fig. 6.2), which reveals that both PCs provide almost the same information regardless of the type of pre-treatment. The main difference is observed in data-logger ♯3, which presents certain periods of abnormal values. Thus, it seems that four components properly explain the data variability of the initial temperature matrix.

Checking the distance of observations (i.e., matrix rows) to a given PCA model usually provides useful information for the detection of outliers. However, in this case it is of interest to identify data-loggers (i.e., matrix columns) with an abnormal performance. Thus, both row-centred and column-centred temperature matrixes were transposed and then PCA was applied. The distance to the PCA models fitted with one or two components is depicted in Fig. 6.3.

Data-loggers ♯2, ♯3 and ♯26 clearly present an excessive distance, while ♯5 is close to the threshold borderline. Probes ♯9 and ♯21 appear as outliers more clearly using the column-centre pre-treatment, but the alternative option seems more effective to highlight the unusual pattern of ♯16. Distances to the PCA model effectively reveal sensors with uncommon trajectories, but results do not provide clear evidence about which pre-treatment is more convenient. Calculating these distances with more than 2 components does not seem appropriate here, because PC3 is influenced by abnormal data-loggers (♯9, ♯16 and ♯26) as well as PC4 (♯3 and ♯16), as revealed by Fig. 6.2.

By visually inspecting all trajectories of temperature, it was reported [19] that ♯3 recorded unusual daily peaks in summer at about 2:00 PM, and recovered the common pattern at 8:00 PM approximately. Additionally, ♯2 also underwent atypical

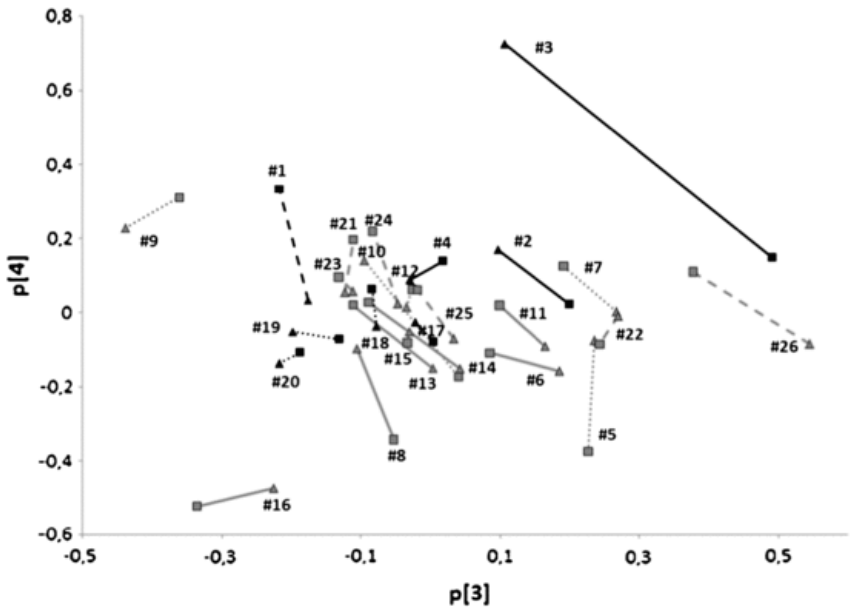

Figure 6.2: Loading plot (p[4] vs. p[3]) of the PCA applied to the initial column-centred matrix of temperature (triangles), overlapped with the equivalent loading plot for the row-centred matrix (squares). Continuous lines: grey (data-loggers on the floor), black (room 4); dotted lines: grey (room 3), black (room 2); dashed grey line (room 1).

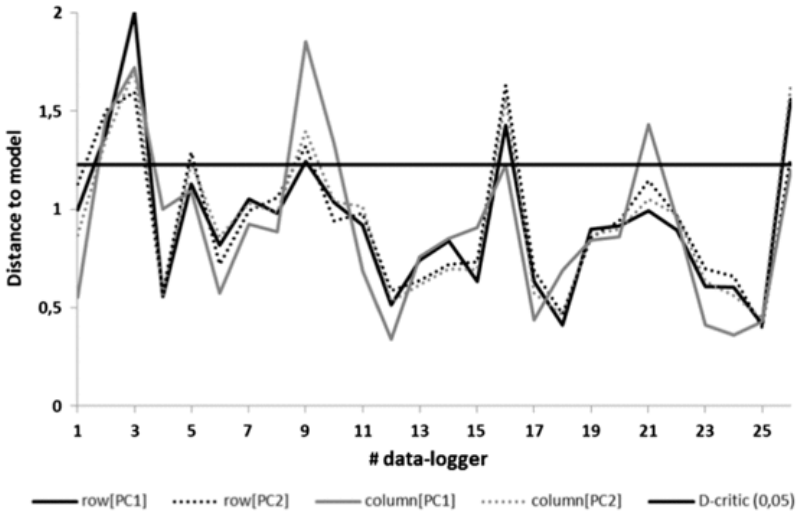

Figure 6.3: Distance to the PCA model with one component (continuous lines) or two components (dotted lines), fitted to the initial matrix of temperature. Prior to applying PCA, the matrix was column-centred (grey lines) or row-centred (black lines) and transposed next. Distances exceeding the critical threshold (D-critic = 0.05) can be regarded as atypical. Labels in the x-axis indicate the sensor code.

fluctuations in winter from about 2:30 PM to 6:30 PM. The time series of ♯9 also reflects sudden peaks of temperature in winter from 8:30 AM to midday (see Fig. 8b of [19]). The reason for such anomalies was the action of direct sunlight incident on these particular probes in a certain daily time frame, which depends on their exact position, height and wall orientation [19].

Probes ♯16 and ♯26 present an excessive distance to the models, but no unusual performance was detected in the previous reported study of the data [19]. A further careful analysis of their trajectories has revealed that ♯26 underwent an abnormal peak of temperature in the warm period from 7:30 AM to 11:00 AM (Fig. 6.4). Similarly, it turns out that ♯16 registered higher temperatures during a short time interval, around 1:00 PM, due to direct sunshine that reached the probe about that time.

The uncommon performance of ♯21 revealed by Fig. 6.3 is probably due to a slightly different shape of the trajectory as a result of very high temperatures recorded in summer. Actually, this data-logger was installed on a south-facing wall, which received more sunlight. The high p[1] value of ♯21 in Fig. 6.1b is an indication of the higher temperature.

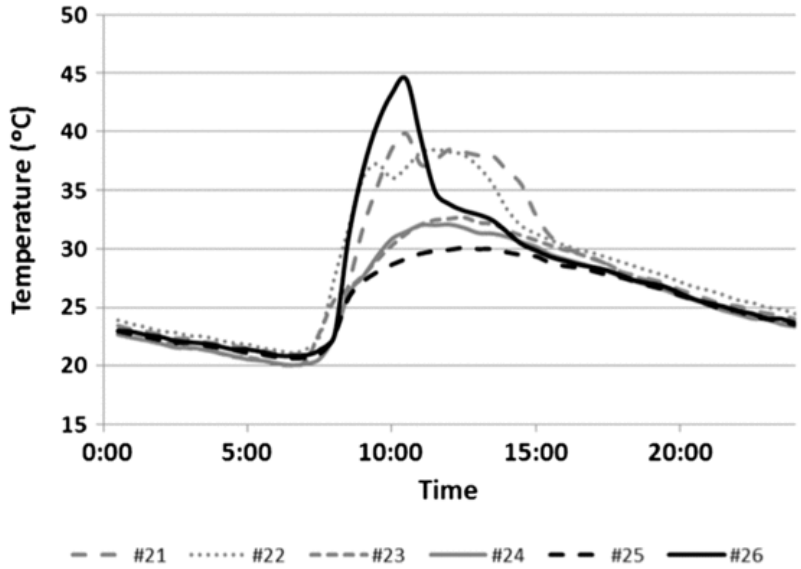

Figure 6.4: Mean daily trajectories of temperature. For data recorded by data-loggers in room 1 during five days (9^{th} - 13^{th} June 2009).

Those probes that registered abnormal temperature trajectories may account for the data variability of certain PCs. Thus, another way to identify atypical trajectories is to check the loading plots with different combinations of PCs. Fig. 6.5 shows the best combination that leads to the identification of ♯2 as an outlier. The uncharacteristic pattern is more apparent using the row-centre pre-treatment. The same occurs in the case of ♯3 in the loading plot of p[3] vs. p[2] (Fig. 6.6b), while a further component (PC4) is required with the alternative pre-treatment (Fig. 6.6a). Furthermore, the atypical trajectory of ♯16 is also more clearly identified with the row-centre pre-treatment (Fig. 6.7). Loading plots with different combinations of PCs were also visually inspected in order to identify the irregular performance of ♯9 and ♯26, but it was unclear which pre-treatment resulted more effective.

Generally speaking, results suggest that the row-centre pre-treatment is more convenient for three reasons: (i) PC1 is stronger correlated with mean temperature allowing an easier physical interpretation, (ii) PC2 provides information that discriminates better the different shape among trajectories, and (ii) the identification of abnormal patterns is more apparent in the loading plots (Figs. 6.5-6.7).

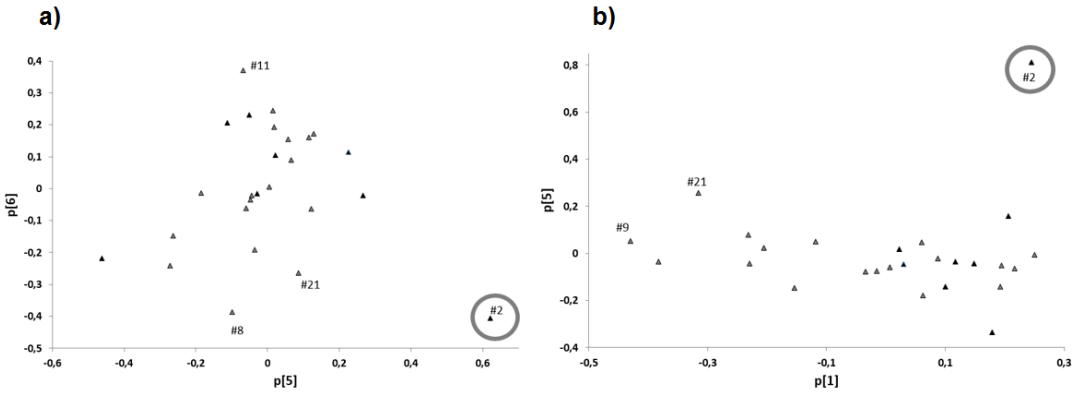

Figure 6.5: Loading plot of the PCA applied to the initial matrix of temperature, choosing the best combination of PCs that highlights probe ♯2 as an outlier. a) Plot of p[6] vs. p[5], column-centred data; b) plot of p[5] vs. p[1], row-centred data.

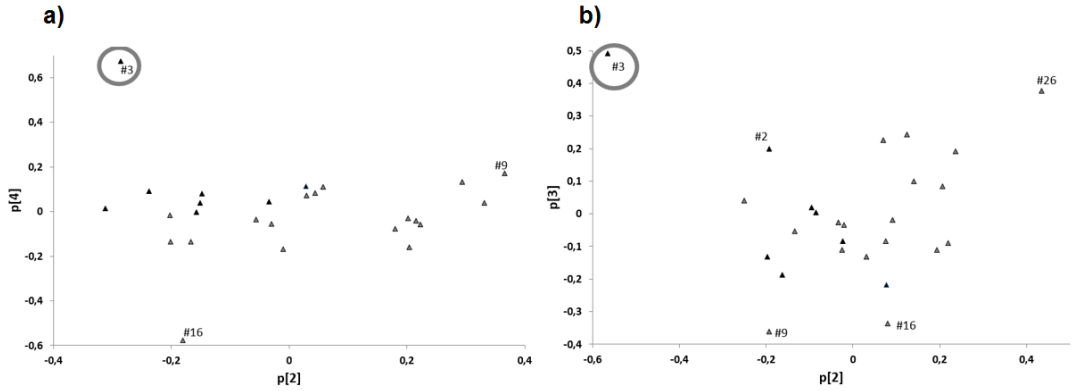

Figure 6.6: Loading plot with the best combination of PCs that highlights abnormal temperatures from probe ♯3. a) p[4] vs. p[2], column-centred data; b) p[3] vs. p[2], row-centred data.

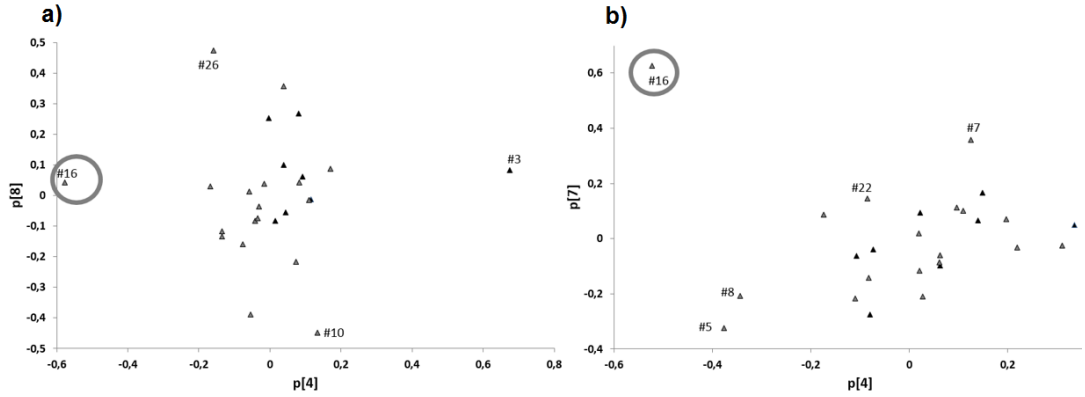

Figure 6.7: Loading plot with the best combination of PCs that highlights abnormal temperatures from probe ♯16. a) p[8] vs. p[4], column-centred data; b) p[7] vs. p[4], row-centred data.

6.3.2. Selection of time periods

By applying PCA to the initial data matrix, a careful analysis of the scores would be necessary to study if the latent correlation structures are maintained throughout the year, but an alternative procedure is proposed here. Once it was determined that the row-centre pre-treatment seems more adequate in this case, the monitored period was split into a few stages. For this purpose, CUSUM charts were obtained for different time series of average daily temperatures: (i) mean value recorded by all data-loggers (except ♯1), (ii) data from the outdoor probe (♯1), and (iii) from two nearby weather stations (Capri and Naples). These charts are displayed in Fig. 6.8, while Fig. 6.9 shows the equivalent charts obtained with RH recordings. As the average of each time series is different (19.18 °C in Pompeii, 18.25 °C in Capri and 17.17 °C in Naples), the charts were properly scaled in order to achieve an easier comparison. For this reason, the vertical scale has been removed.

The observed changes of trend (dates *a, b, c, d* in Fig. 6.8) will obviously vary from year to year, but it is quite remarkable that they appear exactly on the same dates for the weather stations in Naples and Capri, which are located at about 25 - 30 km from Pompeii. Actually, the four time series of temperature are highly correlated (r >0.96, p <0.0001). The decreasing trend (negative slope) observed in Fig. 6.8 from dates $b-c$ (winter) implies that lower temperatures were recorded, while the opposite applies for summer. The charts reveal two climatic periods which will be referred to hereafter as "cold" (11/5/2008 to 3/29/2009) and "warm" (7/23/2008 − 9/13/2008 and 5/9/2009 − 7/30/2009). During the warm period, the average

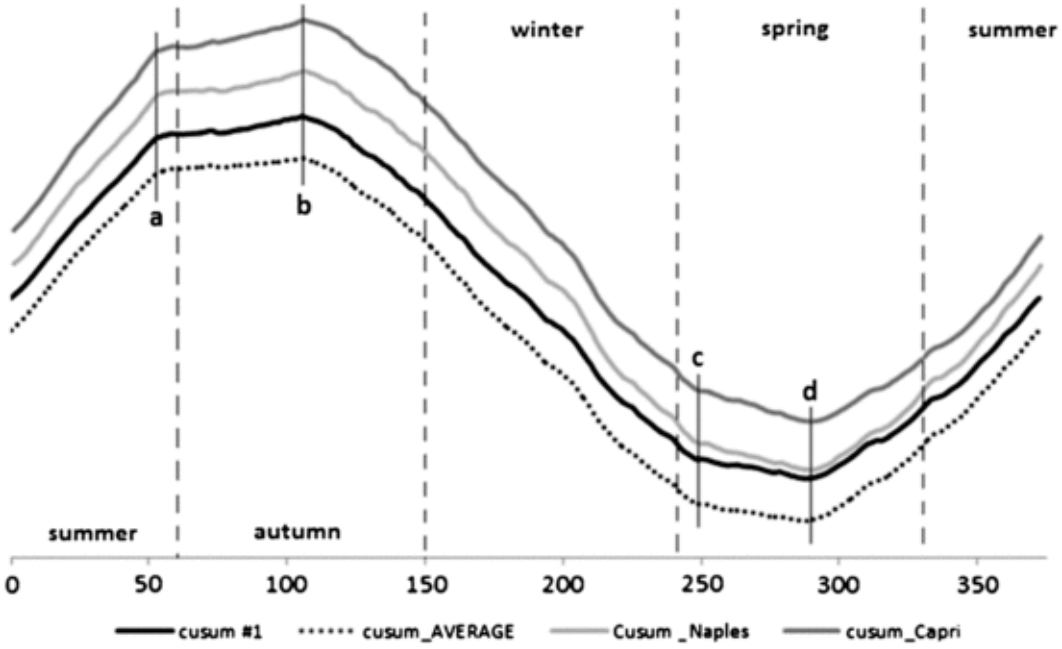

Figure 6.8: CUSUM charts of temperature. (i) Daily mean temperatures recorded by ♯1 during the whole monitoring period of 372 days (x-axis), (ii) average temperature from all data-loggers (except ♯1), and (iii) temperature recorded daily in two nearby weather stations (Capri and Naples). Day 0 is 7/23/2008. Date *a*: 9/13/2008, *b*: 11/5/2008; *c*: 3/29/2009; *d*: 5/9/2009. Vertical dashed lines delimitate the seasons.

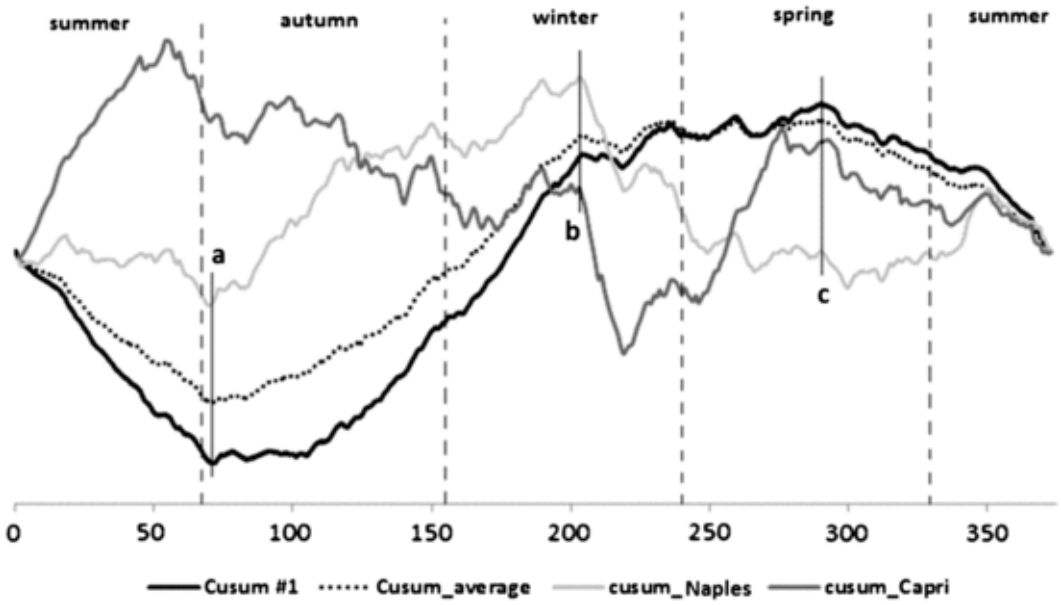

Figure 6.9: CUSUM charts of RH. (i) Daily mean RH recorded by ♯1 during the whole monitoring period of 372 days (x-axis), (ii) average RH from all data-loggers (except ♯1), and (iii) RH recorded daily in two nearby weather stations (Capri and Naples). Day 0 is 7/23/2008. Date *a*: 10/1/2008, *b*: 2/12/2009; *c*: 5/12/2009.

temperature was 27.6 °C in Pompeii, 25.2 °C in Capri and 24.2 °C in Naples. In the cold period, the mean was 11.52 °C in Pompeii (indoor data-loggers), 10.89°C (outdoor probe ♯1), 11.7 °C in Capri, and 10.6 °C in Naples. Two shorter transition periods are also identified: autumn 2008 (from *a* to *b*) and spring 2009 (from *c* to *d*). Both stages are relatively short, and consequently were disregarded for further multivariate analysis.

Regarding RH values for the whole monitored period, recordings from ♯1 are strongly correlated (r =0.970) with the average RH from the other data-loggers. Consequently, their CUSUM charts present a similar shape (Fig. 6.9). In contrast, RH data from Capri are weakly correlated with those from Ariadne's house (r =0.158, p =0.002) as well as from probe ♯1 (r =0.125, p =0.016) probably because Capri is a small island with hygrometric conditions strongly affected by the proximity of the sea. As a result, the shape of Capri's chart is rather different from the others, and was disregarded. Conversely, CUSUM charts for RH in Naples and Pompeii are somewhat similar, but the former does not reflect the shift in date *c*. The reason could be the presence of Mount Vesuvius between both locations.

Based on the CUSUM chart of RH data from Pompeii, three dates reflecting changes

of trend were identified (a, b, c in Fig. 6.9). As a result, three periods were considered: humid (10/1/2008 - 2/12/2009), dry (7/23/2008 - 10/1/2008 and 5/12/2009 - 7/30/2009), and a transition stage (2/12/2009 - 5/12/2009). The term "dry" evokes absence of rain and might be misleading, but it is used here meaning that RH was lower than the average recorded during the whole monitored period, while the opposite applies to "humid". Given the considerable duration of the transition stage (3 months), it was decided to split the initial RH matrix into 3 sub-periods for subsequent PCA studies.

The dates reflecting changes of trend in Figs. 6.8 and 6.9 are not coincident, which indicates that splitting the time series of temperature and RH into common periods is not always the best approach. Thus, in similar studies of microclimatic monitoring, a preliminary study using temperatures from nearby weather stations seems convenient to establish different climatic sub-periods throughout the year, but RH data cannot always be used for comparison purposes.

6.3.3. PCA of temperature and RH by periods

One PCA was carried out with temperatures recorded during the cold period after row-centring the data. The alternative pre-treatment was not considered, given its drawbacks discussed above. The same procedure was applied to the warm period as well as to the three RH matrixes (dry, transition and humid stages). The variance explained by PC1 is quite different comparing the warm and cold periods, as well as between the dry and humid stages (Table 2). PC2 does not satisfy the cross-validation criterion either in the warm ($Q^2 = -0.059$) or in the humid periods ($Q^2 = 0.034 < 0.039$), probably due to the presence of abnormal patterns. By checking Q^2 values in Table 2, it seems that three PCs capture the systematic data variability because the Q^2 of further PCs is rather small in most cases.

Distances to the model depicted in Fig. 6.3 were recalculated for each sub-period, though considering only one component (Fig. 6.10). Probes ♯3, ♯16 and ♯26 present an excessive distance in the warm and dry periods. The same applies to ♯2 but in the cold and humid periods. The transition phase of RH captures intermediate conditions and the distances are also somewhat in-between, with the exception of ♯16.

The comparison of Figs. 6.3 and 6.10 leads to interesting conclusions. All probes with an excessive distance to the PCA model in Fig. 6.3 are also outliers in Figs. 6.10a or 6.10b (♯2, ♯3, ♯9, ♯16, and ♯26). The only exception is ♯21, which is only atypical according to Fig. 6.3. Conversely, Fig. 6.10 reveals an abnormal pattern for ♯1 both in temperature and RH that is not reflected by Fig. 6.3 and was

	Temperature								Relative humidity								
	Warm period				Cold period				Dry period				Humid period				
PC	R^2_{raw}	R^2_{clean}	Q^2_{raw}	Q^2_{clean}	R^2_{raw}	R^2_{clean}	Q^2_{raw}	Q^2_{clean}	R^2_{raw}	R^2_{clean}	Q^2_{raw}	Q^2_{clean}	R^2_{raw}	R^2_{clean}	Q^2_{raw}	Q^2_{clean}	Q^2_L
1	74.1	80.1	71.8	77.9	48.0	47.6	38.0	39.0	70.8	74,9	68.2	72,4	53.4	42,7	45,5	36,5	3.7
2	8.3	5.1	-1,7	3,7	20.8	19.0	12,2	15,9	10.2	7,6	6,7	4,9	15.9	21,7	1,8	-6,3	3.9
3	6.3	4.2	6,3	2,3	8.3	10.2	7	10,2	5.5	5,4	4,5	4,5	10.5	12,2	7,4	6,8	4.0
4	2.3	2.2	1,8	0,6	6.3	4.5	6,2	1,7	2.7	2,7	0,9	1,3	4.8	6,3	2	5,9	4.2
5	1.9	2.1	0,3	0,7	3.8	3.9	2,9	3,7	2.3	1,9	1,7	0,8	3.1	4	-1,2	2,9	4.4
6	1.6	1.3	1,3	0,5	3.0	2.6	3,3	-2,9	1.7	1,3	0,6	0,3	3.1	2,6	2,7	2,5	4.6
7	1.1	1.1	1	0,4	1.8	2.3	-4.5	1,9	1.3	1,1	0,7	0,6	1.8	2,4	1,2	0,8	4.8
8	1.0	0.7	0,8	0,4	1.7	1.8	0,8	1	1.1	0,9	0,6	0,6	1.3	1,5	0,7	1,3	5.0

Table 6.2: Summary overview (R^2: variance explained, Q^2: cross-validated variance, Q^2_L: threshold value) of 8 components obtained from four PCA models: temperature (warm or cold period) and RH (dry or humid period) using row-centered data. All values are expressed as percentage. Two types of models were fitted: using all "raw" data of the period, and using "clean" data (leaving as missing values the abnormal trajectories). Periods: warm (7/23/2008 - 9/13/2008 and 5/9/2009 - 7/30/2009), cold (11/5/2008 - 3/29/2009), dry (7/23/2008 - 10/1/2008 and 5/12/2009 - 7/30/2009), and humid (10/1/2008 - 2/12/2009).

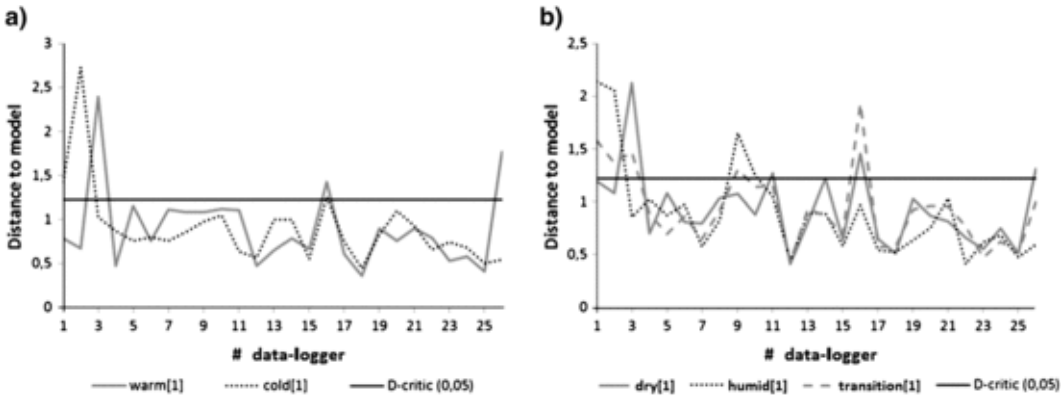

Figure 6.10: Distance to the PCA model with one component per periods: a) temperatures, b) RH data. Matrices were row-centred and transposed next prior to PCA. Horizontal line: critical threshold ($\alpha = 0.05$). Labels in the x-axis indicate the data-logger code.

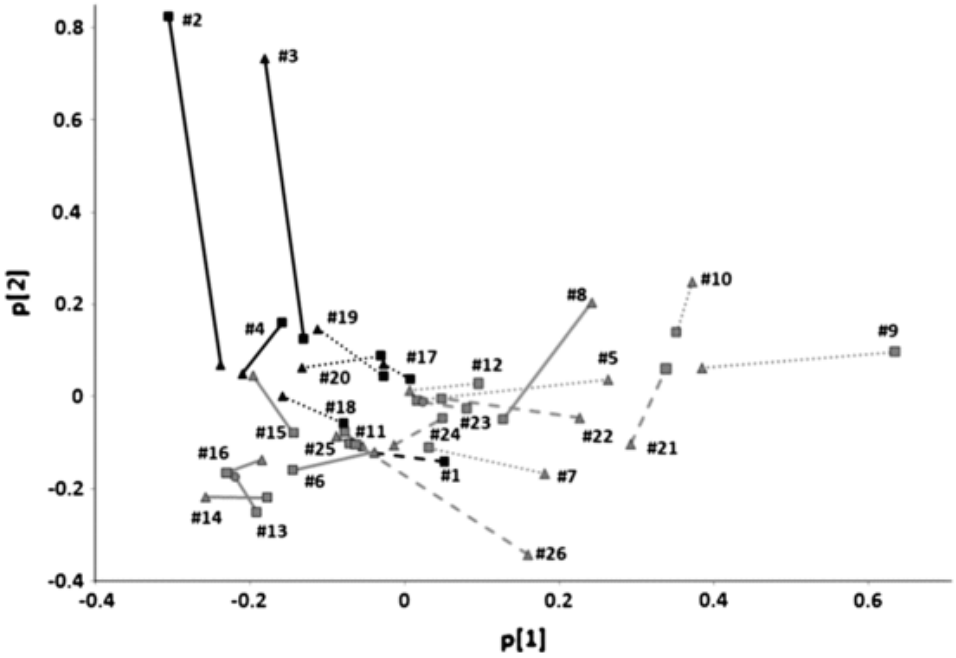

Figure 6.11: Loading plot (p[2] vs. p[1]) of the PCA applied to the row-centred temperatures. PCA for data recorded in the warm period (triangles), overlapped with the equivalent loading plot for the cold period (squares). Line codes as in Fig. 6.2.

not identified in a previous work [19]. As this probe was installed outdoors, results suggest that it registered a slightly different microclimate.

The unusual performance of data-logger ♯2 is detected in Figs. 6.3 and 6.5. Similarly, ♯3 appears as an outlier in Figs. 6.2, 6.3 and 6.6. More precisely, Fig. 6.11 reveals that ♯2 and ♯3 were very atypical in the cold and warm periods, respectively. The reason was the incidence of direct sunshine on the probes, which varies throughout the year. This issue was already discussed previously [19], but Fig. 6.11 highlights that abnormal patterns may occur only in particular sub-periods.

PC2 accounts for the differences of shape among trajectories. To identify which temperature trajectories have mostly changed their profile, we computed the difference of p[2] loadings between periods (i.e., $p[2]_{warm} - p[2]_{cold}$). The representation of these values on a normal probability plot (Fig. 6.12) provides useful information, because those points separated from the tilted line can be regarded as outliers. This is the case for ♯2, ♯3 and ♯26, also identified as atypical in Figs. 6.3 and 6.10a. The abnormal pattern of ♯21 detected in Fig. 6.3 is not apparent in Fig. 6.10, but it

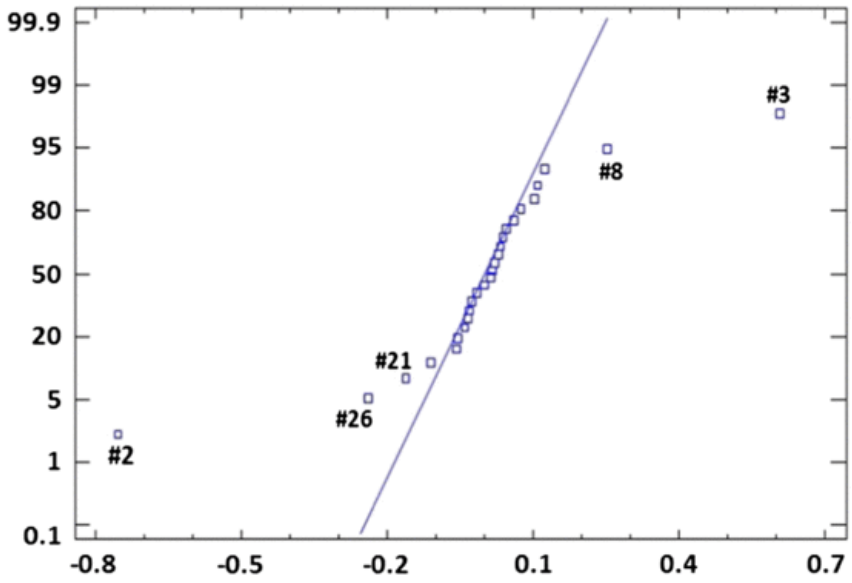

Figure 6.12: Normal probability plot of $p[2]_{warm}$ minus $p[2]_{cold}$ (i.e., difference of PC2 loadings for the warm and cold periods of temperature).

shows up in Fig. 6.12. Finally, the normal probability plot also indicates certain unique pattern for data-logger ♯8 that was not identified above. In summary, nearly 1/3 of the probes (♯1, ♯2, ♯3, ♯8, ♯9, ♯16, ♯21, and ♯26) presented a certain atypical performance, which is excessive. A good microclimate monitoring system should be installed by carefully selecting the position of probes in order to capture the variability due to common causes, avoiding unusual trajectories affected by special circumstances that occasionally arise.

Fig. 6.13 compares p[1] and p[2] loadings for the three periods of RH. The CUSUM chart of RH in Pompeii from dates *b* to *c* (Fig. 6.9) is nearly horizontal, which implies that the transition stage was characterised by measurements around the mean RH of the whole period. Consequently, this stage was expected to present certain intermediate performance between the dry and humid periods (i.e., circles should appear in Fig. 6.13 in the middle of triangles and squares). However, this is not always true, as in the case of ♯16, also reflected by Fig. 6.10b. Similarly, Fig. 6.13 suggests that ♯1, ♯2, ♯3, and ♯9 underwent a relevant shift between the dry and humid periods, which highlights an atypical performance also identified in Fig. 6.10b.

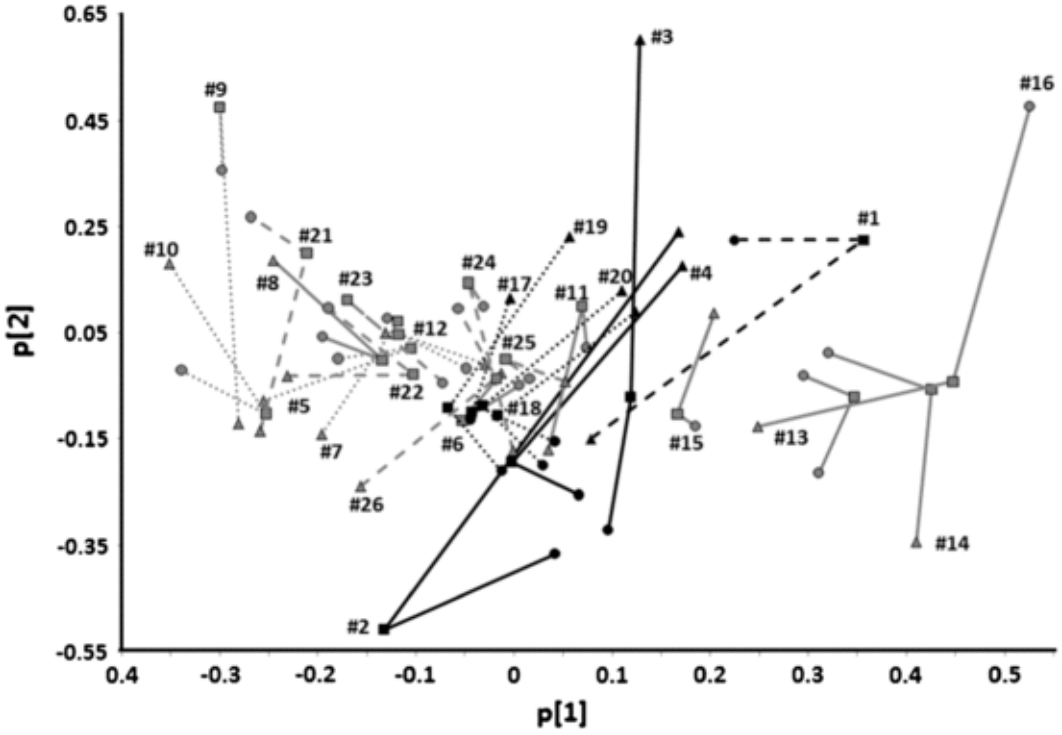

Figure 6.13: Loading plot (p[2] vs. p[1]) of the PCA applied to the row-centred RH data. PCA for data recorded in the dry period (triangles), overlapped with the equivalent loading plots for the transition (circles) and humid period (squares). Line codes as in Fig. 6.2.

6.3.4. PCA of temperatures by periods (excluding outliers)

Direct sunshine on specific probes caused sudden peaks of temperature at particular times, which can be regarded as a mistake in the experimental setup, because this circumstance should always be avoided. However, choosing the right position of probes in open-air sites for long-term monitoring is not straightforward, as it is necessary to calculate the trajectory of solar radiation incident on all walls, which changes during the day and also throughout the year. As the presence of atypical patterns due to this reason strongly affects the multivariate analyses, we wondered what would happen if the problem of incident sunshine had not occurred. Trying to simulate this situation, the abnormal data of probes ♯2, ♯3, ♯9, ♯16 and ♯26 were discarded after carefully checking the trajectories, and were left in the matrix as missing values. PCA models were repeated, and results are shown in Table 2 ("clean" data) and Fig. 6.14. By checking the Q^2 values, it turns out that three PCs capture the systematic data variability because the Q^2 of further PCs is rather small in most cases and close to the threshold limit. The same result was deduced from the "raw" data, but this conclusion is more clearly derived if data are "cleaned" prior to PCA.

Lines in Fig. 6.14 are rather vertical with a few exceptions (♯5 and ♯21), which implies that p[1] values are strongly correlated between both periods (r =0.845). By contrast, in the case of p[2], the correlation is negative and statistically significant ($r = -0.484$, p =0.012), which was rather unexpected. The interpretation of this result is somewhat unclear, but in any case it implies that the underlying correlation structure is not maintained, and the shape of temperature trajectories changes throughout the year.

Data-logger ♯5 appears in Fig. 6.14 as somewhat uncommon because its p[2] loading is almost the same for both periods. The reason could be that ♯5 was placed inside a glass box that protects a mosaic on the floor of room 3, resulting in higher temperatures (warm period) caused by a greenhouse effect.

Fig. 6.14 shows a certain arrangement of probes according to the room where they were installed. Data-loggers in room 4 (continuous black lines) tend to appear on the left side, which implies that they recorded lower temperatures in average. The reason seems to be the protection from sunlight produced by the opaque roof that covers room 4, while the others are sheltered by transparent sheets that cause an undesirable greenhouse effect. Conversely, probes ♯9, ♯10 and ♯21 recorded higher temperatures, probably because they were installed on walls oriented to the south-east that received more sunshine. Given the excessive temperatures registered in summer, the transparent roof in rooms 1−3 was replaced in December 2009 by fibre cement roof sheets.

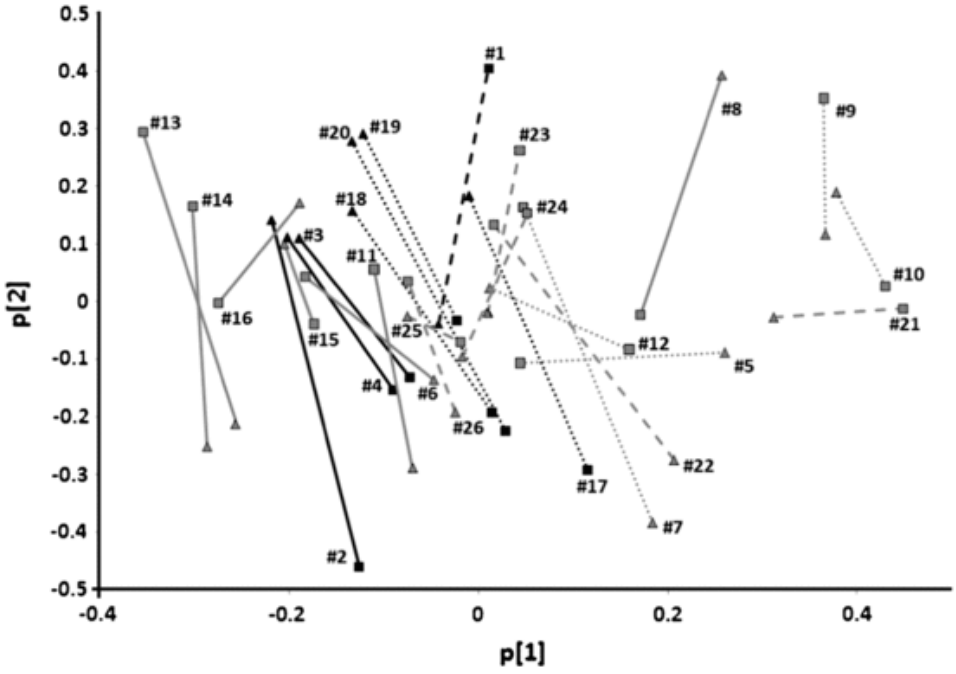

Figure 6.14: Loading plot (p[2] vs. p[1]) of the PCA applied to the row-centred temperatures (without abnormal trajectories). PCA for data recorded in the warm period (triangles), overlapped with the equivalent loading plot for the cold period (squares). Line codes as in Fig. 6.2.

As discussed above, PC2 provides information about the different shape of trajectories, but it would be interesting to obtain a more specific interpretation for this component. Actually, understanding the differences among trajectories is of relevant interest in microclimate monitoring studies [18], and might lead to control charts useful to assess if the relationships among sensors are maintained in long-term periods. To further study this issue, multiple linear regression was applied to fit the 52 values (26 data-loggers $\times$ 2 periods) of p[2] shown in Fig. 6.14 as a function of different parameters extracted from the data, such as daily means and variances of the period, mean daily variation, mean daily range, etc. A similar procedure was applied in a previous work [18]. Despite trying several parameters, it was not possible to obtain a good predictive model.

6.3.5. PCA of RH by periods (excluding outliers)

The main outcome of studying the transition period of RH independently was the identification of ♯16 as an outlier. Having discarded the atypical trajectories as explained for temperature, and in order to simplify the study, only two periods were considered to carry out the PCAs: dry (7/23/2008−10/1/2008 and 3/29/2009 − 7/30/2009) and humid (10/1/2008 − 3/28/2009). The relative position of data-loggers in the resulting loading plot (Fig. 6.15) is basically maintained for both periods. Actually, the correlation of p[1] loadings between periods is statistically significant (r =0.854) as well as in the case of p[2] (r =0.500, p =0.009), which is in contrast with the negative correlation obtained for temperatures. Data-logger ♯1 appears in Fig. 6.15 as slightly atypical in the humid phase which is also reflected by Fig. 6.10, probably because it measures outdoor conditions.

Winter is characterised by lower temperatures and higher RH, while the opposite applies to summer (see Fig. 3 of [19]). Moreover, probes that recorded higher temperatures on average are also those with lower RH (see Fig. 14 of [19]). For this reason, p[1] loadings in Fig. 6.14 (temperatures) and Fig. 6.15 (RH) are negatively correlated ($r = -0.881$, p <0.0001). Probes ♯9 and ♯21, which were installed on south-facing walls, registered the lowest RH values that correspond to highest temperatures, with marked daily fluctuations. Conversely, the highest RH measurements were recorded by three probes on the floor (♯13, ♯14 and ♯16), probably as a result of the diffusion of water vapour by capillarity through the ground.

Multiple linear regression was applied to predict the 52 values of p[2] in Fig. 6.15 using different parameters obtained from the data as predictive variables, and the following equation was found (6.1). The coefficient of determination is R^2 =0.497, and all regression coefficients are statistically significant ($p < 0.001$).

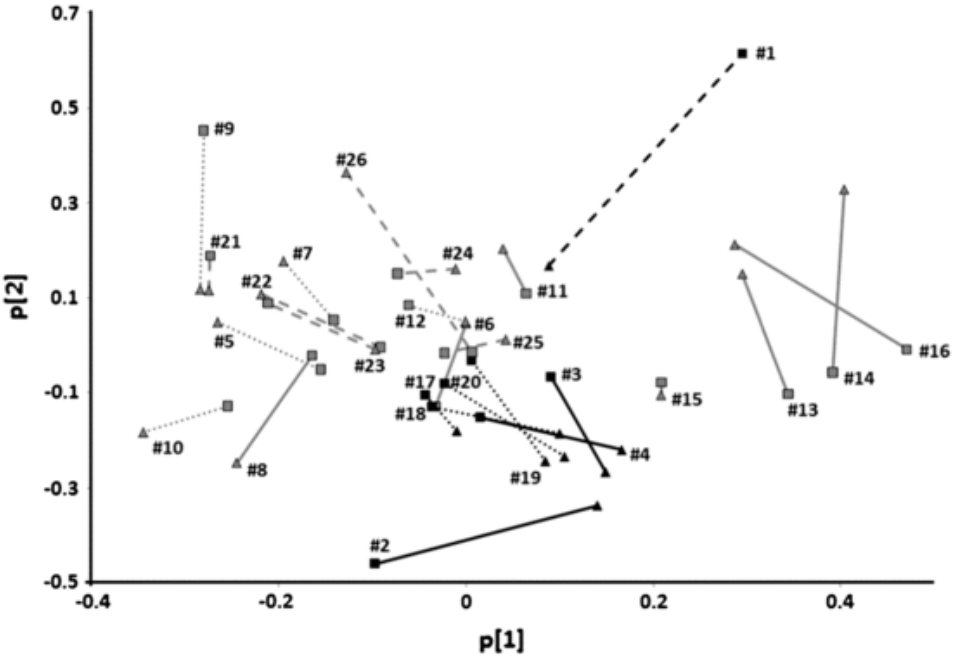

Figure 6.15: Loading plot (p[2] vs. p[1]) of the PCA applied to the row-centred RH data (without abnormal trajectories). PCA for data recorded in the dry period (triangles), overlapped with the equivalent loading plot for the humid period (squares). Line codes as in Fig. 6.2.

$$p[2]_{RH} = -4.01 + 0.00356 \times VarRH + 0.0406 \times MRH + 0.0287 \times MT \quad (6.1)$$

In this model, VarRH is the variance of all RH recordings in the sub-period, MRH is the mean RH, and MT is the mean temperature. VarRH is significantly correlated with $p[2]_{RH}$ (r =0.387, p =0.005). Variables MRH and MT are also correlated (r = −0.918, p <0.0001). Thus, the information that better characterises the different shape among RH trajectories is related with the variance.

Data-loggers tend to be clustered in Fig. 6.15 according to their position in Ariadne's house. Those in rooms 2 (dotted black lines) and 4 (continuous black lines) are close to each other and tend to present lower p[2] loadings, which implies according to eq. 1 that the variance (VarRH) was lower (i.e., trajectories more flat). The reason seems to be that room 2 is the only one delimited by four walls, while room 4 is protected by an opaque roof, which would explain why hygrometric conditions resulted more stable. Conversely, data-loggers in rooms 1 and 3 (dashed and dotted grey lines, respectively) appear in Fig. 6.15 also quite close to each other and are characterised by: (i) lower p[1] loadings, which involves lower RH values and higher temperatures caused by the transparent roof, and (ii) higher p[2] values, which implies trajectories with greater variance (VarRH) (i.e., daily cycles more pronounced) due to the transparent coverage.

6.4. Conclusions

The present work discusses the best pre-treatment prior to applying PCA to data from a multivariate microclimate monitoring system in an open-air archaeological site. The data structure is analogous to the case of continuous chemical processes monitored with multiple sensors. In such processes, data are commonly column-centred before carrying out the multivariate analysis. However, in this case it turned out that working with row-centred data presents advantages for two reasons. Firstly, PC1 accounts for the mean temperature recorded by each data-logger, due to the high correlation between such means and p[1], while PC2 provides information that discriminates the different shape among trajectories. Secondly, the identification of abnormal patterns is more apparent in the score plots.

Another outcome of the work is the advantage of dividing the monitored period into several stages, taking into account that weather conditions are not constant

throughout the year. By applying PCA to each sub-period, the detection of abnormal patterns was more straightforward. These periods were determined by CUSUM charts obtained with the mean daily values of data-loggers and from two nearby weather stations. With this methodology, it was possible to characterise the microclimate in the archaeological site and assess the differences among probes according to their position in Ariadne's house. The different characteristics of the four rooms were reflected in the results. The data could also have repeatability such that you can make protection interventions furniture on the walls at certain times of the year to protect themselves.

Chapter 7

Multivariate thermo-hygrometric characterisation of the archaeological site of Plaza de l'Almoina (Valencia, Spain) for preventive conservation

Multivariate thermo-hygrometric characterisation of the archaeological site of plaza de l'Almoina (Valencia, Spain) for preventive conservation. Fernández-Navajas, A., Merello, P., Beltrán, P., García-Diego, F.-J. *Sensors* 2013, 13 (8), 9729-9746.

Abstract: Preventive conservation requires monitoring and control of the parameters involved in the deterioration process, mainly temperature and relative humidity. It is important to characterise an archaeological site prior to carrying out comparative studies in the future for preventive conservation, either by regular studies to verify whether the conditions are constant, or occasional ones when the boundary conditions are altered. There are numerous covered archaeological sites, but few preventive conservation works that give special attention to the type of cover installed. In particular, there is no background of microclimatic studies in sites that are in the ground and, as in the Plaza de l'Almoina (Valencia, Spain), are buried and partially covered by a transparent roof. A large effect of the transparent cover was found by the sensors located below this area, with substantial increases in temperature and a decrease in the relative humidity during the day. Surrounding zones also have values above the recommended temperature values. On the other hand, the influence of a buried water drainage line near the site is notable, causing an increase in relative humidity levels in the surrounding areas. Multivariate statistical analyses enabled us to characterise the microclimate of the archaeological site, allowing future testing to determine whether the conservation conditions have been altered.

Keywords: microclimate monitoring; archaeological preservation; temperature and relative humidity sensors.

7.1. Introduction

Preventive conservation of archaeological sites is understood as the whole control process of the deterioration factors in order to prevent damage to the cultural heritage before it occurs and minimise future interventions [1].

The conservation of an archaeological site is particularly influenced by the thermohygrometric features of the environment in which it is located, which may lead to material disintegrations and biological problems, etc. Thus, monitoring and control of the physical parameters of temperature and relative humidity become a priority [7].

It is important to characterise an archaeological site with a view to carrying out comparative studies in the future for its preventive conservation, either regularly, in order to verify whether the conditions are constant, or occasionally, when the boundary conditions are altered. It is also important after any change in the environment to first ascertain if the resulting microclimate is suitable according to the

experience of other researchers and standards, and, secondly, if deterioration in the site occurs, to determine the microclimate that has led to this phenomenon.

The control of these parameters has been studied in churches [22], [26], [27] and museums [16], [18], [28], [29]. Microclimatic monitoring studies have also been conducted in open archaeological sites [19], [31]. In the case of the ruins of Ariadne's house in Pompeii [19], as a consequence of this study it was possible to propose corrective measures on the covers that helped improve preventive conservation of the site and its frescoes.

In the case of closed or buried archaeological sites (hypogeum) under climate control systems, it is very important to control the operation of the latter, as well as to prevent harmful combinations of temperature and relative humidity that may lead to the appearance of fungi (high temperature and humidity) or drying of the substrate. A monitoring study of temperature and relative humidity (RH) was carried out at the hypogeum archaeological site of Carcer Tullianum (Rome, Italy) [32]; in that work, statistical tools for exploratory purposes, such as box-and-whisker plots, were used, but statistical comparative techniques were not applied, which is one of the aims of this paper.

There are many examples of covered and visited archaeological sites that can be found, as well as the archaeological crypt in Paris (France), the ruins of the History Museum of Barcelona (Spain), the Saint Laurent church and Saint Oyand crypt (Archaeological Museum of Grenoble, France), and the archaeological site of Saint-Pierre Cathedral in Geneva or the Carcer Tullianum [32].

The authors of [113] discuss the installation of different types of coverage on archaeological remains. Thus, rooftops with different designs and structures are installed, but which could be included in two general classes: opaque or transparent covers. Opaque covers are more effective, but generally hamper the visitor's view, so there are many cases in which it was decided to install a transparent cover. However, it is in the case of transparent covers where the control of thermo-hygrometric parameters is most needed [19].

L'Almoina Archaeological Centre (Valencia, Spain) comprises an area of about $2,500\ m^2$. It houses the archaeological excavations performed between 1985 and 2005 in the city of Valencia [43]. This work has led to the discovery of several monumental buildings, inscriptions, loose architectural elements, more than $1,000$ coins and 500 exhibition quality ceramic pieces [44], and has also given rise to a vast body of technical documentation.

The most interesting facet of this site is the buildings, a continuous overlapping

of constructs, forming a complete and well-preserved compendium of history and urban development of the city of Valencia from its founding to the present. Among them, we find the Islamic Alcazar [45], the first city (the Republican) represented by the thermals [46], remains of the Roman Empire (the forum and the Curia) [47], [48], and martyrdom and Episcopal area from the Vizigothic stage [48], [49].

An intervention was conducted in the years 2005-2007 for the development and construction of the Archaeological Centre. To protect the ruins, a concrete structure adapted to the unique archaeological site was built. In addition, as shown in Fig. 7.1, a glass cover (25 × 25 m) was installed, which allowed passers-by a glimpse of the archaeological remains.

This work deals with the multivariate analysis of microclimatic conditions at the archaeological site of the Plaza de l'Almoina, which allows us to characterise the site with the aim of carrying out comparative studies in the future for preventive conservation of this site when implementing changes in the climate control system or in the architectural design. To this end, we shall perform different statistical analyses, not frequently used in cultural heritage, such as mean daily trajectories, bivariate plots and cluster analysis, with the aim of illustrating mainly restorers and conservators of archaeological sites how to proceed when monitoring systems are affected by technical and economic limitations, resulting impossible to install an ideal sensor network.

7.2. Materials and Methods

7.2.1. Description of Data Loggers

Each RH data logger (Datalog Hygrochron DS1923) contains a humidity sensor with an accuracy of ±5 % [100]. Although this model can also record temperatures, it was decided to use independent devices (Datalog Thermochron DS1922L) for the temperature monitoring [101], which has the same accuracy (±0.5 °C) as the DS1923. The reason was to expand the data storage capacity of the monitoring system. A set of 22 data loggers, 11 of each model, were purchased directly from the manufacturer (Maxim Integrated Products, Inc., Sunnyvale, CA, USA) and calibrated prior to their installation, as described below. These devices resemble button-like batteries, with 17.4 mm of diameter and 5.9 mm of height. Each pair of DS1923 and DS1922L data loggers was placed close to each other.

Figure 7.1: Plan of the archaeological site and location of sensors.

7.2.2. Installation of Data Loggers

The monitoring study started on 22 February 2010 and ended on 5 July 2010, when 11 probes were installed in the archaeological site of Plaza de l'Almoina (location shown in Fig. 7.1). The monitoring period was selected as it provided a representation of cold and warm season, especially considering that the summer is the most interesting period because it presents the most unfavourable microclimatic conditions for conservation given the location of the archaeological site and the transparent cover installed.

Meteorological data on temperature and RH provided by the Environment Department of the Universitat Politècnica de València are also available, and will serve as an outdoor reference (♯OUT). In order to analyse the effect that light passing through the skylight (Fig. 7.2) has on the archaeological site, sensor ♯6 was installed immediately below it (Fig. 7.3.a).

All probes were placed on the ground (Fig. 7.3), except probe ♯2, which was placed in a recess in the archaeological stone wall. Note that at the west of the archaeological site a boundary water pipe from the 1920's was located (Fig. 7.1), not canalised with PVC, so sensor ♯1 was located just near the wall facing the pipe (Fig. 7.3.b).

7.2.3. Calibration of Sensors

Calibration of the sensors was performed with two calibration experiments separated in time, in order to study if measurements from one or more sensors were biased compared to the average recorded by all sensors. Thus, the average sensor bias was corrected for all data. The calibration procedure and the results of the bias can be found in [19] because the sensors were the same.

7.2.4. Frequency of Data Recording

The monitoring study began on 22 February 2010 and ended on 5 July 2010, resulting in a total period of 133 days. All data loggers were programmed to register one measurement every 30 min, which implies 1,440 recorded values per month (i.e., 30 days $\times$ 24 h/day $\times$ 2 data/h).

Figure 7.2: Light coming from the skylight, which affects only part of the archaeological site.

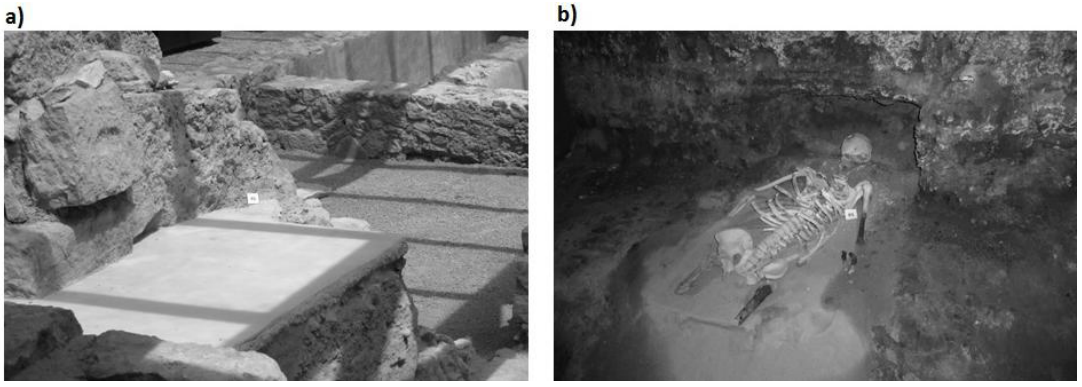

Figure 7.3: Location of sensors with singular trajectories. (a) Location of sensor ♯6, just below the skylight; (b) Location of sensor ♯1, next to skeletal remains (the water pipe is located just above).

7.2.5. Statistical Analyses

Normal Probability Plot

Normal distributions are extremely important in statistics, and are often used in the natural and social sciences for real-valued random variables whose distributions are unknown [124]. The normal probability plot is a graphical technique for normality testing, assessing whether or not a data set is approximately normally distributed. The data is plotted against a theoretical normal distribution, so that the points should approximately follow a straight line, and those departures from this line indicate departures from normality. This is a quantitative technique suitable for researchers trained in statistical analysis.

In our case, we are interested in detecting those sensors whose differences from the average are abnormal. We work on this paper with two different averages. First, we work with the average of all sensors (calculated considering sensors from ♯OUT to ♯11). Second, since we are interested in detecting differences within the archaeological site, we work with the average of inner sensors (calculated considering sensors from ♯1 to ♯11).

Daily Mean Trajectories

Mean daily trajectories are used in several fields of science, but rarely applied in microclimate monitoring of cultural heritage [19]. Mean daily trajectories are calculated as the average of the data from each sensor per fraction of time (in this case, every hour) for the entire date range of interest. This plot summarises the information of the selected time period, avoiding excessively large plots and stationary periods and allowing simple comparison of different sensors. This technique enables us, for example, to detect anomalous data quickly and effectively, such as time bands where direct sunlight affects the paintings, causing a rise in temperature.

Cluster Analysis

Cluster analysis is the name of a group of multivariate techniques whose primary purpose is to gather objects based on their characteristics, attempting to maximise the homogeneity of objects within clusters while simultaneously maximising the

heterogeneity between clusters [125].

In this study, the aim of using cluster analysis was to define a taxonomy of sensors, to characterise the different zones of the archaeological site from their average and daily variability in RH and temperature.

In this paper, the squared Euclidean distance is used as a measure of similarity between observations and hierarchical method of k-means is applied. Note that analyses were also performed for the normalised data (both variables having equal weight in the analysis); as the obtained results were identical, it was decided to present the results for the original variables because of their physical interpretation. All cluster analyses were performed using the software SPSS 16 [126].

Contour Plots

The purpose of including this type of graph in the article is twofold: on one hand they are useful as preliminary study to give an overview of the microclimatic situation of the site; on the other hand, they serve to discuss how the proposed techniques improve the results obtained from contour plots.

These plots were made with a CAD program, connecting each sensor to the closest one with a straight line, forming a triangle. Each line is graded according to the initial sensor value and the final one, resulting in a number of marks where each represents a value of the physical parameter. Linking the marks of the same value by splines, you get a line plot representing an approximation of the gradient of the physical parameter.

7.3. Results and Discussion

7.3.1. Classical Data Analysis

Descriptive Data Analysis of Mean Trajectories

Knowledge about ideal or limit values of microclimate parameters for conservation of cultural heritage is still poor [32]. The Italian UNI 10829 [83] and DM 10/2001

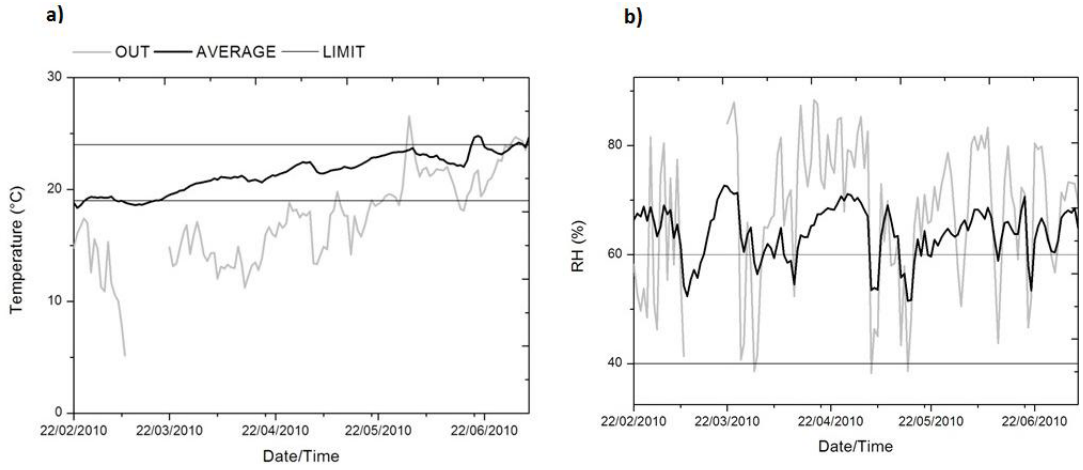

Figure 7.4: Daily averaged data for the whole monitoring period (48 data/day), for the outdoor sensor and the average of interior sensors (11 data/day). The value 0 on the horizontal axis coincides with the date 22 February 2010. (a) Temperature; (b) relative humidity (RH).

[7] are currently the approved standards on this matter. According to [7] and [83], the recommended range of RH and temperature for stones and rocks is 40-60 % and 19-24 °C, and a maximum daily variation of 6 % in RH is recommended, although there is no available data for temperature.

Fig. 7.4.a allows us to detect the growing trend for the temperature data in the monitoring period, as expected. Moreover, Fig. 7.4 verifies how, a priori, the architectural design of the archaeological site mitigates the high variability of the Mediterranean climate of the city of Valencia (Spain), in temperature and especially in RH.

Contour Plots of Temperature, RH and Water Vapour Pressure

To produce these contour plots, data from sensor ♯2 were removed from the graphs, as it was installed in a recess of the wall without contact with soil moisture, resulting in a distortion of the plots.

Fig. 7.5.a shows how temperature is influenced by the effect of the glass cover, which caused an anomalous performance of sensor ♯6, placed just below the skylight. In the case of RH (Fig. 7.5.b), the influence of the transparent cover results in a rise in

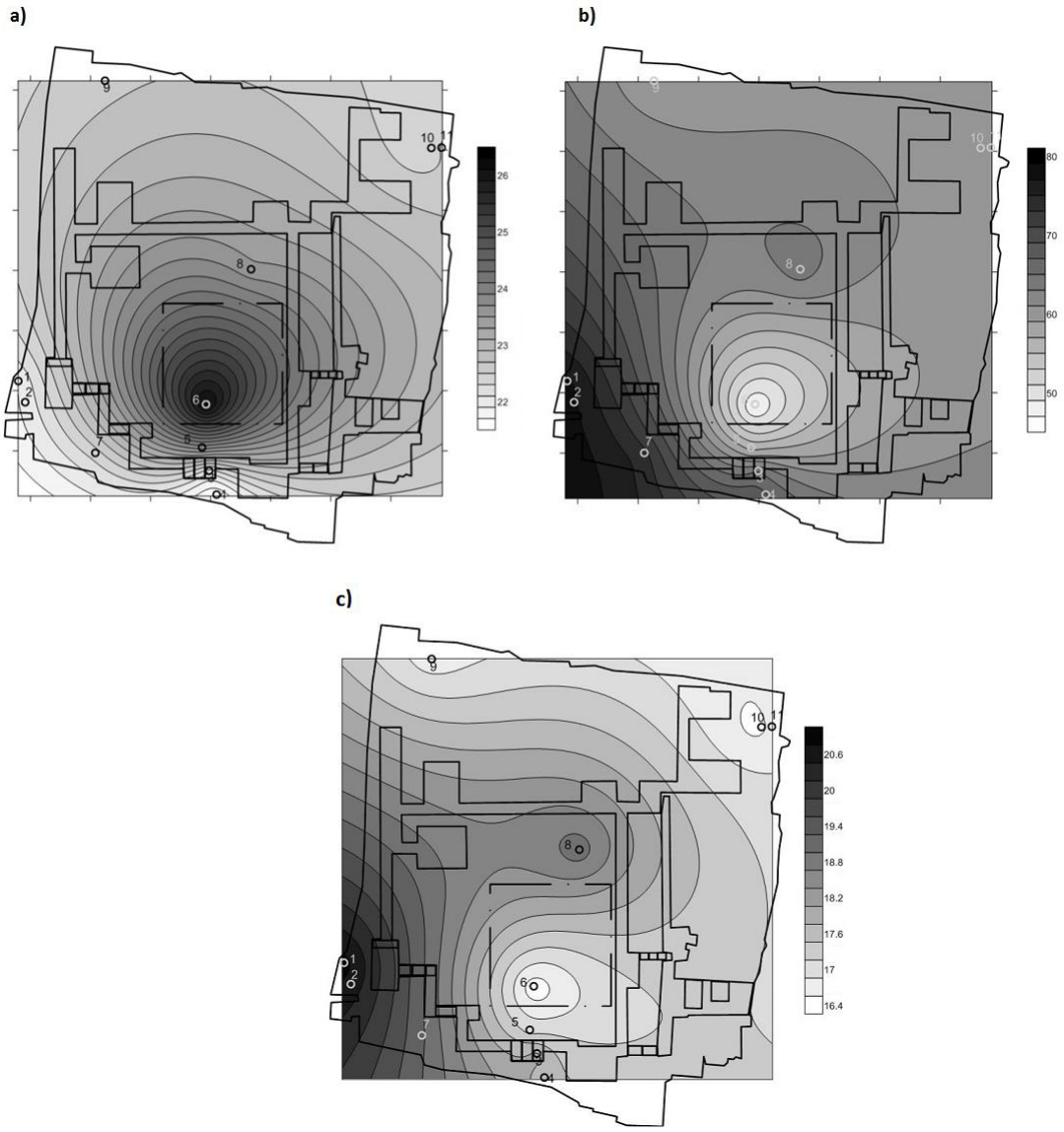

Figure 7.5: Contour plots, averaged data from May to July 2010 from 00:00 to 23:59 h (3,120 data/sensor), (a) temperature (°C); (b) relative humidity (RH, %); (c) water vapour pressure (mbar).

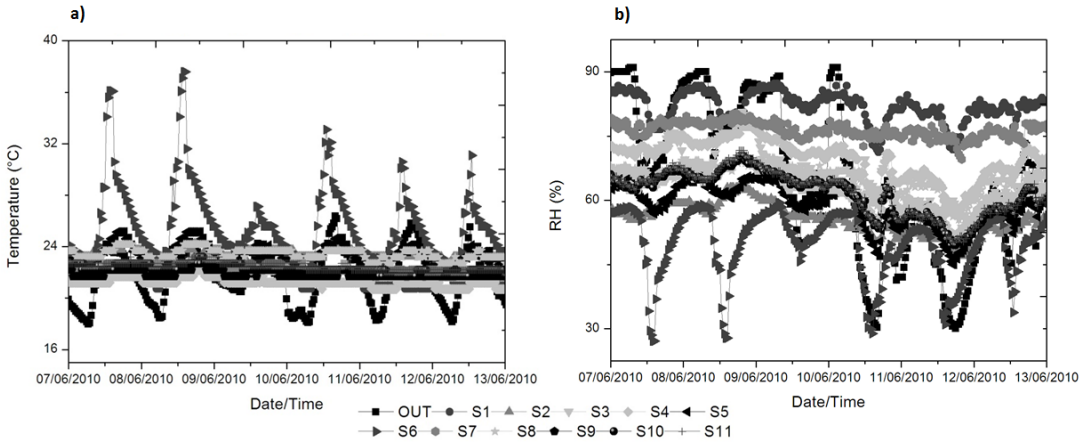

Figure 7.6: Time series of all sensors, for the week from 7 July 2010 to 13 July 2010, (a) temperature; (b) relative humidity (RH).

temperature and consequently a decrease in RH. As Fig. 7.5.b shows, the remaining areas are influenced by the RH gradient, which decreases as we move away from the water drainage line as an effect of the movement of the water as indicates the water vapour pressure (Fig. 7.5.c). Note that, if there is a different pressure between areas in a closed site, as pressure tends to equalize, there will be movement of the water content.

Temperature graphs and RH gradients are widely used in cultural heritage [1], [127], but are limited because they rely on the concept of representing infinite points from a finite number of sensors. In our case, it is clear that under the skylight, where there is only one sensor (♯6), the graph is distorted and centred on this sensor.

To avoid this problem, in the following sections a more comprehensive and quantitative methodology is applied to characterise the archaeological site. These techniques surmount the inherent difficulties of interpretation of a large number of sensors as shown in Fig. 7.6, where it is very difficult to draw useful conclusions.

7.3.2. Multivariate Methodology Proposed

Detecting Singular Trajectories (Normal Probability Plot)

In this paper, we shall consider as outliers those values exceeding a maximum variation every half hour [128] which can be ruled out because they distort the

conclusions. In the case of time series of physical parameters such as temperature and RH, we define as outliers those incorrect records that exceed the acceptable values for a physical parameter trajectory. In our case, the software used [128] highlights those records that exceed a maximum variation every half hour defined by the user; in this case, it was fixed in a range of ±8 °C in temperature and ±20 % RH. In this case, no outliers which could be eliminated were identified.

However, sensors with unusual behaviours or distinct from the rest may appear, for which the information is of great interest to understand the reality of the archaeological site.

To detect the sensors with singular trajectories, the following technique is proposed. We represent in a normal probability plot the centred data (mean subtracted) of all sensors, so that those sensors with abnormal distance to the average appear displaced from the control line. As indicated in the methodology section, the first analysis is performed considering the average of all sensors (from ♯OUT to ♯11), while the second analysis considers only those sensors located inside the archaeological site (from ♯1 to ♯11). Notice that we do not analyse the distribution of all recorded data but only the differences from the average, which should be expected to follow a normal distribution.

In Fig. 7.7 we observe that for the temperature data, during the entire monitoring period, the outdoor sensor appears as abnormal, both for day and night. However, sensor ♯6 comes up as abnormal (Fig. 7.7.a) during daylight hours, as this sensor is immediately below the transparent cover, so that the incidence of sunlight causes an increase in temperature during the day.

Another option is to subtract the average obtained from all sensors inside the archaeological site, as they are the ones that will be taken as a reference, so we can avoid peculiarities introduced by the high variability and significant differences in mean of the outdoor sensor (♯OUT). This approach allowed us to draw relevant conclusions, especially for the non-summer period (from February to May) where the temperature variability is lower and the inclusion of more extreme data, such as the outdoor sensor, in the calculation of the mean may bias the results and differences.

Thus, in Fig. 7.8, when considering the average of the inner sensors (Fig. 7.8.a), we can see how it is possible to appreciate the anomaly of sensors ♯6 and ♯OUT, whereas when the outdoor sensor is included in calculating the average (Fig. 7.8.b), these differences are concealed.

In the case of RH (Fig. 7.9), the anomalous behaviour of sensor ♯6 is noteworthy,

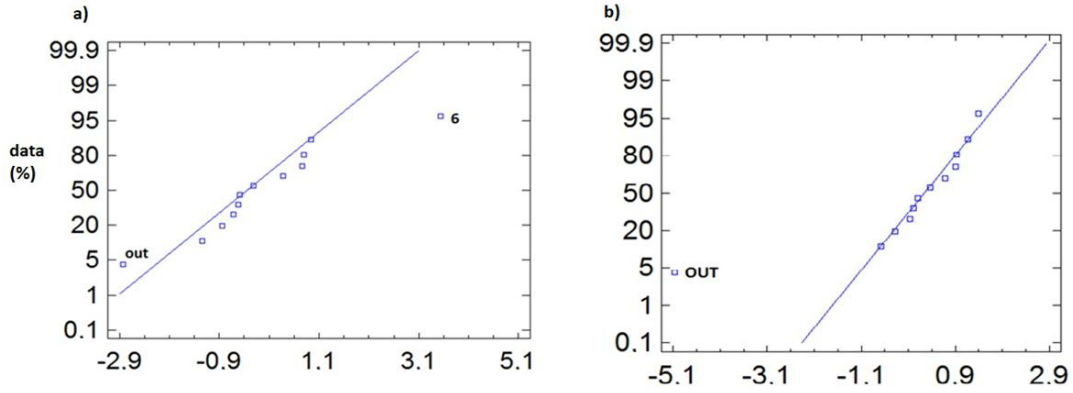

Figure 7.7: Normal probability plot of temperature, from February to July 2010, for centred data (subtracting the average from ♯OUT to ♯11). (a) From 8:00 to 19:59 h, with ♯6 and ♯OUT appearing as anomalous sensors (3,192 data/sensor); (b) from 20:00 to 7:59 h (3,192 data/sensor). At night, only ♯OUT stands out as anomalous sensor.

notably how the temperature increases due to the skylight, resulting in a drop in RH. On the other hand, sensors ♯1 and ♯7 present higher RH values, these sensors being located in the area closest to the water pipe.

No differences were found between the results of RH analyses for different statistics, because the RH average for outdoors was similar to the average for the inner sensors.

This technique for detecting singular trajectories, combined with the study of different factors (such as day/night cycles, seasons, or discussing the use of more accurate averages) allows us to specifically identify those sensors with different behaviour. However, to study and characterise the singular behaviour of these sensors in detail, below we analyse the mean daily trajectories (Fig. 7.10).

It is notable how the trajectory shape of sensor ♯6 corresponds with that of the outdoor sensor, both in temperature and RH (Fig. 7.10), accentuating the differences between night and day compared to all the other inner sensors, which have a highly damped trajectory. However, sensor ♯6 has a parallel offset with respect to the outdoor sensor, with an average temperature around 6 °C higher and a RH average about 20 % lower, due to the overheating caused by the direct impact of sunlight, noticeably surpassing the values recommended by the standards [7], [83].

On the other hand, the cluster formed by sensors ♯1 and ♯7 maintains a nearly constant value of RH throughout the day, but with values 18 % higher than the

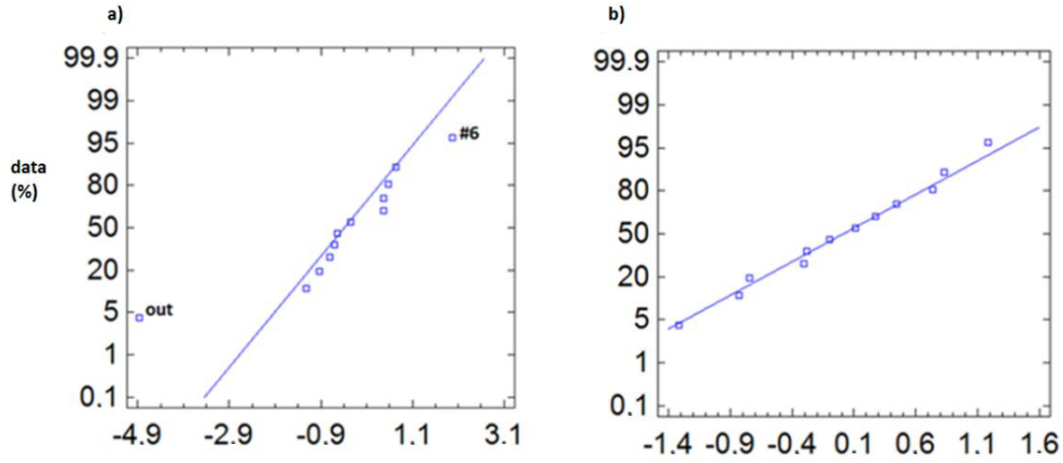

Figure 7.8: Normal probability plot of temperature for data from February to May 2010, from 8:00 to 19:59 (1,608 data/sensor), (a) data centred by the average of the inner sensors from (♯1 to ♯11); (b) data centred by the average of the all sensors (from ♯OUT to ♯11).

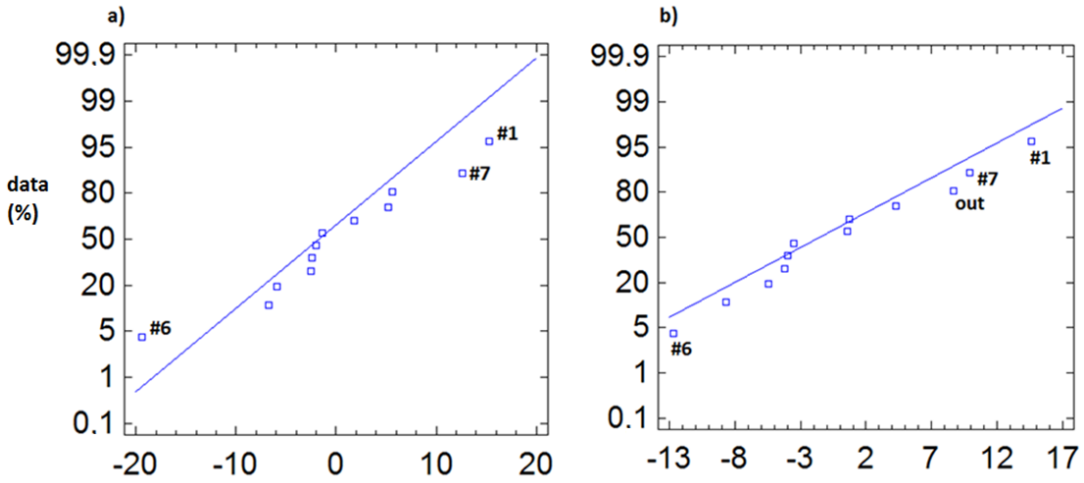

Figure 7.9: Normal probability plot of RH, for centred data (average of all sensors), from May to July, (a) from 8:00 to 19:59 h (1560 data/sensor); (b) from 20:00 to 7:59 h (1,560 data/sensor).

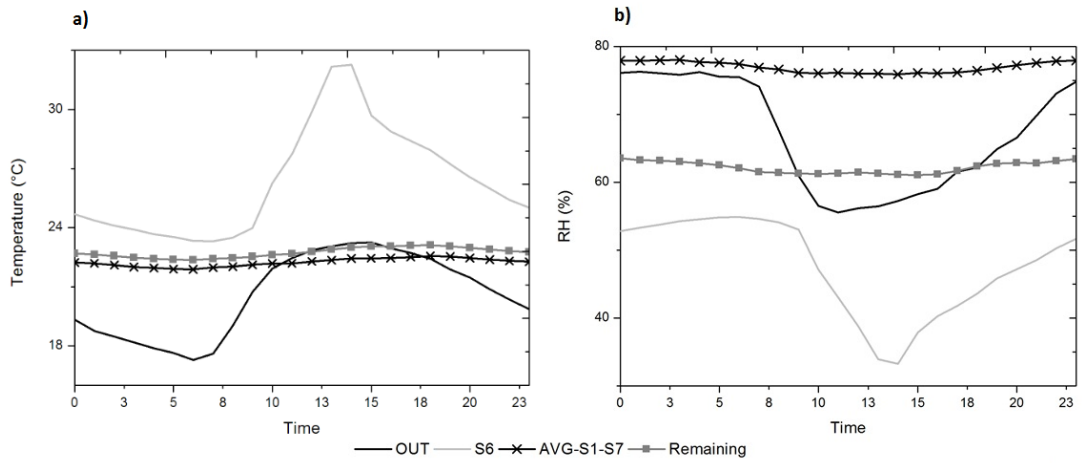

Figure 7.10: Mean daily trajectories, from May to July 2010. (a) For temperature data of sensors ♯OUT, ♯6 and the average of the remaining sensors; (b) for relative humidity (RH) data of sensors ♯OUT, the cluster composed by ♯1 and ♯7, sensor ♯6 and the average of the remaining sensors.

rest of the inner sensors, due to the extra contribution of absolute humidity caused by the water pipe. This does not occur with temperature, which has very similar values of the other sensors.

Analysis of the Remaining Sensors

Next, we carefully analyse possible differences, more subtle than those highlighted above, which may occur in the rest of sensors inside the archaeological site. To do so, cluster analysis is performed on the average and mean daily variation of temperature and RH, so that is possible to empirically identify different clusters of sensors.

According to the study aim of identifying areas with singular behaviour inside the archaeological site a solution for temperature is selected with 4 clusters. The solution was chosen after analysing the results for the highest and lowest number of clusters (Table 7.1) and the distance matrix (Table 7.2).

In Table 7.1 we can identify the sensors that comprise each cluster. As seen in Table 7.1, there are two clearly differentiated main clusters (C1, C4), whose distance from the centres of all clusters is always greater than 6 °C. C1 is the cluster that

Cluster		C1	C2	C3	C4
Sensors		OUT	1,3,4,7,9,10,11	2,5,8	6
Centres (°C)	average	20.59	22.30	23.76	26.33
	Daily variation	7.39	0.71	1.61	9.76
Fraction of sensors		1/12	7/12	3/12	1/12

Table 7.1: Results of cluster analysis of temperature for data from May to July, from 00.00 to 23.59 h (3,120 data points/sensor).

	C2	C3	C4
C1	6.89	6.60	6.21
C2		1.72	9.91
C3			8.55

Table 7.2: Matrix of distances (in °C) between the final cluster centres for cluster analysis of temperature data.

contains the outdoor sensor and is characterised by a high daily variability, while cluster C4 contains sensor ♯6, located under the skylight and characterised by very high temperature levels during daylight hours (which gives it a higher mean and a much higher variability than the rest of the archaeological site sensors).

As seen in Table 7.1, there is a predominant cluster (C2) containing 7/12 of the sensors, and a second cluster (C3) of sensors similar to those of C2 (centre distance = 1.72 °C), but characterised by greater variability. Let us analyse the differences between these two clusters by comparing the mean daily trajectories (Fig. 7.11).

Fig. 7.11 shows the difference in averages previously indicated by cluster analysis. The difference in variability occurs due to an increase of temperature during daylight hours, caused by the proximity of sensors to the skylight area. Thus, the trajectory shape of cluster 3 is similar to that of sensor ♯6 and the outdoor sensor, as shown in Fig. 7.10. However, these sensors have an average approximately 3 °C lower than the average of sensor ♯6.

For RH, a solution with five clusters was selected (Table 7.3). The consistency of this solution can be determined by results shown in Table 7.4 (distance matrix). In Table 7.3 we can identify the sensors that comprise each cluster. As seen in Table 7.3, there are three different main clusters (C1, C2, C4), whose distance from the centres of all clusters is always greater than 10 % of RH. C1 is the cluster that

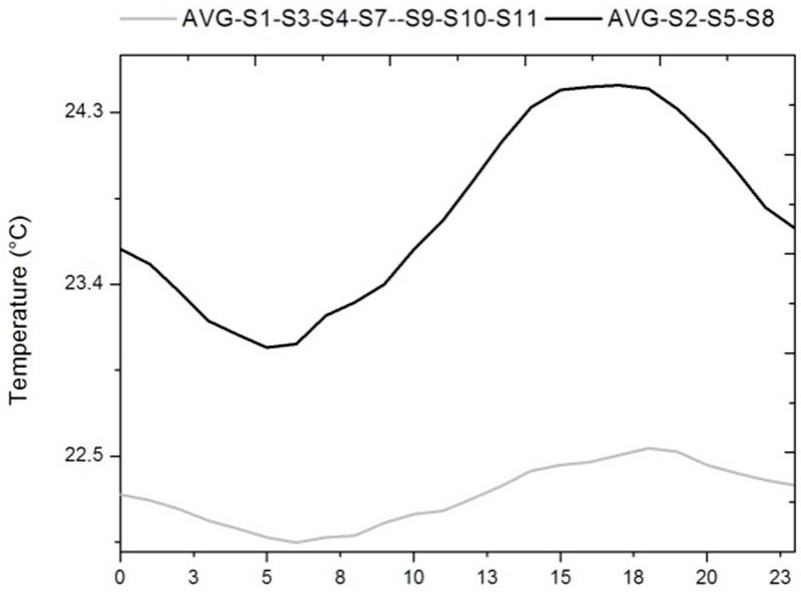

Figure 7.11: Mean daily trajectory of temperature for the average of sensors contained in cluster 2 and 3.

contains the outdoor sensor and is characterised by a high daily variability; cluster C2 is composed of sensors ♯1 and ♯7, which are located closer to the drain and which present the highest levels of RH (constant during all the day); finally, C4 contains sensor ♯6, located below the skylight and characterised by very low levels of RH during daylight hours (with a low average and high variability).

As seen in Table 7.3, there is a large cluster (C3) containing 5/12 of the sensors, and a second cluster (C5) of sensors similar to cluster C3 (centre distance = 7.58 % of RH), but characterised by a higher average and variability. Let us analyse the differences between these two clusters comparing the mean daily trajectories (Fig. 7.12).

Cluster		**C1**	**C2**	**C3**	**C4**	**C5**
Sensor		OUT	1,7	2,5,9–11	6	3,4,8
Centres (%)	average	66.93	76.94	59.37	47.64	66.82
	daily variation	38.13	7.54	8.73	24.43	10.18
Fraction of sensors		1/12	2/12	5/12	1/12	3/12

Table 7.3: Results of cluster analysis of RH for data from May to July 2010, from 00.00 to 23.59 h (3,120 data points/sensor).

	C2	C3	C4	C5
C1	32.18	30.35	23.66	27.95
C2		17.61	33.82	10.46
C3			19.60	7.58
C4				23.89

Table 7.4: Matrix of distances (in % of relative humidity (RH)) between the final cluster centres for cluster analysis of RH data.

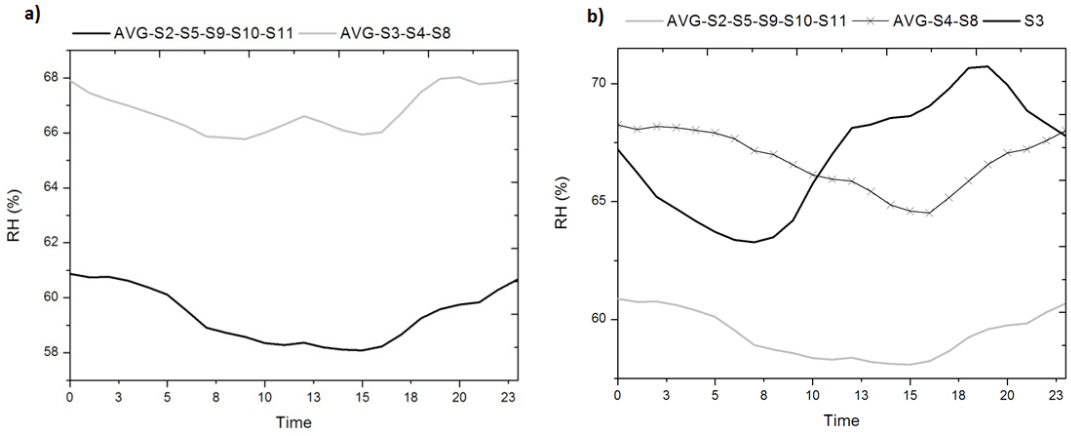

Figure 7.12: Mean daily trajectory of relative humidity of cluster analysis results. (a) The average of sensors contained in cluster 3 and 5; (b) The average of sensors contained in C3, and cluster 5, represented separately sensor ♯3 and average ♯4 and ♯8.

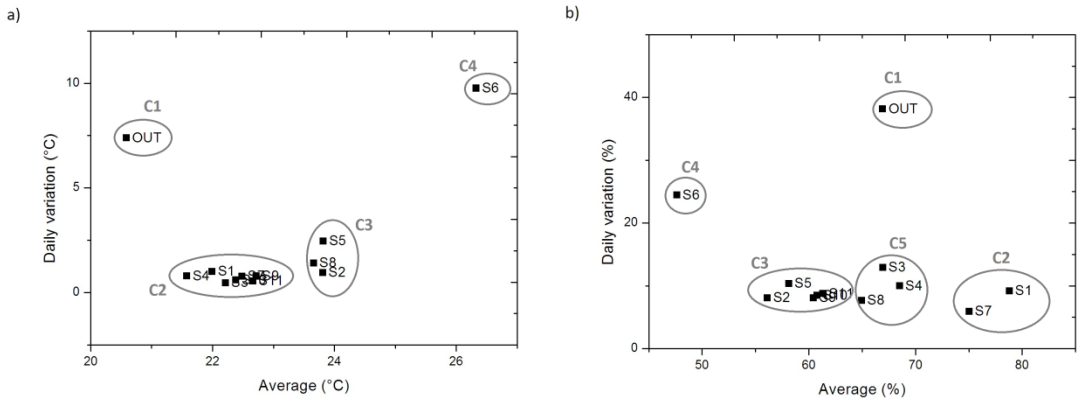

Figure 7.13: Bivariate plot of average versus mean daily variation, from 22 February 2010 to 5 May 2010, from 00:00 to 23:59 h (6,384 data points/sensor), (a) temperature; (b) relative humidity.

An alternative approach for identifying clusters of sensors is proposed. Next, we represent the bivariate plots of temperature and RH for the average versus the mean daily variation. Thus, we can identify visually in Fig. 7.13 different clusters of sensors, coinciding with the results obtained by cluster analysis.

As shown in Fig. 7.12, cluster 5 is composed by sensors ♯3, ♯4 and ♯8 due mainly to having an average greater than C3. By means of the bivariate plots (Fig. 7.13) we observe that sensor ♯3 has more variability, a parameter that captures the amplitude of the trajectory but not its form. Thanks to the representation of the mean daily trajectories (Fig. 7.12.b), we can see the singular form of the trajectory of sensor ♯3 which, contrary to what happens to the rest of sensors, undergoes an increase of approximately 8 % of RH during the day. This occurs to sensor ♯3 because it is in the direct path of the air outlets of the climate control system, so its trajectory reflects the system shutdowns and the cooling strategies followed.

This approach enables us to identify clusters of sensors with similar average and amplitude, as well as allowing comparisons between RH and temperature. Here, it is important to mention the difference between ♯5 and ♯8 in temperature, where these sensors are strongly influenced by the entry of light from the skylight. However, the results in RH differ from those obtained for temperature, as the water pipe apparently smooths the effect of the temperature rise caused by the skylight (which should result in lower RH values).

7.4. Conclusions

Characterising an archaeological site is of great importance, with the aim, on one hand, of carrying out comparative studies in the future when implementing changes in climate control systems or in the architectural design, and on the other hand, to study any future deterioration of the archaeological site, which may be related with microclimate conditions.

The complexity of the data collected and the limitation of the location of the sensors make it difficult to draw relevant and reliable conclusions through standard techniques, such as contour plots or temporal trajectory analysis. The present work is mainly intended for restorers and conservators of archaeological sites.

Three statistical methodologies that are simple to operate have been proposed (two qualitative and one quantitative), which can replace more complex multivariate statistical techniques such as cluster analysis. These proposed techniques are normal probability plot (quantitative), bivariate plots and mean daily trajectories (qualitative), which have been useful in characterising the archaeological site in detail, highlighting the differences between areas.

The results of these techniques have revealed the significant influence of the skylight on the temperature and RH, causing sharp rises and falls during daylight hours. Sensors placed in the vicinity of the cover, but not immediately below, have different behaviour from the other inner sensors. In the case of sensor ♯3, it was possible to detect the direct impact of air from the conditioning system and how the trajectory reflects its operation. Possible solutions to this problem might be installing an external cover over the skylight, painting the glass of the skylight, etc.

On the other hand, a boundary water pipe clearly configures an RH gradient, which decreases as we move away from the pipe. This effect is important to emphasise, as the presence of old water pipes in urban archaeological sites should not be unusual. Piping makes regular monitoring necessary because water may leak, affecting the conservation of the archaeological sites.

When implementing any solution, it would be advisable to perform a short-term monitoring during summer (since it is the most conflictive microclimatic period) and especially in the area immediately below the skylight and its surroundings. Since the current number of sensors has allowed us reaching useful conclusions we consider this an adequate proportion of sensors (in terms of cost-result) whenever working with the appropriate techniques.

Chapter 8

Characterisation of thermo-hygrometric conditions of an archaeological site affected by unlike boundary weather conditions

Characterisation of thermo-hygrometric conditions of an archaeological site affected by unlike boundary weather conditions. Merello, P., Fernández-Navajas, A., Curiel-Esparza, J., Zarzo, M., García-Diego, F.-J. *Building and Environment* 2014, 76, 125-133. DOI: 10.1016/j.buildenv.2014.03.009

Abstract: This paper applies statistical techniques to analyse microclimatic data (temperature and relative humidity) recorded at the archaeological site of Plaza de l'Almoina (Valencia, Spain). This study has allowed us to quantify the effect of certain measures that were adopted for preventive conservation. The first monitoring campaign took place in 2010 at this archaeological site, showing harmful effects on the conservation state of the remains due to the presence of a skylight that partly covers the remains and causes a greenhouse effect. This skylight was covered with a water layer to prevent overheating of this archaeological site. However, this layer was removed in 2013 due to water leaks, and the indoor conditions changed. Over the summer, a temporary canvas was installed over the skylight to avoid heating of the archaeological site below by preventing the incidence of direct sunlight. The main importance of this work was to characterise the effect of unlike boundary weather conditions of different years in the indoor microclimate of the archaeological site, and to study the effect of the new boundary situation. This paper shows that the removal of water from the skylight caused a temperature increase inside the museum; meanwhile, the subsequent installation of the canvas cover allows appropriate daily cycles of temperature and relative humidity, especially in areas under the skylight. This work also shows that the replacement of a water ditch near the archaeological site by a PVC pipe was also detected by the sensors due to the difference in water vapour pressure.

8.1. Introduction

Preventive conservation of artworks has been improved in recent decades through scientific research that has provided a better understanding of the deterioration processes. The main causes of deterioration are environmental: temperature, humidity, light and atmospheric gases. Additional causes include mechanical damage due to inappropriate maintenance and assembly, chemical damage from contact with reactive materials and damage caused by biological organisms, plants, insects and animals. All these factors can be controlled in most cases, although the effect of some of them such as air pollutants can rarely be eliminated.

By controlling these factors, it is possible to significantly slow the deterioration processes, but not to stop them completely. The methodology of preventive conservation is therefore indirect: deterioration is reduced by controlling its causes [129].

Currently, there is growing interest in monitoring the climatic parameters in cultural heritage [10]-[21]. In the case of archaeological sites, temperature differences

between various minerals in block surfaces and differences in surface and substrate temperature are sources of thermal stress. Experience shows that thermal and humidity stresses are important causes of micro-fractures between the mineral grains of blocks [130]. Moreover, thermal variations affecting mechanisms, such as salt crystallisation, may indirectly induce damage. Thermal cycles are more important for surfaces exposed to direct solar radiation [130]. The study of microclimatic conditions surrounding archaeological sites is essential to prevent deterioration and identify eventual consequences of corrective measures [131]-[134].

Some authors have studied the materials composing the roofs [135] and walls [136] of buildings and how they affect the thermal comfort inside, but always focused on the welfare of people, rarely in terms of preventive conservation of archaeological heritage. In our case, we must take into account both the people who visit the museum and the archaeological remains. Nor should we forget the importance of the microclimate on the energy demand in public buildings in the context of climate change [137].

The city of Valentia (Valencia, Spain) was founded by the Romans in 138 BC, and the exact founding point where the city started is located in Plaza de l'Almoina. Evidence of Roman settlement can still be seen in the excavated remains of the Roman forum and baths [42].

The archaeological subsurface gathers a group of monumental buildings that form a complete compendium of history and urban development of Valencia, from its origins until today.

L'Almoina is an archaeological museum located in a building about 3 m below the current city sidewalk level. The archaeological remains are covered by a concrete structure, which forms an elevated plaza above the sidewalk. This cover connects with sidewalks through steps with different heights along its perimeter due to the slope of the sidewalk. There is no vertical retaining wall inside the museum to isolate the remains from water diffusion through capillarity from the surrounding areas. The archaeological remains cover an area of 2500 m^2 and retain vestiges ranging from the second century BC (Roman) until the fourteenth century (medieval).

In 2007, an external concrete structure adapted to the archaeological site was built, and a skylight (25 $\times$ 25 m) covered with a water layer was installed, allowing passers-by a glimpse of the archaeological remains below.

Preventive conservation of the archaeological site at Plaza de l'Almoina includes maintaining stable and adequate temperature and relative humidity levels and managing light exposure, among others. An initial campaign of thermo-hygrometric

monitoring in Plaza de l'Almoina [50] showed a relevant effect of the skylight on the variations in temperature and relative humidity, causing sharp rises and falls during daylight hours. Possible solutions to this problem were proposed [50], based on the experience of a previous monitoring study in the ruins of Ariadne's house in Pompeii [19].

In early summer 2013, water leaks from the skylight occurred, dripping onto the archaeological site. As an initial solution, Valencia City Council, which manages the archaeological site, eliminated the water from the skylight to prevent further leaks. Later, in August, the City Council placed a waterproof canvas over the skylight, preventing rainfall leakage and the direct impact of sunlight.

Moreover, in the year 2011 a water ditch built with porous bricks passing near the archaeological site [50] was substituted by PVC pipe (11 cm of diameter). In general, microclimatic characterisation of an archaeological site must be repeated whenever environmental or boundary conditions change [50], [103]. So, a second monitoring campaign in Plaza the l'Almoina was carried out in 2013.

In [138], the same problem of comparing the effect on thermo-hygrometric conditions of implemented measures is described, aimed at attributing the different levels of temperature and RH to these corrective actions. In this paper, the same data selection is performed and the selected data periods have similar outdoor environmental conditions (mainly in temperature). Now, the same procedure is applied in a buried archaeological site.

The main aim of this work is to assess the effect of different corrective measures and changes implemented in the archaeological site of Plaza de l'Almoina using statistical methods sparsely used in cultural heritage and with proven effectiveness [50], [19], [131] as well as to quantify the improvements achieved by the proposed solution which could be taken as an example for other similar archaeological sites in the future.

8.2. Materials and methods

8.2.1. Data loggers and installation

The same data-loggers were installed as in the first monitoring campaign [50], in the same place (in this paper, sensor positions are shown in Figs. 8.3 and 8.7) and

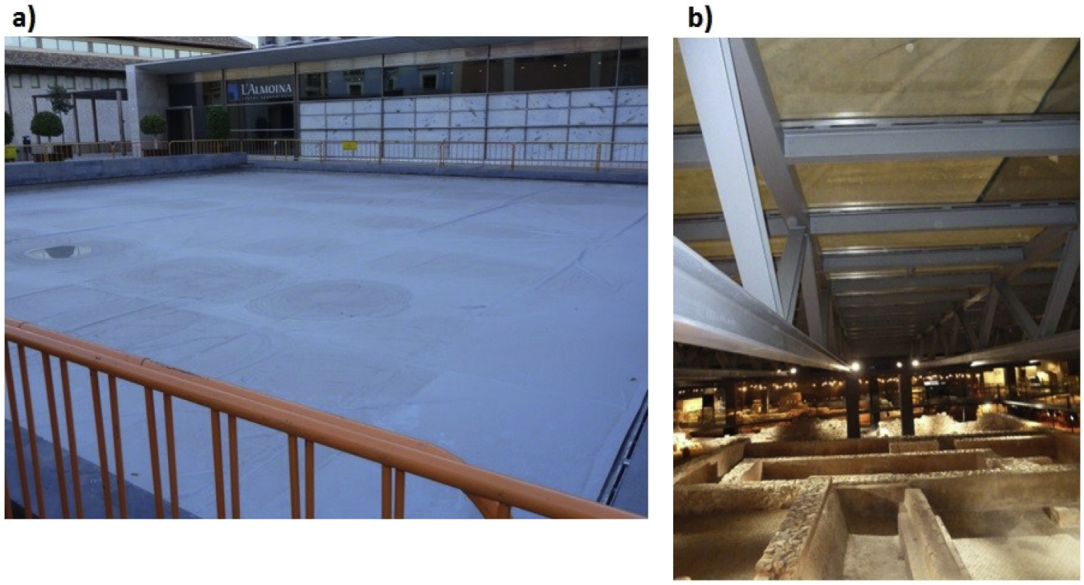

Figure 8.1: Canvas cover, a) viewed from above, b) viewed from below.

with the same calibration methodology.

The second monitoring study began on 22 July 2013 and ended on 11 September 2013, resulting in a total period of 51 days. All data loggers were programmed to register one measurement every 30 min, which entails a total of 2448 recorded values (i.e., 51 days × 24 h/day × 2 data/h).

Sensor coded as number 8 (♯8) was stolen; therefore no data are available for this location. Sensors ♯3 and ♯4 were manipulated by third parties causing data loss for one week, from 09/05/2013 (at 18:00) to 09/11/2013 (at 23:59).

8.2.2. Corrective action implemented

As aforementioned, on 20 August 2013 the City Council of Valencia installed a canvas cover directly on the skylight. The canvas was white and 625 m^2 in area. It was installed directly onto the glass without a fixing system (Fig. 8.1).

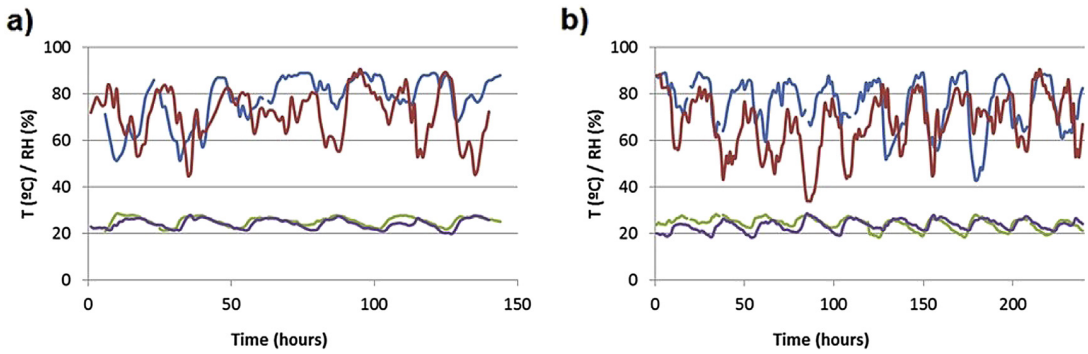

Figure 8.2: Similarity of periods selected from the first (2010) and second (2013) campaign. a) Data for 2010 and 2013 before installing the canvas. Value 0 on the horizontal axis coincides with 06/30/2010 (0:00 h) and 07/31/2013 (0:00 h, period A). b) Data for 2010 and 2013 after installing the canvas. Value 0 on the horizontal axis coincides with 06/25/2010 (0:00 h) and 08/20/2013 (0:00 h, period B). Legend: blue line corresponds to RH data in 2013, red to RH data in 2010, green to temperature data in 2013 and violet to temperature data in 2010.

8.2.3. Statistical analyses

Data selection

In order to compare data obtained in the first monitoring campaign (2010, before removing the skylight water and installing the canvas) with data from the second campaign (2013), a data selection was performed because the two periods monitored are very different: the entire year was monitored in 2010, while only summer was monitored in 2013.

As was done in [138], to compare the effect on thermo-hygrometric conditions of implemented measures and in order to attribute the different levels of temperature and RH to these corrective actions, the time periods compared must have similar outdoor environmental conditions, mainly of temperature. This is necessary to avoid the confusion of effects such as attributing differences, for example, to a warmer period.

In this paper, we work with two different data matrices that correspond to similar thermo-hygrometric outdoor conditions (Fig. 8.2): one matrix to compare data recorded in 2010 with data registered in 2013 before installing the canvas, and another matrix to compare data recorded in 2010 with data obtained in 2013 after installation of the canvas cover (Table 8.1).

Period	Description	Data	Selected dates 2010	Selected dates 2013
A	Data 2010 vs. data 2013 before canvas installation	288 (6 days)	06/30/2010 – 07/05/2010	07/31/2013 – 08/05/2013
B	Data 2010 vs. data 2013 after canvas installation	480 (10 days)	06/25/2010 – 07/04/2010	08/20/2013 – 08/24/2013 and 08/31/2013 – 09/04/2013

Table 8.1: Selected dates with similar outdoor conditions, to be used in the data analyses.

The results are discussed according to international standards [7], [83]. The recommended range of RH and temperature for stones and rocks is 40-60 % and 19-24°C, and a maximum daily variation of 6 % in RH (no recommended daily variation is available for temperature).

Contour plots

Contour plots were analysed in this paper as done in [50], [131]. These plots were obtained with a CAD program. The graduation of the parameter was obtained by triangulation from the physical parameter value (its daily mean value) in a sensor and its closest neighbour. This was performed for all sensors. Next, equal graduation points were connected with splines, obtaining a contour plot for the physical parameter.

Mean daily trajectories

Plots of mean daily trajectories allow us to condense the information of large time periods and discern differences between sensors by visual inspection [19], [50], [131]. In this work, mean daily trajectories were calculated as the average of the data recorded from all sensors per fraction of time (in this case, every hour) for the entire period of interest.

Normal probability plot

The normal probability plot is a graphical technique for normality testing, assessing whether or not a data set is approximately normally distributed. This plot has been previously used for detecting anomalous behaviour of thermo-hygrometric parameters in cultural heritage [50]. We are interested in detecting those sensors whose differences from the average are abnormal. For this purpose, we worked with the average of inner sensors (calculated considering sensors from ♯1 to ♯11) since the main interest was to characterise differences inside the archaeological site.

Analysis of variance (ANOVA)

To study the effect of the waterproof canvas installed, different ANOVA models were tested for data recorded in 2013, considering the following factors: day, sensor (from ♯1 to ♯11) and canvas (0 = no installed vs. 1 = installed, depending on the state of the skylight during this period). ANOVAs were performed using the software Statgraphics 5.1 [103].

ANOVA analyses were carried out for all data recorded in 2013 without selecting any time interval, since the entire monitoring period corresponds to summer and differences between periods can be studied with the factor day.

8.3. Results and discussion

8.3.1. Microclimate characterisation after removing the skylight water layer (period A)

This section studies the effects on the microclimate inside the archaeological site in 2013 as a result of removing the water on the skylight. For this purpose, data recorded in 2013 were compared with data registered in 2010 (period A), when conditions for conservation of the archaeological site were unfavourable [50].

The main change in the mean temperature of the archaeological site as a result of emptying the skylight (Fig. 8.3.a and Fig. 8.3.b) is a generalised increase of this parameter, especially in those sensors located below the skylight (♯6), as a

consequence of the direct impact of sunlight on the glass and the non−existent energy filter effect of the water.

Regarding the water vapour pressure (Fig. 8.3.c and Fig. 8.3.d), the substitution of the water ditch by a PVC pipe has substantially modified the gradient; whereas in 2010 it ran from west to east, in 2014 it is less pronounced and runs from north to south.

As shown in Fig. 8.4.a and Fig. 8.4.b the mean daily temperature trajectory of the outdoor sensor is almost coincident in both years, which implies that both periods are comparable and the differences observed in sensor ♯6 are a consequence of having removed the water layer from the skylight. Thus, sensor ♯6 has increased its mean daily temperature. Its mean daily maximum reaches 37 °C, a value that is detrimental to conservation of the archaeological site, as it exceeds 24 °C, which is the temperature recommended by the standards [7], [83]. The remaining sensors inside the archaeological site have also increased their temperature by 2 °C on average. Note that in 2013 the average trajectory of inner sensors at the archaeological site was above 24 °C during the monitored period, which is the recommended temperature value for preservation of the remains [7], [83].

Fig. 8.4.c and Fig. 8.4.d shows that removing the water from the skylight has caused an increase in temperature (Fig. 8.4.b) as well as a drop in RH in the areas immediately under the glass, primarily reflected by the trajectory of sensor ♯6, which shows a mean daily variability in both years of roughly 14 % of RH, which is higher than the standard recommended value (6 %). On the other hand, the adjacent water ditch [132] caused higher levels of RH in sensors ♯1 and ♯7 in 2010 (Fig. 8.4.c), as a result of substitution of the water ditch by a PVC pipe in 2013. There is no such contribution by capillary action and the trajectories in sensors ♯1 and ♯7 resemble the trajectories of sensors ♯2, ♯5, ♯9−11 (Fig. 8.4.d).

Notice the shift recorded by sensor ♯3, which in 2010 captured the effects of the climate control system and presented an inverted trend compared to the rest of sensors. In 2013, this sensor underwent a very similar pattern to sensors ♯2, ♯5, ♯9 − 11. The reason could be that the climate control strategy was changed; the air conditioning system was working intermittently in 2010 depending on the needs of the archaeological site, whereas in 2013 it was working continuously throughout the day.

The normal probability plot in Fig. 8.5 helps us identify those sensors whose differences compared to the inner average depart from normality.

In the case of temperature (Fig. 8.5.a), sensor ♯6, which is located directly below

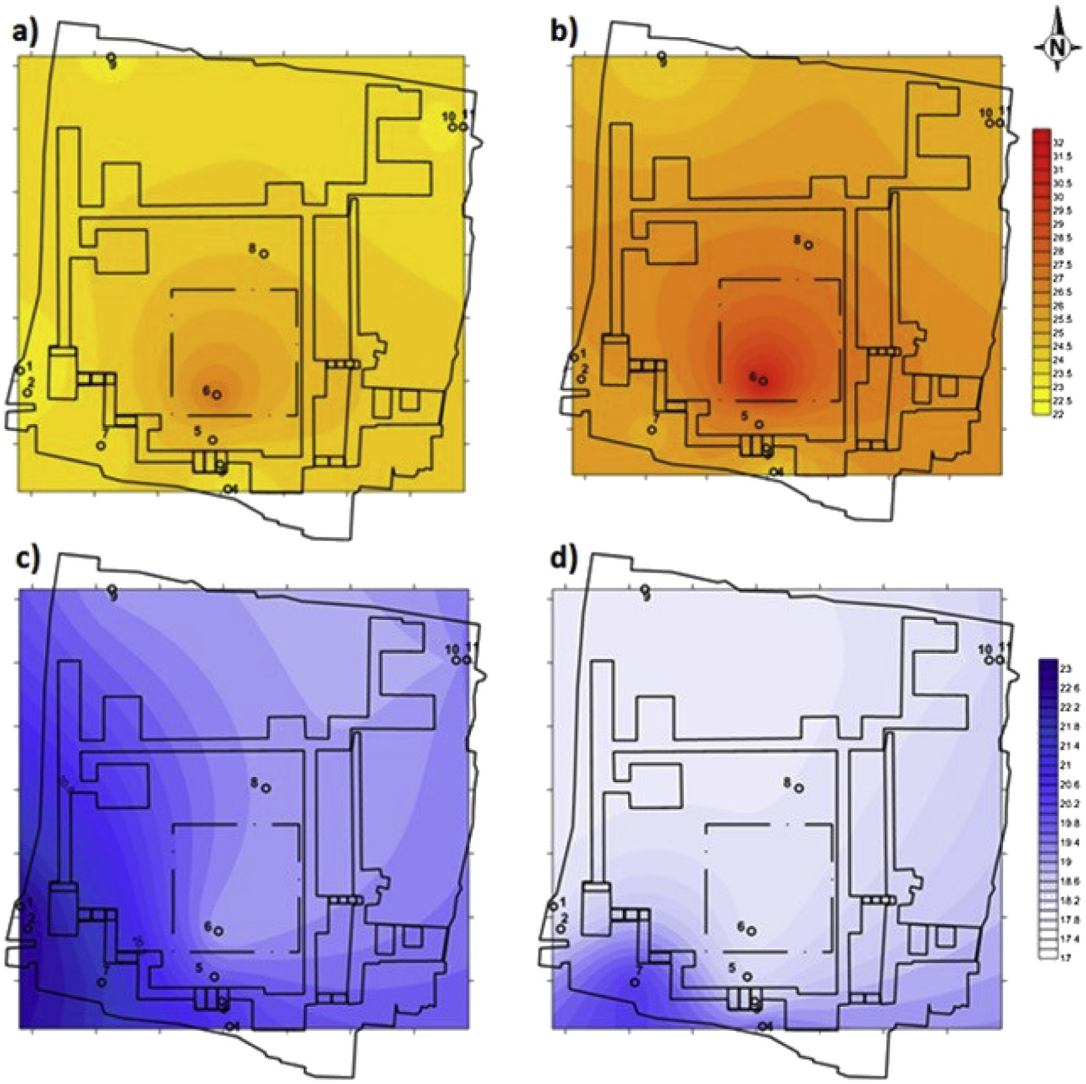

Figure 8.3: Contour plots (period A), a) of temperature (°C) in 2010, b) of temperature (°C) in 2013, c) of water vapour pressure (mbar) in 2010, d) of water vapour pressure (mbar) in 2013.

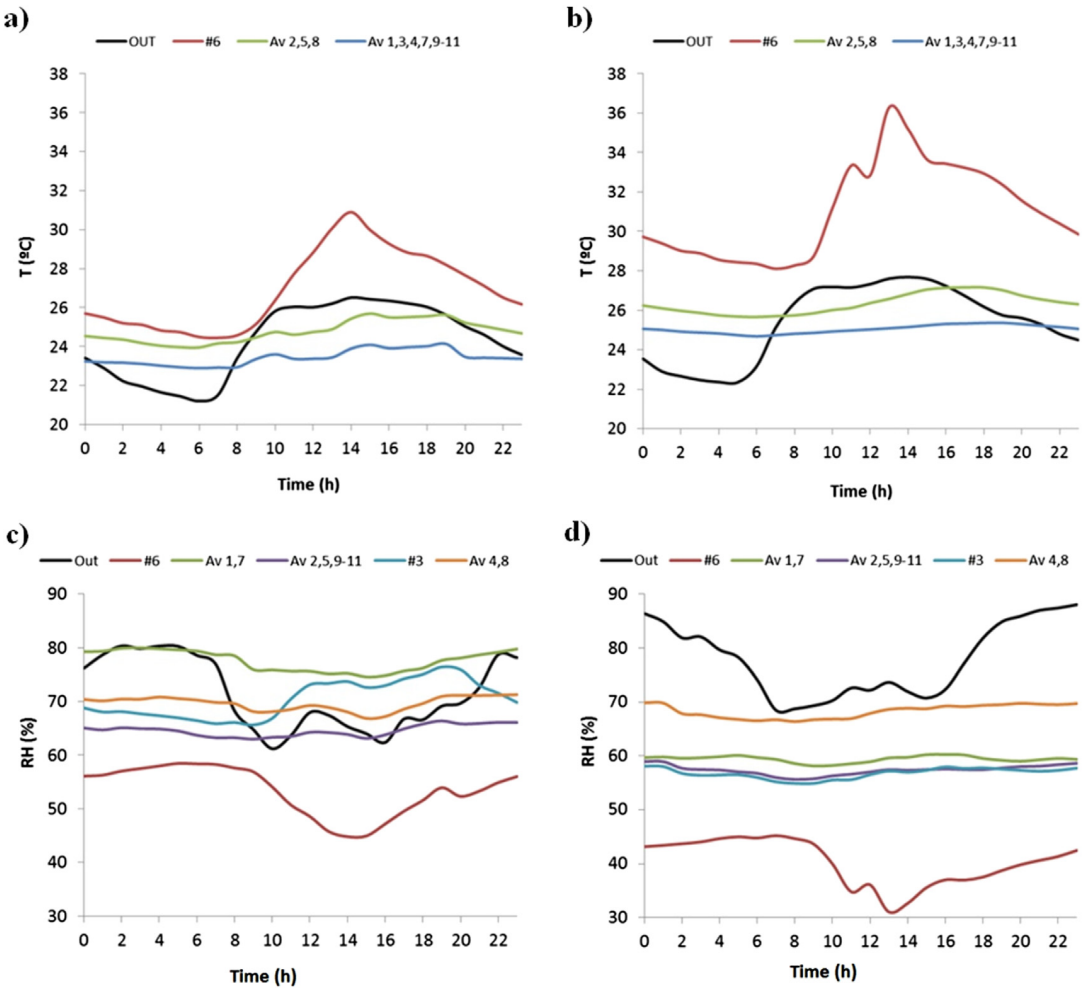

Figure 8.4: Mean daily trajectories of sensors contained in clusters defined in [136]. a) Temperature in 2010 (period A). b)Temperature in 2013 (period A). c) RH in 2010 (period A). d) RH in 2013 (period A).

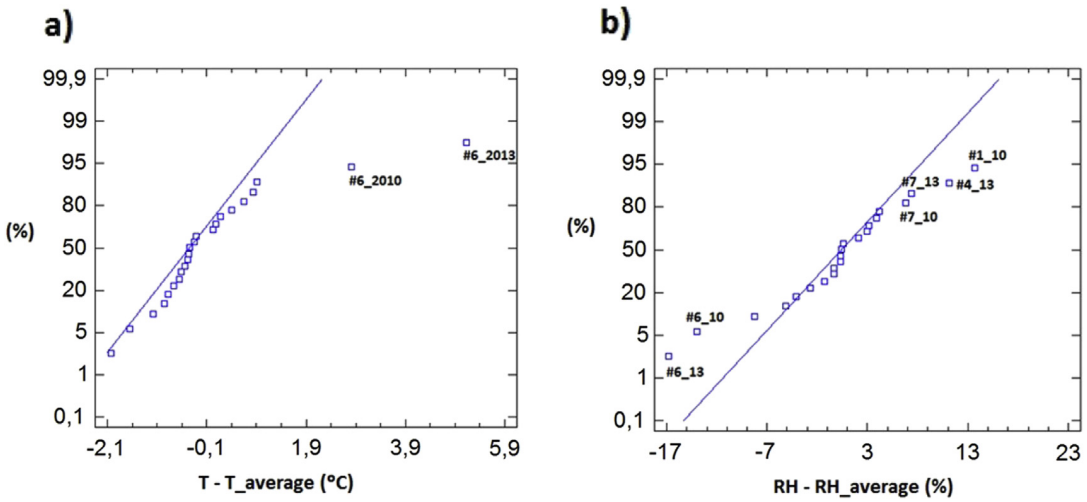

Figure 8.5: Normal probability plot comparing data recorded in 2010 with data recorded in 2013 (period A), for a) temperature difference of each sensor with respect to the inner average this year, b) RH difference of each sensor with respect to the inner average this year.

the skylight, appears further away from the normal trend followed by all sensors of the archaeological site and this difference has increased as a result of emptying the skylight.

For RH (Fig. 8.5.b), the abnormality of sensor ♯6 is more noticeable in 2013 than in 2010, mainly due to the decrease in the daily minimums (Fig. 8.4.c and Fig. 8.4.d). On the other hand, sensor ♯1, which recorded abnormally high RH values in 2010 as a result of water infiltration by capillarity from the nearby water ditch, presents normal behaviour in 2013 after substituting it by a PVC pipe.

Finally, note that sensor ♯4 appears as anomalous in RH in 2013 (Fig. 8.5.b) because its mean daily trajectory of RH is very similar in both years (2010 and 2013, Fig. 8.4.c and Fig. 8.4.d), while the other sensors have substantially changed in 2013, thus changing the inner average of RH, and now ♯4 appears as one of the wettest sensors, in accordance with the results shown by the contour plot of water vapour pressure (Fig. 8.3.c and Fig. 8.3.d).

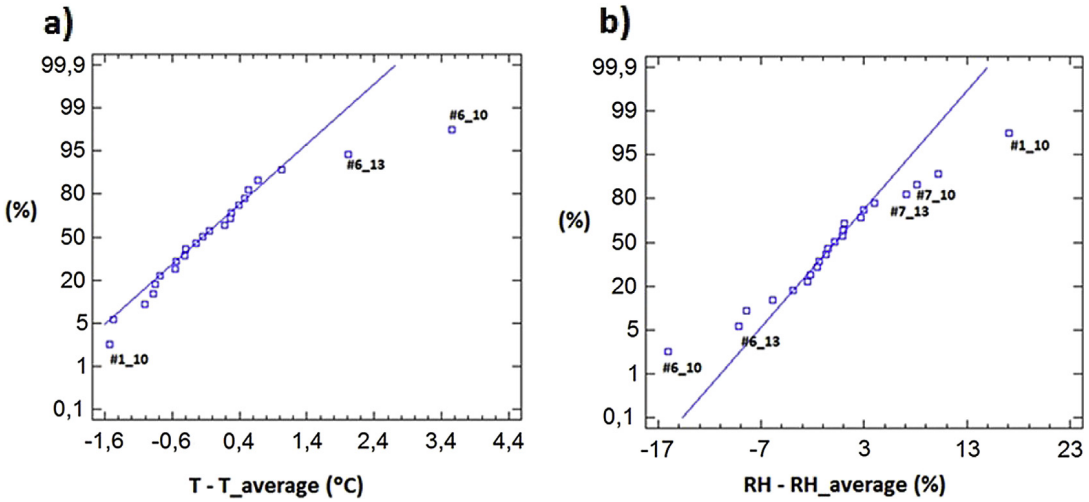

Figure 8.6: Normal probability plot comparing data recorded in 2010 with data registered in 2013 (period B), for a) temperature difference of each sensor with respect to the inner average this year, b) RH difference of each sensor with respect to the inner average this year.

8.3.2. Microclimate characterisation after installing the canvas (period B)

In this section we assess whether installation of the canvas cover has improved the microclimatic conditions affecting the ruins in 2010 [50].

As was done for data recorded before installing the canvas cover (period A), a normal probability plot was represented (Fig. 8.6) for the differences compared to the inner average, in order to identify which sensors have a different behaviour compared to the general trend followed inside the archaeological site in that particular time period (2010 and 2013, period B).

Sensor ♯6 is the most anomalous in temperature, especially in 2010 when no cover was installed, exceeding the inner mean temperature by 3.54 °C. In 2013, when the canvas was installed (period B), sensor ♯6 exceeds the inner mean temperature by approximately 1.8 °C.

As in Section 8.3.1, after substituting the water ditch with a PVC pipe, sensor ♯1 reflects RH values similar to the average. However, sensor ♯7 continues recording RH values above the average in 2013, which may indicate that the contribution of moisture received by this sensor is not related to the water pipe but with the

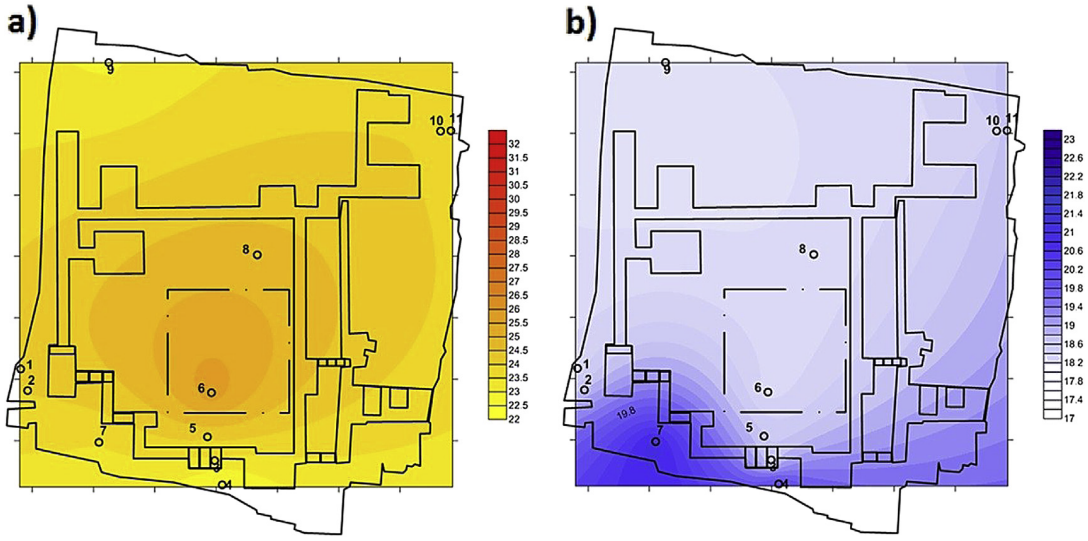

Figure 8.7: Contour plots in 2013 (period B), a) of temperature (°C), b) and water vapour pressure (mbar).

waterproofing of the town square located immediately above this area of the archaeological site.

On the other hand, the temperature increase caused by the skylight during daylight hours resulted in remarkable differences to the average RH in 2010 (♯6_2010, RH values 16.09 % lower than average), and after installing the canvas cover (noted as _C) these differences were smoothed (♯6 _C, RH values 8.27 % below average).

Note that Normal probability plots have also been performed for amplitudes (daily maximum minus minimum), maximums, minimums, and for the differences of these parameters compared to the inner average. As the results were similar, only the plots for the mean value are presented here to simplify the discussion.

8.3.3. Comparison of data recorded in 2013, before and after installing the canvas cover

The temperature gradient after installing the canvas cover (Fig. 8.7.a) remains centred on the skylight, as the major source of heat inside the archaeological site. However, thanks to the installed cover, the place has a more uniform temperature at the different areas and the average temperature in the areas near the skylight has decreased.

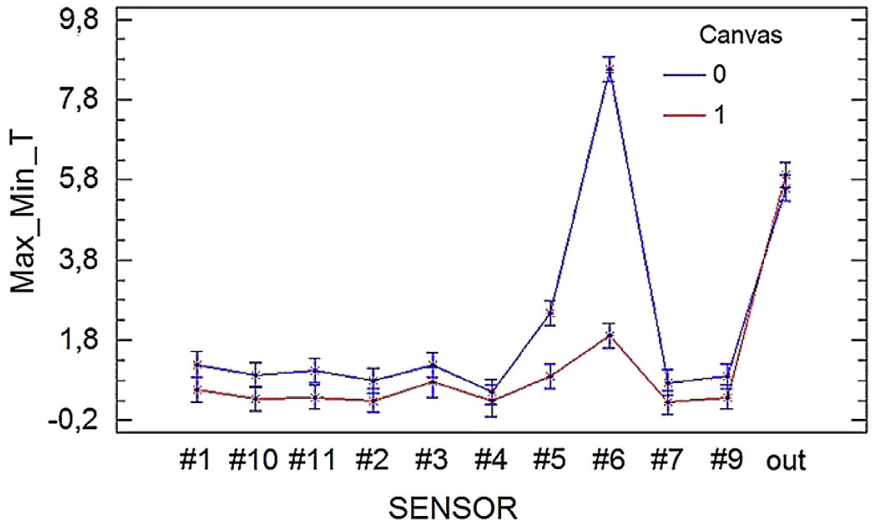

Figure 8.8: ANOVA interaction plot, with the daily amplitude of temperature as dependent variable and "sensor" and "canvas" (takes the value 1 when the canvas was installed and 0 otherwise) as factors. ANOVA analyses were performed for the data recorded in 2013 without selecting dates.

In 2013, the substitution of the water ditch by a PVC pipe was reflected in the water vapour pressure gradient (Figs. 8.3.d and 8.7.b).

Higher levels of water vapour pressure at sensor ♯7 reflect the lower waterproofing of the urban square bounding at the southwest with the archaeological site.

The effect of the canvas cover on the thermo-hygrometric parameters, considering the emptying of the skylight (data 2013), was also studied by statistical techniques.

As explained in the Materials and Methods section, in order to quantify and empirically evaluate the effect of the canvas cover on the thermo-hygrometric parameters at the archaeological site, analysis of variance (ANOVA) was applied for data recorded in 2013, considering the amplitude (max−min) of temperature (and RH) as independent variables and two factors (sensor and canvas).

The two factors and their interaction were statistically significant (p-value <0.00001) and relevant in practice. Especially noteworthy is the effect of the canvas installation on sensor ♯6 (immediately below the skylight) and ♯5 (in surrounding areas), which have reduced their daily amplitude by 6.7 °C and 1.6 °C, respectively (Fig. 8.8).

It should be kept in mind that the differences reflected by ANOVA for the factor "canvas" are not attributable to a relevant difference in the outdoor temperatu-

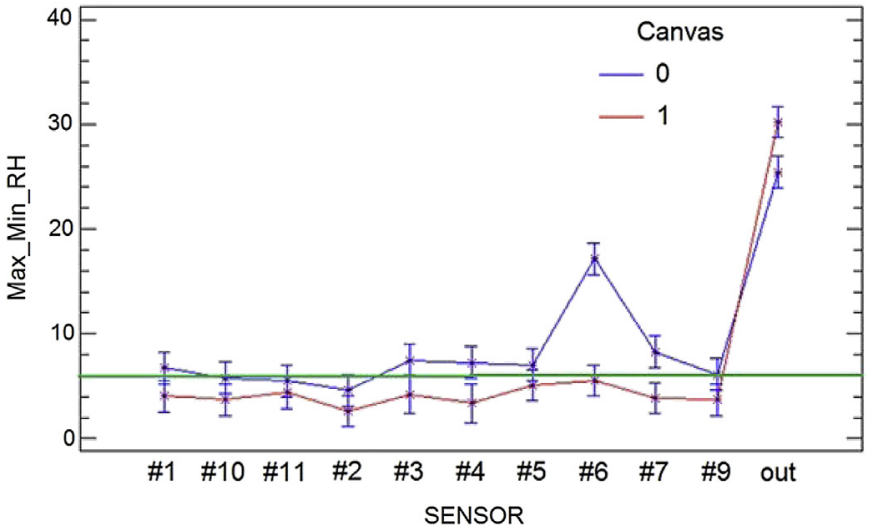

Figure 8.9: ANOVA interaction plot, with the daily amplitude of RH as dependent variable and "sensor" and "canvas" (takes the value 1 when the canvas was installed and 0 otherwise) as factors. ANOVA analyses were performed for the data recorded in 2013 without selecting dates. Green horizontal line indicates the variability of RH recommended by the standards (6 %) [50], [103].

re values in the compared periods, because the least significant difference (LSD) intervals of outdoors sensor overlap, and thus their differences are no statistically significant.

To assess whether the differences are also relevant in practice for the canvas factor in those sensors displaying little reduction in variability, an ANOVA analysis was performed eliminating data from sensors ♯6 and ♯5. In such case, both factors (canvas and sensor) are significant (p-value $<$ 0.00001), but the interaction between them is not statistically significant (p-value=0.46). This result indicates that the effect on the daily variability caused by installing the canvas is relevant, but approximately the same for all sensors.

In the case of RH, both factors and their interaction were significant (p-value$<$0.00001). The installation of the canvas cover reduced the daily amplitude of RH by 11.8 % and 1.7 % for sensors ♯6 and ♯5, respectively. Their mean daily amplitudes now being below the 6 % recommended by the standards (Fig. 8.9).

As for temperature, ANOVA of RH was performed removing data corresponding to sensors ♯6 and ♯5, both factors being significant (p-value$<$0.00001), but not their interaction (p-value=0.11). Again, it can be deduced that the effect on the daily

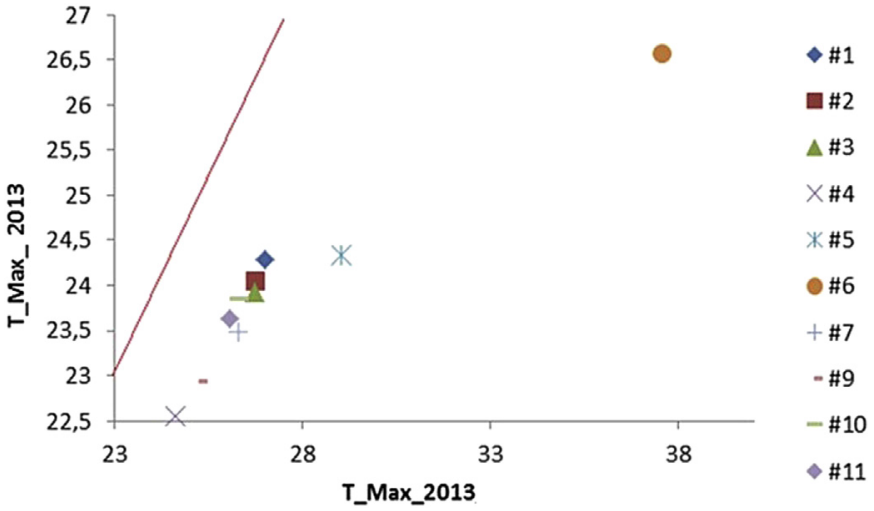

Figure 8.10: Bivariate plot of the mean daily maximum temperature, before (horizontal axis) and after (vertical axis) installing the canvas cover (2013). The red line represents the scenario in which the mean maximum temperature reached without cover is identical to that achieved after installing the canvas.

variability caused by installing the canvas is relevant and the same for all sensors. The interpretation of the interaction can similarly be deduced in the bivariate plot (Fig. 8.10).

The vertical distance to the red line measures the change undergone after installing the canvas cover. Thus, ♯6 is the sensor that has most decreased its mean maximum of temperature (Fig. 8.10), distantly followed by sensor ♯5. The other sensors have dropped their mean maximum by an average of 2.24 °C, which coincides with the non-significant interaction of the canvas and sensor factors in the ANOVA analysis when data from sensors ♯5 and ♯6 are removed. Results are similar for the mean minimum of RH, as the maximums of temperature are significantly correlated with the minimums of RH (p-value < 0.001) with a correlation coefficient of -0.8.

8.4. Conclusions

Recorded thermo-hygrometric data have allowed us to quantify the increase of the daily temperature maximums (and the consequent decrease in the RH minimums) in 2013 as a result of removing the water layer on the skylight (prior to installation

of the canvas cover), especially in those areas immediately below it.

On the other hand, installation of the canvas has improved temperature and humidity conditions for conservation of the archaeological remains, because the covering has created a microclimate more stable and less harmful for conservation purposes according to the recommended values of temperature and relative humidity indicated by the international standards.

The canvas cover has been a provisional solution, whose effectiveness has been proven in view of the results presented here, and a definitive solution more in keeping with the aesthetics of the public square that houses the archaeological site could be designed.

The substitution of the water ditch by a PVC pipe has decreased the RH levels of sensor ♯1. However, sensor ♯7 maintains similar RH levels; this suggests that the supply of moisture in this area comes from a different waterproofing of the area under which it is located.

The proposed methodology resulted in a useful procedure to compare results from unlike boundary weather conditions, based on comparing data from different campaigns in order to determine the effect of a corrective measure using statistical techniques. This methodology allowed us to evaluate the three changes implemented in 2013 at Plaza de l'Almoina and their surroundings, as well as the effects that these changes have had on the thermo-hygrometric conditions of the site, always taking into account that they have a direct impact on the conservation based on the international standards. The satisfactory results of this study can be taken as an example by similar archaeological sites to study and quantify the adequacy of corrective actions.

Chapter 9

Study of the effect of the strategy of heating on the mudejar church of Santa María in Ateca (Spain) for preventive conservation of the altarpiece surroundings

Study of the effect of the strategy of heating on the mudejar church of Santa María in Ateca (Spain) for preventive conservation of the altarpiece Surroundings. García-Diego, F.-J., Fernández-Navajas, A., Beltrán, P., Merello, P. *Sensors* 2013, 13 (9), 11407-11423.

ABSTRACT: The mudejar church of Santa María (Ateca) is valuable for its architecture and the altarpiece contained inside. Ateca is a village in Zaragoza (Spain) with continental climate characterized by cold winters and hot summers. In this paper we are interested in analysing the effect of temperature and relative humidity (RH) changes produced by the heating system on the altarpiece. A monitoring system comprised by 15 temperature and 15 relative humidity sensors was installed with a recording frequency of one data point per minute. The main contribution of this paper is the quantitative study of the effect of the heating system on the thermo-hygrometric parameters using statistical techniques such as ANOVA, mean daily trajectories or bivariate plots, and the proposal of an innovative dynamic contour plot. As results, the heating system produces a substantial increase of temperature and a decrease of RH causing an hourly variation of these physical parameters, which is detrimental to the conservation of the altarpiece, especially in its higher areas.

Keywords: preventive conservation; Spanish cultural heritage; temperature and humidity sensors; climate control system.

9.1. Introduction

In last decades an increasing interest has developed in all areas of conservation, with an interdisciplinary approach. Preventive conservation, as a method of work, aims to control the deterioration of the artwork before it occurs. Currently, preventive conservation measures are acknowledged as important for safeguarding cultural heritage (CH), both in terms of preserving CH and also reducing the cost of future conservation measures [2].

It is recognized that works of art in unheated churches often remain in relatively good condition over centuries, while rapid signs of degradation are observed after heating has been introduced [139]. The indoor climates of unheated buildings are essentially governed by the outside climate modified by the building envelope. The standards [7], [83] recommend that, for the best preservation of materials which are sensitive to moisture, the relative humidity (RH) ranges should replicate the long-term local climate and that the RH fluctuations centred on this local RH level must be kept to a minimum. Heating can introduce serious destabilization to the natural indoor climate in a church.

In particular, wood is a material that undergoes noticeable changes in response to variations in the physical parameters (RH and temperature) characterizing the

environment in which it is placed. The main mechanical properties of wood are its elastic and strength properties. In general, many mechanical properties are affected by changes in moisture content below the fibre saturation point [140]. At constant moisture content and below approximately 150 °C [140], mechanical properties are approximately linearly related to temperature.

The wood supports of paintings are complex structures in themselves [141], which may experience uneven moisture changes, and consequently uneven dimensional responses, on opposite faces of a panel owing to a lower permeability of the painted face to the flow of moisture [142]. Dimensional change is perhaps the most important consequence of moisture interaction with wood affecting any artwork. Wood shrinks as it loses moisture and swells when it gains moisture. Therefore, these contractions and expansions hinder predicting the dimensional change of a given wooden object accurately and the empirical formulae given in wood handbooks can merely be used to estimate the changes [143].

In recent decades an increasing interest has appeared in knowing how RH and temperature can modify the mechanical properties of wood producing deterioration in artworks where this is the main material or base. Some papers have studied this concept from an experimental approach [144]-[147]. In [147], numerical modelling was used to follow the evolution of the moisture content gradient and the stress field resulting from the restrained differential dimensional response across a wooden cylinder, simulating sculptures. However, these studies relate to equilibrium conditions which do not usually coincide with the dynamically changing environments to which historic wooden objects are often exposed. For this reason, in later works [148]-[150] historic wooden objects have been monitored *in situ*. In relation to artworks exposed to heating systems inside churches, some studies performed in churches in Norway have helped to establish that the need for conservation is due to the fact that the climate in heated churches in cold climates is unfavourable for painted wooden objects [151], [152].

In particular, recent works in the literature [139], [153], [154] analyse the influence of RH and temperature on the state of conservation of altarpieces located in churches. In [153], triangulation laser displacement sensors were applied to the continuous *in situ* monitoring of the response of wooden altarpiece in the church of Santa María Maddalena in Rocca Pietore (Italy), to fluctuations in temperature and relative humidity caused by the use of a heating system. In another paper [139], the evolution of cracks in some figures of the altarpiece was monitored according to RH variations, and the main conclusion obtained was that the variation in the moisture content caused dimensional changes in the wood; the response, however, was characterized by ranges and rates which varied considerably with the thickness of the wooden elements. The authors of [154] employed Digital Speckle Pattern Inter-

ferometry (DSPI) and Speckle Decorrelation (DIC) to perform condition surveys of a wooden altarpiece in the church of Hedalen, Norway. The authors of [154] only consider an easy sampling method to be used as an alternative to visual inspection of the piece under study by conservators, but they do not perform an exhaustive monitoring of the physical parameters that are influencing the deterioration.

None of the aforementioned studies analyse in depth and quantitatively the behaviour of the temperature and RH with a mesh of sensors located at different heights and orientations in the altarpiece. One of the main contributions of this work is to consider the effect of the microclimate on the different parts of the altarpiece.

Ateca is a village in the province of Zaragoza in the region of Aragon (Spain). Located at the southwest of the province, at the confluence of the rivers Jalón and Manubles, Ateca is at 606 m above sea level (Latitude: 41°19'51" N, Longitude: 1°47'36" O) [51].

The mudejar parish church of Santa María is located at the village centre. Mudejar is a style of Iberian architecture and decoration, particularly in Aragon and Castile, dating to the 12th to 16th centuries and strongly influenced by Moorish taste. In contrast to other churches of the same period, mudejar churches are mainly made of brick and plaster, instead of ashlar stone [52]. Santa María of Ateca is a temple of a single nave, a seven-sided polygonal apse and chapels between the buttresses. It has a square tower (Fig. 9.1.a) and two sections, minaret structure with stairs covered by barrel vaults and simple ribbing. The tower was built during the second half of the thirteenth century while the mudejar church was constructed in the fourteenth century.

The altarpiece (Fig. 9.1.b) depicts the most important events in the life of the Virgin Mary, and was made between 1650 and 1657. The author of the relief was Martin of Almunia, from Ateca. Bernardo Ibañes was the author of the sculptures, and they were polychromed by Juan Lobera and his sons Jusepe and Francisco Lobera [53].

Ateca features an extreme climate, with a mean daily RH between 11.94 % and 91.97 % and a mean daily temperature ranging from -5.59 °C to 38.48 °C. Therefore, a single heating strategy was adopted. The church is heated rapidly, shortly before and during religious services, to a more comfortable temperature [54], [55] with a hot air heating system through the church.

The vault had repainting and detachment problems. Thus, in 2011, a restoration work performed by the company Albarium S.L. (Zaragoza, Spain) began. Taking advantage of the installed scaffolding, a monitoring system was installed on the

(a) (b)

Figure 9.1: (a) Exterior photograph of mudejar church of Santa María in Ateca. (b) Altarpiece. Photographs from the Prensa Diaria Aragonesa S.A. archive taken by Santiago Cabello.

altarpiece to control both the dome and altarpiece, which has major conservation problems.

It was decided to implement a monitoring system for recording a full year of data of the physical parameters involved in conservation with more influence on wood, *i.e.*, temperature and humidity, both in the front and the back of the altarpiece.

This paper aims to document the conservation conditions, the possible causes of deterioration and the effect of the heating system on the microclimatic conditions affecting the altarpiece of the church of Santa María in Ateca (Spain), to prolong its preservation as much as possible (with corrective measures if necessary), being the first time that a microclimatic study is performed in a mudejar church. For this purpose, the recorded data are analysed by descriptive univariate and multivariate statistical methods [19], [21] recently employed in cultural heritage, serving this example as a working methodology for similar cases.

9.2. Materials and Methods

9.2.1. Monitoring System

A total of 15 probes were installed, 14 in the interior of the temple distributed in the front and the back of the altarpiece, and an additional probe placed on the sill of a window as an outdoor climate control (Table 9.1). All probes contain an 8-pin small-outline integrated circuit (SOIC), model DS2438 (Maxim Integrated Products, Inc., Sunnyvale, CA, USA) that incorporates a direct-to-digital temperature sensor with an accuracy of ± 2 °C as well as an analogue-to-digital voltage converter which measures the output voltage of a humidity sensor (HIH-4000, Honeywell International, Inc., Minneapolis, MN, USA). Because each DS2438 contains a unique silicon serial number, multiple DS2438s can exist on the same data bus. This allows multiple sensors that can be used in the system simultaneously with only one data line (1-wire communication protocol). The HIH-4000 RH sensors were calibrated in the laboratory with a saturated solution of salt as explained in [16].

As specified by the manufacturer, the voltage output of the HIH-4000 sensors is proportional to voltage supply. Thus, the exact value of the voltage supply was measured for each RH sensor once all probes and connections were installed and the calibration curves of each sensor were corrected.

Sensor (S)	Heigth (H)	Back (B)/ Front (F)	S	H	B/F	S	H	B/F	S	H	B/F
1	10.2	F	2	8.3	B	3	4.7	B	4	12.6	F
5	9	B	6	4.3	B	7	2.9	B	8	12.6	F
9	9	F	10	6	B	11	3.2	F	12	10.5	F
13	7.23	B	14	3.2	B	15	OUTDOOR		-	-	-

Table 9.1: Position in which the sensors were installed, specifying height (meters) and orientation in the altarpiece (Back = B, Front = F).

Three electric wires come out from each probe: one wire for +5 V DC power supply, one for ground and another for data transfer. Measurements were recorded in digital format by a microcontroller, to which all sensors were connected in parallel. Recorded data were downloaded monthly to a pen-drive. At the time the monitoring system was installed, it was decided to study whether there were differences between the different areas of the altarpiece (front vs. back, and height). However, due to technical difficulties during installation, sensors could not be perfectly distributed for a complete statistical sampling; therefore most sensors of the front were located at the top of the altarpiece (Table 9.1).

9.2.2. Data

The sensors were installed on 10/14/2011. As the monitoring period for analysis, we considered those data taken from 10/15/2011 to 09/04/2012, however some data had errors, so a set of 80 days were eliminated, which means a total of 245 available days. The outdoors sensor (♯15) started measuring from 01/04/2012 to 09/04/2012.

The sensors were installed with a data acquisition frequency of 60 data points per hour (1 data point every minute). Thus, each sensor is capable of recording 43,200 data points per month (30 days × 24 h/day × 60 values/h). Therefore, in this study we have a data matrix of 352,800 (245 days × 24 h × 60 min) rows and 15 columns (sensors) each one.

The software used for storage and management of recorded data [128] allows detecting and eliminating those anomalous data caused by a punctual error in the sensor data collection or a numerical register that does not fit within the physically possible minute increments of that parameter. In this case, a minute variation of ±5 °C and ±5 % of RH is considered for removing data.

9.2.3. Statistical Analyses

Different exploratory and comparative statistical analyses are used in this work. In order to study if the differences among different positions of the sensors were statistically significant, a multifactor ANOVA was carried out considering different factors as appropriate. We worked with the following factors: day, height (0-5 m (low), 5-10 m (intermediate), 10-13 m (high)), orientation (B/F), season (10/14/2011 - 3/31/2012 "cold", 4/1/2012 - 5/9/2012 "warm"), and the climate control system (ON/OFF). Different statistical parameters were calculated for each hour and each temperature and RH sensor: the average and the hourly variation.

In order to study the effect of height and orientation where the probe was located, different ANOVA models were tested with these parameters. ANOVAs were performed using the software Statgraphics 5.1 [103].

Mean trajectories allow an easy identification of deviations with respect to the target trajectory when cycles are clearly marked. Mean trajectories is a plot commonly applied in the control of batch chemical processes, however this kind of plot is not frequently used in cultural heritage microclimate monitoring studies [19]. The time series of temperature or RH recorded by one data-logger reflects the parameter evolution along time. Temperature and RH mean daily trajectories were plotted in order to discuss the dissimilarities among probes and to identify abnormal patterns.

We also analyse contour plots, as done in [50]. The graduation of the parameter yields is performed by triangulation from its value in two points connected by a straight line (in this case a sensor and the closest one). After doing this for all sensors, points with equal graduation are connected with splines, obtaining a contour plot of the physical parameter. The dynamic contour plots have been similarly made, but considering as points in the plane the hours of the day and the months of the year.

Finally, bivariate plots have proven to be a simple technique that can be interpreted by visual inspection and giving similar results to cluster analysis [19]. A bivariate plot was obtained to compare the difference between the average value of temperature before switching the heating system and the maximum temperature during the heating period versus $(T_{MAX} - T_{AVG})$ the difference between the average value of RH before switching the heating system and the minimum RH during the heating stage $(RH_{AVG} - RH_{MIN})$.

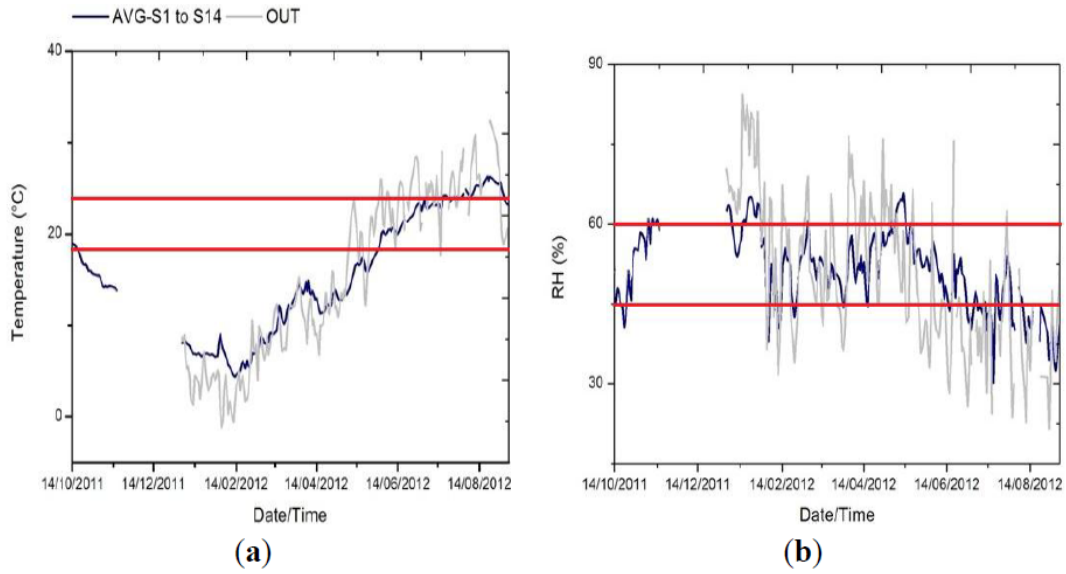

Figure 9.2: Time series of the average of inner sensors (from ♯1 to ♯14) (blue) and the outdoors (whose data begin on 01/04/2012, gray), (a) temperature, (b) RH.

9.3. Results and Discussion

9.3.1. Characterization of the Outdoor and Church Microclimate

Fig. 9.2 shows how the temple smooths the external variability, and it also highlights the extreme climate in Ateca, reaching negative temperatures in winter and above 30 °C in summer. Average trajectories of both parameters (RH and temperature) were inspected for the identification of inappropriate conditions that might be harmful for the wood altarpiece according to the standard UNI [83] and DM 10/2001 [7], which recommend for carved wood conditions of 19-24 °C for temperature (maximum daily variation of 1.5 °C) and 45 %-60 % RH (maximum daily variation of 2 %).

For the monitoring period, approximately 80 % of the points of the hourly average temperature of the altarpiece exceed the recommended values (Fig. 9.2), and the same apply to 32 % of the hourly average RH values.

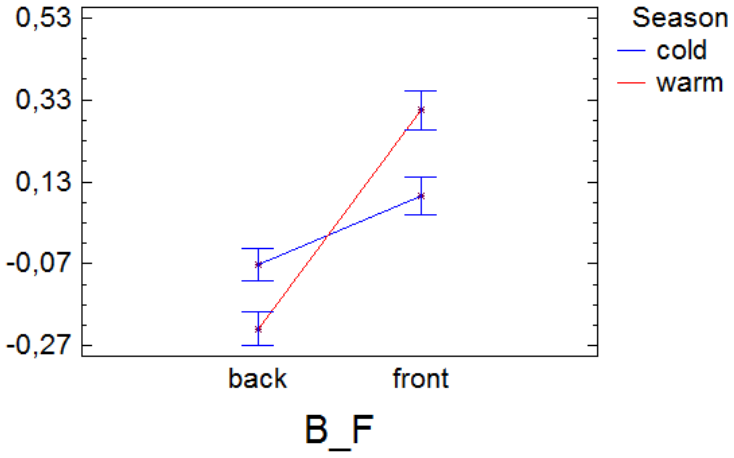

Figure 9.3: Interaction plot of the factors orientation (B/F) and season (cold = blue, warm = red), for the ANOVA analysis of the differences to the average temperature (residuals of an ANOVA of the temperature and the factor season).

9.3.2. Microclimatic Characterization of the Altarpiece

As seen in the previous section, temperature exceeds more often than RH the recommended limits, reaching values predominantly lower than the recommended range because winter temperatures in the temple reach values below 19 °C, while in the case of RH the limits are exceeded mostly in summer. Given the differences between seasons, we have characterized the altarpiece discussing the main differences between the orientation of sensors for the different seasons.

Fig. 9.3 shows the interaction between sensor orientation and the season. In this ANOVA, the factor season is not meaningful ($p - value > 0.05$) because we are working with their residuals to assess differences to the average of that season, *i.e.*, the values of the vertical axis are the differences to the average for that season. However, the interaction is statistically significant.

For temperature, the difference to the average is greater in the front than in the back of the altarpiece. However, that difference becomes even more marked in summer as a result of the higher variability (variance) in the data during this season.

In our opinion, it is possible that the differences between the front and back (B/F) are caused by the hourly variability of temperature. Thus, the ANOVA (Fig. 9.4) indicates that in the case of temperature there are only significant differences between B/F in the cold season, which could indicate that these differences in hourly

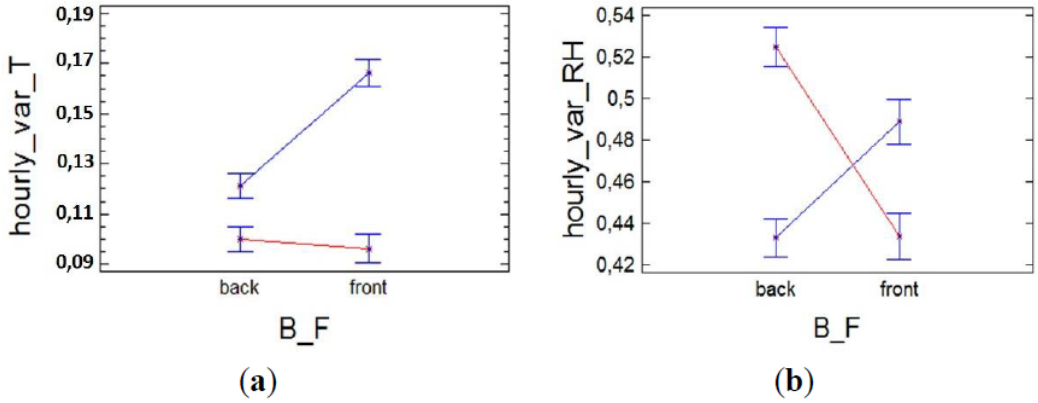

Figure 9.4: Interaction plot of the factors orientation (B/F) and season (cold = blue, warm = red), for the ANOVA analysis of the hourly variation of (a) temperature, (b) RH.

variation are caused in part by the switching of the heating system.

In the case of RH in summer, there is no heating and most RH variability occurs in the back (Fig. 9.4.b). However, in winter the highest variability occurs in the front, which could indicate that this greater variability is induced by the climate control system on the same way that seemed to indicate the temperature. Note that although these differences are small, lower than the sensor error indicated by the manufacturer, due to the fact that an average of a large amount of data is calculated, these differences are relevant.

9.3.3. Analysis of the Effect of The Climate Control System

It is required to determine those specific or regular events that cause an increase of temperature (decrease of RH) due to the switching of the climate control system, and, after studying the mean daily trajectories of the average of all inner sensors for each day of the week, the following events have been detected:

- Saturdays at 20:00, coinciding with the main religious service of the week. These peaks are explained by the switching on of the heating system at 19:00 to heat the temple for the Mass; the heating system shuts off between 20:30 to 20:45, at the end of the religious service. The heating system is switched on from 2/4/2012 to 5/5/2012. From November 2011 to January 2012, Masses were held at another local church due to restoration works.

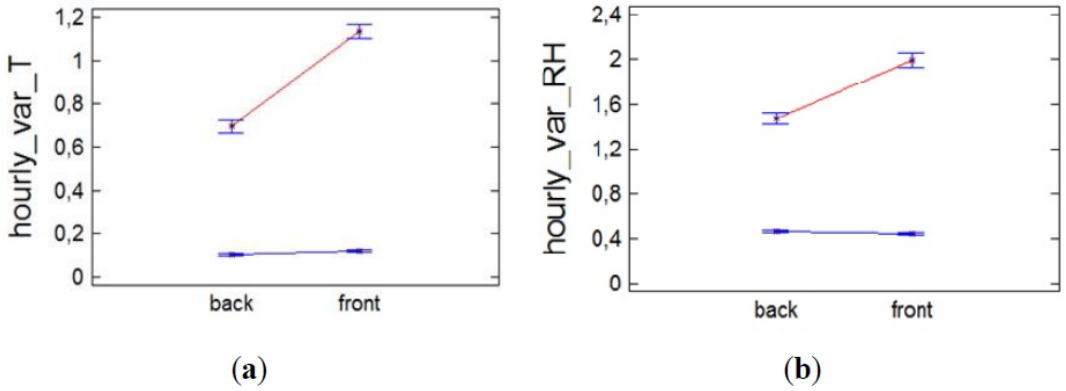

Figure 9.5: Interaction plot of the factor climate control system (blue = OFF, red = ON) and orientation (B/F), for the ANOVA analysis of the hourly variation of (a) temperature, (b) RH.

- The switching on of the heating system during Saint Blas festivity (2/1/2012-2/3/2012).
- The switching on of the heating system from 3/26/2012 to 3/31/2012, coinciding with the preparations for the Easter processions.

ANOVAs were conducted considering as a factor the climate control system, which will take the value "ON" for those cases when it was switched on as a result of an event. In this way we want to analyse if the heating system produces significant changes in temperature and RH.

ANOVA indicated that significant differences exist between the front and the back, and especially for those situations when the heating system is switched on (Fig. 9.5), so next we analyse the mean daily trajectory of the front and back sensors for days when the heating system is switched on (Fig. 9.6). Sensors at the front have all day a temperature approximately 0.5 °C higher (1.5 % lower RH) than those in the back, but when the heating system is switched on the difference between front and back is accentuated reaching 3 °C of temperature (4 % RH).

A contour plot is performed to visually assess those areas that are most affected by the heating system. Notice that temperature and RH are practically constant in the entire altarpiece when the heating system is not working (Fig. 9.7.a and 9.7.c). However, for the hours when the heating system is switched on, there is a vertical gradient of temperature and RH (Fig. 9.7.b and 9.7.d), but with contour plots it is unclear if the differences are significant (both in temperature and in RH), so we

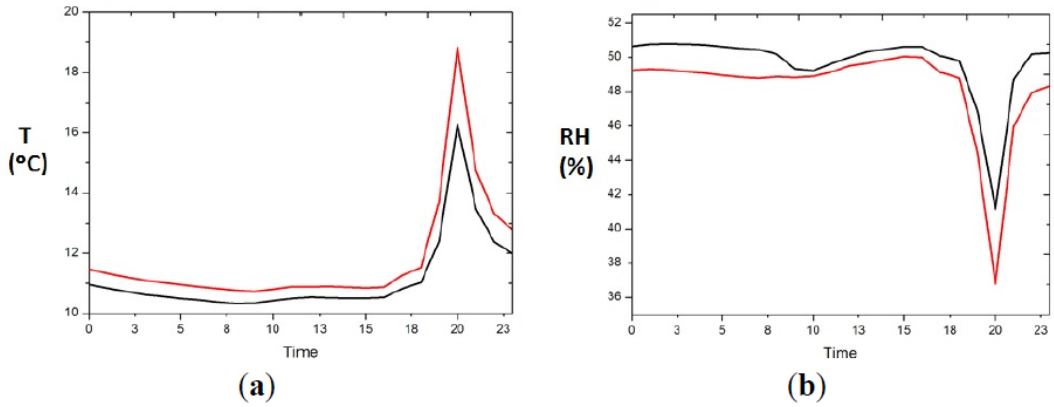

Figure 9.6: Daily mean trajectories for back (black) and front (red), for days when the heating system is switched on, (a) temperature, (b) RH.

perform ANOVA analysis considering the height (low, intermediate and high) as a factor.

The bigger hourly variation clearly occurs as consequence of the heating system and especially in the upper and middle areas of the altarpiece as hot air rises (Fig. 9.8). Note that the hourly variation of temperature and RH exceeds the maximum recommended daily variation for the standards, so considering that these recommended values are for daily variations we can assert that an hourly variation of this magnitude will be very detrimental to the conservation of the altarpiece.

Since most sensors in the front are placed at the top, the B/F effect is possibly masked with the predominant effect of the height when the heating system is switched on (Fig. 9.7.b and 9.7.d). The question arises whether the significant difference between back and front sensors are due to its orientation or rather due to the height at which they are located.

Note that in Fig. 9.4, the hourly variation differences between B/F are not statistically significant for temperature in the warm season (when the heating system does not work). In the case of RH, these differences are significant but with opposite sign (in the warm season there is more variation in the back, and in the cold season in the front).

This suggests that the differences attributed to the factor B/F when the heating system is switched on (Fig. 9.5) would actually be a consequence of the fact that sensors in the front are mostly at the top area (note the similarity in shape between red and lime trajectories in Fig. 9.9). Thus, when the heating system is working the

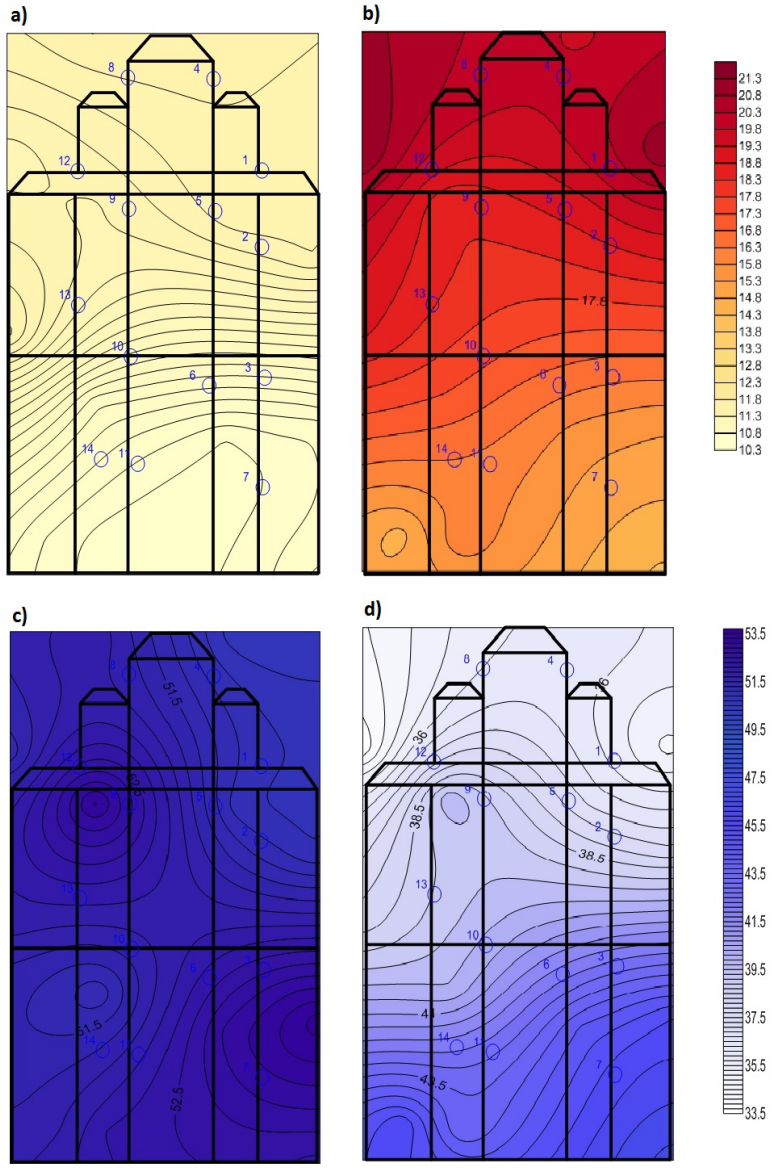

Figure 9.7: Contour plots for days when the heating system is switched on, (a) for the average temperature before switching (2 h), (b) maximum temperature during the heating period, (c) for the average RH before switching (2 h), and (d) minimum RH during the heating period. Circles represent sensors on the back of the altarpiece and squares represent those sensors located in the front of it.

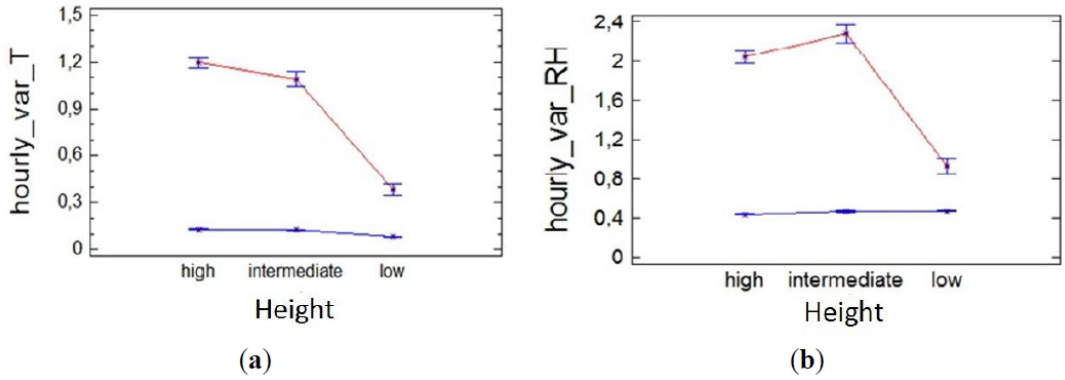

Figure 9.8: Interaction plot of the factors climate control system (blue = OFF, red = ON) and height, for the ANOVA analysis of the hourly variation of (a) temperature, (b) RH.

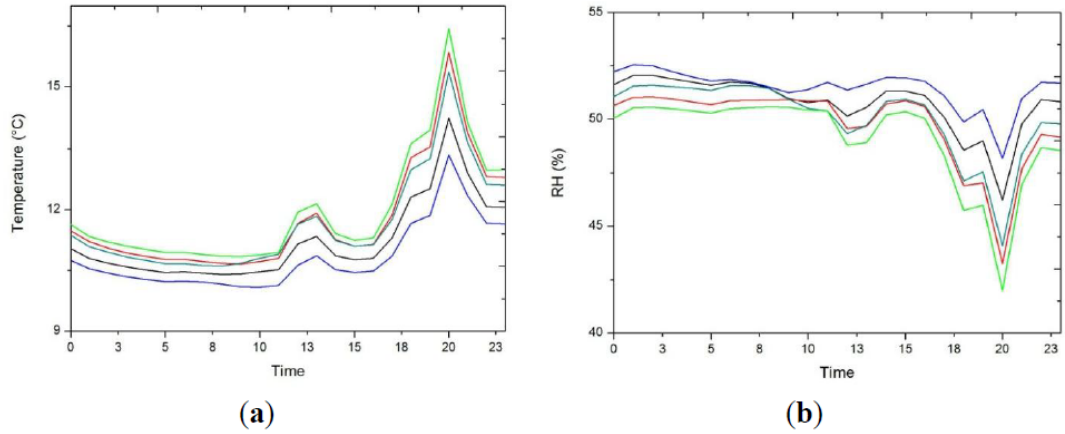

Figure 9.9: Mean daily trajectories, for days when the heating system is switched on, of the average of sensors at the back (black), the average of sensors at the front (red), the average of sensors at low height (blue), the average of sensors at intermediate height (green) and the average of sensors at high height (lime). (a) Temperature. (b) RH. Note the similarity between the red and lime trajectories, although smoothed the red one since it also includes sensors ♯9 and ♯11.

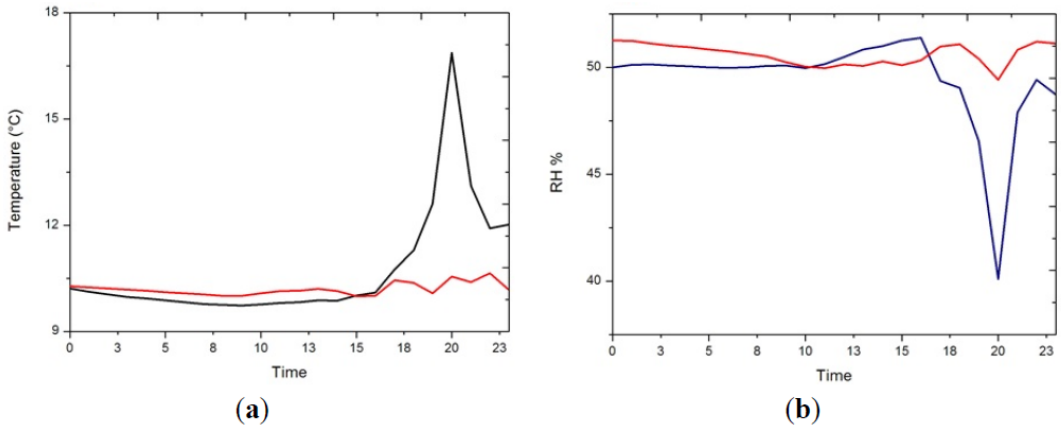

Figure 9.10: Daily mean trajectories of sensors ♯1, ♯4, ♯8, ♯12, for Saturday (black) and Monday (red), from 2/1/2012 to 5/5/2012 (period when heating strategies are followed), (a) temperature, (b) RH.

main differences can be found between heights, masking this factor the difference between B/F, as shown in Fig. 9.7.b and 9.7.d where the gradient is mainly vertical. It would be interesting to investigate the interaction of factor B/F and height, but it is not possible because not all the possible combinations of heights and positions were tested due to technical difficulties during installation.

After performing ANOVA analysis with height factor, we found that the heating system mainly affects the sensors at the upper area (sensors ♯1, ♯4, ♯8 and ♯12). Thus, the normal behaviour of these sensors on days when no religious events take place (Mondays) *versus* days when the heating system is switched on (Saturdays) are compared. In Fig. 9.10 we can observe how when the heating system is switched on an average increase of 7 °C of temperature (and a decrease of 11 % RH) occurs in the range of 1 h.

After verifying that there are significant differences in height as a result of the heating system and evaluate these differences by quantitative (ANOVA) and qualitative (mean daily trajectories and contour plots) methods, we propose to evaluate a bivariate plot to check if they achieve similar results and propose these techniques as an alternative methodology, easier to interpret, to be used primarily by conservators who are non-scientists.

Fig. 9.11 illustrates that the main differences between sensors caused by the heating system are produced according to height. It also appears that there might be some difference, although lower, between front and back as sensor ♯11, located at similar

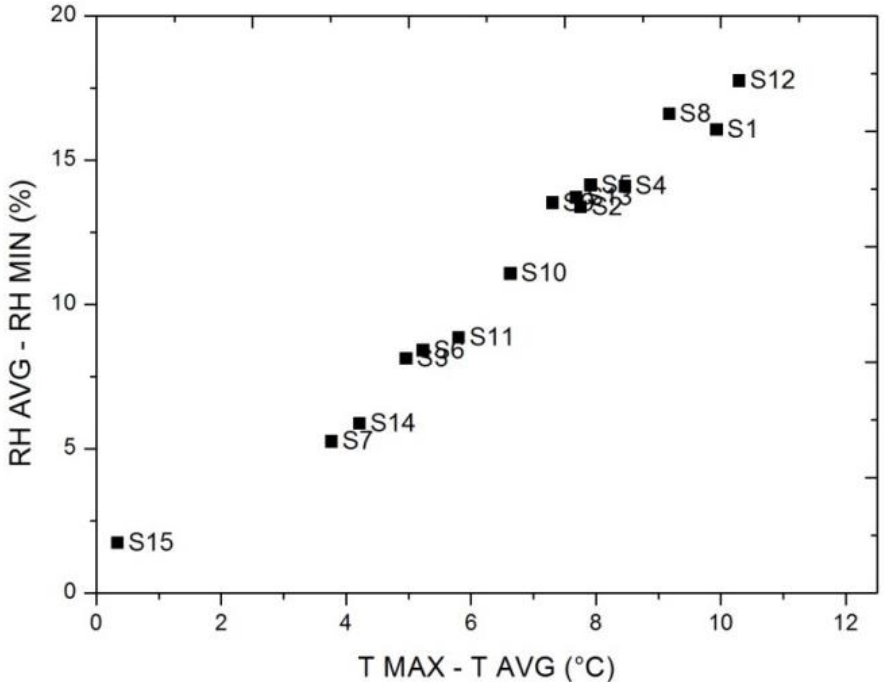

Figure 9.11: Bivariate plot of temperature (horizontal axis) versus RH (vertical axis), of the difference between the average before the heating system is switched on (2 h) and the maximum (minimum for RH) when it is working (from 2/1/2012 to 5/5/2012).

height to ♯14 and ♯7, but in the front, reflects a bigger temperature increase (2 °C) and a bigger RH decrease (3 %). This fact is not clearly reflected in the contour plots (Fig. 9.7), which highlights another benefit of using bivariate plots. However, we note that the interaction between height and orientation (B/F) has not been empirically verified by ANOVA due to complications during installation of the sensors, but possibly there exist significant differences between B/F when the heating system is working.

Then an alternative plot is proposed (Fig. 9.12), for simple visual inspection, to evaluate the differences in mean daily trajectories produced by the heating system (in this case comparing days when a religious event takes place and days when no event takes place) and its dynamic behaviour over the year. In our case, since we already know the sensors which are further noting the changes produced by the heating system (♯1, ♯4, ♯8 and ♯12) we perform this plot for the average temperature of these sensors. However, note that this graph can also be used with the average of all sensors or, for comparative purposes, for one or more sensors separately.

Fig. 9.12 allows us to visually compare the annual change experienced by the mean daily trajectories. Thus, for a traditionally uneventful day (Fig. 9.12.a and 9.12.c) it is observed how temperature remains constant during the day with the annual gradation typical of seasonality of temperature, which is reflected in the plot by almost parallel vertical lines. Similar results are obtained for RH. However, for Saturdays (Fig. 9.12.b and 9.12.d) of those months when the heating system is working (from February to April) an increase of temperature between 19 and 21 h is produced coinciding with the celebration of Mass in the temple (reflected in the chart by "islands" of different tone). We also see that temperature seems to indicate that the first Saturday of September a Mass or concentration of people occurred in the temple. Studying this fact we realize that it coincides with the feast of the Virgin of the Peana (from 6^{th} to 10^{th} September), being the 8^{th} of September Saturday, (Fig. 9.12.b and 9.12.d) the festivity of the Virgin.

This proposed plot allows an easy inspection of a dynamic problem as the temperature variation along the day, also considering its typical variation along the year.

9.4. Conclusions

The techniques used have been able to quantify the effects of the heating system on temperature and RH, parameters that determine the conservation of the altarpiece. These techniques allowed us to determine when the heating effects are more pronounced and their hourly evolution.

A quantitative methodology is proposed, based on ANOVA analysis and a graph of simple interpretation, based on contour plots, that combines the power of mean daily trajectories and the dynamic nature of the time series of temperature and RH.

A proper experimental design is important, however it is not always possible, therefore take into account the deficiencies of the design and employ techniques to surmount them is of great interest.

The "on" switch of the heating system has been detected at different moments due to the celebration of Masses and religious events resulting in a rapid hourly temperature increase of 7 °C and lowering of 11 % of RH in the sensors located at the highest area (♯1, ♯4, ♯8 and ♯12).

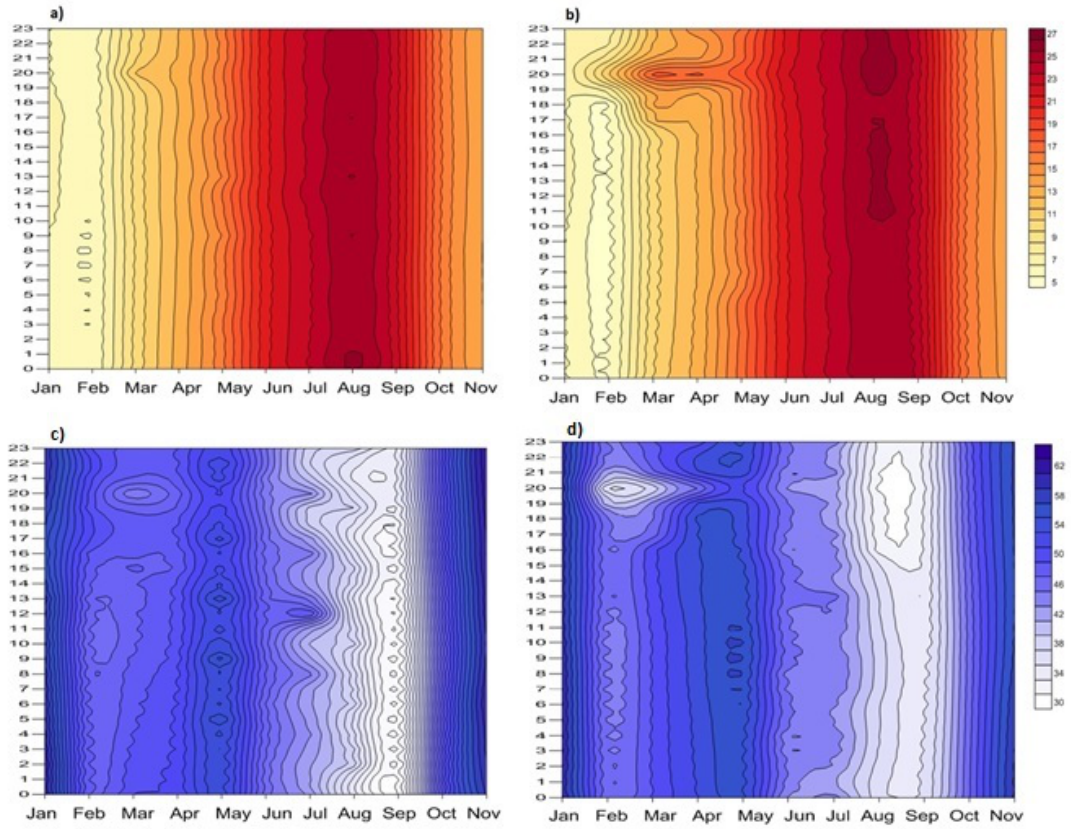

Figure 9.12: Annual contour plot of mean daily trajectories, of the average of sensors ♯1, ♯4, ♯8 and ♯12. The horizontal axis represents the months of the year (from January to November) and the vertical axis the day hours (0-23). (a) Temperature on Mondays, (b) temperature on Saturdays, (c) RH on Mondays, (d) RH Saturdays.

On the other hand, the gas heater emission of CO_2 and H_2O (which would raise the RH) is not affecting that physical parameter, since the figures show when the climate control system is working RH decreases as a result of a temperature increase.

Chapter 10

Software for storage and management of microclimatic data for preventive conservation of cultural heritage

Software for storage and management of microclimatic data for preventive conservation of cultural heritage. Fernández-Navajas, A., Merello, P.,Beltrán, P., García-Diego, F.-J. *Sensors* 2013, 13 (3), 2013, pp. 2700-2718.

ABSTRACT: Cultural heritage preventive conservation requires the monitoring of those parameters involved in the process of deterioration of artworks. Thus, both long-term monitoring of the environmental parameters as well as further analysis of the recorded data are necessary. The long-term monitoring at frequencies higher than 1 data point/day generates large volumes of data that are difficult to store, manage and analyze. This paper presents a software which uses a free open source database engine that allows managing and interacting with huge amounts of data from environmental monitoring of cultural heritage sites. It is of simple operation and offers multiple capabilities, such as detection of anomalous data, inquiries, graph plotting and mean trajectories. It is also possible to export the data to a spreadsheet for analyses with more advanced statistical methods (principal component analysis, ANOVA, linear regression, etc.). This paper also deals with a practical application developed for the Renaissance frescoes of the Cathedral of Valencia. The results suggest infiltration of rainwater in the vault and weekly relative humidity changes related with the religious service schedules.

Keywords: relative humidity and temperature sensors; software; database management; mean trajectories; cultural heritage.

10.1. Introduction

The development of specific software for research purposes, especially in sensors applications, is of high importance in order to adapt to the particular case study and come to relevant conclusions of the recorded data with the maximum possible efficiency [155].

Today, the preventive conservation of the artistic legacy is a priority. Preventive conservation is defined as a working method and a combination of techniques which help in determining and controlling the deterioration process of cultural heritage before it occurs [156].

The practical application of a preventive conservation plan involves the study and control of the risks of deterioration. Objects are influenced by their environment, in terms of stress caused by physical agents such as temperature, humidity, radiation, and chemical agents (e.g., CO_2, SO_2, O_3, mineral salts, etc.), and creating sometimes harmful conditions for preservation [3] - [6]. Specifically, both abrupt changes and inappropriate values of temperature and relative humidity (RH) [7], can cause serious damage to the structure of objects, such as non-isotropic material deformation or detachment in materials of several layers. In hygroscopic materials, such as

wood panels, which are the mainstay of many artworks, mechanical changes and deformations can occur [8]. In the case of frescoes, moisture and soluble salts are the very common causes of degradation; therefore an early detection of inadequate values of these physical parameters is essential to avoid this kind of damage [9].

The study of climatic conditions surrounding the artwork is essential to prevent deterioration [10], [132]-[134], and to identify eventual consequences of corrective measures.

Lately, there is a growing interest in monitoring the climatic parameters in cultural heritage [12], [16] - [19], [21], [32]. The environmental monitoring is performed by a regular data collection, whose frequencies are typically between one datum every hour or every day [12], [22]. Data recorded with very low frequencies of time (e.g., 1 datum/day) is easy to handle, but valuable information may be lost.

Technological changes and the emergence of faster and cheaper microprocessors have opened the possibility to store and work with larger amounts of data, with higher recording frequencies than one datum per hour [19], [21], [28], [98]. It is possible to take a datum every minute without problem in the current systems of data collection and analysis [16], [18]. However, if an accurate grid of the cultural heritage site is monitored, the amount of data recorded increases rapidly arising the need of store and manage them properly. Within a few months of monitoring, the amount of recorded data can easily be a million [18], making it impractical to use standard office software (e.g. MSOffice or OpenOffice). Therefore, it is imperative to develop a database that satisfies requirements of storing large amounts of data, reliability and low-cost compatible with current limited research budgets.

The aim of this paper is to present software specifically developed to store and manage databases (DB) with large storage capacity for environmental monitoring.

This paper presents the application of the DB to the case of the Renaissance frescoes of the Cathedral of Valencia (Spain). During 350 years the frescoes remained in stable conditions of temperature, humidity and lighting, as they were covered by a Baroque vault. In 2004, the vault was removed to restore the frescoes and they were left uncovered with the intention to be contemplated. Furthermore, the outer cover over the vault was reconstructed and waterproofed by an asphaltic roofing sheet which, however, was not tested for tightness and cannot guarantee an absolute waterproofing [16], [18].

To ensure that there is no water infiltration and that the new environmental conditions do not result in a risk for the long-term conservation, it was decided to implement a monitoring system comprised by temperature and RH sensors insta-

lled during the restoration process. The aim of monitoring is two-fold. On one hand, increases of moisture in specific parts of the vault may indicate water infiltration through the roof, which would require corrective measures similar to those specified in [157]. On the other hand, it is of interest to detect diurnal or seasonal excessive thermohygrometric variations that may need corrective measures. In 2006, several salt efflorescence problems were detected in some areas of the frescoes. The monitoring system and management software of the DB can contribute to study the causes of the salt efflorescences [18].

10.2. Materials and Methods

10.2.1. Software Resources

The software is developed with Delphi [158] by the Object Pascal language and Firebird [159] as database engine. Firebird and Delphi are both developed by the same company (Borland, currently disappeared), favoring its compatibility compared to other open source softwares, like PostgreSQL or MySQL.

Firebird is open source software; therefore it is not needed to pay a license fee for download, use or developing of commercial programs (Fig. 10.1). It works on MS Windows systems (XP, Vista and Windows 7) in 32 and 64 bits. Possibly it will work on Linux with a Windows emulator, but it has not been tested yet. It does not consume excessive system resources, works perfectly on a PC with Windows XP and 500 MB of RAM.

The DB is a single file *.FDB that can store millions of data. Currently we manage a DB of over 37 million records with a size of 10.5 GB.

10.2.2. Monitoring System

The monitoring system used in the vault of the Cathedral of Valencia was developed by a multidisciplinary research team. The system consists of a microprocessor and a simple wiring which records data from 32 RH sensors and 32 temperature sensors, placed at different points on the vault and on the surface of the paintings [18]. A frequency of one datum every minute for each sensor is used, generating a volume of more than 2.7 million data per month. RH sensors are formed by an HIH-4000 integrated circuit (Honeywell International, Inc., Morristown, NJ, USA) [160] with

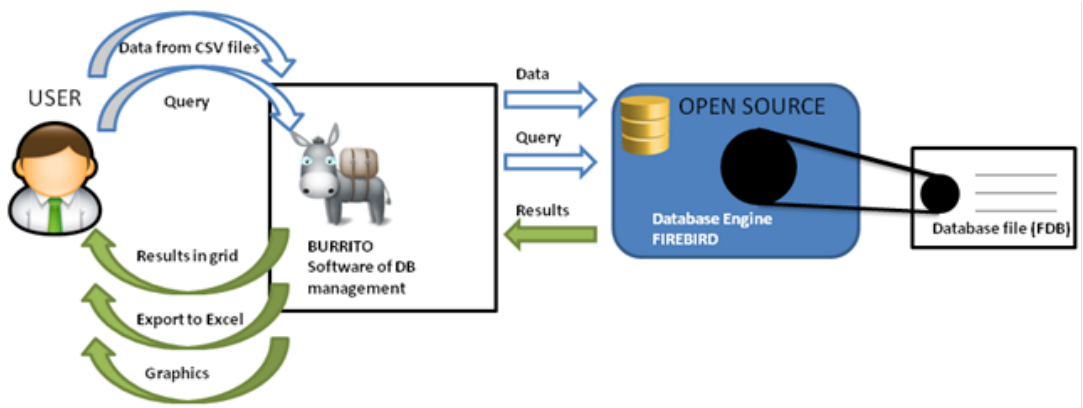

Figure 10.1: Dynamic performance between the software, the database engine and the FDB file.

an accuracy of ± 3.5 % RH. The temperature sensors are formed by a DS2438 integrated circuit (Maxim Integrated Products, Inc., Sunnyvale, CA, USA) [161] with an accuracy of ±2 °C.

In this chapter we analyze the data recorded within the period 01/01/2008 to 31/01/2012 (a total of over 37 million records). Also precipitation rate data obtained from the Spanish National Meteorological Agency [51] is included, for the indicated dates, with a frequency of a datum per day.

10.3. Software description

The software was named as Burrito (donkey in Spanish). It is a graphical interface (GUI) between the user and the engine that drives the DB which stores the information recorded by the monitoring system.

Below, the main features and functions of the software are described.

10.3.1. Data-Logger Database File

The software reads the data recorded by the monitoring system in text format, with CSV extension (comma separated values). These files are quite common in commer-

YEAR	MONTH	DAY	HOUR	MINUTE	SENSOR1	SENSOR2	SENSOR3	...
2011	11	1	0	0	58,96	60,41	56,13	
2011	11	1	0	1	59,09	60,22	56,04	
2011	11	1	0	2	59,04	60,31	56,20	
...								

Table 10.1: Data file structure in table form.

cial data-loggers. The file must comply with the following template (Table 10.1):

YEAR;MONTH;DAY;HOUR;MINUTE;SENSOR1;SENSOR2;SENSOR3...

2011;11;1;0;0;58,96;60,41;56,13

2011;11;1;0;1;59,09;60,22;56,04

2011;11;1;0;2;59,04;60,31;56,2

...

It is not possible to obtain a double-digit accuracy for relative humidity and temperature with the current sensors. For the aim of this research we used the resolution of our data-logger to show that this software can be adapted to situations where different physical parameters are involved, in cases that may require a double-digit accuracy.

The first 5 columns characterize each row, with variables of date and time (year, month, day, hour and minute), and the remaining columns correspond to the sensors (short name) and its data. The sensors can be of different type (RH, temperature, etc.) but it is important that the sensor name matches its short name in the DB (see Fig. 10.4) for the software to automatically assign the data to the sensor. The software is able to incorporate data from a file, regardless the number of columns and rows it has.

10.3.2. Getting Started

Immediately after launching the software the start-up screen appears (Fig. 10.2). From this screen (Fig. 10.2) the software allows quick access to frequently used functions, such as open a DB, add data, query, check the input register, etc. From this screen it is possible to access almost all functions; the additional options are in an attached menu.

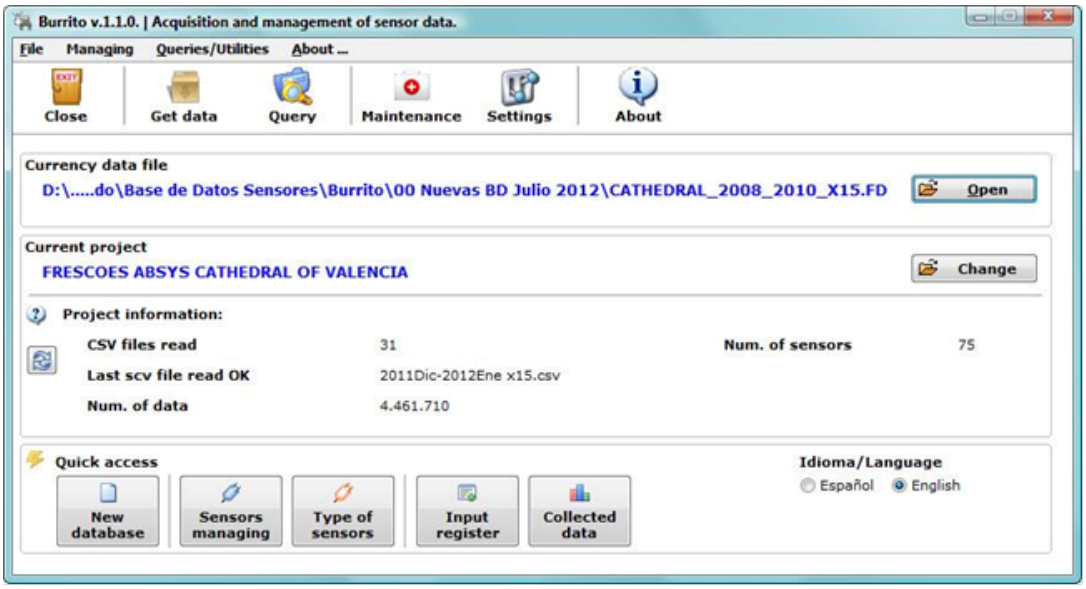

Figure 10.2: Start-up screen of Burrito software.

The data file from data loggers must be in comma separated values (CSV). In the start-up screen, some details of the DB are shown, such as read CSV data files. It is also possible to manage the language in which the program will be handled (Spanish/English).

The first step to store data recorded by a monitoring system is to create the database file, which will be unique and will have FDB extension (Firebird DataBase). It is a single file, making its transport, backup, etc., easier.

The button "New Database" from the "Quick access" panel (Fig. 10.2) creates a new DB. The file must be named and then an empty FDB file will be created ready to save information.

The software allows a single DB to store data from different projects, although this is only recommended in case there is few data per project. Otherwise, a FDB file for each project should be created.

10.3.3. Defining Type of Sensors in the DB

The FDB file is able to store information of any physical parameter such as temperature, RH, lumens, etc., with the condition that data issued have the date and

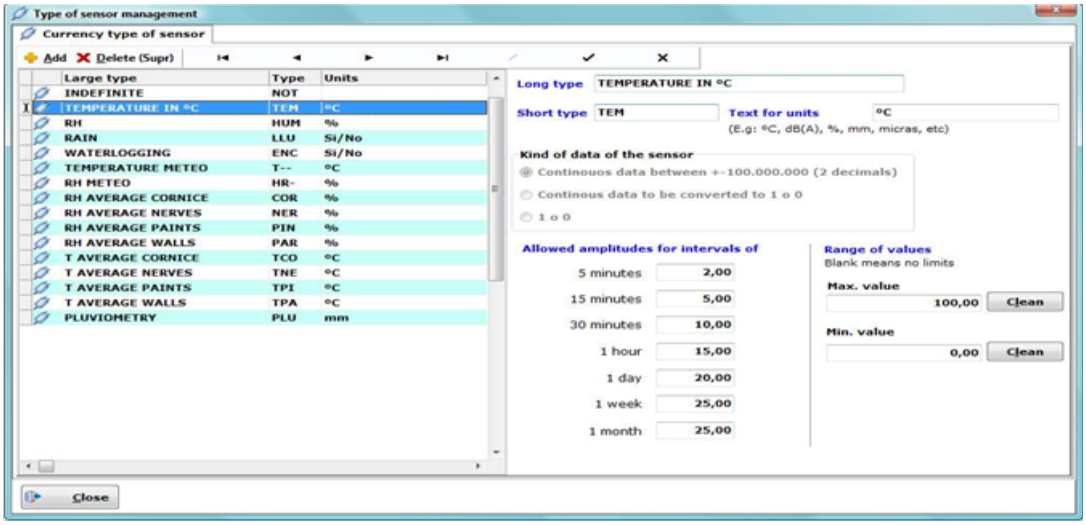

Figure 10.3: Type of sensor management window of Burrito software.

time it was recorded, and their range is 8 bytes.

Given the wide range of physical parameters, before filling the DB, for each physical parameter a different type of sensor must be defined (via the button "Type of sensors" from the "Quick access" panel in the start-up screen, Fig. 10.2).

In an empty DB appears a default data type: "indefinite". This type of sensor must not be used because it is only for software internal use.

Inside the sensor type manager (Fig. 10.3) each sensor is defined by its name and abbreviated units, value range and maximum allowable amplitudes for outlier detection. These errors occur due to faults in the communication between the sensor and microcontroller. Therefore, this fact does not imply a limitation of the software. It is important to fill this information carefully because the program uses it later to define filters and show useful information.

The program automatically numbers each sensor of each type by its abbreviated name (e.g., HUM001, HUM002, $\cdots$, HUMn, TEM001, TEM002, $\cdots$, TEMn etc, for $n = 1, 2, \cdots 999$).

The software, when recording new data, filters the values outside the allowed range and does not include them in the DB or marks them as incorrect. The definition of "Allowed amplitudes" (Fig. 10.3) is implemented for fast detection of anomalous data. For example, for a maximum allowed amplitude of 10 units for the interval

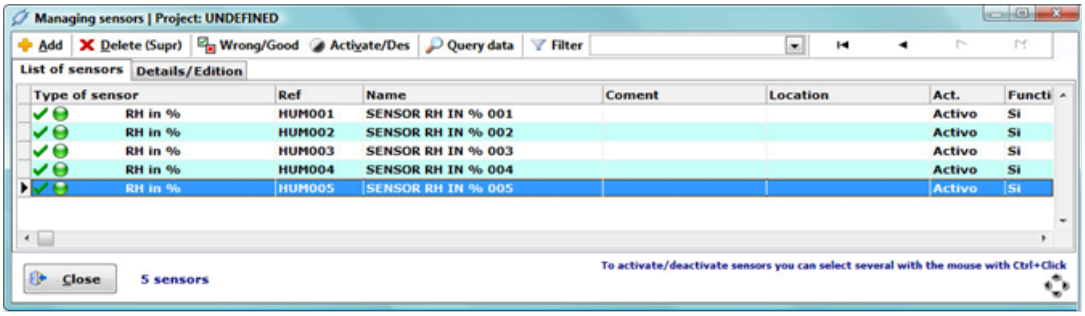

Figure 10.4: Sensors management window.

of one hour (hourly averaged data), if the difference between the minimum and the maximum value is greater than 10, the software will display the data in red, indicating a possible error in the recorded data or unusual circumstances in the time interval.

10.3.4. How to Include Sensors in the DB

After defining the possible types of sensors, it is necessary to indicate the number of sensors and their type (from the already defined categories). This can be performed via the button "Sensors managing" (Fig. 10.4), from the "Quick access" panel in the start-up screen (Fig.e 10.2).

In the sensor management window (Fig. 10.4) several operations on sensors may be performed, such as to mark them as good or bad performance, to enable/disable (note that it is not possible to add data to a disabled sensor), to check how many data have been recorded, to remove a sensor (only if it has not recorded data), etc.

On the other hand, the CSV file (in correct format) will be loaded into DB in the start-up screen (shortcut F2). The software reads the data from the CSV file, indexes and incorporates them into the DB, informing about when the process ends. At the end of the reading, a report with the errors detected and duplicate data found (data previously included for the same sensor and date) is shown.

The software allows a preview of the data and provides options to configure corrective measures if an anomalous datum is detected (with date / time missing, out of range or out of the maximum allowed amplitudes).

Thus, it is possible to perform filtering and elimination of erroneous values on the data collected by columns view. In our experience, approximately 2 % of the data

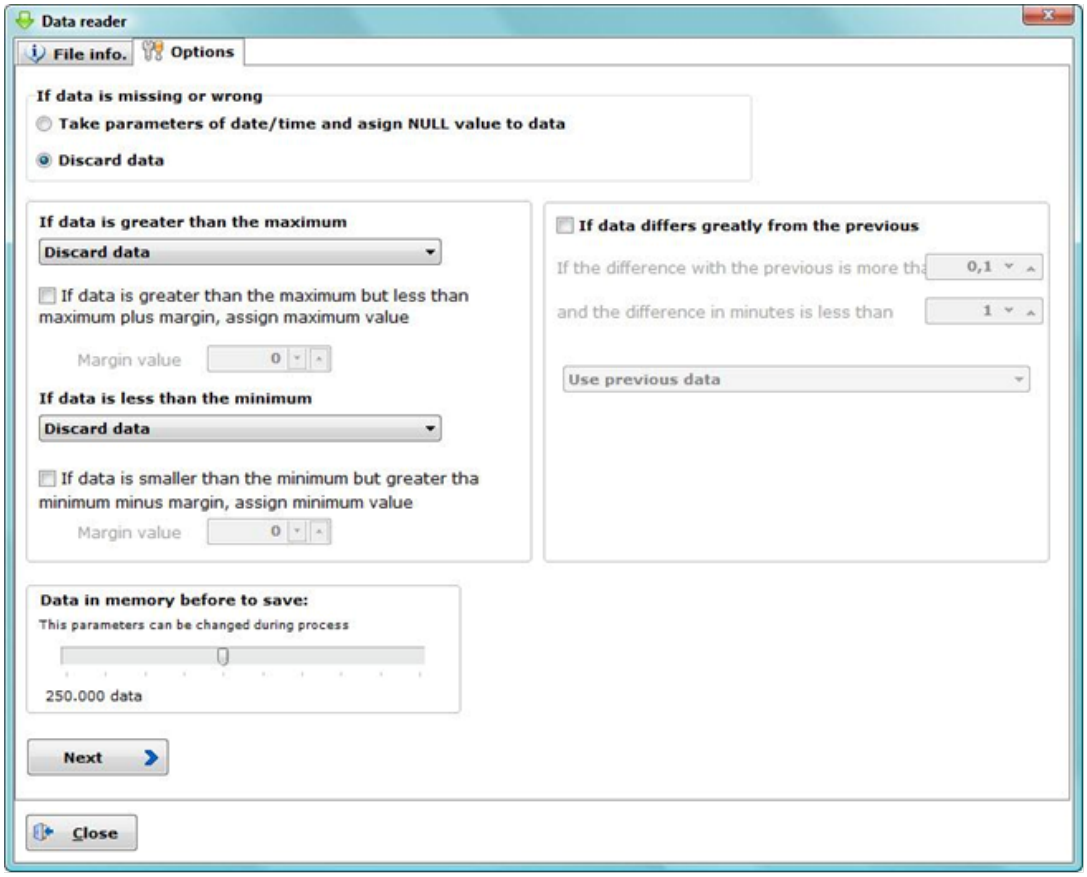

Figure 10.5: Data reader window of Burrito software.

have some type of failure. After studying in detail each anomalous value, three possible actions could be taken (Fig. 10.5): delete, mark as erroneous or edit its value (replacing it by the immediately previous/subsequent correct one).

Information about anomalous data is stored in a LOG extension file, saved in the same directory as the CSV input data file, for future consults.

10.3.5. Input Register

The software keeps a complete register of the information recorded in the DB. This is available by clicking on "Input Register" in the start-up screen (Fig. 10.2). The Input register shows a list (Fig. 10.6) of all read files, specifies if the result of the reading has been correct, the amount of data recorded, the data discarded, quantity

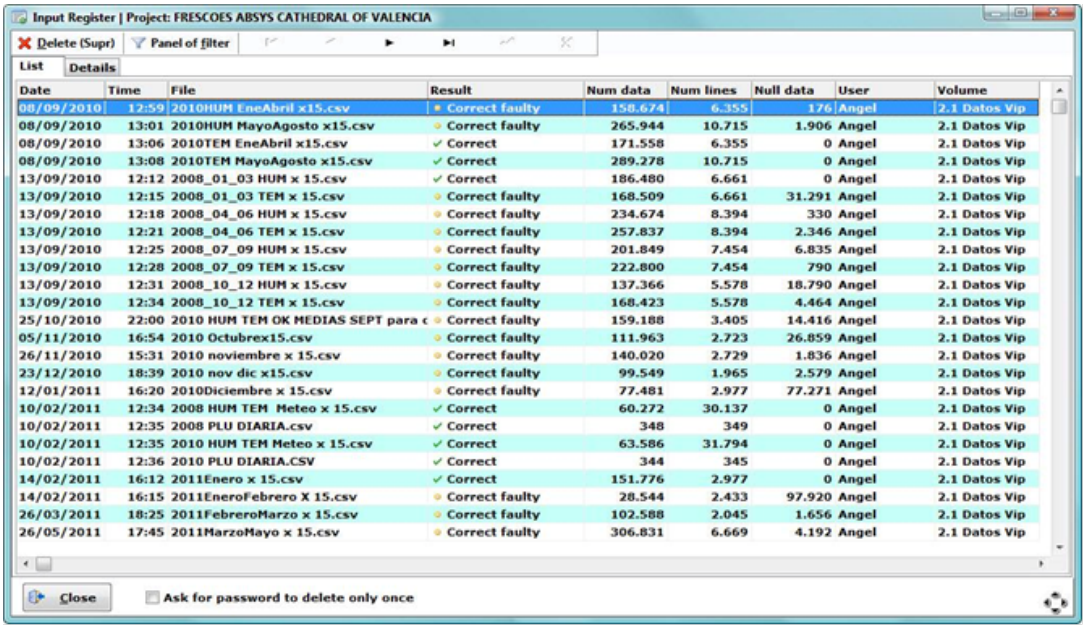

Date	Time	File	Result	Num data	Num lines	Null data	User	Volume
08/09/2010	12:59	2010HUM EneAbril x15.csv	Correct faulty	158.674	6.355	176	Angel	2.1 Datos Vip
08/09/2010	13:01	2010HUM MayoAgosto x15.csv	Correct faulty	265.944	10.715	1.906	Angel	2.1 Datos Vip
08/09/2010	13:06	2010TEM EneAbril x15.csv	Correct	171.558	6.355	0	Angel	2.1 Datos Vip
08/09/2010	13:08	2010TEM MayoAgosto x15.csv	Correct	289.278	10.715	0	Angel	2.1 Datos Vip
13/09/2010	12:12	2008_01_03 HUM x 15.csv	Correct	186.480	6.661	0	Angel	2.1 Datos Vip
13/09/2010	12:15	2008_01_03 TEM x 15.csv	Correct faulty	168.509	6.661	31.291	Angel	2.1 Datos Vip
13/09/2010	12:18	2008_04_06 HUM x 15.csv	Correct faulty	234.674	8.394	330	Angel	2.1 Datos Vip
13/09/2010	12:21	2008_04_06 TEM x 15.csv	Correct faulty	257.837	8.394	2.346	Angel	2.1 Datos Vip
13/09/2010	12:25	2008_07_09 HUM x 15.csv	Correct faulty	201.849	7.454	6.835	Angel	2.1 Datos Vip
13/09/2010	12:28	2008_07_09 TEM x 15.csv	Correct faulty	222.800	7.454	790	Angel	2.1 Datos Vip
13/09/2010	12:31	2008_10_12 HUM x 15.csv	Correct faulty	137.366	5.578	18.790	Angel	2.1 Datos Vip
13/09/2010	12:34	2008_10_12 TEM x 15.csv	Correct faulty	168.423	5.578	4.464	Angel	2.1 Datos Vip
25/10/2010	22:00	2010 HUM TEM OK MEDIAS SEPT para c	Correct faulty	159.188	3.405	14.416	Angel	2.1 Datos Vip
05/11/2010	16:54	2010 Octubrex15.csv	Correct faulty	111.963	2.723	26.859	Angel	2.1 Datos Vip
26/11/2010	15:31	2010 noviembre x 15.csv	Correct faulty	140.020	2.729	1.836	Angel	2.1 Datos Vip
23/12/2010	18:39	2010 nov dic x15.csv	Correct faulty	99.549	1.965	2.579	Angel	2.1 Datos Vip
12/01/2011	16:20	2010Diciembre x 15.csv	Correct faulty	77.481	2.977	77.271	Angel	2.1 Datos Vip
10/02/2011	12:34	2008 HUM TEM Meteo x 15.csv	Correct	60.272	30.137	0	Angel	2.1 Datos Vip
10/02/2011	12:35	2008 PLU DIARIA.csv	Correct	348	349	0	Angel	2.1 Datos Vip
10/02/2011	12:35	2010 HUM TEM Meteo x 15.csv	Correct	63.586	31.794	0	Angel	2.1 Datos Vip
10/02/2011	12:36	2010 PLU DIARIA.CSV	Correct	344	345	0	Angel	2.1 Datos Vip
14/02/2011	16:12	2011Enero x 15.csv	Correct	151.776	2.977	0	Angel	2.1 Datos Vip
14/02/2011	16:15	2011EneroFebrero X 15.csv	Correct faulty	28.544	2.433	97.920	Angel	2.1 Datos Vip
26/03/2011	18:25	2011FebreroMarzo x 15.csv	Correct faulty	102.588	2.045	1.656	Angel	2.1 Datos Vip
26/05/2011	17:45	2011MarzoMayo x 15.csv	Correct faulty	306.831	6.669	4.192	Angel	2.1 Datos Vip

Figure 10.6: Input register window.

of data per sensor, the user who has performed the reading, etc.

At the Input Register it is possible to delete a CSV file entry (delete from the DB all data entered by that file). Thus, if a data register error takes place it can be easily corrected.

10.3.6. Inquiring

Inquiring data according to specific criteria is the basic purpose of collecting and storing data. The software allows clearly defining the queries to be launched to the DB. In the start-up screen (Fig. 10.2, button "Query") we can set parameters (Fig. 10.7) to determine a specific inquiry (e.g., date range, sensors, averages, etc.).

The software can provide averaged values (every 5, 15, 30, and 60 minutes, 1 day, 1 week or 1 month). This is very interesting if we work with high frequency monitoring programs which produce huge amounts of data, as it allows showing monitored parameters at shorter intervals without losing relevant information.

For instance, by selecting an hourly average, we get a single datum for every sensor and hour, which will be the average of all the data recorded at that hour (e.g., from

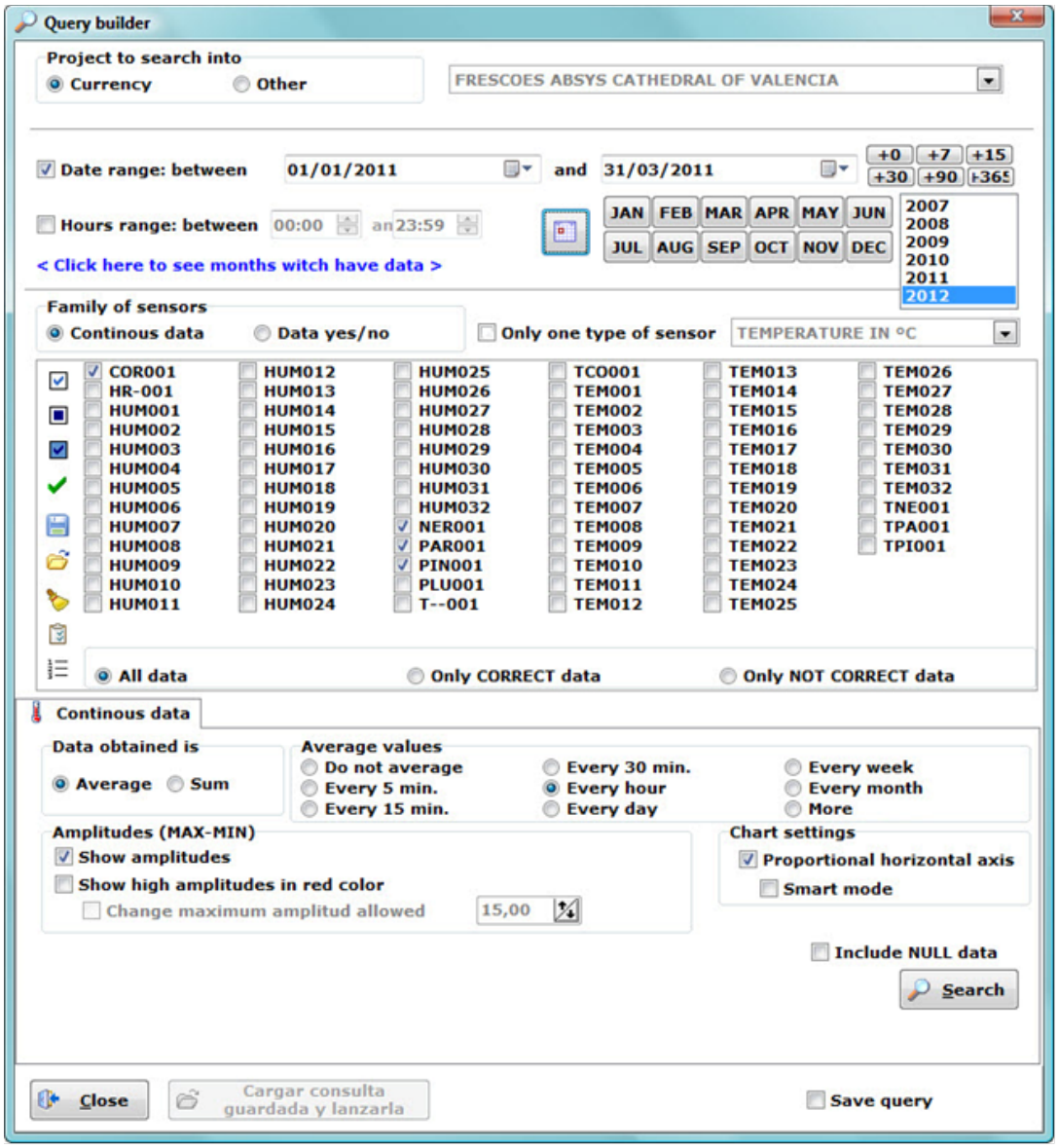

Figure 10.7: Query builder.

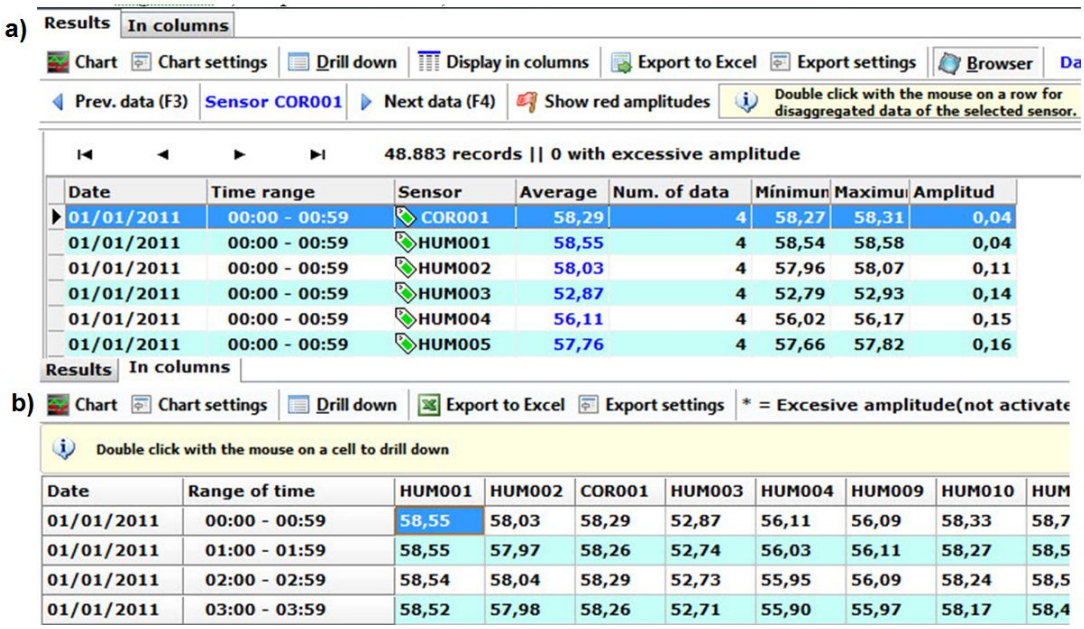

Figure 10.8: (a) Sequential view. (b) Column view.

00:00 to 00:59), for each day of the considered period. Let us note that for averaging per hour it is necessary that the recorded data have a higher sampling frequency than a datum per hour, otherwise the software will show only the available data.

The query results can be displayed in three different ways: sequentially, as columns and as a graph. The sequence (Fig. 10.8.a) shows the results in detail, what is usually impractical because it requires checking many rows. The column view (Fig. 10.8.b) provides less information, although easier to visualize. In the previous display ways, sequential and columns, if you double-click on an item, detailed information of the non-averaged original data is shown. Finally, we can plot a graph (Fig. 10.9), being able to locate every data in the graph and expand its information, in sequential or column view, with a click.

10.3.7. Special Inquiries

The software also allows for special inquiries, as averaging values in the whole period and obtaining mean trajectories. These trajectories are novel and useful in preventive conservation of cultural heritage [19]. Mean trajectories is a plot commonly applied in the control of batch chemical processes because it allows an

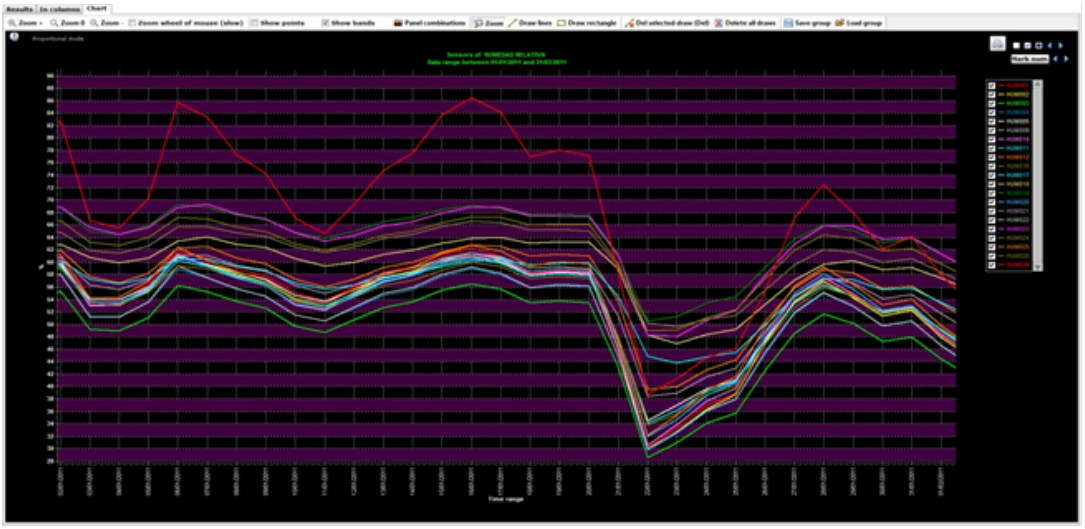

Figure 10.9: Results plotted on a graph (zoom on the figure for more axis detail).

Figure 10.10: Additional options for averaging.

easy identification of deviations with respect to the target trajectory. However, this kind of plot is not frequently used in microclimate monitoring studies of cultural heritage. The chart provides useful information when cycles are clearly marked.

Average in the whole period allows to obtain the daily mean trajectory, weekly mean trajectory and annual mean trajectory, by means of averaging per hour, day of the week (from 1-Sunday to 7-Saturday), week of the year (from 1 to 52), day of the year (from 1 to 366) and month (from 1 to 12), for the whole selected period (Fig. 10.10). Afterwards, these mean trajectories can be plotted.

For instance, if a period from 01/01/2010 to 03/31/2010 is selected, and an averaging per hour in the whole period is performed, 24 data are obtained for each selected sensor (the hourly average from 0 hours to 23 hours, Fig. 10.11). The averaged datum for hour=0 for sensor HUMn (e.g.), is obtained by averaging the data of sensor HUMn taken from 0:00 to 0:59, for the whole indicated period.

In the case of the annual mean trajectory (whether averaging per day of the year, week of the year or month), data from several years must be recorded, otherwise

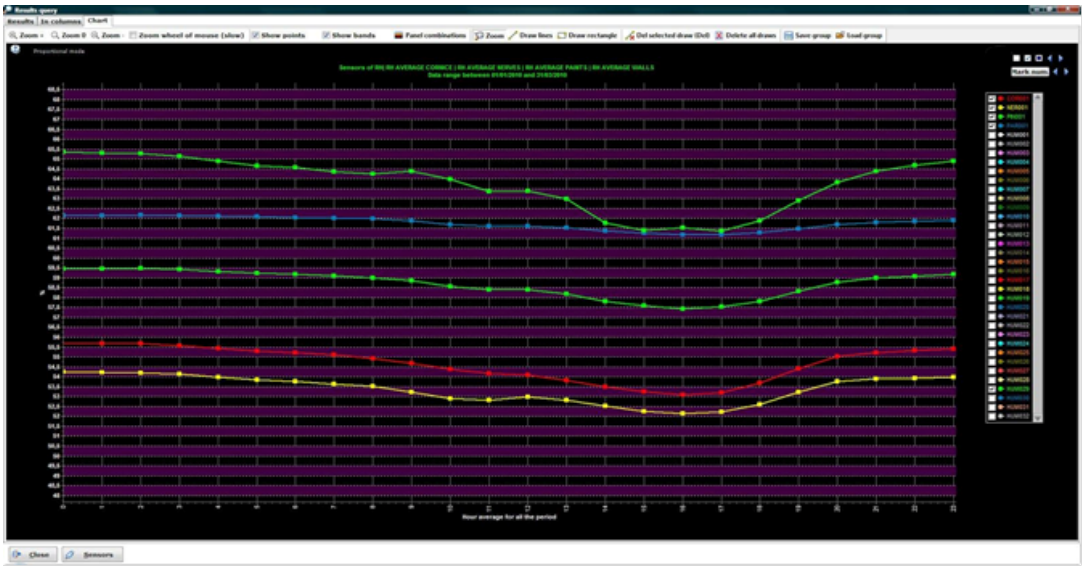

Figure 10.11: Daily mean trajectories of 5 sensors (from 01/01/2010 to 03/31/2010). Zoom on the figure for more axis detail.

the annual mean trajectory will coincide with the trajectory of that particular year.

These tools allow us to find patterns in the trajectories of the sensors that respond to hourly or seasonal changes, and propose appropriate preventive measures. Previous studies have pointed out that the flow of visitors rises RH levels above usual levels inside buildings [98], [162], [163]; therefore, changes of pattern associated with public attendance (like Sundays in churches or museums) could be an interesting subject for study by means of the aforementioned mean trajectories.

10.3.8. Data Exportation

The software combines the storage power of a DB and the flexibility of a spreadsheet. It can export inquiry results into a spreadsheet where statistical analysis can be performed as well as elaborated graphical presentations.

After launching a query and getting the results, both from the column view (Fig. 10.8.b) as from the sequential view (Fig. 10.8.a), data can be exported to a spreadsheet. The sequential view allows choosing the form of export (sequential / columns). Notice that export as columns is usually more useful.

You can also export the hourly or daily variation (absolute difference of two con-

secutive values) in case of averaging per hour or per day. It can be safely said that some cultural heritage conservation standards [7], [83] recommend values for periodic variations (daily and hourly) where the environment can be considered stable, which implies less possibilities of having environmentally-related deterioration problems.

10.3.9. More Duties

Despite the aforementioned functions, the developed software allows to do backup and restoration of the DB, plot graphs of data recorded per month and per sensor, DB maintenance, and other features that allow keeping the recorded data under control.

10.4. Case study. Frescoes of the Cathedral of Valencia

10.4.1. Database and Data Pretreatment

In this case, data recorded by the sensors are written by the microprocessor in CSV format on a USB flash drive connected to the system. Periodically, this flash drive is connected to a computer and, using the software, data are copied to a DB.

A pretreatment was performed on the recorded data. Filtering and elimination of outliers for hourly averaged data by columns view was performed (detecting in red those values with amplitudes greater than those allowed for that type of sensor, see Section 10.3.3). After analyzing the outliers, two different actions were implemented. In those cases where there is more than one consecutive anomalous value (not being able to predict the real values) they were deleted. In cases where the anomalous datum was unique (Fig. 10.12), it was substituted by the immediately previous/subsequent correct value.

10.4.2. Reduced DB for Daily Use

The DB file (FDB extension) has over 37 million data in 2013 and occupies 10.5 GB in the hard drive. The software can handle this amount of data without problems, but inquiries and backups are slow. To speed up the daily work with the data,

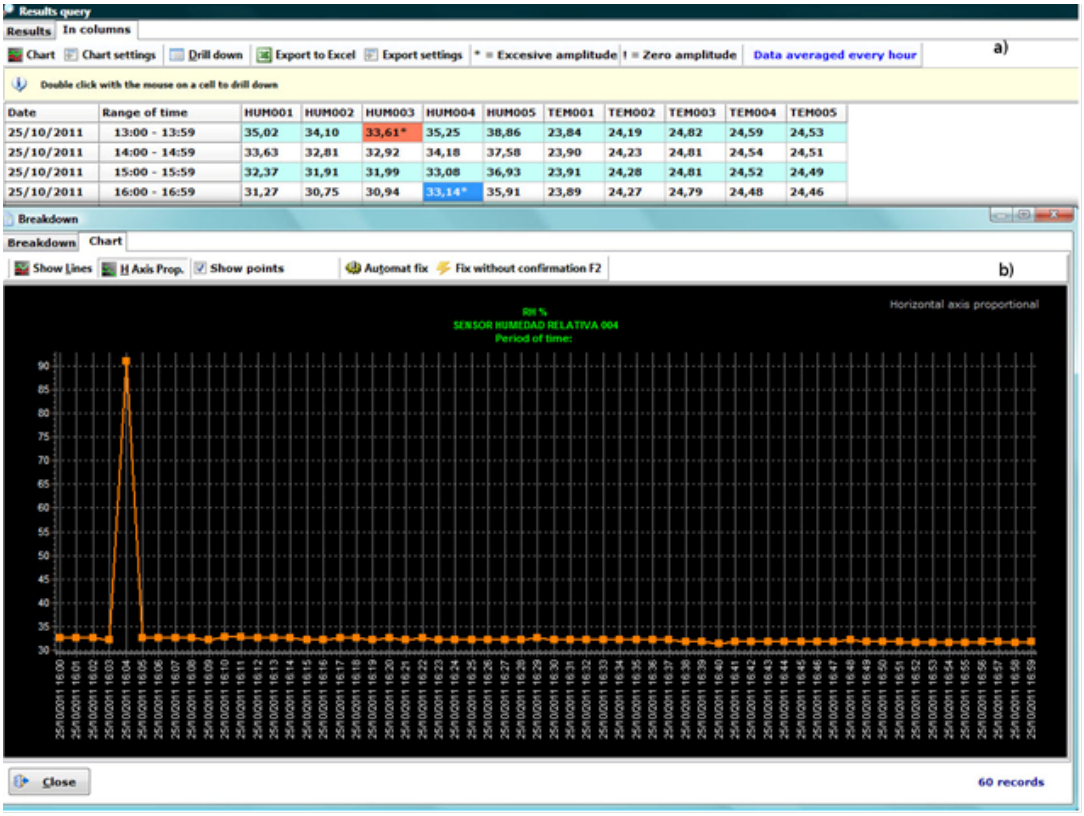

Figure 10.12: (a) Rapid localization of anomalous data in the columns view. (b) Localization of outliers in a graph. Zoom on the figure for more axis detail.

a smaller DB was created by averaging data every 15 minutes. This significantly reduces the size of the DB (from over 37 million to 4 million data) and, consequently, also reduces the processing times for inquiries without losing relevant information.

This reduced DB is generated from an inquiry in the full DB. An inquiry of data averaged every 15 minutes is performed; results are exported to a spreadsheet and saved in CSV format. The present study works with the reduced DB.

10.4.3. Descriptive / Exploratory Analysis

The software allows to easily and quickly perform exploratory analyses. Concerning the utility of these analyses, the salt efflorescences detected in 2006 on the walls and frescoes of the vault of the Cathedral of Valencia, were studied. In order to investigate the causes of the efflorescences, the time series of all sensors were analyzed, especially those located in areas where salt efflorescence appeared.

Previous studies [16], [18] provide information about the vault material and thickness of walls, as well as a sketch showing the location of sensors and their elevations. Notice that the city of Valencia has a Mediterranean climate. Furthermore, the vault is located at an elevation of about 15 meters from the floor; therefore efflorescence problems are caused by the infiltration of water from the roof but not from the ground level.

First, the annual time series for 2010, with data averaged per hour, was plotted (Fig. 10.13). That kind of graph shows an excessive amount of information when large amounts of data are recorded, making it harder to draw useful conclusions.

In order to detect anomalous behaviors in the time series of sensors, mean annual trajectories were studied. For this purpose, an inquiry of monthly averaged data, for the time period from 10/01/2007 to 12/31/2011, was performed using this software. Six annual mean trajectories of RH were compared. The results were exported to MS Excel spreadsheet and plotted as shown in Fig. 10.14. The selected sensors were: two sensors located in the area with salt efflorescences ($SEN3-X$ blue line and $SEN4-X$ violet line), two sensors in the area where the frescoes do not show deterioration ($SEN1-OK$ red line and $SEN2-OK$ yellow line), RH data from outside the Cathedral ($RH-OUT$), and precipitation data ($PLUV$).

Fig. 10.14 shows that the signals from sensors located in areas with salt efflorescences have a higher RH average value than those located in areas without salt efflorescence problems.

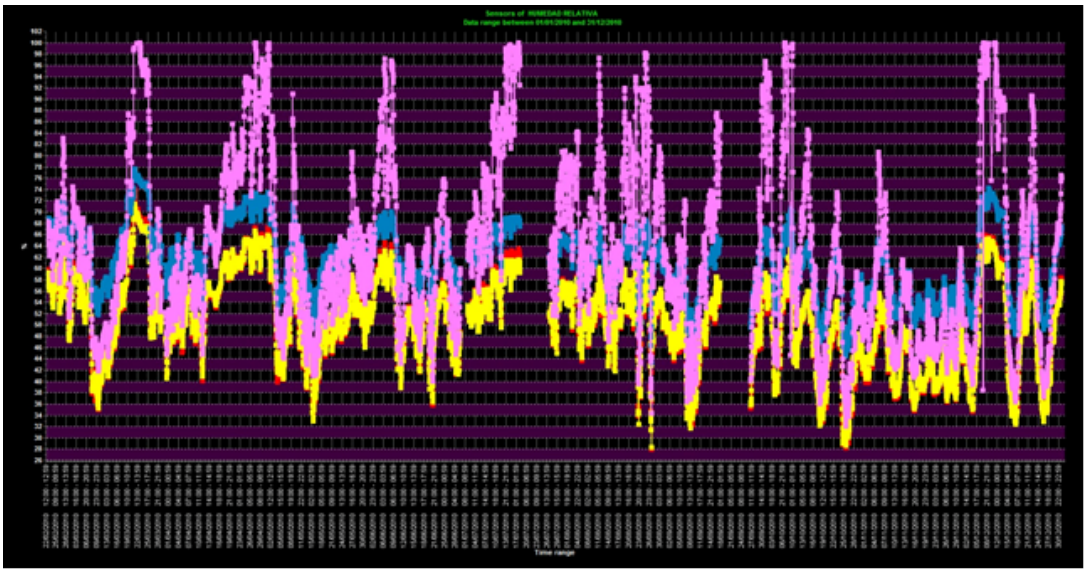

Figure 10.13: Annual time series of hourly averaged data (2010) of four RH sensors, two of them located in the area with salt efflorescence ($SEN3-X$ blue line and $SEN4-X$ violet line) and two sensors in the area where the frescoes do not show deterioration ($SEN1-OK$ red line and $SEN2-OK$ yellow line). Zoom on the figure for more axis detail.

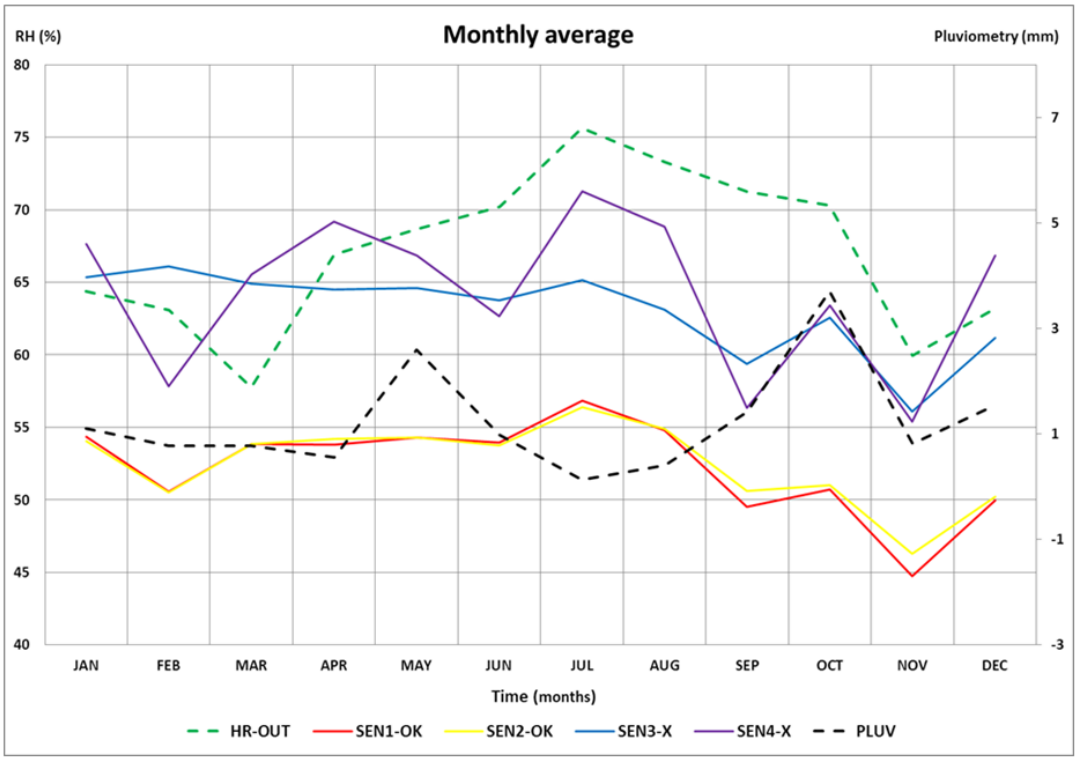

Figure 10.14: The right vertical axis indicates monthly average rainfall data (mm) for *PLUV* sensor. The left vertical axis indicates mean RH (%) for all other sensors.

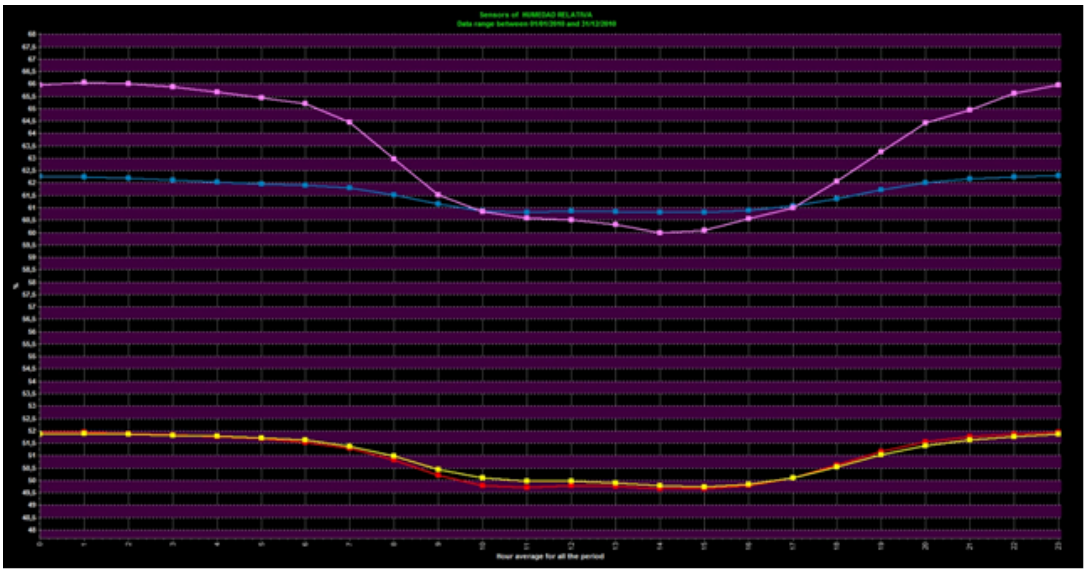

Figure 10.15: Daily mean trajectories in 2010 (from 01/01/2010 to 12/31/2010) of $SEN1-OK$ (red line), $SEN2-OK$ (yellow line), $SEN3-X$ (blue line) and $SEN4-X$ (violet line). The horizontal axis represents time (hour of the day, from 0 to 23) and the vertical axis represents the averaged RH (%). Zoom on the figure for more axis detail.

Regarding the shape of trajectories, all sensors emulate the outside RH trajectory but, obviously, moderated by the effect of walls. However, when the pluviometry exceeds 3 mm per day (October), those sensors in the salt efflorescence area ($SEN3-X$ and $SEN4-X$) follow the precipitation rate pattern, while sensors $SEN1-OK$ and $SEN2-OK$ continue reflecting the external RH trajectory. As the Cathedral was built of limestone, characterized by a high porosity, the aforementioned results may show the possible infiltration of rainwater into the areas where these sensors are located, helping to determine the most convenient conservation measures.

The daily mean trajectories of the aforementioned sensors (Fig. 10.15) were also plotted. Fig. 10.15 condenses the common daily pattern in a single graph (different from Fig. 10.13). This figure detects the difference between those sensors in the area with salt efflorescence problems ($SEN3-X$ and $SEN4-X$) and the ones on the non-problematic area ($SEN1-OK$ and $SEN2-OK$).

The case study of the Cathedral illustrates the power of the software to perform exploratory analyses and find atypical behaviour patterns in the data, helping to extract useful information.

10.4.4. Advanced Statistical Analysis Applications

As mentioned, this software allows data preparation for exportation and analysis with other software, for example by applying more complex statistical analyses.

In previous studies [16], [18] Principal Component Analysis (PCA) was applied, allowing identifying different patterns in the sensors trajectories and relating them to the conservation problems detected in some areas of the frescoes.

The software, with its ability to quickly obtain averaged data, illustrates that the PCA results in this particular case did not vary substantially if performed with data taken every minute, data averaged every 15 minutes or averaged per hour [16], [18].

Let us note that as we refer to averages the reader may wonder why it is needed to record a large volume of data (with a frequency of 1 datum/minute) if the obtained results when one datum per minute is considered agree with those when analyses are performed with one datum per hour. Notice that the difference is that, when working with hourly averaged data, each datum is obtained as an average of the 60 data (1 datum/minute) available for each hour. The results may differ significantly in certain cases when a value is arbitrarily taken at one particular minute in this interval of one hour. The power and confidence of the statistical analysis performed increases in direct proportion to the sample size used [164], [165].

This fact increases the interest of monitoring with frequencies near 60 data per hour (1 datum/minute) and, therefore, the need to develop software able to manage such volumes of data.

The software also helped with the interpretation of the second component PC2, since in a previous study [16] was established that PC2 discriminates sensors according to the shape of the trajectory. This shape is related to hourly, daily or monthly variations, therefore the physical interpretation of PC2 was determined obtaining and studying hourly, daily and monthly averages by means of this software.

10.5. Conclusions

The developed software (Burrito) is a graphic user interface (GUI) that allows the interaction with a DB specifically created to store huge amounts of data such as those generated from environmental monitoring of cultural heritage. The software

intends to be easy to use and powerful, allowing detection of anomalous data, inquiring, plotting mean trajectories and other features which contribute to simplify the management of large amounts of data generated from a long-term monitoring. The software exports the results to a spreadsheet, allowing for advanced statistical studies like PCA.

This software also allows obtaining different averages, which, together with a large amount of data, would give rise to future studies aimed at determining the optimal frequency of monitoring.

This software presents as a novelty the representation of mean trajectories. The graph provides useful information when cycles are clearly marked because it allows an easy identification of periodic deviations with respect to the target trajectory. The plot of mean trajectories is commonly applied in the control of batch chemical processes. However, this kind of plot is not frequently used in microclimate monitoring studies of cultural heritage [19].

Burrito is a low-cost and affordable software because it uses free open source software as database engine; it also runs smoothly on older computers with Windows XP as operating system.

This software was specifically designed to manage data generated from long-term monitoring of cultural heritage. However, it could be useful in other scientific fields where obtaining relevant information from data recorded by sensors is necessary, such as agricultural studies where agricultural productivity is related with different physical parameters (RH, temperature, sunshine, rainfall) or solar energy studies related to insolation.

Chapter 11

General Discussion of Results

11.1. Achievement of objectives

The attainment of the objectives of this PhD dissertation is discussed in this chapter. As shown in table 11.1, all objectives have been achieved and are presented in different chapters of this work. The results of our studies have led to eight scientific publications in international journals indexed in the Journal Citations Report (JCR ®) and several contributions at international conferences.

The objectives have been achieved as follows:

- **O1**: an exhaustive study of the literature has been performed and is distributed in the introduction of the different chapters as the review has been particularized according to the materials and the building method used in the site (wood, frescoes, stone, etc.).
- **O2**: the present work reports, probably for the first time, the advantages of PCA in the multivariate microclimate monitoring of an open-air archaeological site. Also, the best pretreatment for the detection of abnormal patterns is discussed and may serve as guidance for other similar sites.
- **O3**: it has been possible to characterize the dynamic microclimate variations of the mudejar church of St. María in Ateca, as well as to evaluate the perfor-

CHAPTER	3	4	5	6	7	8	9	10
O1	X							
O1.1	X							
O1.2	X							
O1.3	X							
O2				X				
O2.1				6.3.1				
O2.2				6.3.2				
O2.3				6.3.3-6.3.5				
O2.4				6.3.5				
O3							X	
O3.1							9.3.1-9.3.2	
O3.2							9.3.3	
O3.3							9.3.3	
O4		X			X		X	
O4.1		4.3.2-4.3.6			7.3.2		X	
O4.2		4.3.2			7.3.1			
O4.3		4.3			7.3.2			
O5								X
O6	X	X			X		X	
O6.1	X	X						
O6.1.1	3.3.1	4.3						
O6.1.2	3.3-3.4	4.3-4.4						
O6.2					X			
O6.2.1					7.3.2			
O6.2.2					7.4			
O7			X			X		
O7.1			X					
O7.1.1			5.2					
O7.1.2			5.2.5					
O7.2						X		
O7.2.1						8.3		
O7.2.2						8.3		

Table 11.1: Achievement of objectives. Sections in which specific objectives have been achieved are indicated.

mance of the heating system using different data analysis techniques: ANOVA, mean trajectories, contour plots and bivariate plots.

- **O4**: A proper experimental design is important, however it is not always possible to take into account the deficiencies of the design and it is of great interest to employ techniques to overcome them. In this PhD dissertation a methodology combining different statistical techniques (such as bivariate plots, mean trajectories, normal probability plot or ANOVA) has been proposed for a simple use by curators and restorers.

- **O5**: Burrito software has been imprived by implementing special filters that easily allow performing bivariate plots and mean trajectories.

- **O6**: the microclimatic characterization of the three studied cultural heritage sites has been useful to assess the causes of detrimental microclimatic conditions damaging the remains and proper corrective actions have been proposed. A change of roofs was proposed in Ariadne's house, and it was performed within 2009-2010. An opaque coverture for the skylight of the Archaeological Museum of l'Almoina was recommended and implemented in summer 2013. Finally, a control of the heating system in the mudejar church of Santa María in Ateca was suggested.

- **O7**: after the corrective actions taken in Ariadne's house and the Archaeological Museum of l'Almoina, a second monitoring campaing was performed in both sites. Our analysis methodology has allowed concluding the adequacy of these corrective measures, as they have led to more constant microclimatic conditions similar to those termo-hygrometric values recommended by the international standards.

11.2. Future lines of research

This PhD dissertation leads to different fields and future research lines are opened. On one hand, the possibility of extending the analysis methodology and microclimatic characterization to other cultural heritage of interest arises.

On the other hand, another research line deals with the study of other parameters involved in the deterioration process, as lighting or ventilation dynamics, together with the study of displacements and cracks.

Finally, this Phd dissertation can be regarded as a first step that can be completed

with analysis of materials and the interaction of both data, to determine how the microclimate has an effect on with the materials found at the studied site and conclude how the first determines the degradation of the latter.

Chapter 12

General Conclusions

The microclimate characterization of open-air or semi-confined archaeological site is of great importance, with the aim, on one hand, of carrying out comparative studies in the future when implementing changes in climate control systems or in the architectural design, and on the other hand, to study any future deterioration of the archaeological site, which may be related with microclimate conditions. The complexity of the data collected and the limitation of the location of sensors makes it difficult to draw relevant and reliable conclusions through standard techniques, such as contour plots or temporal trajectory analysis. The present work is mainly intended for restorers and conservators of archaeological sites.

Descriptive tools used in this PhD dissertation have been effective for highlighting the dissimilarities among probes in cultural heritage sites. Several analyses not frequently applied in microclimatic monitoring of cultural heritage have been used (mean trajectories, normal probability plots and biplots), and also other multivariate statistical techniques (Principal Component Analysis and cluster analysis) and Analysis of Variance (ANOVA) have been applied.

Three statistical methodologies that are simple to operate have been proposed (two qualitative and one quantitative), which can replace more complex multivariate statistical techniques such as cluster analysis. These proposed techniques are normal probability plot (quantitative), bivariate plots and mean daily trajectories (qualitative), which have been useful in characterising the archaeological sites in detail.

The mean daily trajectories provide useful information about the difference in average values and shapes among data-loggers. This type of plot is rarely applied in microclimate monitoring where trajectories of a few days randomly chosen are usually presented.

Also, a new graph of simple interpretation, based on contour plots, that combines the power of mean daily trajectories and the dynamic nature of the time series of temperature and RH.

The proposed methodology resulted in a useful procedure to compare results from unlike boundary weather conditions, based on comparing data from different campaigns in order to determine the effect of a corrective measure using statistical techniques. This methodology allowed us to evaluate changes implemented as well as the effects that these changes have had on the thermohygrometric conditions of the site, always taking into account that they have a direct impact on the conservation based on the international standards. The satisfactory results of this study can be taken as an example by similar archaeological sites to study and quantify the adequacy of corrective actions.

The methodology of data analysis applied here is also of interest for similar studies aimed at comparing thermohygrometric data recorded in different periods, because it is necessary to avoid the confusion of effects that appears when the average conditions of the periods are different.

Few works have monitored microclimate environments of outdoor or semi-confined archaeological sites. Therefore our results can serve as a guide for the installation of a microclimatic monitoring system in similar archaeological sites. The differences among probes suggest that at least four data-loggers per room would be required to assess the effect of different factors and to detect abnormal trajectories. One or more control sensors are also recommended. Regarding the number of walls of the room, rooms with four walls will require less number of sensors at wall levels, where two different orientations might be enough. At floor level, north orientation and a complementary one (south or east) should also be monitored. If several lodgings present similar characteristics, orientation, size and number of walls, it seems sufficient to monitor just one of them. Furthermore, the microclimate should only be studied in those dates when the most damaging environmental conditions for the site take place. Consequently, ambient conditions in similar studies as Pompeii should be basically monitored in summer.

According to the developed methodology, different analyses (mean trajectories, biplots and special filters) have been implemented in a software for storage, management and analysis of microclimatic databases of cultural heritage, which can be

used in other disciplines.

12.1. Ariadne's House (Pompeii)

The multidisciplinary study developed in Ariadne's house (environmental study, electromagnetic radiation measurement, study of materials and photography) allowed documenting its state of conservation and evaluating the most convenient procedures for a preventive conservation as well as increasing the knowledge about the materials used in its construction, its pictorial procedure and the process of deterioration for the discussion of a future restoration. The study of materials and the photographic study have also shown the relevance of monitoring the environmental conditions in order to stop the deterioration caused by salts crystallization.

The results of the microclimatic study reveal that summer conditions in Pompeii are more unfavorable for the conservation of frescoes according to the standards recommendations because the microclimate was too dry and hot. It was found an effect of roof type, wall orientation and sensor height on microclimate conditions. Higher RH values were recorded by data-loggers on the floor, and the south orientation was characterized by lower RH values because it tended to receive more sunlight radiation.

The microclimatic study suggests that the deterioration process has been accelerated due to the transparent rooftop used. Then, it was determined that the optimal cover should be opaque and as isolated as possible. Therefore the decision on changing the rooftops was taken and within 2009-2010 they were replaced.

The effectiveness of such measure was assessed in a second microclimatic study. The statistical analysis has revealed a considerable reduction of about 3.5°C in the maximum daily values reached in summer at rooms 1 and 3 caused by the roof change. This corrective measure has lowered the maximum temperatures and has also increased the RH and minimum temperatures, which entails an attenuation of daily variations of thermohygrometric conditions. Thus, the roof change has created a microclimate more stable and less harmful for the conservation of frescoes.

Moreover, a study was conducted using PCA aimed at discussing the best pretreatment prior to applying PCA to data from a multivariate microclimate monitoring system in an open-air archaeological site considering that the data structure is analogous to the case of continuous chemical processes monitored with multiple sensors. It turned out that working with row-centred data presents advantages in

front of the column-centred in order to a better identification of abnormal patterns and a more informative PC2.

Furthermore, it turned out the advantage of dividing the monitored period into several stages by CUSUM charts, taking into account that weather conditions are not constant throughout the year, which helps this in the detection of abnormal patterns.

12.2. L'Almoina archaeological site

The results of a microclimatic monitoring study in 2010 have revealed the significant influence of the skylight on the temperature and RH, causing sharp rises and falls during daylight hours. Also it was possible to detect the direct impact of air from the conditioning system and how the trajectory reflects its operation.

In 2013 two corrective actions were implemented: first, the water of the skylight was removed and, after, it was covered with a white canvas.

A second monitoring campaign in summer 2013 has allowed us to quantify the increase of the daily temperature maximums (and the consequent decrease in the RH minimums) as a result of removing the water layer on the skylight (prior to installation of the canvas cover) as well as the installation of the canvas has improved temperature and humidity conditions for conservation of the archaeological remains, because the covering has created a microclimate more stable and less harmful for their conservation.

On the other hand, a boundary water pipe clearly configured an RH gradient in 2010, which decreases as we move away from the pipe. The substitution of the water ditch by a PVC pipe has decreased the RH levels and our sensors and analysis procedures have been able to detect this modification.

12.3. Mudejar church of Santa Maria (Ateca)

The techniques used have been able to quantify the effects of the heating system on temperature and RH on the conservation of the altarpiece, determining the "on"

switch of the heating system at different moments due to the celebration of Masses and religious events and how it results in a rapid hourly temperature increase of 7 °C and a decrease of 11 % RH in the sensors located at the highest position.

References

[1] Camuffo, D. *Microclimate for Cultural Heritage*. Elsevier Science, Amsterdam, 1998.

[2] Kontozova-Deutsch, V.; Cardell, C.; Urosevic, M.; Ruiz-Agudo, E.; Deutsch, F.; Van Grieken, R. Characterization of indoor and outdoor atmospheric pollutants impacting architectural monuments: the case of San Jerónimo Monastery (Granada, Spain). *Environ Earth Sci* 2011, 63, 1433-1445.

[3] Camuffo, D. Modern technology: A new opportunity or a new challenge for the indoor conservation of the cultural heritage? *European Cultural Heritage Newsletter on Research* 1997, 10, 77-83.

[4] Herráez, J.A.; Rodríguez, M.A. *La Conservación Preventiva de las Os de Arte; Instituto del Patrimonio Histórico Español (IPHE)*. CSIC, Madrid, Spain, 1999; p. 645.

[5] Conrad, E. The realistic preservation environment. Available online: http://www.archives.gov/preservation/storage/realistic-preservation-environment.html (accessed on December 2012).

[6] Spolnik, Z.; Worobiec, A.; Injuk, J.; Neilen, D.; Schellen, H.; van Grieken, R. Chemical characterization of airborne particles in St. Martinus Cathedral in Weert, The Netherlands. *Microchim Acta* 2004, 145(1-4), 223-27.

[7] DM 10/2001: *Atto di Indirizzo sui Criteri Tecnico-scientifici e Sugli Standard di Funzionamento e Sviluppo dei Musei*. Ministero per i Beni e le Attività Culturali. Rome (Italy): Gazzeta Ufficiale della Repubblica Italiana (Official Bulletin of Italian Republica); 2001. DL 112/1998 art. 150 comma 6.

[8] Bacci, M.; Cucci, C.; Azelio, A.; Grazia, A. Innovative Sensors for Environmental Monitoring in Museums. *Sensors* 2008, 8, 1984-2005.

[9] Olmi, R.; Bini, M.; Ignesti, A.; Priori, S.; Riminesi, C.; Felici, A. Diagnostics and monitoring of frescoes using evanescent-field dielectrometry. *Meas Sci Technol* 2006, 17, 2281-2288.

[10] Stewart, J.; Julien, S.; Staniforth, S. *An integrated monitoring strategy at Chedworth Roman Villa (Gloucestershire)*. In Preserving Archaeological Remains in Situ?, Proceedings of the 2nd Conference, London, UK,12-14 September 2001; Taryn, J., Nixon, P., Eds.; Museum of London Archaeology Service, London, UK, 2004; p.179-87.

[11] Lopez-Arce, P.; Garcia-Guinea, J. Weathering traces in ancient bricks from historic buildings. *Build Environ* 2005, 40(7), 929-941

[12] Lillie, M.; Smith, R.; Reed, J.; Inglis, R. Southwest Scottish Crannogs: using in situ studies to assess preservation in wetland archaeological contexts. *J Archaeol Sci* 2008, 35(7), 1886-1900.

[13] Lourenço, P.B.; Luso, E.; Almeida, M.G. Defects and moisture problems in buildings from historical city centres: a case study in Portugal. *Build Environ* 2006, 41(2), 223-34.

[14] Zítek, P.; Vyhlídal, T. Model-based moisture sorption stabilization in historical buildings. *Build Environ* 2009, 44(6), 1181-7.

[15] Angelini, E.; Grassini, S.; Corbellini, S.; Parvis, M.; Piantanida, M. A multidisciplinary approach for the conservation of a building of the seventeenth century. *Appl Phys A-Mater* 2010, 100(3), 763-9.

[16] García-Diego, F.-J.; Zarzo, M. Microclimate monitoring by multivariate statistical control: the renaissance frescoes of the cathedral of Valencia (Spain). *J Cult Herit* 2010, 11(3), 339-344.

[17] Nava, S.; Becherini, F.; Bernardi, A.; Bonazza, A.; Chiari, M.; García-Orellana, I.; Lucarelli, F.; Ludwig, N.; Migliori, A.; Sabbioni, C.; Udisti, R.; Valli, G.; Vecchi, R. An integrated approach to assess air pollution threats to cultural heritage in a semi-confined environment: the case study of Michelozzo's Courtyard in Florence (Italy). *Sci Total Environ* 2010, 408(6), 1403-1413.

[18] Zarzo, M.; Fernández-Navajas, A.; García-Diego, F. Long-term monitoring of fresco paintings in the cathedral of Valencia (Spain) through humidity and temperature sensors in various locations for preventive conservation. *Sensors* 2011, 9, 8685-8710.

[19] Merello, P.; García-Diego, F.-J.; Zarzo, M. Microclimate monitoring of Ariadne's house (Pompeii, Italy) for preventive conservation of fresco paintings. *Chem Central J* 2012, 6, 145.

[20] Huijbregts, Z.; Kramer, R.P.; Martens, M.H.J.; Van Schijndel, A.W.M.; Schellen, H.L. A proposed method to assess the damage risk of future climate change to museum objects in historic buildings. *Build Environ* 2012, 55, 43-56.

[21] Pérez, M.C.; García Diego, F-J.; Merello, P.; D'Antoni, P.; Fernández-Navajas, A.; Ribera-Lacomba, A.; Ferrazza, L.; Pérez-Miralles, J.; Baró, J.L.; Merce, P.; D'Antoni, H.; Curiel, J. Ariadne's house (Pompeii, Italy) wall paintings: a multidisciplinary study of its present state focused on a future restoration and preventive conservation. *Mater Constr* 2013, 63 (311), 449-467.

[22] Camuffo, D.; Bernardi, A.; Sturaro, G.; Valentino, A. The microclimate inside the Pollaiolo and Botticelli rooms in the Uffizi Gallery. Florence, *J Cult Herit* 2002, 3, 155-161.

[23] Pavlogeorgatos, G. Environmental parameters in museums. *Buil Environ* 2003, 38, 1457-1462

[24] Gysels, K.; Delalieux, F.; Deutsch, F.; Van Grieken, R.; Camuffo, D.; Bernardi, A.; Sturaro, G.; Wieser, M. Indoor environment and conservation in the Royal Museum of Fine Arts, Antwerp, Belgium. *J Cult Herit* 2004, 5, 221-230.

[25] Saunders, D. Climate change and museum collections. *Stud Conserv* 2008, 53, 287-297.

[26] Corgnati, S.P.; Filippi, M. Assessment of thermo-hygrometric quality in museums: Method and in-field application to the "Duccio di Buoninsegna" exhibition at Santa Maria della Scala (Siena, Italy). *J Cult Herit* 2010, 11, 345-349.

[27] Legnér, M. On the early history of museum environment control: National museum and Gripsholm Castle in Sweden, C. 1866-1932. *Stud Conserv* 2011, 56, 125-137.

[28] Camuffo, D.; Sturaro, G.; Valentino, A. Thermodynamic exchanges between the external boundary layer and the indoor microclimate at the Basilica of Santa Maria Maggiore, Rome, Italy: the problem of conservation of ancient works of art. *Bound Lay Meteorol* 1999, 92, 243-262.

[29] Tabunschikov, Y.; Brodatch, M. Indoor air climate requirements for Russian churches and cathedrals. *Indoor Air* 2004, 14(Suppl 7), 168-174.

[30] Kisternaya, M.; Kozlov, V. Preservation of historic monuments in the "Kizhi" Open-Air Museum (Russian Federation). *J Cult Herit* 2012, 13, S74-S78.

[31] Maekawa, S.; Lambert, F.; Meyer, J. Environmental monitoring at Tiwanaku. *Mater Res Soc Symp Proc* 1995, 352, 885-892.

[32] Visco, G.; Plattner, S.H.; Fortini, P.; Di Giovanni, S.; Sammartino, M.P. Microclimate monitoring in the Carcer Tullianum: temporal and spatial correlation and gradients evidenced by multivariate analysis; first campaign. *Chem Cent J* 2012, 6(Suppl 2), S11.

[33] Varas, M.J.; Vicente-Tavera, S.; Molina, E.; Vicente-Villardón, J.L. Role of canonical biplot method in the study of building stones: An example from Spanish monumental heritage. *Environmetrics* 2005, 16, 405-419.

[34] Ribera, A.; Olcina, M.; Ballester, C. *Pompeya Bajo Pompeya, las Excavaciones en la Casa de Ariadna*. Fundación MARQ, Valencia, 2007.

[35] World Monuments Fund. *World Monuments Watch: 100 Most Endangered Sites*. World Monuments Fund, New York, USA, 1996.

[36] Anter, K.F. Colours in Pompeiian cityscape: Adding pieces to the puzzle. *Color Res Appl* 2006, 31(4), 331-340.

[37] Harris, J. Protecting Pompeii and the Italian heritage in 2012. Available at: http://www.i-italy.org/bloggers/18935/protecting-pompeii-and-italian-heritage-2012 (Accesed on 11/27/2013)

[38] Pesando, F. *Domus: edilizia privata e società pompeiana fra III e I secolo a.C. "L'Erma" di Bretschneider*, Rome, 1997.

[39] Video describing Ariadne's House in Pompeii. Available at: http://vimeo.com/3123842. (Accesed on March 2013).

[40] Pictures of Ariadne's House (Regio VII, Insula 4). Available at: http://www.pompeiiinpictures.com (Accesed on March 2013).

[41] Pesando, F. *La Casa de Ariadna de Pompeya: redescubrimiento de una domus*. In Ribera, A.; Olcina, M.; Ballester, C.; Pompeya bajo Pompeya, Las excavaciones en la Casa de Ariadna, Valencia, Spain, 2007.

[42] Prythercha, D.L.; Boira, J.V. City profile: Valencia. *Cities* 2009, 26(2), 103-15.

[43] Escrivá, V.; Pascual, P.; Ribera, A. L'Almoina Centro arqueológico de Valencia. *Revista de Arqueología* 1989, 99, 40-50.

[44] Álvarez, N.; Ballester, C.; Espí, I.; Mañez, J.; Marín, C.; Pascual, G.; Ribera, A. Las cerámicas de tres nuevos depósitos votivos de fundación de las excavaciones de l'Almoina (Valencia). *Societé Française d'Etude de la Ceramique Antique en Gaule* 2003, 1, 369-395.

[45] Martí, J.; Pascual, J. *El Desarrollo Urbano de Madina Balansiya Hasta el Final del Califato*. In Ciudad y territorio en Al-Andalus; Cara, L., Ed.; Athos-Pérgamos, Granada, Spain; 2000, p. 500-536.

[46] Ribera, A. The Roman foundation of Valencia and the town in the 2nd-1st c. B.C. Early Roman towns in Hispania Tarraconensis. *J Roman Archaeol* 2006, 62, 75-90.

[47] Ribera, A. The discovery of a monumental circus at Valentia (Hispania Tarraconensis). *J Roman Archaeol* 1998, 11, 318-336.

[48] Jiménez, J.L.; Ribera, A. *La Fundación de la Ciudad. Urbanismo y Arquitectura de la Valencia Romana y Visigoda*. In Historia de la Ciudad I. Recorrido Histórico por la Arquitectura y el Urbanismo de la Ciudad de Valencia; Ayuntamiento de Valencia: Valencia, Spain, 2000; p. 9-37.

[49] Ribera, A.; Soriano, R. *Los Cementerios de Época Visigoda*. In Saitabi 46; Universitat de Valencia: Valencia, Spain, 1996; p. 195-230.

[50] Fernández-Navajas, A.; Merello, P.; Beltrán, P.; García-Diego, F-J. Multivariate thermo-hygrometric characterisation of the archaeological site of plaza de l'Almoina (Valencia, Spain) for preventive conservation. *Sensors* 2013, 13, 9729-9746.

[51] AEMET. Agencia Española de meteorología. Available online: http://www.aemet.es/es/portada (Accessed on 24 August 2013).

[52] Turismo de Zaragoza. Iglesia de Santa María de Ateca. Available online: http://www.turismodezaragoza.es/provincia/patrimonio/mudejar/iglesia-santa-maria-ateca.html (Accessed on 24 August 2013).

[53] Sánchez, L. El retablo mayor de la Iglesia Parroquial de San María de Ateca. Descripción y aportaciones documentales. *Aragonia Sacra* 2004-2005, 18, 201-260.

[54] Bordass, W; Bemrose, C. *Heating Your Church*. Church House Publishing, London, UK, 1996.

[55] Padfield, T.; Bollingtoft, P.; Eshoj, B.; Christensen, M.C. *The Wall Paintings of Gundsomagle Church*. In Preventive Conservation: Practice, Theory and Research; Roy, A., Smith P., Eds.; International Institute for Conservation: London, UK; 1994, p. 94-98.

[56] Arnold, A.; Zehnder, K. *Monitoring wall paintings affected by soluble salts*. In The Conservation of Wall Paintings, 2nd ed.; Cather, S., Ed.; Courtauld

Institute of Art and the Getty Conservation Institute: London, UK, 1996; pp. 103-136.

[57] La Gennusa, M.; Rizzo, G.; Scaccianoce, G.; Nicoletti, F. Control of indoor environments in heritage buildings: Experimental measurements in an old Italian museum and proposal of a methodology. *J Cult Herit* 2005, 6, 147-155.

[58] Ariño, X.; Saiz-Jiménez, C. Deterioration of the Elephant Tomb (Necropolis of Carmona, Seville, Spain), *Int Biodeter Biodegr* 1997, 40, 233-239.

[59] Miriello, D.; Barca, D.; Bloise, A.; Ciarallo, A.; Crisci, G.M.; De Rose, T.; Gattuso, C.; Gazineo, F.; La Russa, M.F. Characterisation of archaeological mortars from Pompeii (Campania, Italy) and identification of construction phases by compositional data analysis. *J Arch Sci* 2010, 37, 2207-2223.

[60] Volpin, S.; Appolonia. L. *Le analisi di laboratorio applicate ai beni artistici policromi.* Collana i Talenti, Il Prato, 1999.

[61] Creagh, D.; Bradley, D. *Radiation in Art and Archeometry.* Elsevier, Amsterdam, 2000.

[62] Van der Weerd, J.; Van Veen, M.K.; Heeren, R.M.A.; Boon, J.J. Identification of pigments in paint cross sections by reflection visible light imaging microspectroscopy. *Analytical Chemistry*, 2003, 75 (4), 716-722.

[63] Ferro, D. *La microscopia elettronica a scansione per la storia, per l'arte, per la conservazione.* Istituto Centrale per la Patologia del Libro, Roma, 2007.

[64] Nevin, A.; Melia, J.L.; Osticioli, I.; Gautier, G.; Colombini, M.P. The identification of copper oxalates in a 16th century Cypriot exterior wall painting using micro FTIR, micro Raman spectroscopy and Gas Chromatography-Mass Spectrometry. *J Cult Herit* 2008, 9, 154-161.

[65] Botticelli, G. *Metodologia e Restauro delle Pitture Murali.* Edizioni Centro Di, Firenze, 1992.

[66] Mora, P.; Mora, L.; Philippot, P. *La conservazione delle pitture murali.* Editrice Compositori, Bologna, 2002.

[67] Martinez, M.C.I.; Seoane, A.N.; Romani, J.R.V. *Study of the deterioration of the ancient stone walls of San Antolin de Toques in Galicia, Spain, and the influence of the substitution of traditional lime mortars*, Proceedings of the 1997 5th International Conference on Structural Studies, Repairs and Maintenance of Historical Buildings, STREMAH V; San Sebastian, Spain, 1997; Code46967., Vol. 3, p.221-231.

[68] Augusti, S. *La tecnica del´antica pittura parietale pompeiana.* Gaetana Macchiaroli Editore, Nápoles, 1950.

[69] Durán, A.; Pérez-Maqueda, L.A.; Poyato, J.; Pérez-Rodríguez, J.L. A thermal study approach to roman age wall painting mortars. *J Therm Anal Calorim*, 2010, 99 (3), 803-809.

[70] Pérez, C.; Ferrazza, L.; Doménech, M.; Sarrió, F.; Ribera, A. *Las pinturas murales de la Casa de Ariadna en Pompeya: Un ejemplo de estudio e investigaciones científicas aplicados en el proyecto de conservación y restauración, La Ciencia y el Arte II.* Ciencias experimentales y conservación del Patrimonio Histórico, Ministerio de Cultura, Madrid, Spain, 2010.

[71] Peña-Poza, J.; Conde, J.F.; Palomar, T.; Agua, F.; García-Heras, M.; Villegas, M.A. Environmental evaluation of the holdings at the CCHS-CSIC Tomás Navarro Tomás library. *Revista Espanola de Documentacion Cientifica* 2011, 34, 65-78.

[72] Grinzato, E.; Bressan, C.; Marinetti, S.; Bison, P.G.; Bonacina, C. Monitoring of the Scrovegni Chapel by IR thermography: Giotto at infrared. *Infr Phys Tech* 2002, 43, 165-169.

[73] Palombi, L.; Cecchi, G.; Lognoli, D.; Raimondi, V.; Masotti, L. *A fluorescence imaging lidar for the control of cultural heritage*, Proceedings of SPIE - The International Society for Optical Engineering, 2007, vol. 6750, art. no. 675002.

[74] Bonizzoni, L.; Caglio, S.; Galli, A.; Poldi, G. Comparison of three portable EDXRF spectrometers for pigment characterization, *X-Ray Spectrom* 2010, 39, 233-242.

[75] López, M.C.; Medina, V.J.; Adroher, A.M.; García, A. Estudio de materiales y técnica de ejecución de los restos de pintura mural romana hallados en una excavación arqueológica en Guadix (Granada). *Espacio, Tiempo y Forma, Serie I, Prehistoria y Arqueología* 2000, 13, 253-278.

[76] Edreira, M.C.; Feliu, M.J.; Fernández-Lorenzo, C.; Martín, J. Roman wall painting characterization from Cripta del Museo and Alcazaba in Mérida (Spain): chromatic, energy dispersive X-ray fluorescence spectroscopic, X-ray diffraction and Fourier transform infrared spectroscopic analysis. *Analyt Chim Acta* 2001, 434 (2), 331-345.

[77] Schirripa, G. Virtual restoration: detection and removal of craquelure in digitized image of old paintings. Proceedings of SPIE - The International Society for Optical Engineering 8084, 2011, art. no. 80840B.

[78] Dellepiane, M.; Venturi, A.; Scopigno, R. Image guided reconstruction of unsampled data: a filling technique for cultural Heritage models. *Int Journal of Computer Vision* 2011, 94, 2-11.

[79] Moon, T.; Schilling, M.R.; Thirkettle, S. A note on the use of false-color infrared photography in conservation. *Stud Conservat* 1992, 37, 42-52.

[80] Klein, M.E.; Aalderink, B.J.; Padoan, R.; De Bruin, G.; Steemers, T.A.G. Quantitative hyperspectral reflectance imagining. *Sensors* 2008, 8, 5576-5618.

[81] Veniale, F.; M.; Setti, M.; Lodola, S. Diagnosing stone decay in built heritage. Facts and perspectives. *Mater Constr* 2008, 58, n°289.

[82] Liu, B.; Chen, X.; Fang, D.; Perrone, A.; Pispas, A.; Vainos, N.A. Environmental monitoring by thin film nanocomposite sensors for cultural heritage preservation. *Jour Alloys Comp* 2010, 504, S405-S409.

[83] UNI 10829. *Works of Art of Historical Importance. Ambient Conditions for the Conservation. Measurement and Analysis.* UNI Ente Nazionale Italiano di Unificazione, Milano, Italy, 1999.

[84] ASMETEC. 2011. Meteolite UV 400 description of UV-filter-sleeves UV-400. Available at: www.asmetec.de

[85] Gurioli, L.; Cioni, R.; Sbrana, A.; Zanella, E. Transport and deposition of pyroclastic density currents over an inhabitated area: the deposits of the AD 79 eruption of Vesuvius at Herculaneum, Italy. *Sedimentology* 2002, 49 (5), 929-953.

[86] Selim, A. *I colori pompeiani.* Rome, 1967.

[87] Corpora, H.; Quaresima, R. *Malte storiche e da restauro: stato dell'arte, considerazioni e prospettive alla luce della normativa esistente.* Edizioni Il prato, Padova, 2007.

[88] Baglioni, P.; Bitossi, G.; Fratini, F.; Rescic, S.; Dei, L. *Salt crystallization in porous materials: physicochemical aspects and effects of antiscaling additives.* In Proceedings: Science and technology for cultural heritage - Atti II Convegno naz. Chmica dei beni culturali della Società Chimica Italiana, Torino, 23-26 giugno 2003, Istituti editoriali e poligrafici internazionali MMIV.

[89] Castellano, A.; Cesareo, R.; Buccolieri, G.; Donativi, M.; Palama, F.; Quarta, S.; De Nunzio, G.; Brunetti, A.; Marabelli, M.; Santamaria, U. Detection of detachments and inhomogeneities in frescos by Compton scattering. *Nucl Instrum Meth A* 2005, 234, 548-554.

[90] Zehnder, K. Long term monitoring of wall painting affected by soluble salts. *Environmental Geology* 2007, 52 (2), 395-409.

[91] García-Diego, F.-J.; Bravo, J.M.; Pérez-Miralles, J.; Estrada, H.; Fernández-Navajas, A. Development of a low cost airborne ultrasound sensor for the detection of brick joints behind a wall painting. *Sensors* 2012, 12, 1299-1311.

[92] Castriota, M.; Cosco, V.; Barone, T.; De Santo, G.; Carafa, P.; Cazzanelli, E. Micro-Raman characterizations of Pompei's mortars. *J Raman Spectrosc* 2008, 39(2), 295-301.

[93] Maguregui, M.; Knuutinen, U.; Castro, K.; Madariaga, J.M. Raman spectroscopy as a tool to diagnose the impact and conservation stateof Pompeian second and fourth style wall paintings exposed to diverseenvironments (House of Marcus Lucretius). *Journal of Raman Spectroscopy* 2010, 41 (11), 1400-1409.

[94] Genestar, C.; Pons, C.; Más, A. Analytical characterisation of ancient mortars from the archaeological Roman city of Pollentia (Balearic Islands, Spain). *Analytica Chimica Acta* 2006, 557, 373-379.

[95] Bernardi, A. Microclimate in the British Museum. London. *Museum Manag Curat* 1990, 9, 169-182.

[96] Bernardi, A.; Camuffo, D. Microclimate in the Chiericati Palace Municipal Museum. Vicenza. *Museum Manag Curat* 1995, 14, 5-18.

[97] Loupa, G.; Charpantidou, E.; Kioutsioukis, I.; Rapsomanikis, S. Indoor microclimate, ozone and nitrogen oxides in two medieval churches in Cyprus. *Atmos Environ* 2006, 40, 7457-7466.

[98] Vuerich, E.; Malaspina, F.; Barazutti, M.; Georgiadis, T.; Nardino, M. Indoor measurements of microclimate variables and ozone in the church of San Vincenzo (Monastery of Bassano Romano - Italy): a pilot study. *Microchem J* 2008, 88, 218-223.

[99] Verdecchia, F.; Zoccatelli, C.; Norelli, E.; Miandro, R. Integrated monitoring network for surface deformation in Capo Colonna archaeological area, Crotone. Italy. *IAHS-AISH P* 2010, 339, 345-351.

[100] Hygrochron Temperature/Humidity Logger iButton with 8KB Data-Log Memory. Maxim Integrated Products. Available at: http://datasheets.maxim-ic.com/en/ds/DS1923.pdf (Accessed on September 2013)

[101] Temperature Logger iButton with 8KB Data-Log Memory. Maxim Integrated Products. Available at: http://datasheets.maxim-ic.com/en/ds/DS1922L-DS1922T.pdf. (Accessed on September 2013)

[102] ASTME 104-02. *Standard Practice for Maintaining Constant Relative Humidity by Means of Aqueous Solutions*. West Conshohocken, PA: ASTM Intl., 2012.

[103] Statgraphics Software. Available at: http://www.statgraphics.net (Accessed on September 2013)

[104] De los Rios, A.; Cámara, B.; García del Cura, M.A.; Rico, V.J.; Galván, V.; Ascaso, C. Deteriorating effects of lichen and microbial colonization of carbonate building rocks in the Romanesque churches of Segovia (Spain). *Sci Total Environ* 2009, 407, 1123-1134.

[105] Cooke, R.U.; Smalley, I.J. Salt weathering in deserts. *Nature* 1968, 220, 1226-1227.

[106] Paradise, T.R. Limestone weathering and rate variability, great temple of Amman, Jordan. *Phys Geogr* 1998, 19(2), 133-146.

[107] Winkler, E.M. Weathering rates as exemplified by Cleopatra's needle in New York city. *J Geol Educ* 1965, 13, 50-52.

[108] Winkler, E.M. Important agents of weathering for building and monumental stone. *Eng Geol* 1966, 1, 381-400.

[109] Winkler, E.M.; Wilhelm, E.J. Salt burst by hydration pressures in architectural stone in urban atmosphere. *Geol Soc Am Bull* 1970, 81, 567-572.

[110] Nord, A.G. Efflorescence salts on weathered building stone in Sweden. *Geol Fören Stock För* 1992, 114(4), 423-229.

[111] W*ü*st, R.A.J.; Schlüchter, C. The origin of soluble salts in rocks of the Thebes mountains, Egypt: The damage potential to ancient Egyptian wall art. *J Archaeol Sci* 2000, 27(12), 1161-1172.

[112] Coperture: lastre in fibrocemento ecologico (Edilit SpA). Available at: http://www.edilit.com. (Accesed on March 2013).

[113] Laurenti, M.C. (Ed). *Le Coperture delle Aree Archeologiche*. Museo Aperto, Gangemi editore, Roma, 2006.

[114] Raich, A.; Çinar, A. Statistical Process Monitoring and Disturbance Diagnosis in Multivariable Continuous Processes. *AIChE J* 1996, 42, 995-1009.

[115] Martin, E.; Morris, A. An overview of multivariate statistical process control in continuous and batch process performance monitoring. *T I Meas Control* 1996, 18, 51-60.

[116] Chen, G.; McAvoy, T.J. Predictive on-line monitoring of continuous processes. *J Process Contr* 1998, 8, 409-420.

[117] Goulding, P.R.; Lennox, B.; Sandoz, D.J.; Smith, K.J.; Marjanovic, O. Fault detection in continuous processes using multivariate statistical methods. *Int J Syst Sci* 2000, 31, 1459-1471.

[118] Nomikos, P.; McGregor, J.F. Multivariate SPC charts for monitoring batch processes. *Technometrics* 1995, 37, 41-59.

[119] Kourti, T. Application of latent variable methods to process control and multivariate statistical process control in industry. *Int J Adapt Control* 2005, 19, 213-246.

[120] Kourti, T. *Analysis, monitoring, control and optimization of batch processes: multivariate dynamic data modeling.* In: Koch M editor. PAT Applied in Biopharmaceutical Process Development And Manufacturing. CRC Press, Florida; 2001, p.43-76.

[121] Fernández, A. *La pintura y los mosaicos de La Casa de Ariadna.* In: A. Ribera, M. Olcina, C. Ballester editors. Pompeya bajo Pompeya, La Casa de Ariadna. Valencia, Spain, 2007, p.67.

[122] Camacho, J.; Picó, J.; Ferrer, A. Bilinear modelling of batch processes. Part I: Theoretical discussion. *J Chemometr* 2008, 22, 299-308.

[123] Zarzo, M.; Ferrer, A. Batch process diagnosis: PLS with variable selection versus block-wise PCR. *Chemom Intell Lab Syst* 2004, 73, 15-27.

[124] Casella, G.; Berger, R.L. *Statistical Inference.* Duxbury Press: North Scituate, MA, USA, 2001.

[125] Hair, J.F.; Anderson, R.E.; Tatham, R.L.; Black, W.C. *Análisis Multivariante.* Prentice Hall Iberia, Madrid, Spain, 1999.

[126] IBM Software, SPSS 16. Available online: http://www-01.ibm.com/software/es/analytics/spss/ (accessed on 25 June 2013).

[127] Horemans, B.; Schalm, O.; de Wael, K.; Cardell, C.; van Grieken, R. *Atmospheric Composition and Micro-Climate in the Alhambra Monument, Granada (Spain), in the Context of Preventive Conservation.* In Proceedings of the IOP Conference Series: Materials Science and Engineering, Sharjah, United Arab Emirates, 7-8 December 2011; Volume 37, p. 012002.

[128] Fernández-Navajas, A.; Merello, P.; Beltrán, P.; García-Diego, F.-J. Software for storage and management of microclimatic data for preventive conservation of cultural heritage. *Sensors* 2013, 13, 2700-2718.

[129] Ward P. *The nature of conservation: a race against time.* Oxford University Press, California, 1990.

[130] Ponziani, D.; Ferrero, E.; Appolonia, L.; Migliorinia, S. Effects of temperature and humidity excursions and wind exposure on the arch of Augustus in Aosta. *J Cult Herit* 2012, 13, 462-8.

[131] García-Diego, F.-J., Fernández-Navajas, A.; Beltrán, P.; Merello, P. Study of the effect of the strategy of heating on the mudejar Church of Santa Maria in Ateca (Spain) for preventive conservation of the Altarpiece surroundings. *Sensors* 2013, 13, 11407-23.

[132] Staniforth, S. *Benefit versus costs in environmental control.* In Managing Conservation: Papers Given at a Conference Held Jointly by the Unit-ed Kingdom Institute for Conservation and the Museum of London; Keene, S., Eds.; The United Kingdom Institute for Conservation: London, UK, 1990; p. 28-30.

[133] Staniforth, S.; Ballard, W. M.; Caner-Saltik, E. N.; Drewello, R.; Eck-mann, I.-L.; Krumbein, W. E.; Padfield, T. *Group report: what are appropriate strategies to evaluate change and to sustain cultural heritage?* In Durability and Change: The Science, Responsibility, and Cost of Sustaining Cultural Heritage; Krumbein, W.E., Brimblecombe, P., Eds.; John Wiley and Sons Inc: New Jersey, USA, 1992; p. 175.

[134] Staniforth, S.; Griffin, I. *Damp problems in the Chapel at Cliveden.* In The Conservation of Heritage Interiors, Proceedings of Conference Symposium 2000, Ottawa, Canada, May 17 to 20 2000; Canadian Conservation Institute: Ottawa, Canada, 2000; p. 177-84.

[135] Ouldboukhitine, S.E.; Belarbi, R.; Djedjig, R. Characterization of green roof components: measurements of thermal and hydrological properties. *Build Environ* 2012, 56, 78-85.

[136] Kumar, A.; Suman, B.M. Experimental evaluation of insulation materials for walls and roofs and their impact on indoor thermal comfort under composite climate. *Build Environ* 2013, 59, 635-43.

[137] Ouedraogo, B.; Levermore, G.J.; Parkinson, J.B. Future energy demand for public buildings in the context of climate change for Burkina Faso. *Build Environ* 2012, 49, 270-82.

[138] Merello, P.; García-Diego, F.-J.; Zarzo, M. Evaluation of corrective measures implemented for the preventive conservation of fresco paintings in Ariadne's house (Pompeii, Italy). *Chem Cent J* 2013, 7(1), 87.

[139] Bratasz, L.; Kozlowski, R.; Camuffo, D.; Pagan, E. Impact of indoor heating on painted wood: Monitoring the altarpiece in the church of Santa Maria Maddalena in Rocca Pietore, Italy. *Stud Conserv* 2007, 52, 199-210.

[140] Green, D.W.; Winandy, J.E.; Kretschmann, D.E. *Mechanical Properties of Wood*. In Wood Handbook, Wood as an Engineering Material; Forest Products Laboratory: Madison, WI, USA; 2010.

[141] Uzielli, L. *Historical Overview of Panel-Making Techniques in Central Italy*. In The Structural Conservation of Panel Painting; Dardes, K., Rothe, A., Eds; The Getty Conservation Institute: Los Angeles, CA, USA; 1998, p. 110-135.

[142] Rachwal, B.; Bratasz, L.; Lukomski, M.; Kozlowski, R. Response of wood supports in panel paintings subjected to changing climate conditions. *Strain* 2012, 48, 366-374.

[143] Simpson, W.T. *Drying and Control of Moisture Content and Dimensional Changes*. In Wood Handbook, Wood as an Engineering Material; Forest Products Laboratory: Madison, WI, USA, 2010.

[144] Mecklenburg, M.F.; Tumosa, C.S.; Erhardt, D. *Structural Response of Painted Wood Surfaces to Changes in Ambient Relative Humidity*. In Wood Handbook, Wood as an Engineering Material; Forest Products Laboratory, Madison, WI, USA; 2010.

[145] Bläuer, B.C.; Zehnder, K.; Domeisen, H.; Arnold, A. Climate control for the passive conservation of the Romanesque painted wooden ceiling in the church of Zillis (Switzerland). *Stud Conserv* 2001, 46, 251-268.

[146] Bernikola, E.; Nevin, A.; Tornari, V. Rapid Initial Dimensional Changes in Wooden Panel Paintings due to Simulated Climate-Induced Alterations Monitored by Digital Coherent Out-of-Plane Interferometry. *Appl. Phys. A* 2009, 95, 387-399.

[147] Jakiela, S.; Bratasz, L.; Kozlowski, R. Numerical modelling of moisture movement and related stress field in lime wood subjected to changing climate conditions. *Wood Sci Technol* 2008, 42, 21-37.

[148] Olstad, T.M. *Mediaeval Wooden Churches in Cold Climate Parish Churches or Museums?* In Preventive Conservation: Practice, Theory and Research; Roy, A., Smith, P., Eds.; International Institute for Conservation: London, UK; 1994, p. 99-103.

[149] Richard, M. *The Transport of Paintings in Microclimate Display Cases*. In Preventive Conservation: Practice, Theory and Research; Roy, A., Smith, P., Eds.; International Institute for Conservation: London, UK; 1994, p. 185-189.

[150] Knight, B. *The Effects of the Real Environment on Real Objects.* Ancient Monuments Laboratory English Heritage, London, UK, 1998.

[151] Marstein, N.; Stein, M. Advanced Measuring of the Climatic Conditions in the Medieval Wooden Churches in Norway. In Proceedings of the ICOM Committee for Conservation: 8th Triennial Meeting, Sydney, Australia, 6-11 September 1987; p. 889-896.

[152] Olstad, T.M.; Stein, M. *Saving Art by Saving Energy.* NIKU Temahefte (2); Norwegian Institute for Cultural Heritage Research, Norway, 1996.

[153] Bratasz, L.; Kozlowski, R. Laser sensors for continuous in situ monitoring of the dimensional response of wooden objects. *Stud Conserv* 2005, 50, 307-315.

[154] Lasyk; Kukomski, M.; Olstad, T.M.; Haugen, A. Digital speckle pattern interferometry for the condition surveys of painted wood: Monitoring the altarpiece in the church in Hedalen, Norway. *J Cult Herit* 2012, 13, 102-108.

[155] Ren, H.; Halvorsen, M.B.; Deng, Z.D.; Carlson, T.J. Aquatic Acoustic Metrics Interface Utility for Underwater Sound Monitoring and Analysis. *Sensors* 2012, 12, 7438-7450.

[156] Koller, M. *Learning from the History of Preventive Conservation.* In Preventive Conservation: Practice, Theory and Research, Proceedings of the Ottawa Congress, Ottawa, Canada, 12-16 September 1994; Ashok, R., Smith, P., Eds.; International Institute for Conservation of Historic and Artistic Works, London, UK, 1994; p.1-7.

[157] Bernardi, A.; Todorov, V.; Hiristova, J. Microclimatic analysis in St. Stephan's church, Nessebar, Bulgaria after interventions for the conservation of frescoes. *J Cult Herit* 2000, 1, 281-286.

[158] Embarcadero. Delphi vendor and distributor. Available online: http:// www.embarcadero.com (Accesed on December 2012).

[159] Firebird. Database engine. Available online: http://www.firebirdsql.org/ (Accesed on December 2012).

[160] Honeywell. HIH-4000 Series integrated circuit humidity sensor datasheet. Available online: http://sensing.honeywell.com/product%20page?prid=53944 (Accessed on December 2012).

[161] Maxim Integrated Products. DS2438 Smart Battery Monitor datasheet; Available online: http://pdfdata.datasheetsite.com/pdf1/Maxim/DS2438.pdf (Accessed on December 2012).

[162] Foster, M.; Tadj, O. Occupant control of passive systems: The use of Venetian blinds. *Build Environ* 2001, 36(2), 149-55.

[163] Maekawa, S. *Preventive Strategies for Reducing the Impact of Visitors on the Microenvironment of Caves at the Mogao Grottoes*. In Preventive Conservation: Practice, Theory and Research, Proceedings of the Ottawa Congress, Ottawa, Canada, 12-16 September 1994; Ashok, R., Smith, P., Eds.; International Institute for Conservation of Historic and Artistic Works: London, UK, 1994; 76-79.

[164] Adcock, C.J. Sample size determination: A review. *J R Stat Soc D* 1997, 46 (2), 261-283.

[165] Branscum, A.J.; Johnson, W.O.; Gardner, I.A. Sample size calculations for studies designed to evaluate diagnostic test accuracy. *J Agr Biol Environ Stat* 2007, 12, 112-127.

Index of Figures

Index of Tables